ALTERED EXPRESSION OF THE NON-PHOSPHORYLATION ELECTRON TRANSPORT CHAIN EFFECTS GROWTH AND STRESS TOLERANCE IN *ARABIDOPSIS THALIANA*

BY CHEVAUN SMITH

A THESIS SUBMITTED FOR THE DEGREE OF DOCTOR OF PHILOSOPHY

AT

THE SCHOOL OF BIOLOGICAL SCIENCES

FLINDERS UNIVERSITY

JANUARY 2010

ABBREVIATIONS

ADP	Adenosine Diphosphate
ANGIS	Australian National Genomic Information Service
AOX	Alternative Oxidase
At	*Arabidopsis thaliana*
ndb	external alternative NAD(P)H dehydrogenase
ATP	Adenosine Triphosphate
bp	Base Pairs
BSA	Bovine Serum Albumin
Ca^{2+}	Calcium
CAC	Citric Acid Cycle
CEl	Cell Intensity File
cDNA	Complementary DNA
DH	Dehydrogenase
DNA	Deoxyribose Nucleic Acid
DPI	Dipenyleneiodonium
dsRNA	double-stranded RNA
EDTA	Ethylenediaminetetraacetic Acid
EGTA	Ethylene Glycol Bis(2-aminoethyl Ether)-N,N,N',N'-tetraacetic Acid
EPR	Eectron paramagnetic resonance
ETC	Electron Transport Chain
$FADH_2$	Flavin Adenine Dinucleotide [reduced]
FDR	false discovery rate
g / mg	grams / milligrams
µg / ng	micrograms / nanograms
GC-RMA	Guanine Cytosine Robust Multi-Array Analysis
gDNA	Genomic DNA
hpRNA	Hairpin RNA
IM	Inter Membrane Space
K^+	Potassium
Kb	Kilobase

KCN	Potassium Cyanide
kDa	kilodalton
L / ml / µl	litre / millilitres / microliters
LB	Luria Broth
M / mM	molar / millimolar
µM / nM	micromolar / nanomolar
MAS5	Affymetrix Microarray Suite version 5
MATDB	MIPS *Arabidopsis Thaliana* Database
mETC	Mitochondrial Electron Transport Chain
MIPS	Munich Information Centre for Protein Sequences
mRNA	Messenger RNA
MS	Murashige and Skoog
Na^+	Sodium
NaCl	Sodium Chloride
NAD+	Nicotinamide Adenine Dinucleotide
NAD(P)H	NADH and NADPH
NADH	Nicotinamide Adenine Dinucleotide [reduced]
NADP	Nicotinamide Adenine Dinucleotide Phosphate
NADPH	Nicotinamide Adenine Dinucleotide Phosphate [reduced]
NCBI	National Centre for Biotechnology Information
NDA	NAD(P)H dehydrogenase Internal
NDB	NAD(P)H dehydrogenase External
NDC	NAD(P)H dehydrogenase membrane spaning
NDE	NAD(P)H dehydrogenase External
NDI	NAD(P)H dehydrogenase Internal
NEB	New England Biolabs
NPT	Neomycin phosphotransferase
ORF	Open Reading Frame
PCA	Principal Component Analysis
PCR	Polymerase Chain Reaction
PTGS	Post Transcriptional Gene Silencing
QRT-PCR	Quantitative Real Time Polymerase Chain Reaction
RE	Restriction Enzyme
REBASE	Restriction Enzyme Recognition Sites

RISC	RNA Induced Silencing Complex
RNA	Ribonucleic Acid
RNAi	RNA Interference
ROS	Reactive Oxygen Species
Rpm	Revolutions per Minute
RGR	Relative Growth Rate
RT-PCR	Reverse Transcriptase Polymerase Chain Reaction
SAP	Shrimp Alkaline Phosphatase
SDS-PAGE	Sodium Dodecyl Sulphate Polyacrylamide Gel Electrophoresis
siRNA	Small Interfering RNA
T_a	PCR cycle annealing temperature (°C)
T_m	PCR cycle melting temperature (°C)
UCP	Uncoupling Proteins
µE	Micro Einstein's
UQ	Ubiquinone
UTR	Untranslated Region
v / v	Volume / Volume
w / v	Weight / Volume
Wt	Wild Type

ABSTRACT

The branched respiratory pathway of plants contains a cyanide-insensitive alternative pathway. The alternative pathway is of particular interest due to the apparent wasteful activity of the non-phosphorylating NAD(P)H dehydrogenases. Seven putative alternative NAD(P)H dehydrogenase genes have been identified from the *Arabidopsis thaliana* genome however, there have only been five activities characterised experimentally. Thus it is not known which gene encodes which activity in *A. thaliana* mitochondria. The three main aims of this study were to generate a transgenic *A. thaliana* line with complete suppression of the *ndb4* gene to confirm that it encodes an external NAD(P)H dehydrogenase and its calcium dependence. It was also hoped to elucidate the role of these alternative NAD(P)H dehydrogenases by reducing or eliminating expression of all four external NAD(P)H dehydrogenases in one plant line. The third aim was to look at the response of the alternative pathway including Alternative Oxidase (AOX) to stress growth conditions, specifically salinity stress.

RNAi technology was used to generate transgenic *A. thaliana* plants. The *ndb4* lines showed a range of suppression which lead to the up-regulation of *Atnbd2* in some lines and *Aox1a* in all lines, which was confirmed at the protein level. It was determined that *ndb4* encodes a calcium independent NADH dehydrogenase, where *ndb2* is likely to have calcium dependent NADH activity. Silencing lines of an *Atndb* region indicated the plant was not viable without any of the external dehydrogenases present. Microarray data indicated an altered expression profile in *ndb4* knock-down lines which significantly impacted several anti-oxidant pathways, both in and outside the mitochondria indicating the altered *ndb4* resulted in a change in the global expression pattern of the cell.

The involvement of this alternative pathway in a stress response may be linked to its capacity to uncouple carbon metabolism from adenylate control and/or the minimisation of the formation of destructive reactive oxygen

species (ROS). Salinity stress is a widespread, adverse environmental stress, which leads to an ionic imbalance, hyperosmotic stress, and oxidative stress, the latter being the result of reactive oxygen species formation. We have shown that salinity stress of *A. thaliana* plants resulted in the formation of ROS, increased levels of Na^+ in both the shoot and the root and an increase in transcription of *Aox1a*, *ndb2* and *ndb4* genes, indicating the formation of a bridged non-phosphorylating electron transport chain in response to salinity stress. Furthermore, plants constitutively over-expressing *Aox1a*, with increased AOX capacity, showed lower ROS formation, 30-40% improved growth rates and lower shoot Na+ content compared to controls, when grown under salinity stress conditions, the *ndb4* knock-down plants responded to salinity stress with the same trend. This was even further supported when plants had both an external dehydrogenase and AOX up regulated. Thus, more active alternative pathway in roots and shoots can improve the salt tolerance of *A. thaliana* as defined by its ability to grow more effectively in the presence of NaCl, and maintain lower shoot Na^+ content. AOX does have an important role in stress adaptation in plants, and these results provide some validation of the hypothesis that AOX can play a critical role in cell re-programming under salinity stress.

DECLARATION

I certify that this thesis does not incorporate without acknowledgement any material previously submitted for a degree or diploma in any university; and that to the best of my knowledge and belief it does not contain any material previously published or written by another person except where due reference is made in the text.

Chevaun Smith

PUBLISHED WORK

Part of the work in this thesis has been published or is in preparation for publishing.

Published

Smith, C.A., Melino, V.J., Sweetman, C., and Soole, K.L. (2009) Manipulation of alternative oxidase can influence salt tolerance in *Arabidopsis thaliana*. *Physiological Plantarum* **137**; 459-72

Prepared for Publication

Smith C.A., Barthet, M. M., Simms, R. M., Yilmaz, O., Smith, P. M. C., Whelan, J., Soole, K., Day, D. A. Altered NDB4 expression in *Arabidopsis* impacts relative growth rate and leaf area. For submission to Plant Physiology.

ACKNOWLEDGEMENTS

Firstly I would like to thank my supervisors Assoc/Prof Kathleen Soole and Dr Ian Menz for their supervision and support throughout this project. Thanks especially to Kathy for reading through all the edits

.

I would also like to thank to the Soole Lab members who have been around while doing my PhD and helped in many ways big and small, Tania Kurek, Crystal Sweetman, Pip Cook, Vivek Vijayraghavan, Crista Burbidge and Lidia Mischis. All these lab members have offered support and advice during my PhD which has been greatly appreciated, especially Lidia with her green thumb knowledge.

I would especially like to thank my close friends who have been there when the times were good and bad, Mel G, Patrick, Lexi, Drew, Bart, Mel P, Ana, and Mel S. I couldn't have done it without you or the many coffee sessions we had together.

Thanks to all the other students and staff on the third floor for their help and guidance throughout the year. I would also like to thank all the technical staff who were able to help with equipment when needed. Also special thanks again to Mel G who helped with all the last minute things I really appreciated it!

Lastly a special thanks to my family who supported me during my PhD and pretended to understand when I told them about the great results and the disasters. I couldn't have done it without all of you!

TABLE OF CONTENTS

TABLE OF FIGURES

DATA TABLES

1 INTRODUCTION

1.1 Mitochondria

Mitochondria are made up of two highly specialised membranes, which make up two compartments; the internal matrix and the inter membrane space, as seen in Figure 1.1. Within the inner membrane are the components of the Electron Transport Chain (ETC) that leads to the production of ATP. Mitochondria are the site of oxidative phosphorylation in eukaryotes.

1.2 The Electron Transport Chain

The primary features of the mitochondrial electron transport chain found in plants are similar to those of the electron transfer chain in mitochondria isolated from other eukaryotes, consisting of four integral multiprotein complexes (Siedow *et al.* 1995) (Figure 1.2). Complex I or NADH dehydrogenase, which is rotenone-sensitive (Finnegan et al., 2004), oxidizes NADH and transfers the electron to ubiquinones, a small lipid-soluble electron and proton carrier. For every electron pair oxidized from NADH by Complex I, four protons are pumped from matrix into the inter-membrane space. Succinate is oxidized to fumarate by Complex II or succinate dehydrogenase and then feed the electron to ubiquinone pool via FADH2 and a group of iron-sulfur protein. Complex II is inhibited by a substrate analog to succinate, malonate (Finnegan et al. 2004)(Finnegan et al. 2004)(Finnegan et al. 2004). Complex III or cytochrome bc_1 complex oxidized ubiquinol (the reduced form of ubiquinones) and distributes the electron to cytochrome *c* via an iron iron-sulfur centre, two *b*-type cytochrome (b_{565} and b_{560}) and a membrane-bound cytochrome c_1. Oxidation per pair electron by Complex III causes four protons pumped to the inter-membrane space. Antimycin A and myxothiazol are the inhibitors for Complex III (Finnegan *et*

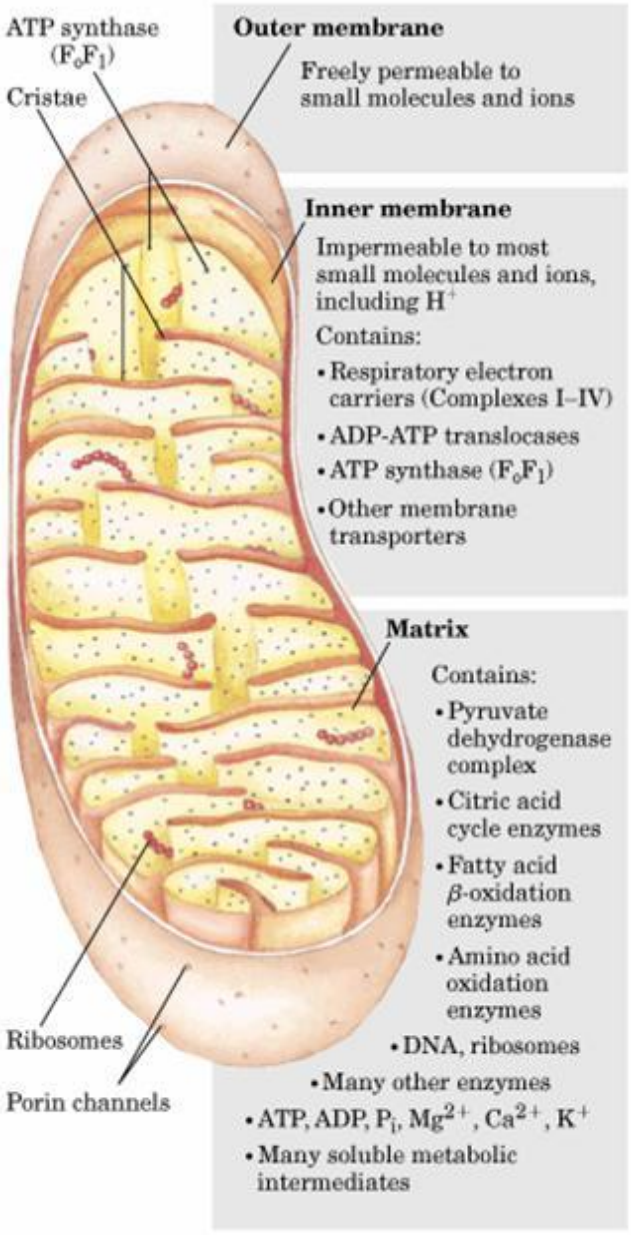

Figure 1.1 The Mitochondria (Nelson *et al.* 2000)

The following figure shows the three compartments the Matrix, the Inner membrane and the Outer membrane.

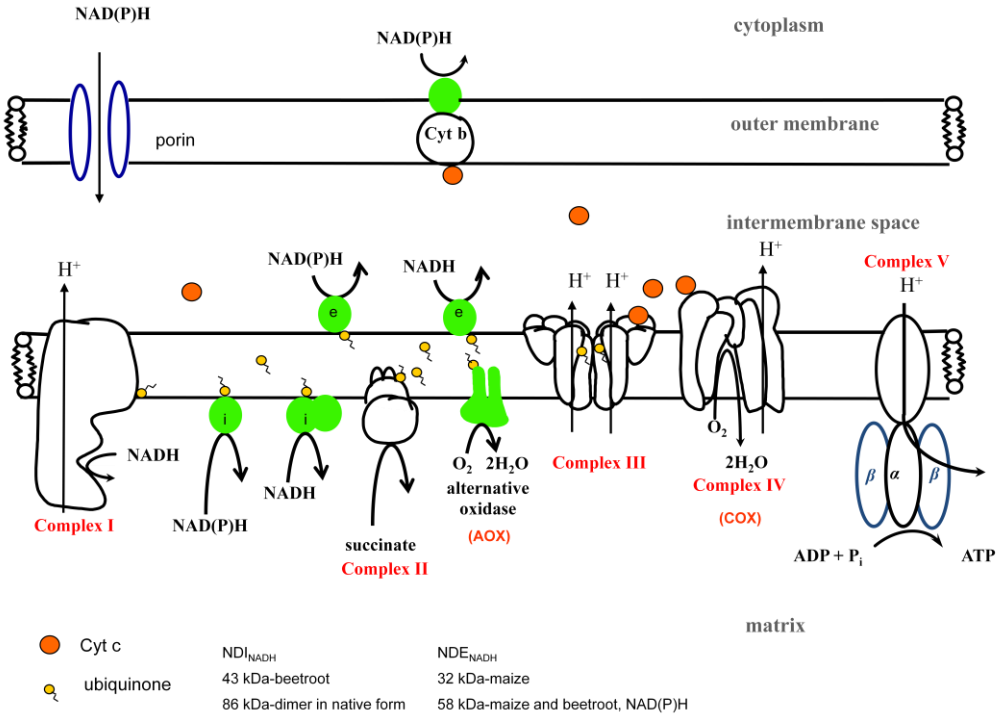

Figure 1.2 The electron transport chain containing the alternative enzymes

Organization of the electron transport chain and ATP synthesis in the inner membrane of plant mitochondria. In addition to the five standard protein complexes found in nearly all other mitochondria, the electron transport chain of plant mitochondria contains five additional enzymes marked in green. None of these additional enzymes pump protons.

al. 2004). Complex IV or cytochrome *c* oxidase transfers electron from cytochrome *c* to O_2 (oxygen) as the final electron acceptor, producing two molecules of H_20 for every four electron. When a pair of electron is transferred to O_2 by Complex IV, two protons are pumped across the inner membrane. The activity of Complex IV is inhibited by cyanide, carbon monoxide and azide (Finnegan *et al.* 2004). The series of proton pumping from matrix to the inter-membrane space creates proton-motive force that drives ATP production through ADP phosphorylation catalysed by F1F0 ATP synthase. The involvement of cytochrome *c* in this electron transport makes this pathway called cytochrome pathway.

This flow of electrons through the protein pumping complexes results in the generation of an electrochemical proton gradient across the inner mitochondrial membrane. When the gradient is established it is used to drive the synthesis by the mitochondrial ATP synthase or Complex V, through which protons flow passively back into the matrix via a proton pore associated with Complex IV. This is why oxygen consumption is said to be coupled to ATP synthesis.

1.3 Plant Mitochondria

Mitochondria play an essential role in diverse metabolic pathways in plants, including the production of ATP and the biosynthesis of carbon skeletons and metabolic intermediates, such as heme and amino acids. They also play roles in pathogen and stress responses and are intimately involved in the process of programmed cell death (Mackenzie *et al.* 1999; Lam *et al.* 2001).

Respiration is an important determinant of plant growth and development. As well as the cytochrome pathway (Phosphorylating pathway) mentioned above, plant mitochondria are unique in that they contain three unique non-phosphorylating respiratory pathways (Finnegan *et al.* 2004). These additional energy-dissipating components include the type II NAD(P)H dehydrogenases, the alternative oxidase (AOX) and uncoupling proteins

(UCP) (Picault *et al.* 2004; Rasmusson *et al.* 2004). The presence of AOX is characterised by the ability of plant mitochondria to respire in the presence of cyanide, which is a known potent inhibitor of cytochrome oxidase (Finnegan *et al.* 2004).

AOX is not limited to just plants, but also found in many algae, fungi and certain protozoa (Siedow *et al.* 1995), as well as recently being found in all kingdoms of life except the Archaebacteria (McDonald 2008). AOX has recently been found in 20 animal species, and as AOX has been identified in several sponges, members of the most primitive animal phylum, it suggests AOX was subsequently lost by vertebrates and arthropods (McDonald 2008). This enzyme branches from the respiratory chain at ubiquinone and catalyses the oxidation of ubiquinol, reducing oxygen to water with no proton translocation (Finnegan *et al.* 2004) (Figure 1.3). The type II NAD(P)H dehydrogenases provide an alternative entry point into the cytochrome pathway before ubiquinone. Both of these pathways are mediated by NAD(P)H: UQ oxidoreductases which are located on the inner mitochondrial membrane. There is a pathway associated with the oxidation of cytosolic NADH and NADPH, which is facilitated by at least two external NAD(P)H:UQ oxidoreductases, whose active sites face the cytoplasm (external). Matrix NADH and NADPH is oxidised via two internal NAD(P)H:UQ oxidoreductases which have their active sites facing the matrix (internal) (Figure 1.3).

The NAD(P)H:UQ oxidoreductases have been grouped into two classes, type I (NDH1) and type II (NDH2) NAD(P)H dehydrogenases (Yagi 1991). The two classes are characterized by differences in energy transduction, cofactors and polypeptide composition (Finnegan *et al.* 2004). The type I NAD(P)H dehydrogenases are Complex-like enzymes, and the type II NAD(P)H dehydrogenases unlike type I do not translocate protons, have non-covalent bound FMN, don’t have iron sulphur clusters and are usually comprised of one subunit, and are rotenone insensitive. These are referred to as the alternative NAD(P)H dehydrogenases, in this thesis. This does not mean that they only operate when Type I dehydrogenases are not functioning, but can oxidise NAD(P)H in the presence of a functional Complex I. Of the seven

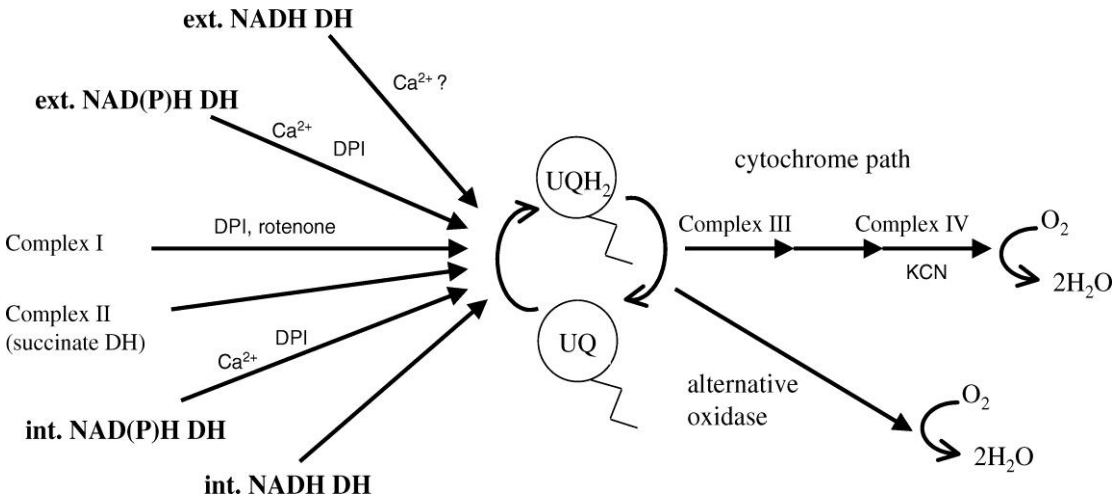

Figure 1.3 Schematic view of the plant mitochondrial electron transport chain (Rasmusson *et al.* 2004)

Multiple dehydrogenases reduce a common pool of ubiquinone, which is then oxidized by either the traditional cytochrome pathway or the alternative oxidase. Inhibitors are rotenone, DPI and KCN. Activators are Ca^{2+}.

genes encoding putative type II NAD(P)H dehydrogenases in *A. thaliana* three have been determined to be external dehydrogenases, (NDE)(*ndb1*, *2*, and *4*) the NDB family and three determined to be internal NAD(P)H dehydrogenases, (NDI) (*nda1* and 2 and *ndc1*) the NDA family(Michalecka *et al.* 2003; Elhafez *et al.* 2006), while the remaining cDNA, *ndb3* has not been able to be cloned and hence could be a pseudogene or have very restricted expression (Escobar *et al.* 2004). Using proteolytic digestion after in vitro import of each gene product, it has been confirmed that of the NAD(P)H dehydrogenases, the NDB family, are located on the external side of the inner membrane and that two NAD(P)H dehydrogenases (the NDA family) are located on the inner side of the inner membrane (Elhafez *et al.* 2005). The regulation of distribution of flux through each DH is not yet well understood, however the optimal conditions for each NAD(P)H DH activity is discussed in the relevant Sections below .

1.4 Pre genome analysis of the alternative pathway enzymes

1.4.1. Identification of alternative NAD(P)H dehydrogenases

External NAD(P)H oxidation was first demonstrated in lupin cotyledon mitochondria (Humphreys *et al.* 1956). This activity has now been detected in many plant species. The enzymes found in various tissue types have reported a wide range of Km values for external NAD(P)H activity depending on the assay conditions (Moller *et al.* 1993). External NAD(P)H oxidation has a total requirement for calcium (Coleman *et al.* 1971), hence the activity of external dehydrogenases can be inhibited by calcium chelators such as EGTA, EDTA and citrate. As NADPH oxidation is inhibited to a greater extent than NADH oxidation at the same inhibitor concentration for the sulfhydryl reagents, p-chloromercuribenzoate, n-ethylmaleimide and mersalyl inhibitors (Arron *et al.* 1979; Arron *et al.* 1980; Nash *et al.* 1983b) it has led to the proposal that NADH and NADPH were oxidised by separate enzymes. This was further supported by differential stimulation of NADH oxidation over NADPH oxidation during cold storage (Fredlund *et al.* 1991b; Zottini *et al.*

1993).

Fungal mitochondria contain combinations of internal and external rotenone-insensitive NADH and NADPH dehydrogenases, and these have been useful in helping to identify related bacteria enzymes (Michalecka *et al.* 2003). Additionally (Melo *et al.* 2001), identified an external NAD(P)H dehydrogenase in *Neurospora crassa*, as well an internal NADH dehydrogenase. These discoveries in yeast, fungi and bacteria have provided means of identifying related plant enzymes (Moore *et al.* 2003). The comparison of the NAD(P)H dehydrogenases between *N. crassa, Saccharomyces cerevisiae,* mammals and plants is compared in Figure 1.4.

1.4.2. Protein Purification

Attempts to purify the NDE enzymes in various species have resulted in the isolation of both NADH-specific (NDE $_{NADH}$) and NAD(P)H non-specific enzymes (NDE $_{NAD(P)H}$) suggesting the presence of multiple NDEs on the outer surface of the inner membrane (Finnegan *et al.* 2004). Several early purification efforts with different species indicated that 2 or 3 proteins with NAD(P)H dehydrogenase activities could be isolated from soluble fractions of plant mitochondria (Knudten *et al.* 1994). After several years, four different proteins emerged as potential alternative NAD(P)H dehydrogenases (Rasmusson *et al.* 2004). A 43 kDa protein which has NADH and NADPH activity has been purified from red beet root (Luethy *et al.* 1991a; Menz *et al.* 1996b), and thought to be the internal NAD(P)H DH.

A 58 kDa potential NAD(P)H dehydrogenase has been isolated from red beet root and maize, and was located to the external side of the inner membrane (Luethy *et al.* 1995). An antibody raised to this 58 kDa protein cross-reacted with several plant species and not with the rat liver mitochondria, further confirming it to be a potential candidate for the external NAD(P)H dehydrogenase. In 1996, Menz and Day supported that a 58 kDa protein, which was isolated from a soluble fraction from beetroot mitochondria had

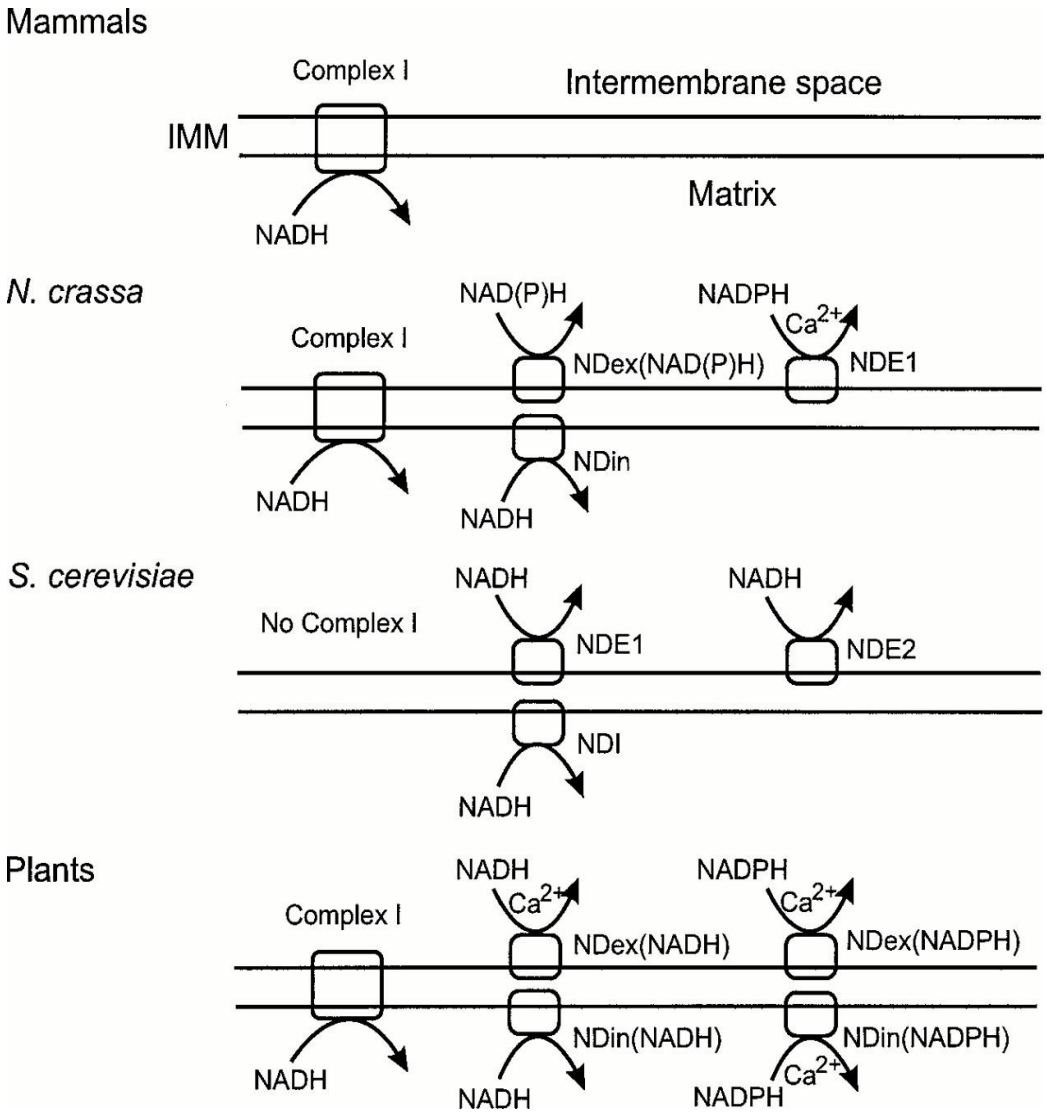

Figure 1.4 NAD(P)H dehydrogenases in the respiratory chain of mitochondria from mammals, *N. crassa*, *S. cerevisiae*, and plants (Moller 2001)

The NAD(P)H dehydrogenases of the alternative respiratory chain of mitochondria in mammals, *N. crassa, S. cerevisiae*, and plants.

NADH DH activity. In 1996 Menz and Day also purified a 43 kDa protein with NAD(P)H dehydrogenase activity in this soluble fraction of beetroot mitochondria. An antibody cross-linking experiment was done using an antibody raised to this protein, and located the 43kDa protein to the internal side of the inner membrane. This antibody also reacted with a protein in potato tuber and soybean mitochondria (Menz *et al.* 1996b). Using size exclusion chromatography, the 43 kDa protein was determined to be an 86 kDa dimer, in its native form. This study elucidated that there were two separate enzymes from NADH and NADPH oxidation as the protein was only capable of inhibition rotenone-insensitive NADH-specific oxidation.

1.4.2.1 Activators

Soole *et al.* (1990) have indicated that internal NADH dehydrogenase in plants are specific for NADH and are not reliant on calcium. On the other hand, in contrast to this, Moller (2001) provided evidence that the internal NAD(P)H dehydrogenase has a moderately high affinity for NADPH and is calcium specific. For the external NAD(P)H dehydrogenases, these are stimulated by calcium, indicating external oxidation is dependent on calcium, and hence have a specific requirement for calcium (Zottini *et al.* 1993; Finnegan *et al.* 2004). The stimulation of NAD(P)H oxidation by calcium has been shown to affect the enzymes activity (Soole *et al.* 1990).

1.4.2.2 Inhibitors

Currently for both internal and external NAD(P)H dehydrogenases there is no biological/ cellular function allocated to genes. The use of inhibitors is helpful in allocating function to protein, but unfortunately there is a lack of specific inhibitors for this enzyme family. External NAD(P)H dehydrogenases are inhibited by calcium chelators such as EGTA, EDTA and citrate. The effect with EGTA is more noticeable when mitochondria are incubated with EGTA before the addition of NAD(P)H, indicating that once activated, the calcium is tightly bound and therefore unavailable to EGTA or other chelators (Moller *et*

al. 1981). Inhibition of the external NAD(P)H dehydrogenases was also shown with sulhydryl reagents, although NADPH oxidation is inhibited to a greater extent that NADH oxidation with the same inhibitor concentration (Nash *et al.* 1983a). Dipenyleneiodonium (DPI) is a potent inhibitor of internal NAD(P)H dehydrogenases, and the use of the differential response to this inhibitor suggested that internal NAD(P)H dehydrogenase activity was facilitated by two separate enzymes. DPI also inhibits external NAD(P)H-dependent oxygen uptake, with inhibition at much lower concentrations for NADPH, compared to NADH (Melo *et al.* 1996). Flavone platanetin (Roberts *et al.* 1995), and dicumarol (Rasmusson *et al.* 1991) also have shown potential as NAD(P)H dehydrogenase inhibitors, but none of these specify either NADH or NADPH when inhibiting.

1.5 Alternative Oxidase

Alternative oxidase (AOX) is the sole component of the “alternative” electron transport pathway that accepts electrons from the UQ pool and it is tightly associated with the inner mitochondrial membrane (Dizengremel 1983; Siedow *et al.* 1992). AOX directly catalyses the two-electron oxidation of UQH_2 and the four electron reduction of oxygen to water (Moore *et al.* 1991). AOX is a non-proton pumping enzyme and hence the energy instead of adding to the proton motive force, is released as heat. This is why AOX is often associated with thermogenic plants. AOX in *A. thaliana* is encoded by a five member gene family with each gene displaying different spatial expression patterns (Thirkettle-Watts *et al.* 2003).

1.5.1. Identification of AOX

Alternative respiratory pathways were first noticed by scientists in specialised flowers due to their thermogenic metabolism, which was first reported in 1778 (Meeuse *et al.* 1969). It was Herk in 1938, who discovered this burst in respiratory pathway was due to a pathway other than the cytochrome

pathway (Finnegan *et al.* 2004). It was latter observed that mitochondrial respiration on D-day flowers was “uncoupled” and not associated with forming a proton gradient (Wilson *et al.* 1971). This observation was due to the presence of the alternative oxidase enzyme (AOX). Elthon *et al.* (1989) confirmed the observation of AOX protein in D-Day flowers, the cytochrome pathway decreased, and AOX increased. Since it was discovered, AOX has been identified in many plants, fungi, yeasts and several protozoans (Chaudhuri *et al.* 1998; Joseph-Horne *et al.* 2000). Recently AOX has been found in all kingdoms of life except the Archaebacteria (McDonald 2009).

1.5.2. Biochemistry

AOX is a quinol-oxygen oxidoereductase and does not pump protons, the oxygenase transfers electrons from ubiquinone to oxygen and generates water, and hence four electrons must be transferred to oxygen. AOX has the ability to reduce oxygen to water, which indicates the presence of a transition metal at the centre of its active site. Minagawa *et al.* (1990) have indicated that AOX requires iron. To confirm that AOX requires iron, Fe^{2+} was removed from the growth medium of a yeast culture, which resulted in the production of an inactive AOX protein. As well as biochemical approaches to confirm that iron was involved in AOX catalysis, gene sequence information was examined. Using sequence homology (Siedow *et al.* 1995) proposed a model that the AOX active site was predicted to be a four-helix bundle located in the C-terminal portion of the oxidase, as does other enzymes that bind iron. Recently using plant AOX expressed in *E. coli*, an EPR signal associated with AOX has confirmed the di-iron centre model (Berthold *et al.* 2002). The functional form of the enzyme is a dimer, with two polypeptides either covalently or non-covalently bound to each other. Since the this model was proposed (Siedow *et al.* 1995), another model has been proposed (Andersson *et al.* 1999), that like the (Siedow *et al.* 1995) model, postulates that the iron binding involves two antiparallel helix pairs combining to form a four helix bundle. To achieve the structure allowing for changes, the E-X-X-H motif (where iron binds) located in the intermembrane space in the

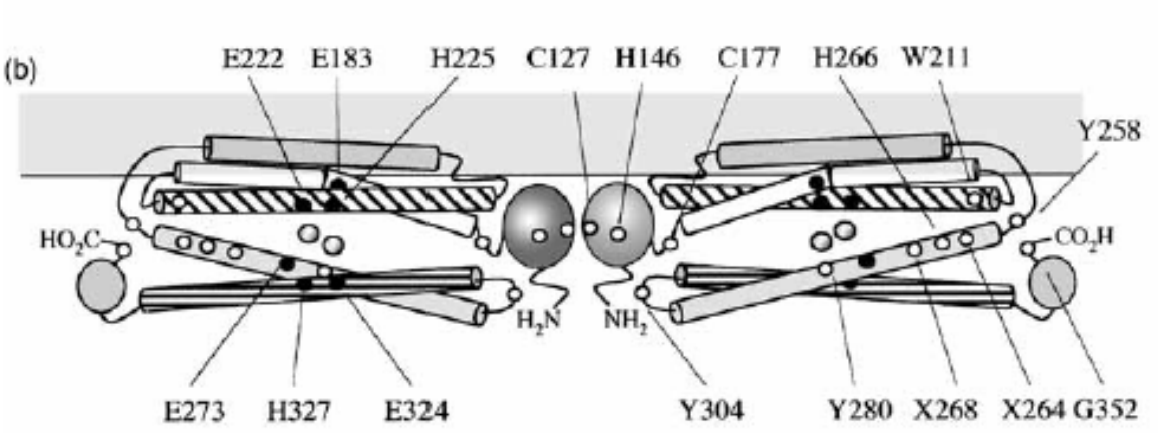

Figure 1.5 The evolution of AOX structural Models (Finnegan *et al.* 2004)
Structural model of Andersson and Nordlund (1999). Proposed helical regions are shown as boxes. The unmodelled N- and C-terminal regions are depicted as ovals. Residues postulated to be involved in iron binding are shown by filled circles, with the positions specified in the left-hand subunit. The relative positions of other key residues mentioned in the text are indicated as open circles, with the positions specified in the right-hand subunit. Numbering is according to the AtAOX1a primary translation product. The drawings are not to scale.

Siedow et al. (1995) model had to be relocated to the matrix. The final model is presented in Figure 1.5 (Finnegan et al. 2004).

1.5.3. Physiological function

The heat generation of AOX activity in the thermogenic physiology of Aroid and other flowers was the first recognised function of AOX (Meeuse 1975). As well as AOX having a role in thermogenisis, it also found to be active during chilling stress as detected by microcalorimetry (Ordentlich *et al.* 1991). Confirming that AOX may play a role in chilling stress, arctic plants have been investigated, and found to have a higher level of alternative pathway activity than temperate species (McNulty *et al.* 1987).

AOX may also work as a bypass to oxidise NADH ad $FADH_2$ under conditions when ADP is a limiting factor. This allows for the glycolysis and citric acid cycle to continue functioning and provide the cell with biosynthetic precursors needed for other reactions.

Although plant mitochondria normally produce ROS, excessive ROS can have devastating effects, by directly inhibiting enzymes and damaging DNA, as well as causing the formation of lipid peroxidises from membrane lipids, causing loss of membrane integrity (Fridovich 1978). It has been suggested that the alternative pathway might also play a function in the reduction state of the UQ pool, by preventing or minimising ROS production (Chapter 5).

1.6 Relationship Between AOX and Alternative NAD(P)H dehydrogenases

Clifton *et al.* (2005) have suggested that there may be a link between the AOX and the alternative NAD(P)H dehydrogenases, in creating their own alternative electron transport chain. Neither the NAD(P)H dehydrogenases or AOX contribute to proton pumping or ATP synthesis and hence bypass

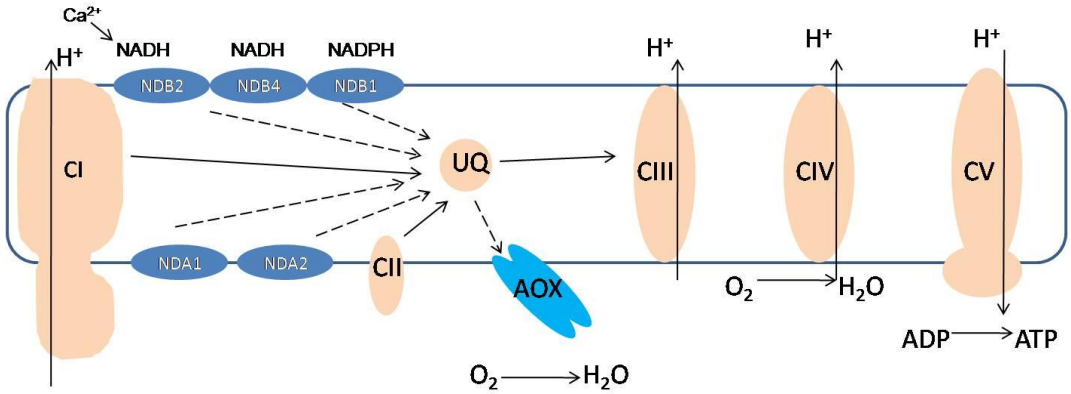

Figure 1.6 Diagrammatic representation of the plant mitochondrial electron transport chain (Clifton *et al.* 2005)

The multi subunit complexes I, II, III and IV and cytochrome c which comprise the cytochrome electron transport chain are shown in beige. The stress inducible alternative external NADH dehydrogenases (NDB) and alternative oxidase (AOX) are shown in blue. The flow of electrons is indicated by arrows with the proposed stress inducible pathway indicated by dotted lines. UQ = ubiquinone.

adenylate control and allow for respiration with flexible levels of energy conservation and respiration control (Figure 1.6)(Clifton *et al.* 2005). Although a linkage between AOX and NAD(P)H dehydrogenases is suggested, these genes display differences in response to the treatments applied, suggesting differential regulation occurs within the alternative gene family. Considine *et al.* (2002) have shown that AOX genes 1a-d in *A. thaliana* are induced by varying stress conditions, and relate to a need under a stress conditions. The AOX2 subfamily are not induced by stress, but display a constitutive or developmental expression, and hence are suggested to have a role in housekeeping in respiratory metabolism.

Co-expression of AOX and NDH has been observed, such as for *Aox1a* and *ndb2* (Clifton *et al.* 2005). This co-regulation may be due to the presence of common sequence elements in their promoters. Due to this co-expression, it has been suggested by Clifton *et al.* (2005) that the products of AOX and NDB2, a terminal oxidase and an external NAD(P)H dehydrogenase, are capable of forming a simple but functional alternative respiratory chain (Figure 1.6). This respiratory chain allows oxidation of cytosolic NAD(P)H in a manner uncoupled from oxidative phosphorylation. This self-contained pathway may be useful in helping maintain redox balance of the cell and turnover of carbon pathways.

1.7 Post genome analysis of the Alternative pathway enzymes

1.7.1. A. thaliana NAD(P)H Dehydrogenases

1.7.1.1 Sequence identification

After initial experiments to purify the alternative NAD(P)H dehydrogenases (Section 1.4.2), more recent work has been at the molecular level using a genome-based approach to identify the gene products and thus proteins responsible for these activities. The genes responsible for both internal and external NAD(P)H oxidation are nuclear in origin (Rayner *et al.* 1983). It was in *Escherichia coli* and *S. cerevisiae* that the alternative NAD(P)H

dehydrogenases were first identified at sequence level (Finnegan *et al.* 2004).

Rasmusson *et al.* (1991) discovered the initial sequence information about plant alternative NAD(P)H dehydrogenases, Rasmusson *et al.* (1999) screened a potato leaf cDNA library with a probe whose sequence similar to NDI from *E. Coli* and discovered two sequence with NADH DH-like features, these were named *St-nda* and *St-ndb*. From mitochondrial import experiments, Rasmusson *et al.* (1999) deduced St-NDA , which was 55 kDa in size, was oriented towards the internal face of the inner mitochondrial membrane, and that St-NDB, 60 kDa in size imbedded in the external face, where they face the inner mitochondrial membrane.

Moore *et al.* (2003) used sequence homology with *S. cerevisiae,* which is known to have at least three non-phosphorylating NAD(P)H dehydrogenases; ScNDE1, ScNDE2 and ScNDI1. The genome sequence database of *A. thaliana,* was blasted with these sequences to help identify *A, thaliana* genes. This approach identified seven putative NAD(P)H dehydrogenases (Table 1.1). Michalecka *et al.* (2003), used a similar strategy and grouped the *A. thaliana* NAD(P)H dehydrogenases based on their similarities to the potato homologs, so that putative internal dehydrogenases were termed NDA, and putative external dehydrogenases were termed NDB. These protein sequences of *A. thaliana* were aligned with the three yeast sequences ScNDE1, ScNDE2 and ScNDI1 and with two potato sequences StNDB and StNDA. An alignment of the internal NAD(P)H dehydrogenase sequences can be seen in Figure1.7.

These NAD(P)H dehydrogenase sequences have been separated into groups based on functional features in their sequences (Moore *et al.* 2003). There are two *A. thaliana* genes that when translated, show closer homology to *S. cerevisiae* internal NAD(P)H DH enzyme ScNDI1 and two that have closer homology to the external NAD(P)H DH enzymes ScNDE1 and ScNDE2 (Figure 1.8). The internal DH *A. thaliana* proteins are shorter than the external DH proteins. Also a difference between the internal and external

Table 1.1 Summary of the *A. thaliana* alternative NAD(P)H dehydrogenases

Gene nomenclature is taken from Mickalecka *et al.* (2003). Where the nda refers to genes encoding an internal NAD(P)H dehydrogenase, and ndb refers to genes encoding an external NAD(P)H dehydrogenase as confirmed Elhafez *et al.* (2006). Each of the *A. thaliana* (AT) NAD(P)H dehydrogenases were assigned a number based on order of identification. Expression is based on Elhafez *et al.* (2006) from Quantitative RT-PCR where tissue with most abundant expression for each gene is identified.

Gene	Locus	Accession No.	Protein Length	Expression
nda1	At1g07180	NM_100592[b]	510	Cotyldeons
nda2	At2g29990	AC004680[c]	508	Coyledons/Flowers
ndb1	At4g28220	NM_118962[b]	571	Buds
ndb2	At4g05020	AY039856[b]	582	Root
ndb3	At4g21490	AL161555[c]	581	Roots
ndb4	At2g20800	AC006234[c]	582	Roots
ndc1	At5g08740	NM_120955[b]	519	Flowers

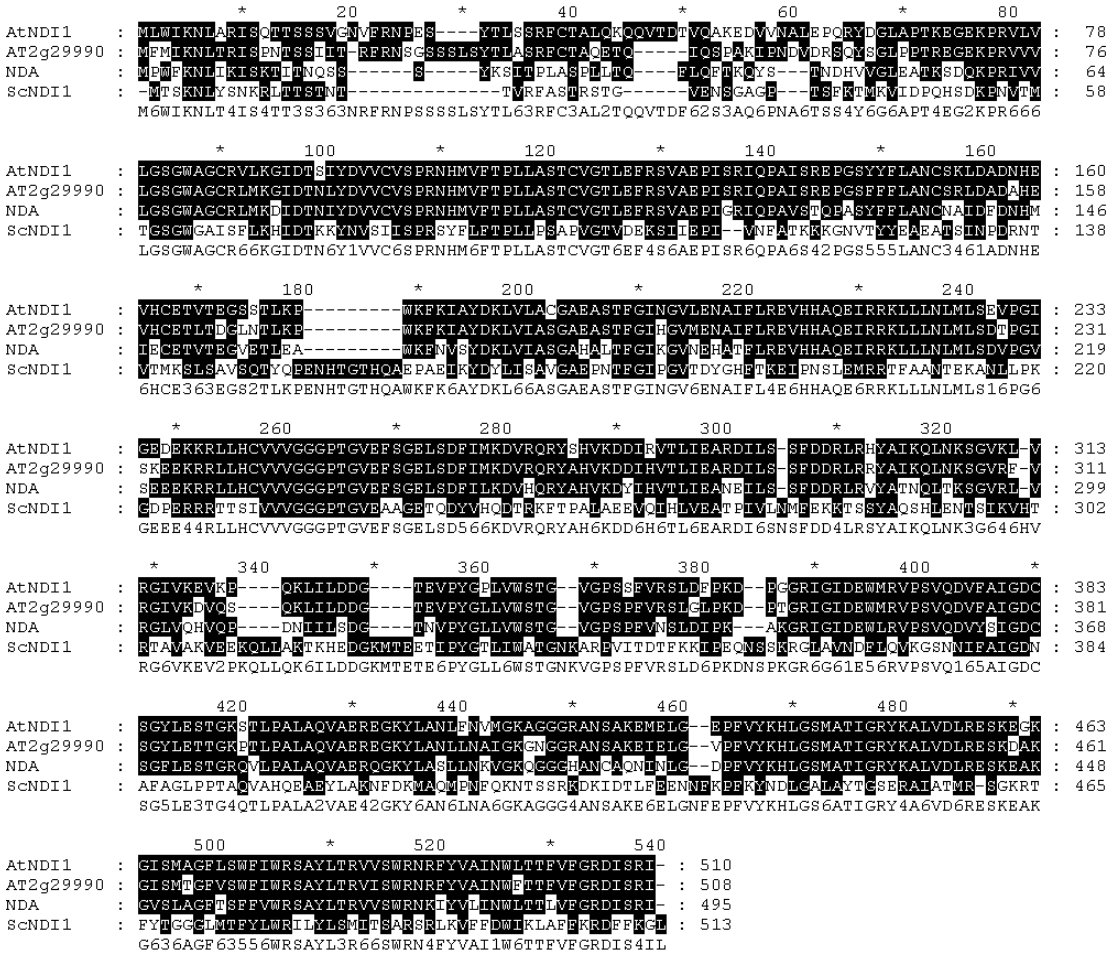

Figure 1.7 An alignment of internal NAD(P)H dehydrogenase amino acid sequences (Finnegan *et al.* 2004)

The sequences from S. cerevisiae (ScNDI1, accession X61590), potato (NDA, accession AJ245861), and *A. thaliana* (AT1g07180, accession AC067971; AT2g29990, accession AC004680) proteins were aligned using ClustalW. Regions of high homology (75% or more) are boxed in black. Dashes represent gaps in the sequence introduced to optimize the alignment.

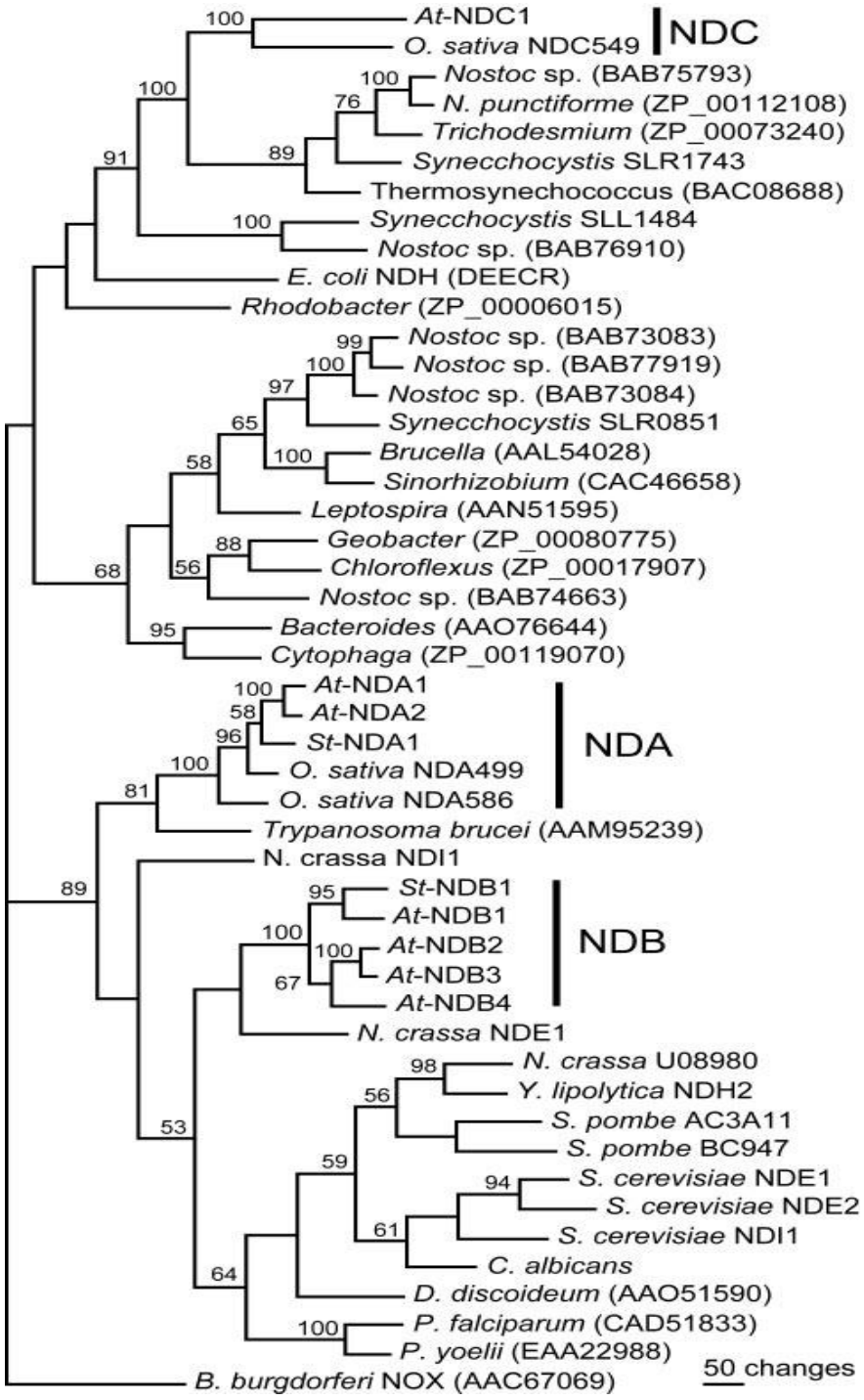

Figure 1.8 Phylogenetic analysis of bacterial, plant, fungal, and protest NAD(P)H dehydrogenase-like protein sequences

Sequences were aligned using ClustalW in MacVector 7.1 software (Accelrys Inc., San Diego). Alignments were manually inspected and edited, assuring correct matches of conserved regions (Michalecka *et al.* 2003).

is that the internal DH proteins have a higher degree of homology with an average of 74% identity, with the external proteins having an average identity of only 58% (Moore *et al.* 2003). The nomenclature for these alternativedehydrogenases changed for the internal dehydrogenases from NDI to what they are now referred to as NDA's and the external dehydrogenases from NDE's to NDB, and the third group known as NDC (Elthon *et al.* 1989). As well as the putative internal NDA and putative external NDB groups Michalecka *et al.* (2003) indicated that there may be a third group of NAD(P)H dehydrogenases with one gene and named NDC. These *A. thaliana* NDI and NDE sequences contain two dinucleotide fold motifs, as does the potato sequence. Of the four NDE three of them contain an insert, hence why the internal genes are shorter. These inserts contain a Ca^{2+} binding EF hand motif which is also found in potato NDB1 (Michalecka *et al.* 2003) (Figure 1.9). This EF hand motif is not found in the internal dehydrogenase sequences.

Recently it has also been discovered that several of the alternative DHs proteins are dual targeted not only to the mitochondria but also to the peroxisomes. There have been reports of over 30 proteins in plants which are dual targeted to the mitochondria and chloroplasts (Millar *et al.* 2006). For the internal dehydrogenases one of these NDC1 is targeted to both the mitochondria and the chloroplast. Three other proteins, the remaining two internal proteins (NDA1 and NDA2) as well as one external protein (NDB1) were found to be dual targeted between the mitochondria and the peroxisome. The remaining proteins did not display peroxisomal targeting (Carrie *et al.* 2008).

1.7.1.2 Internal NAD(P)H dehydrogenases

Internal NAD(P)H dehydrogenases in *A. thaliana* had their sequences identified by (Moore *et al.* 2003) based on homologous sequences with yeast. Using a t-DNA insertion mutation line the expression of an internal NAD(P)H dehydrogenase (AT1g07180) was disrupted. QRT-PCR on

Figure 1.9 Amino acid sequence denoting comparison of EF-hand motif of external NAD(P)H dehydrogenases from various species (Michalecka *et al.* 2003)

The EF hand motif in *A. thaliana* NDB proteins (NDB2, NDB3, NDB4, NDB1) Potato NDB1 (StNDB1), *Plasmodium falciparum* (Pf), *Plasmodium yoelli* (Py), Neurospora crassa (NcNDE1), and *Gallus gallus* troponin C (Trop-C). The known potato EF hand motif (*) is conserved amongst *A. thaliana* NDB sequences except for two position in NDB4. The two *plasmodium* sequences contain no EF hand motifs.

transcripts indicated this gene had been completely silenced but the highly homologous gene (AT2g9990) was still transcribed (Moore *et al.* 2003). When mitochondrial activities were done on this mutant there was loss of matrix NAD(P)H activity. A protein import experiment indicated this internal NAD(P)H dehydrogenase named AtNDI had a molecular weight of approximately 56 kDa (Moore *et al.* 2003). Expression profiles of internal NAD(P)H dehydrogenase genes has indicated that *nda1* and *ndc1* respond to light (Michalecka *et al.* 2003; Escobar *et al.* 2004; Elhafez *et al.* 2006). An examination of tissue specific expression has indicated that nda1 expression is absent from the roots, but that *nda2* and *ndc1* are expressed in most plant tissues (Michalecka *et al.* 2003).

1.7.1.3 External NAD(P)H dehydrogenases

There had been no published data on knockouts or t-DNA inserts in the external dehydrogenase family, at the start of this research project presented in this thesis. Tissue specific expression had been examined for the external dehydrogenases and it was found from mRNA transcripts of *A. thaliana* ndb genes, that *ndb1* was expressed mostly in the buds, *ndb2,3 & 4* in the roots*, nda1* were expressed in the cotyledons, *nda2* in the cotyledons and flowers and *ndc1* in the flowers. However *ndb3* and *ndb4* mRNAs were mostly absent in leaves and *ndb4* transcript was absent in the stems, indicating there is potential for spatial regulation of these genes at the transcript level (Michalecka *et al.* 2003).

1.8 *A. thaliana* Alternative Oxidase

The AOX antibody has proven useful for detecting AOX from many plants and other organisms, including numerous fungi, *Trypanasoma brucei* (Chaudhuri *et al.* 1998), *Acanthamoeba castellanii* and *Dictyostelium discoideum* (Jarmuszkiewicz *et al.* 2002). The AOX antibody detects either one or a few proteins at 35–37 kDa. AOX has the potential to be detected

immunologically in many species there is a highly conserved binding site on the denatured AOX protein, within the sequence R321-A-D-E-A-H-H-RD-V-N-H332 of the *A. thaliana* AOX1a (AtAOX1a) protein (Finnegan *et al.* 2004). The AOX antibody led to the isolation of the *Sauromatum guttatum* SgAox1 cDNA that encodes a 39 kDa protein (Rhoads *et al.* 1991). Since this there have been AOX cDNAs sequences isolated from many species including 28 Animal species (McDonald 2009).

First discovered in soybean (Whelan *et al.* 1996), AOX multi-gene families have also been reported in tobacco (Whelan *et al.* 1996), *A. thaliana* (Saisho *et al.* 1997), rice (Ito *et al.* 1997), mango (Considine *et al.* 2001), maize (Karpova *et al.* 2002) and tomato (Holtzapffel *et al.* 2003). The existence of multiple AOX genes explained why multiple bands have been visualised on immunoblots when using the AOX antibody. Commonly, each gene family member has a specific tissue and developmental stage-dependant expression pattern (Finnegan *et al.* 1997; Ito *et al.* 1997; Saisho *et al.* 1997; McCabe *et al.* 1998; Karpova *et al.* 2002; Holtzapffel *et al.* 2003; Thirkettle-Watts *et al.* 2003). This differential specific expression and tissue patterns for expression of the various AOX genes, may also explain the multiple gene family found.

1.8.1. Physiological Significance of the alternative pathway

Although external NAD(P)H oxidation has been known for quite some time, its physiological importance has yet to be determined (Rasmusson *et al.* 2004). Even for the most studied system, the red beet root, the physiological relevance is not known. However, there are currently many hypotheses for the role that these NAD(P)H dehydrogenases may play in plants.

1.8.1.1 Thermogenesis

The plant *Arum maculatum*, has a thermogenic respiratory burst, where

external NADH oxidation increases along with AOX activity (Leach *et al.* 1996). A closer measurement of the NAD(P)H dehydrogenases indicated that internal NADPH oxidation and external NAD(P)H oxidation increased concomitantly with AOX, but internal NADH remained high during the post thermogenic phase (Finnegan *et al.* 2004). The heat generated during this respiratory burst is for the purpose of pollination and floral development.

1.8.1.2 Turnover of matrix $NADP^+$ and its link to AOX capacity.

Moller *et al.* (1998) and (Agius *et al.* 2001) have determined that $NADP^+$ is present at lower levels in the matrix than $NAD^{+,}$ thus there is need for the capacity to turnover NADPH in the plant mitochondrial matrix. The NAD(P)H/NADP ratio could play a role in the suggested AOX activation thus the presence and activity of the NADPH dehydrogenase will potentially influence AOX capacity. The level of matrix or internal NADPH will depend on the relative NAD(P)H DH dehydrogenase activity which in turn may be regulated by matrix/internal calcium levels, as the protein is suspected to be dependent on calcium (Moller *et al.* 1998).

1.8.1.3 Stress Adaptation

Plants are often put under various stresses, depending on growth conditions, and environmental conditions, such as cold, heat, too much salt and phosphorus. Reactive oxygen species (ROS) are often produced in the mitochondria. This ROS production occurs when oxygen interacts with the reduced form of the electron transport components such as flavones and ubiquinone. Accumulation of ROS in plants will clearly result in a wide variety of deleterious effects through oxidation reactions involving proteins, lipids and nucleic acids (Taylor *et al.* 2002). Alternative NAD(P)H dehydrogenases are flavoproteins, and along with ubiquinone are potential sites of ROS production.

It has been observed that external NADH oxidation only, i.e. not NADPH

oxidation increases during long term chilling stress, such as after storing beetroot tubers at 4^{o}C for 10 weeks (Fredlund *et al.* 1991a). On the contrary external NAD(P)H oxidation did not change in potato leaf mitochondria which were exposed to chilling stress of 2-6 days, but the internal NADH oxidation decreased, as did *Stnda* transcript levels (Svensson *et al.* 2002). It has been suggested that Internal NAD(P)H oxidation decreases due to the ROS production produced during chilling stress to further minimize ROS production.

1.8.1.4 Photosynthetic Metabolism

Svensson *et al.* (2001) have suggested that internal NADH oxidation decreases in the absence of light and increases through leaf growth, suggesting a role for internal NADH oxidation in photosynthesis. It is suggested that the external NADH dehydrogenases operate with alternative oxidase to oxidise excess NADH that is produced under photosynthesis and bypass ATP synthesis, and this allows for continued flux occurring through the photorespiratory cycle (Rasmusson *et al.* 2004).

1.8.1.5 Maintaining Redox Balance

Although the function of these alternative NAD(P)H dehydrogenases is unclear, other roles may be linked to maintaining the redox balance as these dehydrogenase can compensate for when the ETC is compromised. (Zhang *et al.* 1996) confirmed this by showing that external NADH and internal NADH oxidation rates are increased when Complex I is compromised by various inhibitors. There have been instances where mutants have shown increased external NADH oxidation, i.e. in Complex 1 mutants from *Nicotiana sylvestri*s indicate a role of these dehydrogenases in maintaining the redox balance of the cell (Gutierres *et al.* 1997). There has also been observed dramatic increases in external NAD(P)H dehydrogenase activity in an *nda1* T-DNA insertion line of *A. thaliana*. This could be suggesting that this enzyme is acting as a compensatory mechanism with matrix-reducing equivalents

being exported via a malate/oxaloacetate shuttle (Day *et al.* 1981; Moore *et al.* 2003). It has been postulated that the alternative pathway for NAD(P)H oxidation only operates when complex I and the phosphorylating pathway is compromised or saturated. Thus, the non-phosphoryalting pathway would become active and cycle to remove excess NAD(P)H both matrix and/or cytosolic. It is now thought that both may act at the same time with electrons passing through both pathways and thus a better understanding of what regulates electron flux through complex I and the non-phosphorylating dehydrogenases is needed.

1.9 ROS signaling

Plants contain a branched respiratory network containing antioxidant enzymes, antioxidants and enzymes capable of producing ROS. This system is said to be responsible for maintaining and tightly regulating ROS levels (Gechev *et al.* 2006). As well as causing cellular damage, ROS have been suggested to function as signalling molecules which are able to coordinate a range of plant processes (Apel *et al.* 2004; Gechev *et al.* 2006). Some of these plant processes, which ROS could coordinate, are growth and development, stress adaptation or programmed cell death. The oxidised products of ROS damage can also be important secondary signalling molecules (Rinalducci *et al.* 2008). This has lead to a concept of oxidative signalling, rather than oxidate stress. As plants can use ROS as a signalling pathway it suggests that over evolution, plants were able to control ROS toxicity and now use ROS as signalling molecules for more specialised process. (Vanlerberghe *et al.* 2002) have suggested that AOX plays a role in the cell signalling pathway generated by ROS which can lead to cell death. It is thought AOX plays a role in mitochondrial-generated ROS levels, which impacts on the cellular level of anti-oxidant defences resulting from signalling.

1.10 Aims

Moller (2001) provided evidence that the internal NAD(P)H dehydrogenase was allegedly calcium dependent, but none of the internal dehydrogenases or NDC have the EF-hand motif, suggesting the possibility of one of the external dehydrogenases moving internally. Hence further work is needed to confirm the calcium dependence of these dehydrogenases and confirm previous experiments. The other dehydrogenase with speculation is NDC, as experiments indicated it was imported to the matrix but spans the membrane as determined by proteolytic digestion (Elhafez *et al.* 2006), leaving the question open as to which side of the membrane does its active site face? Does it have internal or external NAD(P)H DH activity?

Since sequence information has become available there has also been questions raised to the mis-match between the purified protein sizes for these activities and the predicted sizes for the protein. It is hoped that these questions can be answered by using RNAi knockdown plants and western blots to confirm protein sizes, as have previously been determined, Hence there is still a lot to be determined about these dehydrogenases and it is thought that a transgenic approach towards altering the expression of all these NAD(P)H DH genes may help to resolve these issues.

The overall aims of this work is to help to further understand the role of these alternative dehydrogenases by focusing on the external dehydrogenases and specifically *ndb4*, as little work has been done on this gene. Then to help understand the role between these dehydrogenases and AOX and its response to abiotic stress and specifically salinity stress as little is known about salinity stress and the relationship with AOX and the non-phosphorylating pathway.

To do this I have taken a transgenic approach, which could use either T-DNA lines or RNAi knockdown. I have chosen to use RNAi knockdown lines for this work as it allows to specifically target one individual gene family member

or multiple at the same time. T-DNA lines do not offer this, and further, RNAi often does not result in complete elimination of gene expression and this may be important in genes that are critical for growth and development. This may be why there are few T-DNA lines available for the NAD(P)H dehydrogenase genes.

2 MATERIALS AND METHODS

2.1 Materials

All reagents used were obtained from SIGMA unless otherwise stated. In all molecular techniques, autoclaved HPLC grade water was used. The *A. thaliana* over-expressing *Aox1a* lines were a kind gift from Prof Jim Siedow and Dr Ann Umbach (Developmental, Cell, and Molecular Biology Group, Biology Department, Duke University, Durham, North Carolina). pHellsgate 12 vector was made available from the CSIRO (Wesley *et al.* 2001)

2.2 Plant Growth

A. thaliana ecotype Columbia-0 was used as *A. thaliana* Wt tissue samples. All *A. thaliana* lines were germinated in a Sanyo Versatile Environmental Test Chamber (14 hour light, 10 hour dark cycles, light intensity 100 uE m^{-2} s^{-1}, 23°C). Plants were either grown in soil or in hydroponics. Soil grown plants were grown in a specialised soil mix, CocoMix 3 (Appendix A.5), in an enclosed greenhouse (light intensity 150 uE m^{-2} s^{-1}, 25ºC) and day/night cycles subject to the seasonal variability of the day. Otherwise, plants were grown hydroponically in half complete strength Hoagland's solution (Appendix A.5) in an enclosed greenhouse (light intensity 150 uE m^{-2} s^{-1}, 25ºC) and day/night cycles subject to the seasonal variability of the day. Hydroponic setup was aerated using a Regent Air Pump 6500 set to low speed. Seeds were germinated in preset 0.7 % (w/v) agar bullets containing ½ complete strength Hoagland's solution for plants that were to be grown hydroponically. Agar was poured into sterile 1.5 ml centrifuge tubes and inverted with the lid closed until set. The base of the tube was removed with a sterile blade and stored at 4ºC until required. Seeds were placed in the agar bullet and placed into a rack containing half strength complete Hoagland's solution. The racks were contained in a sealed bag and placed in

Sanyo Versatile Environmental Test Chamber (14 hour light, 10 hour dark cycles, light intensity 100 uE m^{-2} s^{-1}, 23ºC) for 14 days to germinate and grow, after which they were transferred to the hydroponic growth apparatus.

2.3 Bioinformatics and Sequence Analysis

A. thaliana type II alternative NADH dehydrogenase DNA sequences, as well as alternative oxidase sequences used in this study were obtained from the Munich Information Centre for Protein Sequences (MIPS) *A. thaliana* database (Initiative 2000; Schoof *et al.* 2002). The confirmed 5′ and 3′ UTR sequence of all alternative dehydrogenases as well as alternative oxidase were obtained from the National Centre for Biotechnology Information (NCBI) nucleotide sequence database GenBank and these sequences were used throughout this study. The Bioinformatics analysis tool BioManager provided by the Australian National Genomic Information Service (ANGIS) was used to perform all sequence and bioinformatics analysis. The ClustalW (accurate) program (Thompson *et al.* 1994) was used for nucleotide sequence alignments among the type II alternative NADH dehydrogenase family using the default parameters.

2.4 DNA Extraction

DNA extraction was performed according to Meyerowitz method (Chuang *et al.* 2000). Leaf tissue was ground into a fine powder in a 1.5 ml centrifuge tube under liquid nitrogen using a plastic applicator. Tubes remained in liquid nitrogen until required in order to preserve the DNA. Extraction buffer (Appendix A.7), 500µl, was added to each tube and vortexed thoroughly. The homogenate was then mixed with 35 µl of 20 % (w/v) SDS and the tube inverted before being incubated at 65°C for five minutes (Solid State Control Three Block Capacity Dry Block Heater, Ratek Instruments, Australia). The homogenate was then mixed with 130 µl of 5 M KOAc, not pH adjusted

before being inverted and incubated on ice for five minutes and centrifuged at 15,000 g for ten minutes (Eppendorf 5415c centrifuge, Crown Scientific, Minto, NSW, Australia). The supernatant was transferred to a sterile 1.5 ml centrifuge tube and mixed with 640 µl of Isopropyl alcohol and 60 µl 3 M NaOAc not pH adjusted and inverted. The solution was then incubated at -20°C for ten minutes and centrifuged at 15,000 g for ten minutes (Eppendorf 5415c centrifuge, Crown Scientific, Minto, NSW, Australia). The supernatant was discarded and the resultant pellet washed with 300 µl 70 % (v/v) ethanol. The tube was then centrifuged for five minutes at 15,000 g. Ethanol was discarded and the pellet left to air dry removing any residual ethanol in a closed fume hood. The pellet was resuspended in 50 µl HPLC grade water and treated with 20 µl/ml (final) RNase as required. Samples were separated by gel electrophoresis on a 1 % (w/v) agarose gel to confirm presence of DNA.

2.5 RNA Extraction

RNA extraction protocol (Chomczynski *et al.* 1987; Chomczynski *et al.* 2006) was modified to the following. Approximately 1 g of *A. thaliana* leaf tissue was ground using a liquid nitrogen cooled mortar and pestle into a fine powder. Tissue was then placed in an ice cold, sterile 50ml falcon tube containing 10 ml GTC buffer (Appendix A.7). The solution was vortexed and then the homogenate was passed twice through a sterile 21 gauge Livingstone disposable syringe until well homogenized. 0.1 volumes of 2 M NaAc pH 4.0 was added and vortex briefly. Equal volumes of Phenol:Chloroform:Isoamyl Alcohol (25:24:1) pH 4 was added to the solution and vortexed for ten seconds before being incubated on ice for fifteen minutes, inverting every five minutes. Solution was then centrifuged at 4,500 g for thirty minutes at 4°C. Once spun, the tube was left to settle and the top layer of the solution was transferred into a sterile 50ml falcon tube with an equal volume of iso-propanol. Tube was stored overnight at -20°C to enable RNA precipitation. Once precipitated the tube is centrifuged at 6,000 g for

thirty minutes at 4°C. The resultant pellet was then washed twice in 75 % (v/v) ethanol and centrifuge at 4,500 g for five minutes at 4°C. The pellet was then left to dry at room temperature before resuspending in 100 µl of HPLC grade water and stored at -80°C. Concentration of extracted RNA was determined spectrophotometrically (GeneQuant II, Pharmacia Biotech, St. Albans, Hertfordshire, UK) via the equation:

RNA(ng/µl) = Average absorbance at 260 nm (measured in triplicate) x Dilution factor x 40 ng/µl.

2.6 DNase Treatment of RNA

Extracted RNA was treated with 10x reaction buffer and 4 % (v/v) RQI RNase free DNase and incubated at 37°C for thirty minutes (Solid State Control Three Block Capacity Dry Block Heater, Ratek Instruments, Australia).

2.7 Cleanup of DNAse Treated RNA

An equal volume of Phenol:Chloroform:Isoamyl alcohol (25:24:1) (Sigma) was added to the extracted RNA solution and spun at 10,000 g for five minutes (Eppendorf 5415c centrifuge, Crown Scientific, Minto, NSW, Australia). The top layer of the solution was removed and placed in a sterile centrifuge tube with 1/10 volumes of 3 M sodium acetate pH 4 added. Two volumes of 99 % (v/v) molecular grade ethanol were added to the tube before inverting and centrifuging at 8,000 g for fifteen minutes (Eppendorf 5415c centrifuge, Crown Scientific, Minto, NSW, Australia). The supernatant was then removed and the resultant pellet resuspended in two washes of 70 % (v/v) ethanol. Pellet was allowed to air dry and resuspended in 100 µl of HPLC grade water. Samples were separated on a 1 % (w/v) agarose gel to confirm presence of RNA.

2.8 Reverse Transcription PCR

Extracted RNA was reversed transcribed using Stratascript Reverse transcriptase (Stratagene) and $Oligo_{dt}$ primer (15) (Invitrogen, USA) as per manufacturers protocol. The Reverse Transcription cycle consisted of; 65°C for five minutes, 22°C for ten minutes, 42°C for one hour, 70°C for fifteen minutes in a thermocycler (GeneAmp® PCR System Applied BioSystems, Carlsbad, California, USA).

2.9 Primers

All primers used were supplied by GeneWorks Pty Ltd (Aust.). The melting temperature, T_m, for each primer was calculated as per the formula:

$T_m = 64.9°C + 41°C \times (GC\ content – 16.4)/N\ (\#\ bp)$

All primer sequences used and their respective T_m are shown in Table 2.1. The underlined bp within each primer sequence represents the sequences corresponding to the restriction site as specified by the primer name.. The bases flanking the restriction site are required for efficient cutting of the RE of the PCR product ready for cloning. The Bold regions are the attB regions required for gateway cloning

2.10 Polymerase Chain Reaction (PCR)

All PCR reactions were conducted in a GeneAmp® PCR System 2400 thermocycler (Applied BioSystems, Carlsbad, California, USA). Volumes of PCR reaction varied from 25 µl-50 µl in 0.2 ml clear dome cap tubes (Scientific Specialities Inc, USA). Promega reagents were used unless otherwise stated. A standard PCR reaction (50 µl) contained; One x PCR Buffer, 1 unit Taq DNA Polymerase, 50ng/µl forward and reverse primers (GeneWorks), 2 mM $MgCl_2$, varying concentration of template DNA and HPLC molecular grade water (Sigma). The standard PCR cycle consisted of;

94°C for three minutes, 30 cycles of 94°C for thirty seconds, T_A for thirty seconds, 72°C for one minute; 72°C for ten minutes, 4°C to infinity. PCR reactions were separated by gel electrophoresis.

2.10.1. PCR Screen of transformed colonies

A single colony was picked with a sterile toothpick and swirled in 20 µl of TE buffer (10mM Tris-HCl, 1mM EDTA, pH 8.0). The same toothpick was then swirled in 10 ml of LB Media for inoculation and grown overnight at 37°C (for subsequent plasmid extraction). The tube with TE buffer and cells was boiled at 100°C for 5 mins. 2 µl was used as template for PCR screening (Section 2.10).

2.10.2. PCR Cleanup

PCR products were purified using the Wizard® Plus SV minipreps DNA Purification System (Promega, Madison, WI USA) as per the manufacturer's centrifugation protocol.

2.11 Agarose Gel Electrophoresis

Agarose gel electrophoresis was performed as described by Sambrook (Sambrook *et al.* 2001). Analytical grade Agarose (Promega, Madison, WI USA) was dissolved in 1x TAE buffer (Appendix A.6) to 1 % (w/v) as per volume of gel run. Solution was heated in a Sanyo Supershower Wave microwave to dissolve agarose powder. Once cool, 0.5 µl of 10 mg/ml ethidium bromide per 10 ml of TAE was added before being placed into the appropriate gel tray and left to set. Samples to be loaded were mixed with 6x loading dye (Promega, Madison, WI USA) in a 6:1 ratio as required. Gel systems used include the BioRad Mini-Sub Cell GT and the BioRad Wide Mini-Sub Cell (Bio-Rad, CA, USA). The power pack used was the BioRad

Power Pack 300 (Bio-Rad, CA, USA). Gels were viewed under ultra violet light on a BioRad Transilluminator and imaged using a BioRad DigiDoc (Bio-Rad, CA, USA), powered by a Canon® digital camera and the Canon® Utilities Zoom Browser Ex Version 5.5 Software (Tokyo, Japan).

2.12 Nucleic Acid Sequencing

Purified DNA samples were supplied as per facility requirements (Australian Genome Research Facility (Brisbane, Australia). Double stranded plasmids were supplied at between 400-1000 ng with 6.4 pmol of appropriate primer. The cycling conditions used to determine sequence information include; 96°C for one minute, 96°C for ten seconds, 50°C for five seconds, 60°C for four minutes, 10°C soak. Steps 2-4 were cycled thirty times. Samples were shipped overnight at room temperature to the Australian Genome Research facility.

2.13 Restriction Digest

Restriction digests were conducted as per the guidelines as recommended by Promgega (Promega, Madison, WI USA). DNA was digested by treating with a restriction endonuclease over a range of volumes from 10 µl-50 µl. Restriction enzymes (RE) used were supplied from Promega unless otherwise stated and used in conjunction with their compatible buffer. Concentrations of 1 unit per microgram DNA of RE were used in 10x RE buffer. A 10x volume of 1 mg/ml Bovine Serum Albumin (BSA) was also added to each digest reaction which was incubated at 37°C for 1–3 hours (Solid State Control Three Block Capacity Dry Block Heater, Ratek Instruments, Australia). RE used include; BamH1, Xho1, Kpn1, Not1 and Cla1.

2.13.1. Restriction Digest Cleanup

Digested plasmid and PCR products cleaned up using the Wizard® SV gel and PCR Clean-up System kit (Promega, USA) as per the manufacturers processing PCR reactions protocol.

2.14 Shrimp Alkaline Phosphate Treatment of Digested Vector

Exposed 5' phosphate was removed from the vector ends by Shrimp Alkaline Phosphatase (SAP) (Promega, Madison, WI USA). 1 unit of SAP was used with 2-4 µg of vector plasmid DNA and 10x SAP buffer (5 µl) in a total volume of 50 µl and incubated at 37°C for 1 hour. The SAP was de-activated by ten minute incubation at 65°C. The plasmid DNA was extracted with a Promega Wizard®SV Gel and PCR Clean-up System (Promega, Madison, WI USA).

2.15 Competent Cells

The procedure for competent cells was performed as described previously (Sambrock *et al.* 2001). A 10 ml culture of Luria Broth (Appendix A.3) with appropriate antibiotics and a sterile sample of *E. coli* PMC103 was incubated overnight at 37°C on an orbital shaker speed 180 rpm. 50 ml of LB was inoculated with 500 µl of the already prepared overnight PMC103 culture and appropriate antibiotics. The culture was incubated at 37°C on an orbital shaker speed 180rpm until optical density reaches 0.6 at 600 nm. Optical density was measured spectrophotometrically (Beckman DU 640 spectrophotometer). Once optical density was reached, the culture was transferred into a sterile 50 ml falcon tube and centrifuged at 5,000 g for ten minutes at 4°C in a Jovan CR312 centrifuge. The resultant pellet was resuspended in 20 ml ice cold 0.1 M $CaCl_2$ not pH adjusted and incubated on ice for 30 minutes. The solution was then centrifuged at 5,000 g for 10 minutes at 4°C. The supernatant was then discarded and the resultant pellet

was resuspended in 4 ml of ice cold 0.1 M $CaCl_2$ cells were then stored at 4°C until required.

2.16 Transformation of PMC103

Digested and purified vector and DNA were placed in a sterile 1.5 ml centrifuge tube with 50–100 µl of competent cells. Tube was inverted and incubated on ice for thirty minutes. The cells were then heat shocked treated at 42°C for ninety seconds and then immediately returned to ice for two minutes. Between 50-100 µl of LB is added and the microfuge tube is incubated vertically at 37°C for thirty minutes on an orbital shaker speed 180 rpm. The cells were then spread plated using a sterile metal spreader on an appropriately supplemented LB Media plate (Appendix 3). Once dry, the plates were incubated lid down overnight at 37°C, plates are then stored at 4°C until required.

2.17 Glycerol Stock of Bacterial Cells

Overnight cultures of the bacterial strain were grown as previously described. 900 µl of the culture and 100 µl of autoclaved 80 % (v/v) glycerol were added to a1.5ml centrifuge tube and then stored at -80ºC.

2.18 DNA plasmid purification

To purify plasmid DNA, the Wizard Plus SV Miniprep DNA purification system- Centrifugation Protocol (Promega, Madison, WI USA) was followed. 10 ml of culture was centrifuged at 3,500 g for 10 minutes. The DNA was eluted in 100 µl of nuclease free water. The purified plasmids were stored at -20ºC.

2.19 Gateway cloning

2.19.1. Recombination Reaction

The protocol for Gateway® Technology with Clonase™ II was followed, using BP Clonase™ II Enzyme mix to clone PCR products flanked by *att*B sites into a pDONRTM221 vector (BP Recombination Reaction) and LR Clonase™ II Enzyme mix to transfer the PCR product from pDONRTM221 into a pHELLSGATE 12 vector (LR Recombination Reaction) as per manufacturer's guidelines (Invitrogen, USA).

2.19.2. Transforming Competent Cells with pHELLSGATE vector

OneShot® OmniMAXTM 2-T1® chemically competent *E. coli* cells (supplied with the Gateway® Technology kit) were transformed following the manufacturers protocol (Invitrogen, USA), with the modification of 250 µl liquid LB media used in place of SOC medium. Transformed cell mixtures were spread plated on solid LB with the appropriate antibiotic selection and incubated at 37ºC for 12-48 hours.

2.20 Electroporation of pHELLSGATE 12 construct into *Agrobacterium tumefaciens* GV3101

2.20.1. Preparation of Eletrocompetent *A. tumefaciens* GV3101 cells

A. tumefaciens GV3101 cells from a -80ºc glycerol stock were used to inoculate a 10 mL LB culture (25 µg/ml Rifampicin, 25 µg/ml Gentamicin) and left to incubate overnight at 28ºC with shaking. The next day 1 mL of the overnight culture was used to inoculate 100 mL of LB that incubated at 28ºC with shaking for four-five hours until the optical density reached 0.6 measuring spectrophotometrically at 600nm (Beckman DU 640 spectrophotometer, USA). The culture was chilled on ice for ten mins prior to centrifugation at 1,900 g for 20 mins at 4ºC (Jouran CR 312 Centrifuge). The

pellet was resuspended in 100 mL of sterile MiliQ H_2O before repeating the centrifugation step for 15 minutes. The pellet was then resuspended in 10 % (v/v) autoclaved glycerol before centrifugation was repeated again for 30 minutes. The final time the pellet was resuspended in 200 µl of 10% (v/v) glycerol. Cells were aliquoted, and snap frozen using liquid nitrogen and stored at -80ºC.

2.20.2. Electroporation of Electrocompetent *A. tumefaciens* cells with pHellsgate

Electrocompetent GV3101 cells (80 µl) were electropporated with 1µl of plasmid DNA (either empty pHELLSGATE 12 vector or *Atndb* silencing pHELLSGATE 12) (BioRad Gene Pulser II, CA, USA). Parameters used were 1.8kV field strength, 25 µF capacitance, and 200Ω resistance. Once electroporated, the sample was immediately transferred to 1 mL LB media and incubated at 28ºC for 3hrs without agitation. 100 µl of the electroporated mixture was plated onto LB media with 25 µg/ml Rifampicin, 25 µg/ml Gentamicin and 30 µg/ml Spectinomycin to select for transformed colonies.

2.21 Transformation of *A. thaliana* to incorporate pHELLSGATE vector

2.21.1. Floral Dip Method

Floral dip method was used for *A. thaliana* (Clough *et al.* 1998), with a few modifications. The cultures to dip were started when the emergence of flower bolts were evident on Wt plants to dip. A 10 mL starter culture of LB (25µg/ml Rifampicin, 2 5µg/ml Gentamicin and 30µg/ml Spectinomycin) was inoculated with GV31010 cells containing either the empty pHELLSGATE vector or *Atndb* silencing pHELLSGATE 12 vector and incubated overnight at 28ºC with shaking. The next day 250 mL LB culture (25 µg/ml Rifampicin, 25 µg/ml Gentamicin and 30 µg/ml Spectinomycin) was inoculated with the 10 mL overnight culture and incubated at 28ºC with shaking for 24 hours.

The next day the cultures were centrifuged at 600 g for 20 minutes at 4ºC (Sorvall® GSA Rotor). The pellet was then resuspended in 5 % (w/v) sucrose, until the optical density of the solution was between 0.6 and 1.0 measuring spectrophotometrically at 600nm (Beckman DU 640 spectrophotometer, USA). Silwett l-77, (Lehele Seeds, USA) was added to the resuspended *A. tumefaciens* mixture to a final concentration of 0.05 % (v/v). The above ground Sections of the Wt plants were then dipped into the bacterial solution with very gently agitation for approximately 30 seconds. The plants were then wrapped in plastic wrap and laid down overnight in a tray with a black cloth covering the plants to ensure no direct contact with light. The following morning the cloth was removed and plants were stood up and the plastic wrap was removed. Six plants were dipped for each culture. Five days after the initial dipping a second round of dipping occurred following the same method. Plants were then left to grow and set seed.

2.22 Collecting seed

Once seed pods had developed and dried, they were collected from plant and placed in paper bags. This allowed the seeds to dry out. After seeds had dried they were transferred to 1.5 ml centrifuge tubes and stored in a cool dry place. Before using seeds they were vernalized at 4ºC for two days.

2.23 Western Blot

2.23.1. Determination of Protein Concentration

Protein concentration for purified mitochondria was determined using the BCA Protein Assay Kit (Pierce, Rockford, IL, USA) using the micro plate method as outlined according to the manufactures protocol using a Multiskan EX Plate Reader (Labsystems, Adelab, Australia).

2.23.2. SDS Page Gel

Two SDS-PAGE Gels were constructed and run simultaneously. A sandwich of Blotting Apparatus (Hoefer SE250, Holliston, MA, USA) was constructed and placed into a caster platform. 3.5 ml of 10% (v/v) resolving gel (Appendix A.1) were added to each gel sandwich and allowed to set with an overlay of iso-butanol to prevent oxidation. Once set the iso-butanol was removed, the gel sandwich rinsed with MilliQ water. The upper layer of the gel sandwich was filled with 2.5 ml of 4% (v/v) stacking gel (Appendix A.1) before the appropriate size comb was inserted and left to set. Gel cassette was stored at 4°C until required.

2.23.3. Sample Preparation

40 µg of purified mitochondria was used for western blot. 4 x denaturing loading buffer (Appendix A.1) was added and incubated at 95°C for five minutes in a Solid State Control Three Block Capacity Dry Block Heater. (Ratek Instruments, Australia). A volume of 40 µg of each protein sample was then electrophoresed through the precast SDS-PAGE gels immersed in SDS-PAGE Running buffer (Appendix A.1) a Kaleidoscope ladder (BioRad, CA, USA) was also run in each gel. Proteins were separated by gel electrophoresis at 170 volts for approximately 60 minutes in a Hoefer SE 250 western blot gel tank.

2.23.4. Protein Transfer

Seperated proteins were then transferred onto nitrocellulose membrane (BioRad) via the semi-dry blot method. The membrane (4 cm x 8 cm) and ten Whatman filter papers (3 cm x 7 cm) were soaked in transfer buffer for fifteen minutes. Whatman filter papers were layered onto the base of the BioRad Trans-Blot SD transfer cell, five filter papers then the membrane, the SDS-PAGE resolving gel with the stacking gel removed and the remaining five

Whatman filter papers on top. All air bubbles were removed from the assembled layers. Transfer was conducted at 38 MilliAmps for 90 minutes.

2.23.5. Blotting and Immunodetection

The membrane was incubated in Blocking Buffer (Appendix A.2) for one hour on an orbital shaker (Adelab, Adelaide, Australia) speed 2.5 at room temperature before being subjected to one fifteen minute washes in 1x TBST buffer, followed by two five minute washes (Appendix A.2). The primary antibodies used were then diluted as in Table 2.3 in 1x TBST Buffer and then added to the membrane. Incubation occurred overnight at 4ºC on an orbital shaker speed 2.5. The membrane was then washed with a fifteen minute washes in 1x TBST buffer, followed by two five minute washes. The secondary antibody Rabbit-HRP-AntiMouse IgG (DAKO, Australia) was diluted 1:1000 in blocking buffer or Mouse-HRP-Antigoat IgG (DAKO, Australia) was diluted 1:25000 in blocking buffer (for Porin and AOA antibodies) and added to the membrane. Incubation occurred at room temperature for one hour on an orbital shaker speed 2.5. The membrane was then washed with a fifteen minute washes in 1x TBST buffer, followed by two five minute washes. Once drained the membrane was inserted into a plastic sleeve and incubated at room temperature with equal parts of Super Signal West Pico Luminol Enhancer and Stable Peroxide solution (Pierce, Rockford, IL, USA). X-ray film was placed on either side of the membrane and left in the dark for 30 minutes and 1 hour. The film was then developed using Kodak® (Australia) fixer and developer reagents.

2.23.6. Stripping membrane

Stripping buffer (Appendix A.2) was added to membrane and incubated at room temperature for 30 minutes with gentle shaking. The membrane was then rinsed four X for five minutes each in 1 X TBS buffer (Appendix A.2). The membrane was then incubated in Blocking Buffer (Appendix A.2) for one

hour on an orbital shaker (Adelab) speed 2.5 at room temperature prior to use with porin antibody as outlined in Blotting and immunodetection 2.36.

2.24 Mitochondrial isolation

The method used to isolate mitochondria from *A. thaliana* was adapted from (Dry *et al.* 1987). All steps were done at 4ºC. Tissue was rinsed in de-ionised water and drained before weighing. Tissue was then homogenized in 250ml of Isolation Media (Appendix A.8) using a Polytron blender (Kinematica, Australia) at level four for four bursts of three seconds. The homogenate was then filtered through two layers of miracloth and centrifuged in GSA Bottles (Sorvall) at 4066 g for 10 minutes at 4ºC. The supernatant was transferred to clean 250 ml GSA bottle and centrifuged at 16,200 g for 20 minutes at 4ºC. The pellet was then resuspended in 2 mL of Wash media (Appendix A.8) using a paintbrush and the suspension was gently layered onto a continuous Percoll gradient for purification of mitochondria. The gradients were centrifuged at 38,700 g for 40 minutes at 4ºC. Mitochondria were sitting ¾ of the way down the tube where a visible band was noticeable. The mitochondria were collected using a pasteur pipette. The mitochondria were washed twice with wash media at 17,211 g for 20 minutes for the first spin and 10 minutes for the second spin both at 4ºC. The third wash on purified mitochondria was done using Wash Media without BSA for 10 minutes at 17,200 g at 4^{o}C. The clean purified mitochondria were resuspended in 500 µl of Wash media without BSA for use in assays and protein estimations.

2.25 Respiration Assays

Oxygen uptake rates were determined polarographically using a Clark oxygen electrode (Rank Brothers, Cambridge, UK), to measure activities of NAD(P)H DHs and AOX. All assays were conducted in 1 mL of standard reaction media (Appendix A.8), using approximately 80 µg of mitochondrial

protein. The air-saturated O_2 concentration of the medium was assumed to be 240 µM. Matrix NAD(P)H oxidation was assayed in the presence of 3 µM EGTA, 10 mM malate, 10 mM glutamate, 10 mM pyruvate and 1 mM NAD+. State-3 respiration was determined upon addition of 1 mM ADP. Rotenone (50 µM) was added to determine the rotenone resistant activity due to internal NAD(P)H dehydrogenases. The assay for cytosolic rotenone-insensitive NADH oxidation contained 2 mM NADH and 1 mM ADP, and 2 mM $CaCl_2$ was added to determine the maximal rate of NADH oxidation. Cytosolic rotenone insensitive NADPH oxidation was determined in the presence of 2 mM NADPH and 1 mM ADP. The maximal rate of NADPH oxidation was also determined upon addition of $CaCl^2$ (2 mM).

.

2.26 Sterilisation of *A. thaliana* Seeds

In order to prevent the growth of bacteria or fungus on plates, seeds must be sterilised to remove traces of these organisms. Sterilisation of seeds was conducted in a PC2 laminar flow to prevent contamination of mutant lines. Seeds are placed into a 10 ml centrifuge tube and incubated at room temperature in 7 ml 70% ethanol for five minutes. Ethanol was removed from the 10ml centrifuge tube by tipping the tube at a large angle to prevent seed loss. Seeds where then incubated in 6 ml of seed sterilisation buffer (Appendix A.5) at room temperature for fifteen minutes inverting every two–three minutes. Using a paster pipette, seed sterilisation buffer was removed and seeds repeatedly rinsed with 6ml sterile milliQ water until clear. All items (including solutions) used in the sterilisation process were subsequently killed post-sterilisation to prevent spread of mutant seed lines to the outside environment.

2.27 Plating of Seeds

MS media plates containing 30 µg/ml Kanamycin, 1 % (w/v) sucrose (pH

range 5.6-5.8), 0.7 % (w/v) agar, 30 µg/mL Cefotaxime, 100 x Gamborgs vitamin mix, and 0.2165 g of MS powder per 50 mL plate were prepared. Each MS media plate was seeded with 25 seeds of each *A. thaliana* line using a 2µl pipette. Seeds were placed in a 5x5 grid pattern to enable easy identification of transformants. Or for the P1 seeds, up to 400 seeds were placed on each plate to allow for maximum transformants to germinate. Plates were wrapped in Parafilm® and placed in a Sanyo Versitile Environmental Test Chamber (light intensity of 150 uE m^{-2} s^{-1}) at 23°C with 14 hour light/10 hour dark cycles.

2.27.1. Transfer of plants from MS Media to Soil

For resistant plants that had grown on MS Media they were to be transferred to soil to allow the plants to continue to grow and set seed. Plants were carefully removed from MS Media plates with sterile tweezers and gently placed into moist soil. The plants were placed so that the roots were slightly emerged into the soil. Pots were placed in glasshouse (PC2 glasshouse for transgenic lines) light intensity 150 uE m^{-2} s^{-1}, 25ºC) and day/night cycles subject to the seasonal variability of the day.

2.28 Analysis of Segregation Ratios in Mutant *A. thaliana* Lines

Two to four weeks after plating, plates were observed and the number of seeds per plate which had germinated and grew to two leaf stage only, germinated and grew beyond two leaf stage and showed no change (non-viable) were recorded. These data sets were used to determine ratio of resistant to sensitive. It was expected that all seeds would grow on MS media without Kanamycin selection and only those containing the RNAi silencing cassettes would grow on MS+Kanamycin. The ratio between the two data sets will determine the segregation ration of the cassette and the subsequent number of inserts within the genome.

2.29 Growth curves

Growth curves were measured using fresh weight of both leaf and root tissue at various ages (1-6 weeks) for both Wt tissue and RNAi knock-down lines including empty vector control. Fresh tissue from plants grown on either MS Media plates (Appendix A.3) or soil-grown plants material was weighed. RGR was determined by use of the Richards function (Venus *et al.* 1979).
The following equation was used for growth rate

$$RGR = \frac{\ln(M2) - \ln(M1)}{t2 - t1}$$

Where M= weight (g) and t = time (days)

Root length was determined for growth for both Wt tissue and RNAi knock-down lines including empty vector control plants. Measurements were taken directly off MS Media plate using a ruler.

2.30 Physiological measurements.

Leaf area was determined for individual leaves as well as both cotyledons (and whole rosettes, respectively) at three stages of growth, two-cotyledon stage (6-days post-germination), four-leaf stage (15-days post-germination), and 12-15 rosette stage (~5 weeks post-germination). Leaves or whole rosettes were taken from plants grown on either MS Media plates or soil-grown plants depending on stage of growth (e.g. 6-day cotyledon leaf area was determined from plants growing on plates while 5-week measurements were from plants in soil). Leaf area was determined from photocopies of leaves using Image J (NIH). Root length was determined for the first 7 days of growth for both Wt and RNAi knock-down plants. Measurements were taken directly off MS Media plates using a ruler.

2.31 Visual observation

Visual observations of plant growth both on MS Media plates and soil-grown plates were observed and recorded using a Sony Cyber-shot 7.2 Mega Pixel camera (SONY, Australia) for record keeping of noted observations.

2.32 Quantitative Real Time PCR (QRT-PCR)

Total RNA (1 µg) tissue was reverse transcribed into cDNA using StrataScript reverse transcriptase (Stratagene). Target sequences, approximately 100 to 200 bp, near the 3' end of the *nda1*, *nda2*, *ndb1*, *ndb2*, *ndb3*, *ndb4, ndc1*, AtAox1a, *Complex 1* (51 kD subunit) and *Ubiquitin* cDNA (Table 2.2 for primer sequences) were amplified by PCR, isolated and purified and the concentrations of these QRTPCR standards were ascertained by comparison with standards of known concentration using agarose gel electrophoresis with ethidium bromide staining followed by analysis with the Quantity One (Bio-Rad) program. These QRTPCR standards were then used at different concentrations (10^{-2}, 10^{-4}, 10^{-6} and 10^{-8} fmol/µL) for QRTPCR. QRTPCR was performed on the Rotor Gene RG-3000 (Corbett Research) machine using SYBR-Green and Fisher BiothermStar Hot Start Taq Polymerase (Fisher Biotec, Australia). The conditions for QRTPCR for all the genes analyzed were optimized such that only a single specific product devoid of primer dimers was obtained. This was confirmed both by agarose gel electrophoresis of the PCR samples and by a melt curve analysis. The PCR cycle used was 1 cycle of 95°C for 10 minutes; 50 cycles of 95°C for 30 seconds, 54°C for 30 seconds, 72°C for 30 seconds; 1 cycle of 72°C for 1 minute; Melt curve from 72°C to 99°C. Threshold fluorescence was set using the automatic settings of the Rotor-Gene 6 program. The concentration of the target gene cDNA from RNA was calculated from the standard curve generated during each run and normalized against the concentration of *Ubiquitin* cDNA, which itself was ascertained the same way. Replicate experiments (n=3) were performed for each gene.

To determine fold change of QRT-PCR results based on *ndb4* knock-down lines, the empty vector control and/or Wt was set to 1 to determine the respective gene changes for the *ndb4* knock-down lines.

2.33 Salinity Stress

2.33.1. Growth conditions for Wt seeds in liquid culture

Seeds of Wt *A. thaliana* (ecotype *Columbia*) were surface sterilised in petri dishes (6 cm diameter). The seeds were soaked in 70 % (w/v) ethanol with 0.1 % (w/v) Tween-20 (Sigma, USA) for 5 min, 2.5 % (w/v) household bleach with 0.1 % (w/v) Tween-20 for 20 min and then rinsed four times in RO water filtered through a 0.2 micron filter. Seeds were germinated in liquid culture media (Moore *et al*, 2003) (4 g/L MES, 2.15 g/L ½ Murashige and Skoog salts, 2 % (w/v) sucrose, pH 5.8, 1000x Gamborgs Vitamin B5) was inoculated with approximately 50 seeds suspended in filtered RO water (Murashige *et al.* 1962). Alternatively, 250 mL flasks with 80 mL of Liquid Culture media were inoculated with culture (1/2 strength Murashige and Skoog basal salt mixture salts), 2 % (w/v) sucrose, 2 mM 2-(N-Morpholino) ethane-sulfonic acid, pH 5.8, 1 X 1000 Gamborgs Vitamin (B5) and at least 50 seeds, to obtain maximum tissue yield. *A. thaliana* Liquid Cultures were allowed to germinate under 24 h light at 80-100 µE m-2 s-1, 25ºC with shaking at 60 rpm. After 11 days post germination, the Liquid Culture media was replaced with fresh media supplemented with 100 mM NaCl (salt stress treatment) or without NaCl (control treatment), and maintained, for a further 6, 24 or 72 hours.

2.33.2. Determination of Na^+ and K^+ Concentrations Using Flame Photometry for Wt tissue

Fresh leaf and root tissues from each plant were weighed separately, before drying at 80°C for 48 hours and re-weighing. Tissue water content was

calculated as the difference between fresh and dry weights. The dried tissues were then incubated in 50ml of 0.5M HCl for two hours at 50°C. Triplicate samples of each supernatant were quantified for Na^+ and K^+ using a Corning Flame Photometer 410, and standard curves created from a set of NaCl and KCl standard solutions.

2.33.3. Growth conditions for hydroponics salt stressed plants

All plants were grown hydroponically in aerated, half-strength Hoagland nutrient solution, within an enclosed glasshouse (light intensity 150 uE m-2 s-1, 25ºC). Day/night cycles were subject to seasonal variability. Plants were harvested after 5 weeks of growth (including the stress). Salt stress was introduced gradually over 3 days (50 mM NaCl and 0.6 mM $CaCl_2$ each day), then maintained at 150 mM NaCl and 1.8 mM $CaCl_2$ for a further 7 days.

2.33.4. Growth analysis during salinity stress

Growth was recorded by measuring fresh and dry weight of both roots and leaves, before and after salinity stress had been applied for treated plants, as well as untreated plants. Plant growth data from treated and untreated were analysed for RGR by use of the Richards function (Venus *et al.* 1979) Section 2.29 above.

2.33.5. Inductively Coupled Plasma-Optic Emission Spectroscopy (ICP-OES) Analysis of Na+ and K+

After 5 weeks of hydroponic growth (including 10 days of NaCl treatment), *A. thaliana* shoots and roots were separated, washed twice in 5 mM CaCl2 and dried at 80ºC for 48 hours. Samples were sent for ICP analysis, by an inductively coupled plasma-optic emission spectrometer at the Waite Analytical Service, University of Adelaide, Australia, to measure a range of metal ions, including Na^+ and K^+.

2.33.6. ROS Detection

An Amplex Red Hydrogen Peroxide/Peroxidase Assay Kit (Molecular probes, Eugene, OR, USA) was used to measure H_2O_2 production in 5 week old control and stressed plants (Shin *et al.* 2005). The method used was adapted from Shin *et al* 2005. Firstly the harvested tissue was snap frozen with N_2 as soon as harvested. Tissue was ground and kept frozen while transferred and weighed in pre-weighed 1.5ml centrifuge tubes. Samples were then placed into N_2 to keep frozen. After all samples were ground only 12 samples were used at a time to do the assay. (Take out 12 tubes from N_2 and add buffer and vortex for 30 sec. During this procedures, tissue thaws briefly). The harvested tissue was frozen and ground under liquid nitrogen, and 20 mM phosphate buffer (pH 6.5) was added depending on the weight of tissue, with 100 µL being added per 100 mg of tissue. Samples were centrifuge at 8000 g for 10 minutes at 4ºC. 50 µl of the supernatant was used for the assay according to manufactures guidelines.

2.34 Statistical analysis

Data is expressed as mean ± standard error (SE). The statistical Significance of differences found between means was evaluated at the 95% Confidence level by the ANOVA and Multiple Comparisons Tests using the program GraphPad Version 5.02.

2.35 Microarray

Cotyledons from *A. thaliana* plants were harvested at six-days post-germination and frozen in liquid nitrogen.

2.35.1. RNA extraction

RNA was extracted using the QIAGEN RNeasy Plant Mini Kit according to the manufactures guidelines (QIAGEN, USA). 100 mg of tissue was used as starting material. The RLT buffer was used as starting material with *A. thaliana* leaf tissue. The optional DNase digestion was done with DNase I from the RNase-Free DNase Set (QIAGEN, USA). The RNA was eluted in 40 µl of RNase-free water.

2.35.2. Microarray Analysis

Analysis of the changes in transcript abundance between pART and *RNAi knock-down lines* in six-day-old Arabidopsis plants was performed using Affymetrix GeneChip Arabidopsis ATH1 Genome Arrays. Leaf tissue samples were collected in biological triplicate for each line. For each replicate, the quality of RNA was verified using a Bioanalyzer (Agilent Technologies), and spectrophotometric analysis was carried out to determine the A_{260} to A_{280} and A_{260} to A_{230} ratios. Single labelling of chips occurred. Preparation of labelled complementary RNA from 5 μg of total RNA, target hybridization, as well as washing, staining, and scanning of the arrays were carried out exactly as described in the Affymetrix GeneChip Expression Analysis Technical Manual, using an Affymetrix GeneChip Hybridization Oven 640, an Affymetrix Fluidics Station 450, and a GeneChip Scanner 3000 7G at the appropriate steps. Data quality was assessed using GCOS 1.4 before CEL files were exported into Array Assist (version 5.51) for further analysis.

CEL files were subjected to GC-RMA normalization, a variation of the robust multiarray average normalization algorithm. MAS5 normalization algorithms were also carried out to generate present/absent calls across the arrays. Correlation plots were examined between all chips using the scatter plot function, in all cases $r \geq 0.95$ (data not shown). Probe sets determined as absent in 4 out of 6 chips for individual investigation of RNAi, were eliminated

from the analysis. Fold changes for a number of different comparisons were calculated using the Differential Expression Analysis function, and *P* values were calculated using an unpaired *t* test; *P* values were given as uncorrected and after correction for estimation of FDR in multiple comparisons. A method of FDR correction that is based on the Benjamini and Hochberg method (Benjamini et al., 1995) was used. This comparison was KDb4-1 RNAi knock-down line versus pART empty vector control. PCA plots were generated using the PCA tool in Array Assist (version 5.51), reducing the 22,810 gene expression values to two dimension clusters with mean centring and scaling of all variables to unit variance. Principal eigen values associated with the principal axes were also calculated and plotted against their respective percentile contribution to determine the percentage of variance captured. Principal axes 1 and 2 were plotted as those capturing over 94% of the variance in the data set. Cluster images were generated using the hierarchical cluster function in the Array Assist (version 5.51) software package, clustering on both rows and columns using complete linkage and Euclidean distance measures.

2.35.3. MapMan

MapMan software (http://gabi.rzpd.de/projects/MapMan/)(Thimm *et al.* 2004) was used to generate a qualitative global assessment of two-fold or greater transcript abundance changes in the *ndb4* line compared to empty vector controls under normal conditions.

Table 2.1 Primer used

Primers used for cloning, screening and amplification. Restriction enzyme recognition sites and flanking sequences were identified by using REBASE (NEB) website, those sequences are underlined. attB regions for Gateway cloning are in bold. The annealing temperature (Ta) for amplification was calculated from the melting temperature (Tm), Ta=Tm-5ºC, unless otherwise stated.

Name	Primer sequence (5'>3')	Tm (ºC)	Product	Application
At4F1	CGGGATCCCGTTTGGATCTGAGGTTTGAGAAA	60	200bp antisence fragment or 580bp *ndb4* fragment from genomic DNA	Screening
At4R1	CCATCGATGGTGAGTCAAGAGTAGCGTCTG	60	200bp antisence fragment or 580bp *ndb4* fragment from genomic DNA	Screening
pHANF	CACAACAAGTCAGCAAACAG	58	258bp product from genomic DNA	Screening
pHANR	GTGAACATAGTGTCGTCACC	60	258bp product from genomic DNA	Screening
NDB2F	GTGTGAAAAATTCTTCTTC	42	1861bp cDNA product	Amplifying
NDB2R	TAGTGTAACTCGTGAGAG	46	1861bp cDNA product	Amplifying

SenseCasF	CCGCTCGAGCGGAGAGGAGAAGGTCGTCAC	53	173bp cDNA product	Amplifying
SenseCasR	GGGGTACCCCCGCCAGCTCACTTGCTTAC	53	173bp cDNA product	Amplifying
AntisenseCasF	CGGGATCCCGAGAGGAGAAGGTCGTCAC	53	173bp cDNA product	Amplifying
AntisenseCasR	CCATCGATGGCGCCAGCTCACTTGCTTAC	53	173bp cDNA product	Amplifying
pHellsB2F	**GGGGACAAGTTTGTACAAAAAAGCAGGCT** AGAGGAGAAGGTCGTCAC	53	173bp cDNA product	Amplifying
pHellsB2R	**GGGGACCACTTTGTACAAGAAAGCTGGGT** CGCCAGCTCACTTGCTTAC	53	173bp cDNA product	Amplifying
pHellsscreenF	GCTGGCGTAATAGCGAAGAG	54	316 genomic product	Screening
pHellsscreenR	CGGGCGGAAATAGGTAAAG	51	316 genomic product	Screening

Table 2.2 Primers used for QRT-PCR

Primers were used for QRT-PCR amplification

Gene	Forward	Reverse	Size fragment
NDA1	AGAGCAAGGAAGGGAAAG	GAAGTGGAGGGGATATGG	180
NDA2	CTTGGAAGCATGGCTACTAT	CAAAAACGAAAGTGGTGAA	190
NDB1	GAAAAATCTTGGGGGATATT	ATGCTTGCTTTTCAGGTAGA	146
NDB2	GTCTACGCCAGTAAGCAAGT	TGTAACTCGTGAGAGAGAGAGA	151
NDB3	TTTACGCTAGTAAGCAAGTGAG	CCATGATAATTCAAACGAGAG	140
NDB4	TGAGGACACACAAGTGAATATC	TGGCTTCTTCTCACATTTCT	157
NDC1	CCTTTATTACCATTCAGGTTTC	TCAAATACGCCAGTTTTCTC	141
Ubi	GACAGAGCAGAGAACATAAGG	TGGGGATTGGGTAAAGAGG	184
Complex 1-51kDa	AAACAGATCGAAGGACACAC	AGAGCAAGGACTGGAGATG	186

Table 2.3 Antibodies used for protein determination

Antibodies used for western analysis and the concentration that was used for each, with incubation time of the primary antibody.

Antibody	Concentration	Incubation time
NDB4	1:10 000	Overnight
NDB2	1:10 000	Overnight
AOX	1:1000	Overnight
NDB	1:10000	Overnight
AOA	1:500	Overnight
Porin	1:5000	Overnight

3 GENERATION AND CHARACTERISATION OF PLANTS WITH SUPRESSED EXPRESSION OF EXTERNAL NAD(P)H DEHYDROGENASES

3.1 Introduction

3.1.1. NAD(P)H dehydrogenases

Type II NAD(P)H dehydrogenases are non-proton pumping respiratory enzymes, each consisting of one type of polypeptide of 50–60 kDa. They are widely distributed among plants, fungi, protists, many bacteria, and Archaea (Rasmusson *et al.* 2004). These NAD(P)H dehydrogenases work in parallel with complex I, which is a multi subunit proton pumping type I NADH:quinone oxidoreductase (Rasmusson *et al.* 1998). In many organisms the presence of several type II DH isoenzymes potentially increases the catalytic flexibility of respiratory NAD(P)H oxidation. Although there has been different proposed roles for the different homolog genes, in plants, the relative expression of gene homologs varies between tissues (Michalecka *et al.* 2003; Elhafez *et al.* 2006), during development (Svensson *et al.* 2001), in response to light (Svensson *et al.* 2001; Michalecka *et al.* 2003; Escobar *et al.* 2004) and upon several kinds of stress (Svensson *et al.* 2002; Clifton *et al.* 2005; Escobar *et al.* 2006a). The differential gene expression of plant type II NAD(P)HDH homolog's points to diverse physiological roles of the enzymes.

External NADH and NADPH oxidation measured in isolated plant mitochondria is generally dependent on Ca^{2+} (Moller 1997; Rasmusson *et al.* 2004) with NADH oxidation being less sensitive to inhibition by chelators (Arron *et al.* 1980; Moller *et al.* 1986). NADH oxidation has even been observed in the absence of Ca^{2+} for several plant materials (Nash *et al.* 1983a; Zottini *et al.* 1993; Escobar *et al.* 2006b). There is strong evidence in the literature that each gene encoding a dehydrogenase is a separate dehydrogenase which is specific for either external NADH or NADPH in plants (Fredlund *et al.* 1991b; Michalecka *et al.* 2004). However, the absence

of specific inhibitors has made it difficult to study the isoenzymes individually in isolated mitochondria. Several proteins showing NAD(P)H oxidation in the presence of artificial electron acceptors have been purified from different plant species (Luethy *et al.* 1991a; Luethy *et al.* 1995; Menz *et al.* 1996a). However, the requirement for artificial electron acceptor such as quinones, which can affect substrate specificity and Ca^{2+} dependence (Soole *et al.* 1990; Menz *et al.* 1996a; Moller *et al.* 1996), has complicated the catalytic characterization of the purified enzymes. *Neurospora crassa* contains a homolog mainly catalysing Ca^{2+} dependent NADPH oxidation, the external NDE1 (Melo *et al.* 2001), whereas the external NDE2 and NDE3 of *N. crassa* were described as Ca^{2+} independent dehydrogenases accepting both NADH and NADPH (Carneiro *et al.* 2004; Carneiro *et al.* 2007). The substrate specificity has been able to be elucidated in *N. crassa* due to the characterisation of gene deletion mutant and analysis of mitochondria isolated from there mutants.

For plants, a substrate has been identified for the NDB1 homolog of potato, which is an external Ca^{2+} dependent NADPH dehydrogenase. The strategy used was overexpression of the potato NDB gene in tobacco, which resulted in an increase in NADPH oxidation on isolated mitochondria (Michalecka *et al.* 2004). Substantial evidence in potato and *A. thaliana* indicated that NDA1 is a matrix-facing NADH dehydrogenase (Svensson *et al.* 2001; Svensson *et al.* 2002; Moore *et al.* 2003; Elhafez *et al.* 2006). Defining the substrate specificities and Ca^{2+} dependence of the *A. thaliana* homologs is essential for elucidating the physiological roles of these enzymes. In this chapter, I use a plant where one of the external dehydrogenases (*ndb4*) has been knock-downed and observe the changes at transcript, protein and enzyme assay level. It is proposed that this approach will assist in identifying the different substrate specificities ndb enzymes will have for either NADH or NADPH, and which proteins will require calcium stimulation for dehydrogenase activity.

The mRNA sequences of the *A. thaliana* alternative NAD(P)H dehydrogenases were collected from GeneBank (NCBI) and MATDB (MIPS)

database (Table 1.1). The ClustaW tool (ANGIS, Biomanager) was used for pair-wise alignment of each mRNA sequence against *ndb4* mRNA sequence and were viewed in Genedoc. The region of least homology with *ndb4* was highlighted within each pairwise alignment. This would enable an RNAi knock-down construct to be designed for specific knock-down of the expression of *ndb4* without interfering with the expression of the 6 other alternative NAD(P)H dehydrogenases. A sequence of 200 nucleotides was identified initiating within the 5'UTR of *ndb4*, 31 bases from the start site and ending 166 bases after the start site, as having less than 56% identity with the other sequences and a maximum of 12 nucleotides of block identity (Figure 3.1). The sequence identity between *ndb4* and other members of NAD(P)H dehydrogenase gene family was an important parameter considered when designing the primers to prepare the RNAi construct to ensure specificity of target mRNA degradation. Wesley *et al.* (2001) found that the efficiency of knock-down averaged 90% using ihpRNAi constructs with arms of 400-800 nucleotides.

3.2 RNA Interference

Double stranded RNA (dsRNA) is recognised by the cell and triggers the degradation of itself and homologous RNA within the cell (Wesley *et al.* 2001). This process is known as posttranscriptional gene knock-down or RNA interference in animals.

3.2.1. Natural Process

This process of degrading dsRNA is a natural process already occurring in plants and plays a protection role against viral infections, transposons, transgenes and in genomes (Waterhouse *et al.* 2001). It has been found that different forms of silencing are all acting by the same mechanism which is referred to as post-transcriptional gene silencing (PTGS), which has a strong link to RNA interference. When dsRNA is introduced into a system it is

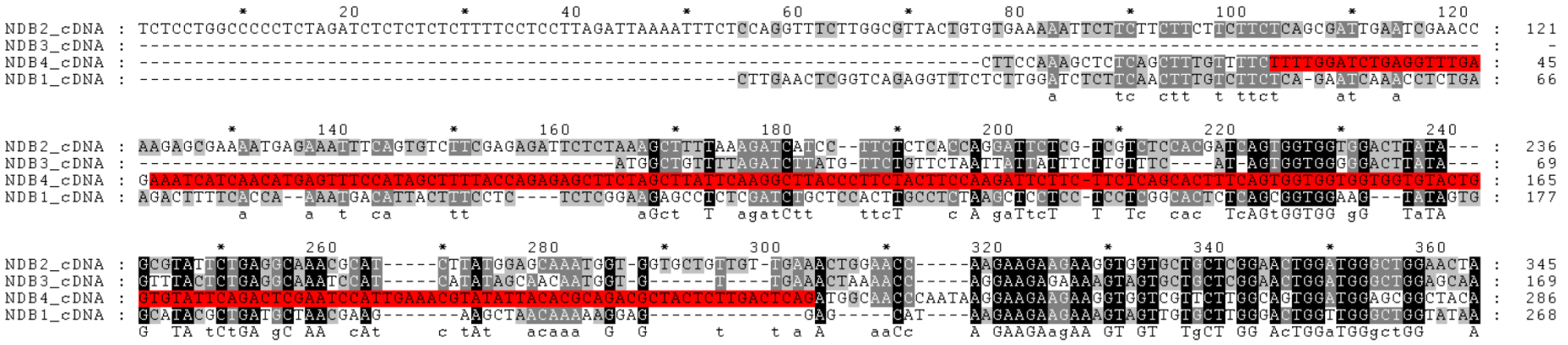

Figure 3.1 *ndb* family alignemnt with knock-down region from *ndb4* highlited in red

Development and characterization of *ndb4* RNAi Arabidopsis lines. Alignment of all four *Arabidopsis* external alternative NAD(P)H dehydrogenases with the 220 bp region used to generate the *ndb4* RNAi lines highlighted in red. Sequence with 100% identity is highlighted in black. A pair wise alignment was done (Section 2.3). The region in red highlights the region selected as *ndb4* knock-down region. The areas of sequence homology are indicated by shading, the dashes (-) represent the gaps inserted to maximise the sequence alignments. *ndb1* has 56% identity with *ndb4* knock-down region, *ndb2* has 48.5% identity, *ndb3* has 50.5% identity.

quickly degraded. When this degradation process occurs it produces ~21 nucleotide blocks from both ends of the dsRNA by the RNaseIII active Dicer like enzyme in *E. coli* or CAF1 homolog in *A. thaliana*. This degradation provided by dicer like enzymes can be visualised in Figure 3.2. To keepgenerating these 21 block nucleotides, every time there is exposed ends a new Dicer enzyme will be attracted to these exposed ends and continue to break the dsRNA up into 21 block nucleotides until the dsRNA is completely broken up (Figure 3.2). When the siRNA duplexes are loaded into the Dicer enzyme they are unwound, using ATP. At this stage the Dicer-siRNA will associate with a ribonuclease complex RISC (RNA- induced silencing complex). The now unwound siRNA directs RISC to the complementary single stranded mRNA for degradation. The dicer complex that is loaded from one end of a dsRNA will cleave the sense strand and hence the complex loaded from opposite end will cleave the anti-sense strand. The experimental induction of PTGS in higher plants as opposed to the natural process will be referred to as RNA interference (RNAi).

3.2.2. Silencing by intron-spliced hairpin RNAs

PTGS can be induced in plants by introducing a vector construct which is designed to express dsRNA or single self-complementary (hairpin) RNA (Wesley *et al.* 2001). This hairpin RNA contains sequences which are homologous to the target gene. Within this vector there is a spacer region between the two complementary regions to help the plasmid with stability. Vector constructs that encode intron spliced RNA with hairpin structure induced PTGS with almost complete efficiency (22 out of 23 transformants) when directed against viruses or endogenous genes (Smith *et al.* 2000). Intron spliced RNA vectors could facilitate the study of the functions of a wide variety of genes in plants, as has been done in nematodes and *Drosophilia* and been quite useful.

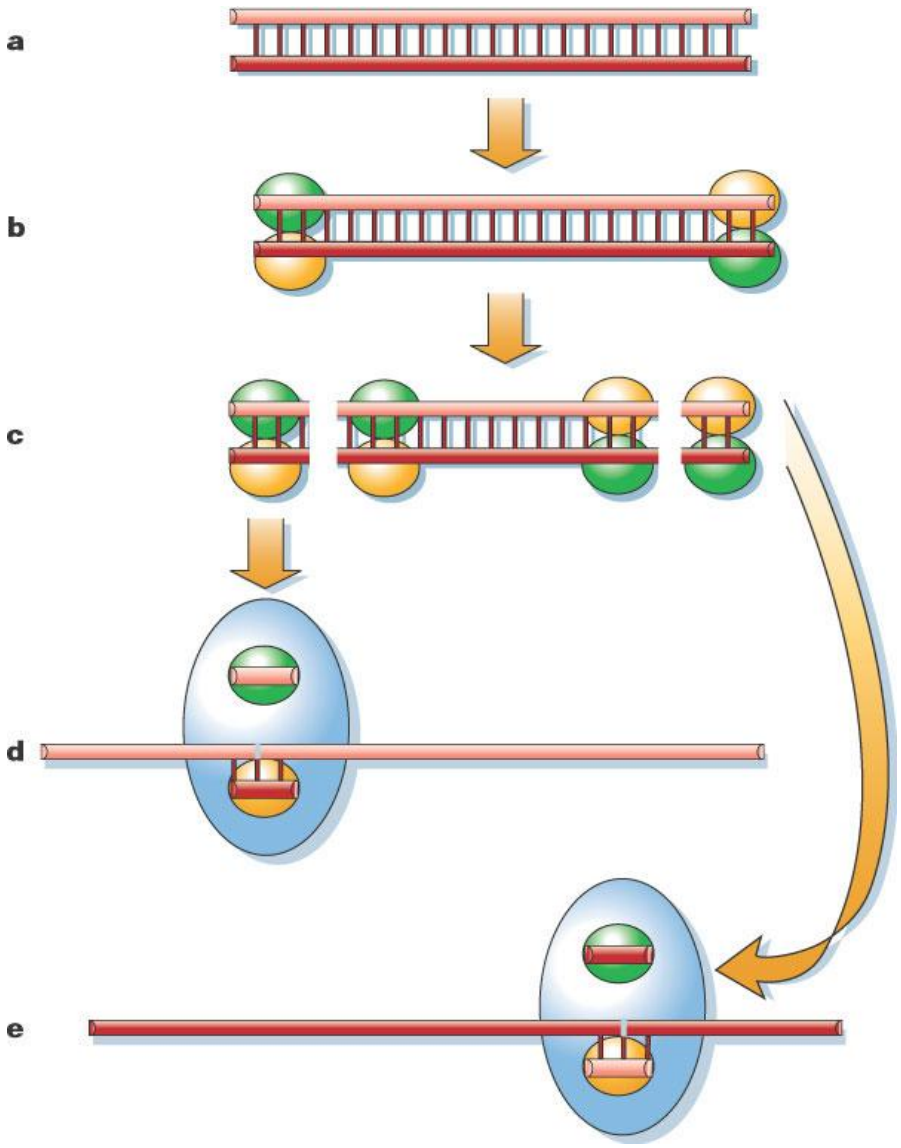

Figure 3.2 Mechanism proposed for dsRNA-induced ssRNA cleavage in PTGS based on RNA interference (Waterhouse *et al.* 2001)

Introduced dsRNA (a) attracts Dicer-1-like proteins to its termini (b). The heterodimer complex at each end cleaves a 21-nucleotide dsRNA fragment (c), and the exposed ends of the shortened dsRNA each attract a new Dicer complex, which cleaves a further 21-nucleotide dsRNA fragment. Dicer complexes loaded from one end of a dsRNA will cleave sense-strand mRNA (d), whereas complexes loaded from the other end will cleave mRNA of the opposite sense (e).

3.3 Aim

The aim of this chapter was to generate homozygous *A. thaliana* knock-down plants for *ndb4* using RNAi silencing, and confirm that these plants were silencing *ndb4* at the transcript and protein level. The transcript levels of other members of the alternative pathway were assessed, to determine if there were any changes as a result of the knock-down of *ndb4*. Using the knock-down plants it was hoped to resolve which enzyme activity is encoded for by *ndb4* in *A. thaliana* and its specificity for NADH or NADPH as a substrate and calcium dependency. In addition, the impact of *ndb4* suppression on the plant phenotype was assessed.

Previously Vanessa Melino an honours student in the lab in 2004 generated the *ndb4* knock-down lines of *A. thaliana* up to the T1 generation. Vanessa Melino did the molecular work for this construct and once had made the RNAi knock-down lines did the floral dipping and collected the initial seed. No analysis was done.

3.4 Results

3.4.1. Generation of *ndb4* knockdown plants

3.4.1.1 Confirmation of silenced expression vector

The *ndb4* knock-down vector had previously been generated by Vanessa Melino, using pHANNIBAL (Wesley *et al*. 2001) as the RNAi knock-down vector and then placed into pART27 (Gleave 1992) for expression in plants. The pHANNIBAL vector uses hairpin RNAi to silence genes (Figure 3.3). The hairpin loop method was chosen for RNAi silencing as has been shown to be efficient at gene silencing in plants. The hairpin RNAi silencing vector against anendogenous gene give highly effective post transcriptional silencing (Waterhouse *et al.* 1998; Chuang *et al.* 2000; Levin *et al.* 2000) and this eliminates the need to generate large populations of lines to ensure the disruption of the function of a given gene (Helliwell *et al.* 2002). Once the

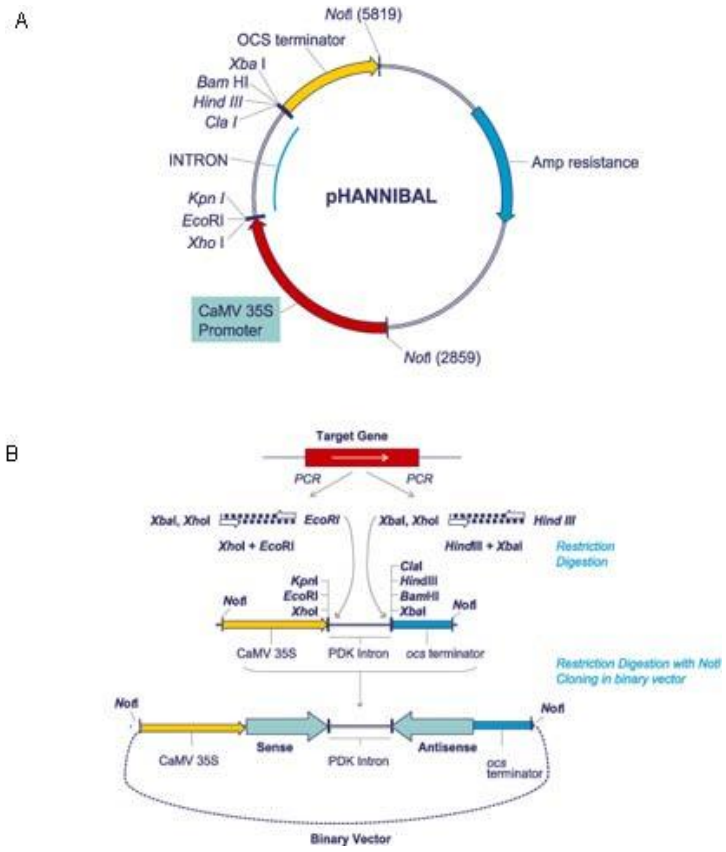

Figure 3.3 Plasmid map of the silencing vector pHANNIBAL (Wesley *et al*. 2001) used for cloning of *ndb4* knock-down region

(A) The pHANNIBAL (Wesley *et al*. 2001) silencing vector map, where the Intron loop is seen between the two cloning sites, as well as containing the CaMV 35S promoter site and OCS terminator sites between the Not I restriction sites. (B) The Cloning sites where RNAi PCR product was cloned in both directions using KpnI and XhoI for sense and BamHI and ClaI for the antisense direction.

two PCR fragments were cloned into pHANNIBAL the binary vector region was ligated into pART27 (Gleave 1992) (Figure 3.4). The cloned pART27 vector was then electroporated into *Agrobacterium tumefaciens*, so that stable transformants of *A. thaliana* could be made. After the parent seed was collected and screened for *ndb4* stable knock-down plants. The floral dipping *A. thaliana* plants that have taken up the vector were resistant to kanamycin and grown on selection plates, the plants that have not taken up the vector were sensitive to kanamycin were bleached out (Figure 3.5). Plants were transferred to soil to allow setting to seed. Genomic DNA extractions were carried out on parent plants to confirm by PCR that the vector was present in the *ndb4* knock-down lines and empty pHANNIBAL control plants. PCR confirmed the presence of both the control empty vector fragment at 258 bp, and for the pHANNIBAL vector containing the *ndb4* fragment seen at 220 bp (Figure 3.6). In addition there was an *ndb4* genomic DNA fragment. The purified empty pHANNIBAL vector and pART vector containing the *ndb4* fragment were used as the positive controls. Once the presence of the vector was known the plants could then be used to generate homozygous lines for further analysis.

3.4.1.2 Generating T1 plants

Once parent seed was collected and dried, the seed was used to generate T1 plants on kanamycin selective plates. The seeds were first sterilised according to Section 2.25. After 2 weeks the plants were of sufficient size to determine the number of inserts present in each line by determining the ratio of bleached plants (sensitive to kanamycin as they don't contain vector) to healthy plants (resistant to kanamycin as they contain vector). Ratios were determined based on this observation and resulted in each line having an expected ratio of close to 3:1 for resistant: sensitive. This confirms only one copy of the vector is present. The living plants will either be heterozygous i.e. vector/no vector or homozygous for vector/vector. The dead bleached plant will be homozygous for no vector/ no vector. Table 3.1 indicates the exact ratios that were generated for each line. After a total of 3 weeks, the living

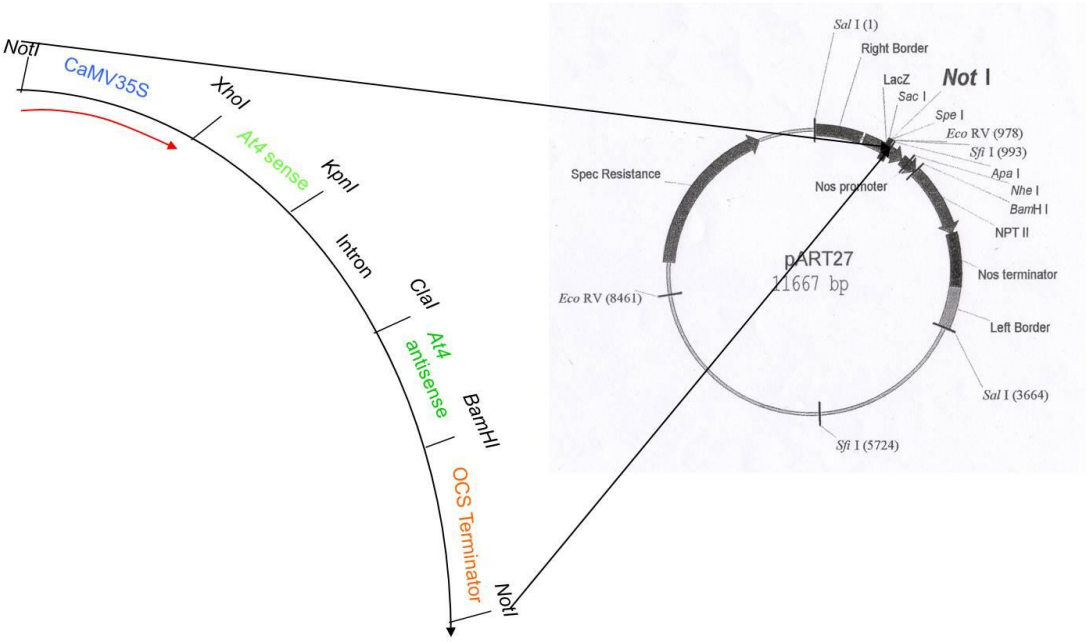

Figure 3.4 pART27 (Gleave 1992) plasmid containing cloned pHANNIBAL (Wesley *et al*. 2001) fragment with both sense and antisense fragment

The region where the hair pin loop is formed with the *ndb4* knock-down region using the intron is shown. The NotI fragment was ligated into pART containing the *ndb4* knock-down region.

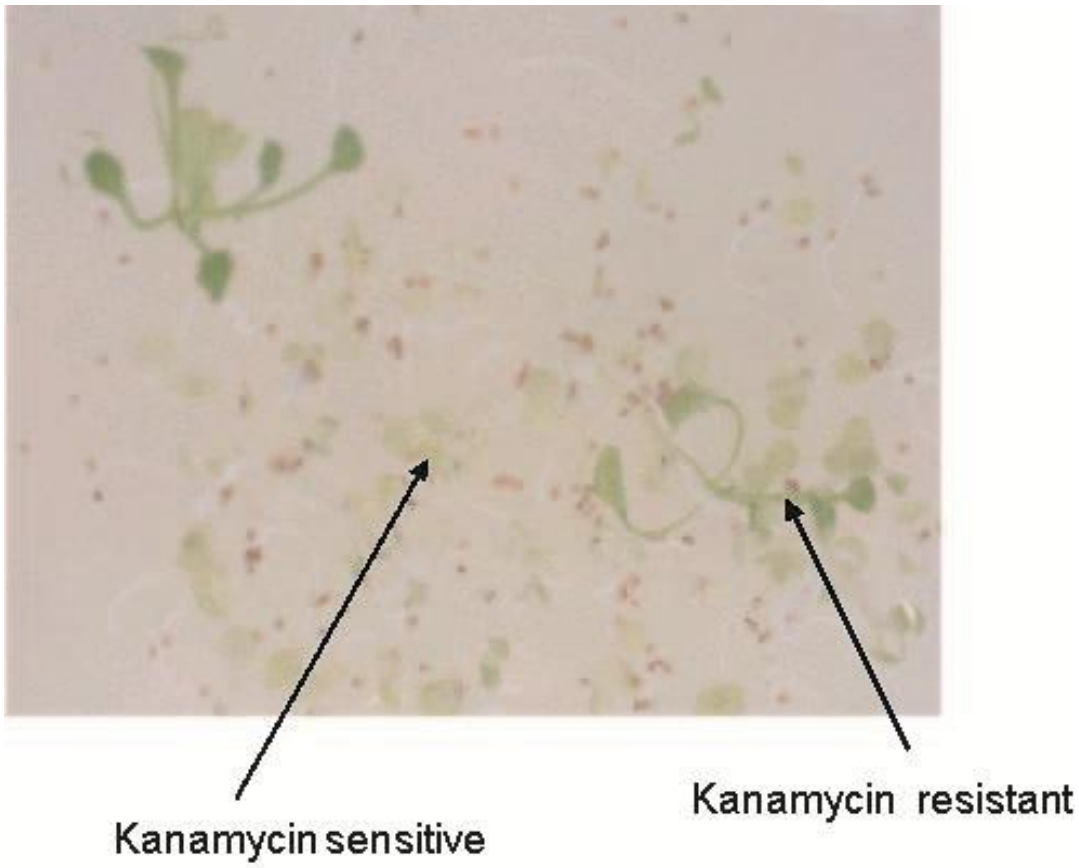

Figure 3.5 transformants on kanamycin selection plates, showing resistant and sensitive plants

Seeds were germinated on MS Media plates with selection. The Kanamycin resistance plants are still green in colour and healthy. The sensitive plants are bleached.

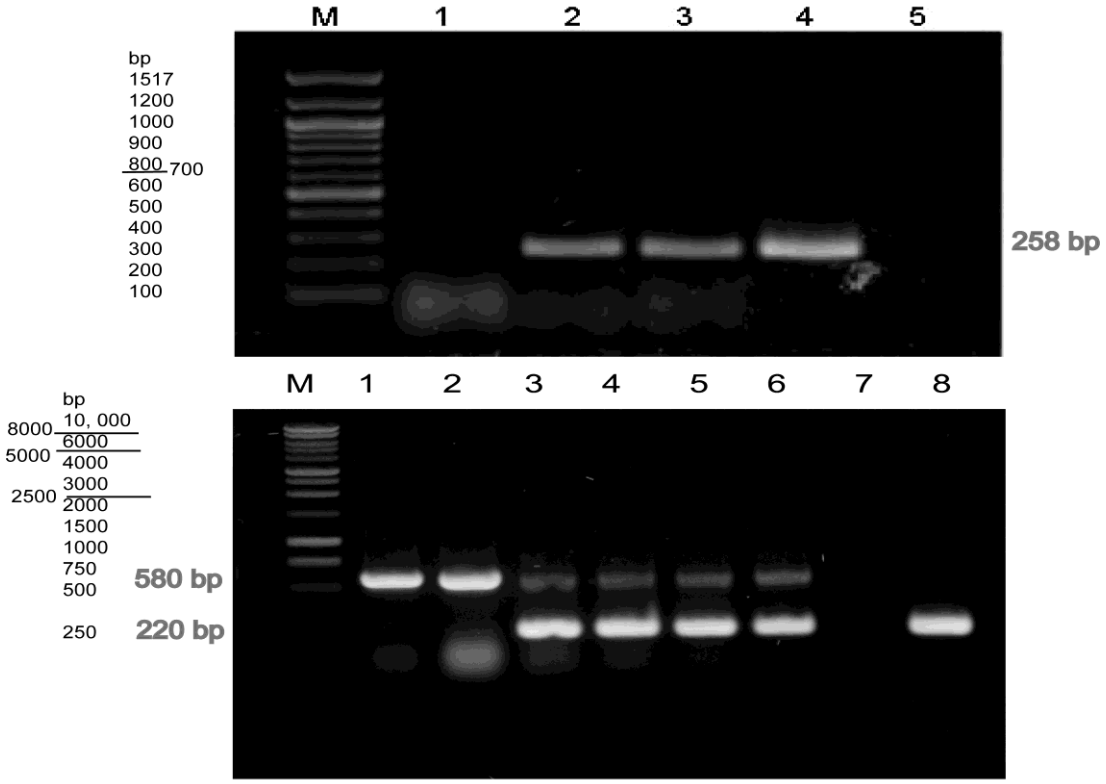

Figure 3.6 PCR Confirmation of pHANNIBAL (Wesley *et al*. 2001) containing *ndb4* knock-down region and pART27 (Gleave 1992) empty control vectors taken up by the plant

PCR on genomic DNA to confirm the presence of the RNAi vector or Control Vector in *plants* a) Control empty vector can be seen at 258 bp. b) pHANNIBAL vector containing *ndb4* fragment can be seen at 220 bp as well as genomic DNA *ndb4* fragment at 580 bp. PCR was conducted as described Section 2.10. Primers used were pHANF and pHANR for empty vector and AT4F1 and AT4R1 for pHANNIBAL containing the *ndb4* knock-down region.

Gel 1

Lane 1 Wt tissue

Lane 2 pART control #1

Lane 3 pART control #2

Lane 4 + control

Lane 5 – control

M 100bp marker

Gel 2

Lane 1 Wt tissue

Lane 2 pART control

Lane 3 KDb4-1

Lane 4 KDb4-2

Lane 5 Kdb4-3

Lane 6 KDb4-4

Lane 7 – control

Lane 8 + control

M 1kp marker

plants were moved to soil to collect the T1 seed to continue the process of generating homozygous plants.

3.4.1.3 Generating T3 homozygous plants

Generation of the homozygous plants for the *ndb4* knock-down lines began by taking T1 seeds which had been generate by previous student and growing them on kanamycin selective plates. Only T1 seeds of kanamycin selective plants with a 3:1 segregation ratio were used to generate T2. A single insert is desired to ensure the disruption of the genome only once, reducing the risk of disrupting a gene involved in an unrelated pathway, leading to phenotypic effects. Initially 15 lines of the T1 seed were tested from 5 independent parents that were dipped with the RNAi knock-down vector (Table 3.1). Plants show kanamycin resistant due to the presence of the NPT II gene in pART vector and this is only evident after 14 days of growth. As well as the T1 seeds, Wt seeds were plated out on the kanamycin selection to confirm that plants without a pART vector conferring resistance will be bleached (Figure 3.5). For the 20 lines tested the ratios of resistant to sensitive were determined (Table 3.1). Figure 3.7 shows the flow chart for generation of T3 homozygous plants.

The T2 seed was germinated on MS agar with kanamycin selection with 15 separate lines grown. T2 seeds will either produce all plants resistant (generating T3 homozygous seed), indicating homozygous lines, or they will generate a 3:1 segregation on resistant to sensitive which is indicating the T2 seed for that line was heterozygous. From the 15 lines plated, 5 individual lines all from separate T2 parental lines were chosen which were homozygous as defined above. These were described as KDb4-1, KDb4-2, KDb4-3 and KDb4-4 and pART control (empty vector control) (Table 3.1). Included in one of these lines is the empty vector control. This empty vector control is used to show that any of the changes in both physiological and molecular analysis were not due to the presence of the knock-down vector.

Table 3.1 Segregation ratios of T1 seed to determine number of inserts

Seed generated from homozygous t2 plants formed T3 homozygous seed, the lines used were 42 a 31 (KD-b4-2), 25 b 23 (pART control), 4 a 31 (KDb4-4), 3 a 31 (KDb4-1), and 2 a 32 (KDb4-3). Chi squares were done to confirm results visualised Appendix 3.

Plant Line	Alive	Dead	Ratio
42 a 31	22	6	1:3.7
25 b 23	22	8	1:2.8
4 a 31	25	8	1:3.1
3 b 22		21	n/a
3 a 31	24	2	1:3.1
26 b 32	14	5	1:2.8
41 a 31		19	n/a
26 b 22		23	n/a
5 a 32	21	13	1:1.6
1 b 21	26	1	1:26 (too high)
2 a 32	21	7	1:3
3 a 24	23	8	1:2.9
1 b 15	22	7	1:12 (too high)
42 a 22	24	9	1:2.7
6 a 25		24	n/a

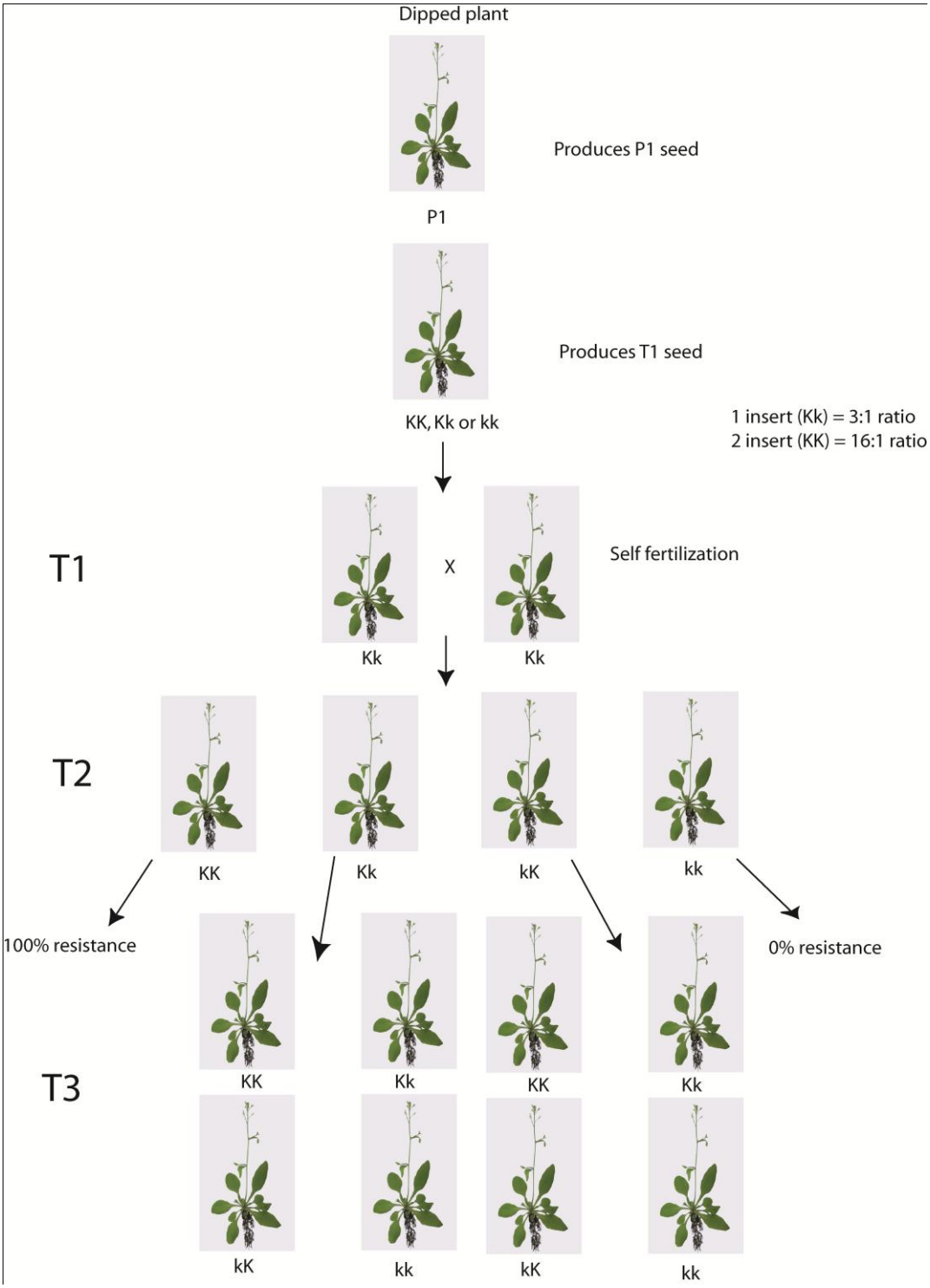

Figure 3.7 Flow chart of generation of T3 homozygous plants

The flow chart shows how T3 homozygous plants are generated based on dipping of plants and generating T1 seed, T2 seed and T3 seed.

Due to self crossing in *A. thaliana* these T3 seeds will produce homozygous T3 plants from which experiments can be conducted.

3.4.1.4 Confirming T3 homozygous plants have RNAi cassette present

In order to detect the presence of the knock-down vector, PCR was conducted. It was expected that for the lines able to grow on kanamycin they would be positive for the presence of the knock-down vector. Genomic DNA was extracted from leaf tissue for the 5 selected homozygous lines. This genomic DNA fragment was used as a template for PCR to confirm the T3 homozygous lines contain the RNAi knock-down vector (Figure 3.8). The PCR confirmed each line contained the appropriate DNA fragments with a band at 220 bp, as well as confirming the DNA fragment band at 258 bp after visualizing bands after gel electrophoresis. The PCR for the *ndb4* knock-down vector produced two bands on the PCR as seen in Figure 3.8. This is due to the whole genomic *ndb4* gene being present in the plants as well as the knock-down vector containing the 220 bp fragment. The genomic *ndb4* gene is larger in size (580 bp) as the region selected for knock-down spans an intron. This band is not seen in knock-down lines as PCR is optimized for the preference of the 258bp band. For each seed generation, this PCR screen should be conducted to confirm that although stable transformants were made that the knock-down vector is still present at each generation.

3.4.2. Determining knock-down efficiency of vector on *ndb4* gene

When the knock-down region was designed it was determined that the 5'UTR was the least similar with the other alternative NAD(P)H dehydrogenase genes. As the family contains four genes, they are very alike in sequence, and hence it was difficult to find a region that was completely unique Quantitative real time PCR was used to determine knock-down efficiency by comparing the transcript level of the gene to Wild Type *A. thaliana* as well as an empty vector control.

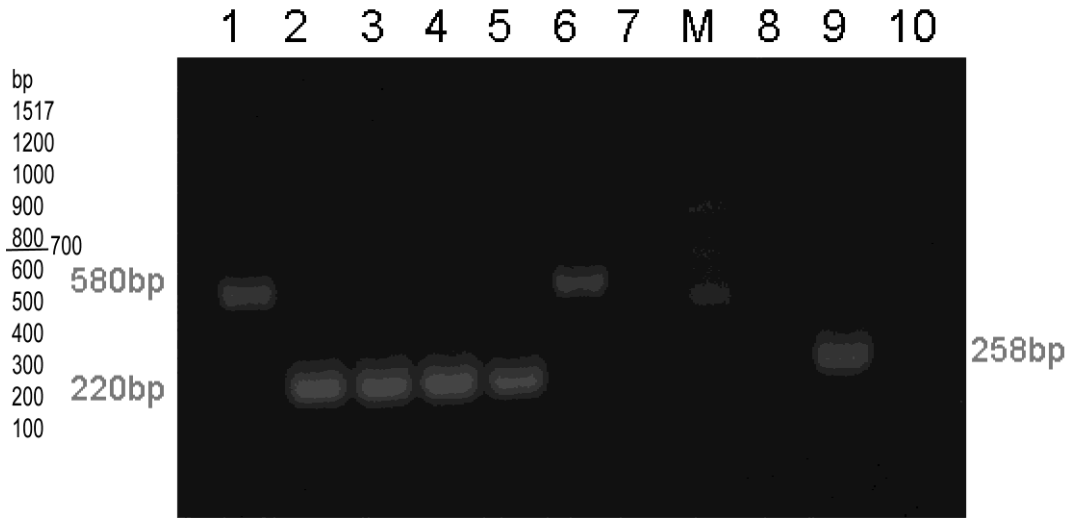

Figure 3.8 PCR conformation that T3 plants contain the *ndb4* knock-down vectors

Lane 1-7 contain PCR products for B4 knock-down vector, at expected size of 220 bp, with genomic *ndb4* at 580 bp. Lane 8-10 contain PCR products for empty vector at expected size of 258 bp. PCR was conducted as described Section 2.10. Primers used were pHANF and pHANR for empty vector and AT4F1 and AT4R1 for pHANNIBAL containing the *ndb4* knock-down region.

Lane 1 Wt tissue
Lane 2 KDb4-1
Lane 3 KDb4-2
Lane 4 KDb4-3
Lane 5 KDb4-4
Lane 6 pART control (empty vector control)
Lane 7 H_20 control
Lane 8 Wt tissue
Lane 9 pART control
Lane 10 H H_20 control
M is 100bp marker

QRT-PCR assays were developed to measure the expression of all the alternative NADPH dehydrogenase genes and *aox1a*. Initially four lines and a control were used to screen for knock-down efficiency. Ubiquitin was used as a reference gene to determine relative values. Ubiquitin had constant absolute values across all samples, indicating it is suitable to use as a reference gene (Appendix B.1 for example of standard curve and amplification). Results from the QRT-PCR indicated that *ndb4* was silenced and the knock-down efficiency varied between each line with KDb4-1 having only 50% knock-down although was significant compared to the pART control line. KDb4-2 however had up to 70% knock-down, and was significantly different compared to pART control as a fold change (Figure 3.9 (A)). KDb4-3 also had 50% significantly lower knock-down expression, and KDb4-4 had significant knock-down of 60%. Absolute (Appendix B.2) and Relative Transcript abundance also indicated the same response (Figure 3.9(B)), indicating that no significant difference between pART control and the Wt indicates that the transformation itself was not having an effect on the *ndb4* gene expression. Once it was confirmed that *ndb4* had been silenced effective, the other alternative enzymes gene expression was assessed.

3.4.3. Transcript analysis of remaining alternative respiratory pathway genes

To look at the expression of the remaining alternative respiratory pathway genes the same QRT-PCR assay was used, with ubiquitin as the reference gene. Results indicated that when there was higher knock-down of *ndb4* as seen in line KDb4-2 there was increased transcript of some of the other alternative genes, mainly *ndb2, nda1* and *aox1a*, (Figure 3.10). *nda1* was significantly increased for all lines. *ndb2* transcript was up regulated significantly in 3 out of the 4 lines, KDb4-2, KDb4-3 and KDb4-4.

When there was only around 50% knock-down of *ndb4* as in KDb4-1 line there were still elevated transcript levels of *aox1a* but not *ndb2* or *nda1*.

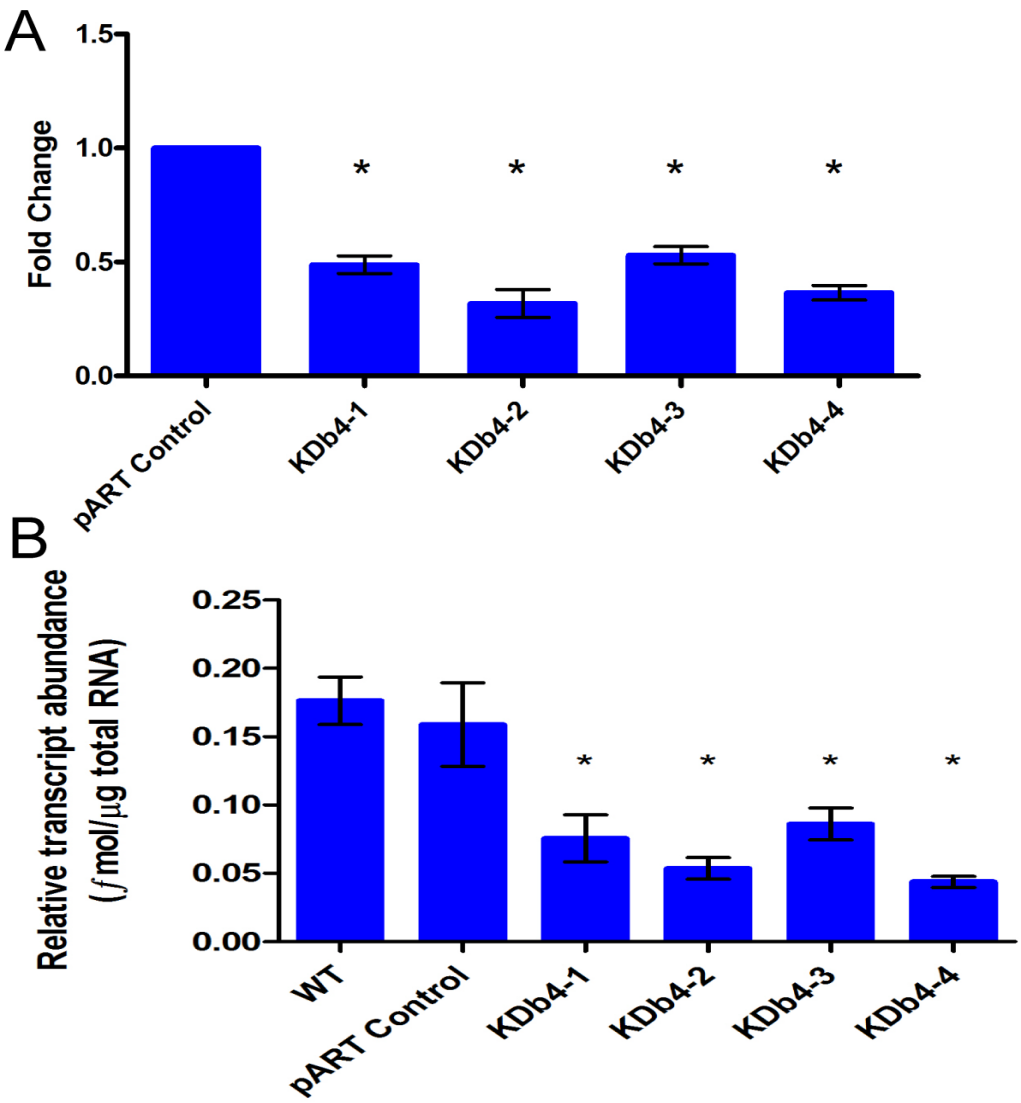

Figure 3.9 Expression of *ndb4* in transformed at Wt plants. (A) Fold change and (B) Relative transcript of *ndb4* in knock-down lines

Relative transcript abundance of *ndb4* in the four independent *ndb4* RNAi lines determined by QRT-PCR. Transcript levels were normalized to the reference gene *Atubiquitin* (At2g17190) and are shown relative to *pART* control, which =1. *pART* control refers to *A. thaliana* plants transformed with empty vector control for comparison to the *RNAi* lines which were generated in this same vector background. Asterisk represents statistically significant differences ($P < 0.05$) between the RNAi lines and control. Values are mean +/- SD for n=6 with * being significantly different from the control at P>0.05. KDb4-1 (Mean diff=0.5117, t=9.201, P<0.001), KDb4-2 (Mean diff= 0.6817, t= 12.26, P<0.001), KDb4-3 (Mean diff= 0.4702, t= 8.454, P<0.001), and KDb4-4 (Mean diff= 0.6350, t= 11.42, P<0.001).

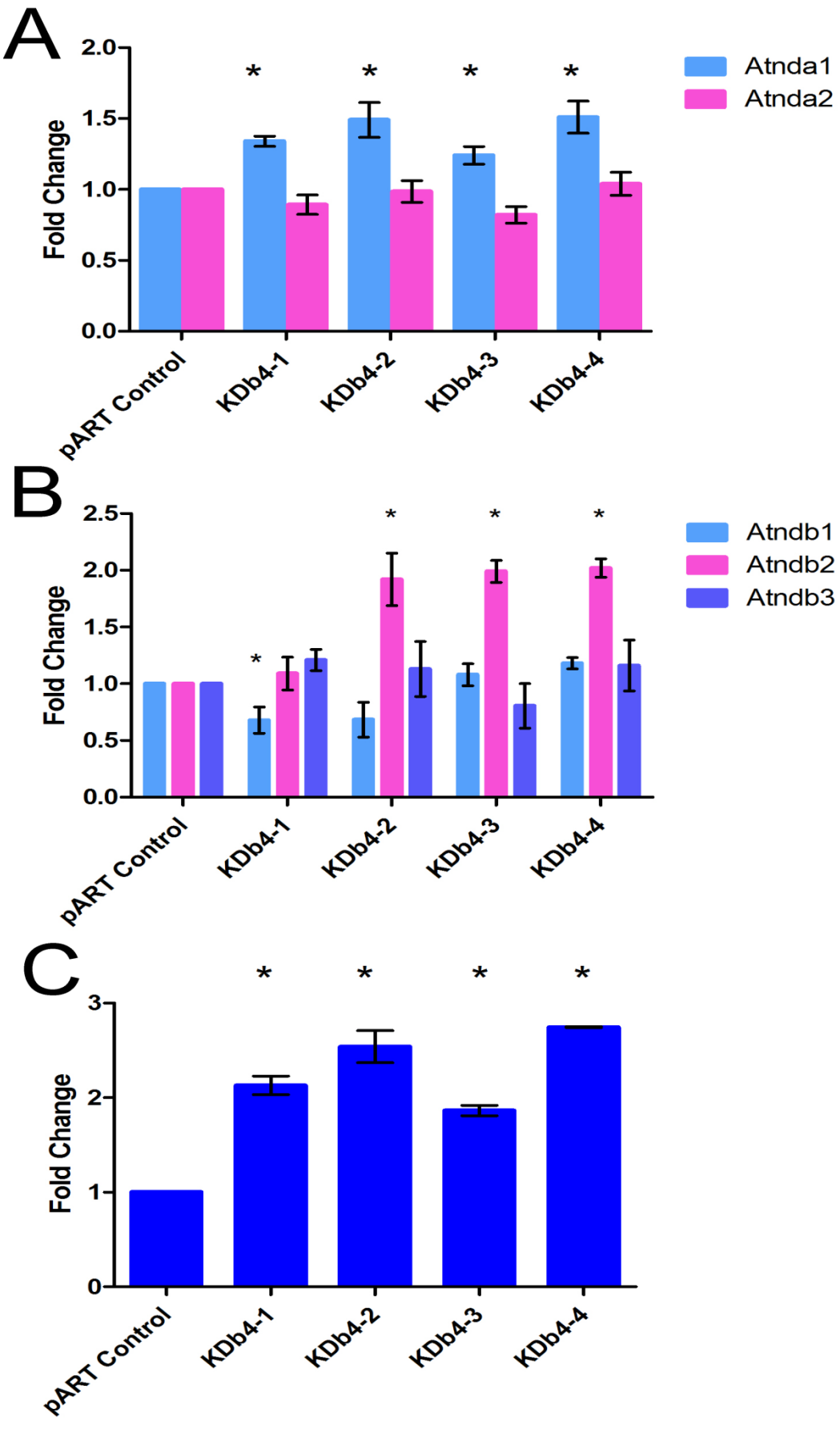
A
Fold Change
2.0
1.5
1.0
0.5
0.0
*
*
*
*
Atnda1
Atnda2
pART Control
KDb4-1
KDb4-2
KDb4-3
KDb4-4
B
Fold Change
2.5
2.0
1.5
1.0
0.5
0.0
*
*
*
*
Atndb1
Atndb2
Atndb3
pART Control
KDb4-1
KDb4-2
KDb4-3
KDb4-4
C
Fold Change
3
2
1
0
*
*
*
*
pART Control
KDb4-1
KDb4-2
KDb4-3
KDb4-4

Figure 3.10 Expression of the alternative pathway genes for *ndb4* knock-down lines

Transcript levels of alternative respiratory enzymes in the *ndb4* mutants. Transcript levels for (A) internal, (B) external NAD(P)H dehydrogenases and C) *aox1a* as determined by QRT-PCR. QRT-PCR transcript profiles for genes of the alternative respiratory pathway of the mitochondria 35 days (10-12 rosette stage). RNA was isolated from cotyledon or rosette leaves, respectively, and reversed transcribed to cDNA for QRT-PCR analysis Transcript levels were normalized to the reference gene *pdf2* (At1g13320) in all cases except 35 day RNAi vs. *pART* control where transcript levels were normalized to the reference gene *Atubiquitin* (At2g17190). In all cases, transcript abundance is shown relative to p*ART* empty vector control which = 1. Values are mean +/- SD for n=3 with * being significantly different from the control at P>0.05. Significance for *nda1*, KDb4-1 (Mean diff=0.3400, t=5.694, P<0.001), KDb4-2 (Mean diff= 0.4900, t= 8.206, P<0.001), KDb4-3 (Mean diff= 0.2400, t= 4.019, P<0.01) and KDb4-4 (Mean diff= 0.5100, t= 8.541, P<0.001). *ndb2* KDb4-2 (Mean diff= 0.9200, t= 8.045, P<0.001), KDb4-3 (Mean diff= 0.9900, t= 8.658, P<0.001) and KDb4-4 (Mean diff= 1.020, t= 8.920, P<0.001). *aox1a* KDb4-1 (Mean diff= -1.130, t= 15.46, P<0.001), KDb4-2 (Mean diff= -1.540, t= 21.08, P<0.001), Kdb4-3 (Mean diff= -0.8633, t= 13.21, P<0.001) and KDb4-4 (Mean diff= -1.745, t= 23.89, P<0.001). *ndb1* KDb4-1 (Mean diff= -0..3210, t= 2.807, P<0.05).

Hence all four lines were significantly increased for *aox1a*. As transcript levels had now confirmed the knock-down of the *ndb4* gene the next step was to look at the biochemistry and any physiological response.

3.4.4. Analysis of the relative protein levels of the alternative dehydrogenases and alternative oxidase in the knock-down lines.

To confirm that the observations seen for transcript levels and activities for the alternative dehydrogenases, resulted in changes in the levels of corresponding proteins, immunoblot analyses were done on the isolated mitochondria. Antibodies were available for NDB2, NDB4, AOX as well as an antibody raised against a homologous region for all NDBs. These four antibodies were used to probe immunoblots of purified mitochondria from wild type tissue, pART control and the KDb4-1 and KDb4-2 lines. An equal amount of purified mitochondrial protein from each plant line was loaded onto the gel, and the resulting blot was also probed with anti-porin antiserum as a loading control.

Initially, the NDB4 antibody was used to confirm that the knock-down of the NDB4 gene resulted in lower amounts of the corresponding protein. There was noticeably less protein present for the two knock-down lines compared to the control at the expected size of 65 kDa (Figure 3.11, 3.12). This was repeated three times from separate mitochondria preparations with similar results. A quantitative program was used to quantitate the amount of protein visualised from the immunoblot. This can be seen in Figure 3.12 where the abundance corresponds to the observations made from the transcript data. The decrease of ndb4 was significant for both KDb4-1 and KDb4-2 The NDB2 antibody was also used to confirm the transcript increase seen with QRT-PCR data. The immunoblot confirmed that the increase in transcript resulted in NDB2 protein and that this may be contributing to the increased NAD(P)H oxidation seen in the KDb4-2 line but not the KDb4-1. The ndb2 antibody detected a protein with a size of 65 kDa, as expected (Carrie *et al.* 2008), this increase compared to pART control for KDb4-2 was significant.

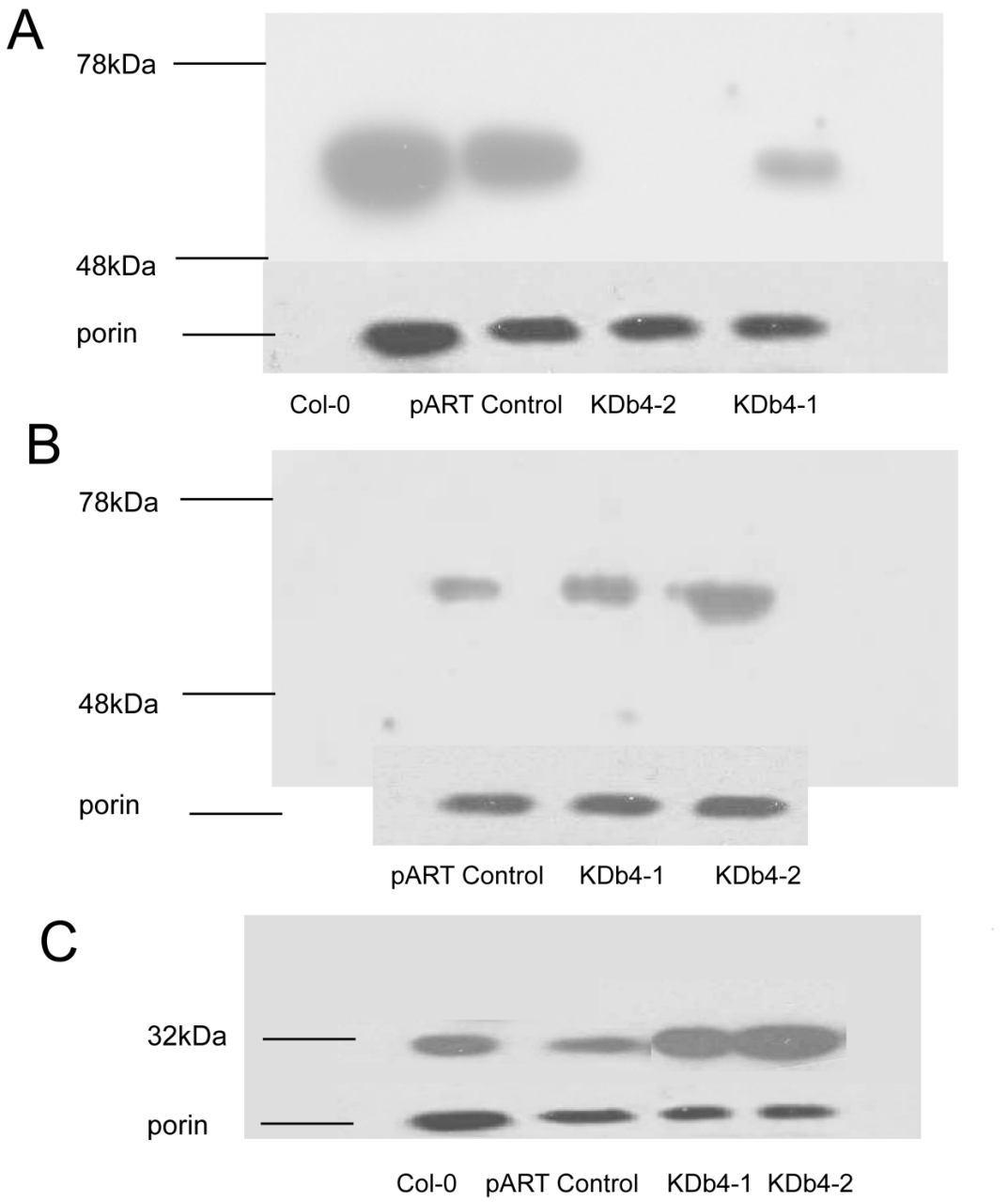

Figure 3.11 Western Blot analysis, to confirm gene transcription changes at the protein level

Isolated mitochondria were resolved on 10% SDS-PAGE, transferred to nitrocellulose, and probed with antibodies against NDB2, NDB4 and Porin. Histograms show protein levels of (A) NDB4, and (B) NDB2, and (C) AOX, in isolated mitochondria from 5-week old *ndb4* knock-down lines. Approximate molecular mass for each protein is given. Isolated mitochondria were resolved on 10% SDS-PAGE, transferred to nitrocellulose, and probed with antibodies against NDB2 NDB4 and the reference protein Porin.

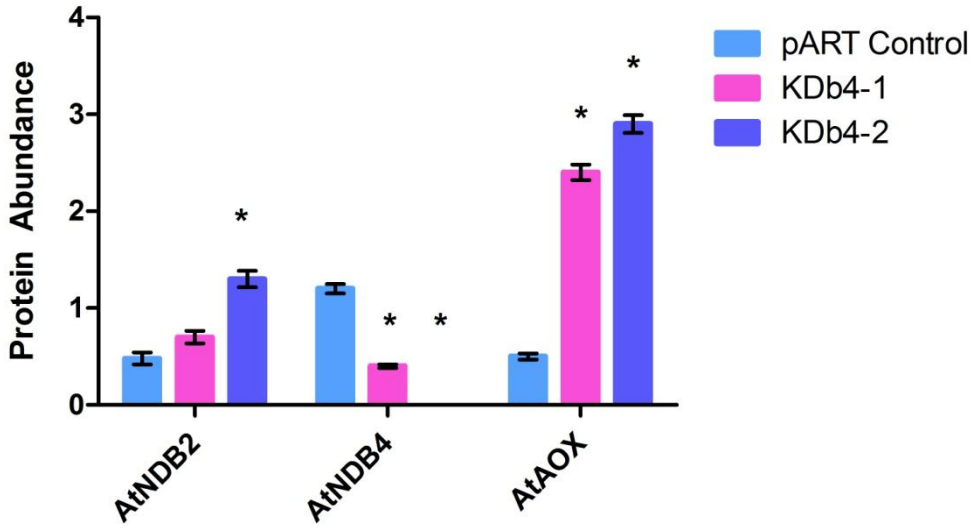

Figure 3.12 Protein abundance for NDB2, NDB4 and AOX

Porin was used as the reference protein for quantification of NDB4 protein levels. The protein abundance is determined from the amount of protein visualised compared to control. Values are mean +/- SE for n=3 * indicates significant difference comparing *ndb4* knock-down lines to pART control.' ndb4, KDb4-1 (Mean diff= -0.8000, t= 9.183, P<0.001), KDb4-2 Mean diff= -1.200, t= 13.77, P<0.001). ndb2, KDb4-2 Mean diff= 0.8200, t= 9.412, P<0.001). AtAOX1a, KDb4-1 (Mean diff= 1.900, t= 21.81, P<0.001), KDb4-2 (Mean diff= 2.400, t= 27.55, P<0.001).

The antibody designed against a homologous region of the amino acid sequence for all the NDB's was also used to probe a blot of isolated mitochondrial protein. This antiserum against this homologous region of NDB protein family was used as crude bleed. There was some non-specific binding of the antiserum to the blot and several bands were detected in the KDb4-2 line, where there was an increase in the *ndb2* gene expression (Figure 3.10). The size of this increased band was only 32 kDa, (Figure 3.13). Interestingly, previous work on beetroot identified a 32 kDa polypeptide which was believed to be responsible for external NAD(P)H oxidation (Luethy *et al.* 1995; Menz *et al.* 1996a). The increase in the 32 kDa band corresponds to the increase in external NAD(P)H oxidation and transcript of *ndb2* seen for this line.

The AOX antibody was also used to confirm that there was an increase at the protein level which corresponded to the increase in *aox1a* transcript data, with the expected size of the reduced form of AOX at 32 KDa (Figure 3.11). The protein increase seen from the immunoblot was quantified from each biological replicate (Figure 3.12), showing a significant increase in the AOX protein level for the KDb4-1, and for KDb4-2 compared to the pART control. For each antibody the membrane used was stripped according to the stripping protocol in Section 2.23.6. The membrane was then probed with the porin antibody which was used as a loading control to confirm that an equal amount of protein had been loaded. It can be seen in from the porin signal that an equal amount of protein had been loaded, confirming the results seen were due to increases in the specific protein rather than due to variation in loading.

3.4.5. Respiratory assays for knock-down *ndb4* lines to determine substrate specificity

3.4.5.1 External NADH Oxidation

The capacity of the external dehydrogenases was measured by adding

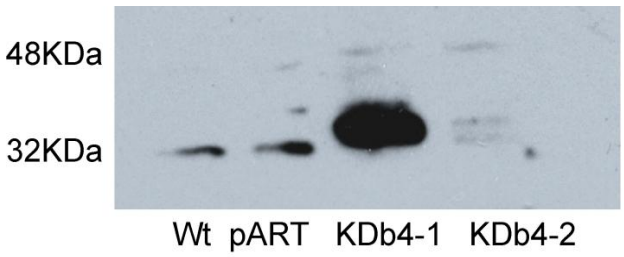

Figure 3.13 Western Blot analysis using an antibody raised to a region of AtNDB that shows high identity amoungst the AtNDB family

Isolated mitochondria were resolved on 10% SDS-PAGE, transferred to nitrocellulose, and probed with antibodies against NDB. Histograms show protein levels in isolated mitochondria from 5-week old *ndb4* knock-down lines, probed with NDB antibody. Protein level of mitochondria from 5 week old *ndb4* knock-down lines and controls. The approximate molecular mass for each protein is given.

NADH to isolated mitochondria and measuring the O_2 uptake rate. Ca^{2+} was added to give maximal activity (Soole *et al.* 1990; Finnegan *et al.* 2004). For the KDb4-1 line, there was a significant decrease in the NADH oxidationrate both in the presence and absence of Ca^{2+}, when compared to the pART line, the empty vector control (Figure 3.14). The calcium-sensitive rate, which is the difference between the - Ca^{2+} and + Ca^{2+} rate was similar for mitochondria isolated from both KDb4-1 and pART plant lines compared to pART control there was significantly less activity for both the – Ca^{2+} rate and + Ca^{2+} rate. Ca^{2+} significantly stimulated the NADH oxidation rate in both the control and KDb4-1 lines to the same amount, suggesting that the lost NADH oxidation activity is calcium independent. Results indicate that the decrease of *ndb4* results in a loss of external NADH activity which is calcium-independent. There was no significant difference between pART control and the line KDb4-2 when comparing NADH oxidation rates in the absence of calcium. In this set of experiments, there was not a significant increase in the NADH oxidation rate in presence of calcium, which was unexpected, but was a trend towards an increase. In the KDb4-2 line, NADH oxidation was significantly increased with the addition of calcium and this Ca-stimulated rate was significantly higher than the Ca^{2+} stimulated rate in pART control (Figure 3.14). The response of NADH oxidation between the different transgenic lines varies and may be a response to the increase in *ndb2* transcript as observed in the KDb4-2 line, which was not observed in the KDb4-1 line (Figure 3.14).

3.4.5.2 External NADPH activity

The external dehydrogenases also exhibit NADPH oxidation activity. There has been much debate as whether this is due to separate dehydrogenase or lack of specificity by the dehydrogenases present. Thus the NADPH oxidation capacity was also determined in these *ndb4* knock-down lines. For the line KDb4-1 there was almost no activity in the absence of calcium and only low activity for the control line, although the difference between these lines for this Ca^{2+} independent activity was significant (Figure 3.14). Once

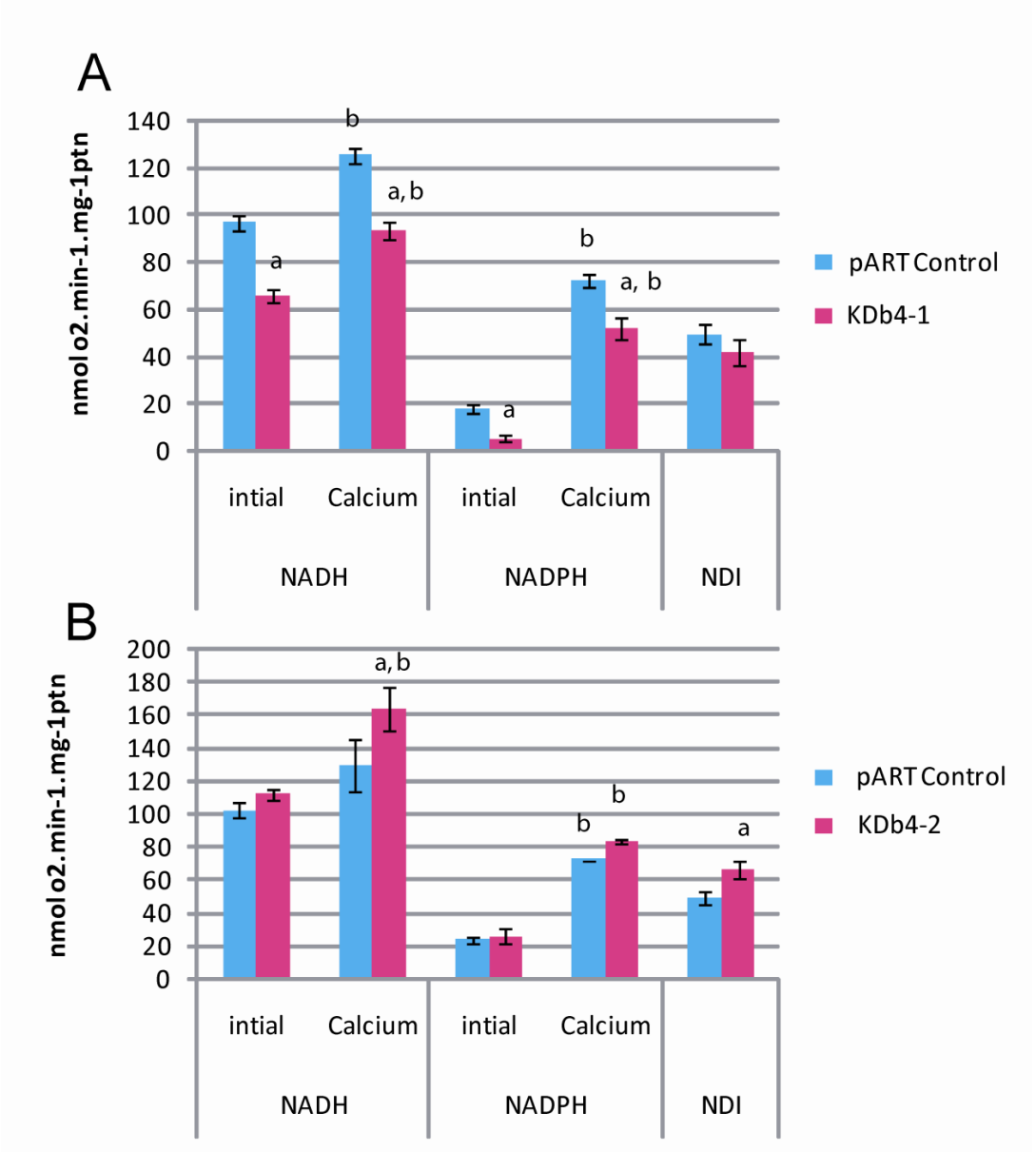

Figure 3.14 NAD(P)H oxidation rates for *ndb4* knock-down lines KDb4-1 and 2

NAD(P)H DH activities measured in intact, isolated mitochondria at 5 weeks of age, from *ndb4* knock-down lines and the pART Control plants. Values are mean +/- SD for n=3 different mitochondrial isolations, with a = significant when comparing control to *ndb4* knock-down line b = significant when comparing inital rate to calcium rate. NADH activity KDb4-1 compared to pART –Ca (Mean diff = -31.06, t= 10.76, P<0.001),+ Ca^{2+} (Mean diff = -31.60, t= 10.95, P<0.001). KDb4-2 compared to pART + Ca (Mean diff= 52.43, t= 9.135, P<0.001). NADPH activity Kdb4-1 – Ca^{2+} (Mean diff= -12.92, t= 4.476, P<0.01), + Ca^{2+} (Mean diff= -20.69, t= 7.166, P<0.001). KDb4-2 + Ca^{2+} (Mean diff= 57.40, t= 10.00, P<0.001). Internal KDB4-2 (Mean diff= 16.44, t= 2.864, P<0.05).

calcium was added there was a significant increase in NADPH oxidation in both plant lines, but the Ca^{2+}-stimulated rate was significantly lower in KDb4-1 line than in pART. The results suggest that calcium is required for activation, in both lines, which has been observed many times for external NADPH oxidation in several plants species (Geisler *et al.* 2007). For the KDb4-2 line there was no significance between the pART control and knock-down line for the -Ca^{2+} rate, but once calcium was added as an activator, there was a significant increase for both control and silenced line. These results indicate that *ndb2* prefers NADH as a substrate and is calcium dependent, whereas *ndb4* uses either NADH or NADPH as a substrate and is calcium independent, although has a preference for NADH.

3.4.5.3 Internal NADH oxidation

The rotenone-insensitive rate of matrix NADH oxidation was determined by the addition of the substrates malate, glutamate and pyruvate to generate NAD(P)H in the matrix. NAD^+ was added to the assay to ensure there was a maximum level of matrix NAD^+ and hence NADH to ensure the internal NADH dehydrogenase activity was fully engaged. EGTA was added to the assay to inhibit any oxidation by the external NAD(P)H dehydrogenases as it is a calcium chelator. For silenced line, KDb4-1, there was a non-significant small decrease in NDI activity while the silenced line KDb4-2 showed a small but significant increase from the control line (Figure 3.14). This small increase correlates with the transcript increase of *nda1*.

3.4.6. Physiological changes of *ndb4* knock-down lines

To determine if the knock-down of *ndb4* had any effect on the growth of the plants a series of growth curves were done for both the roots and leaves. There was some variation between the growth rates of silenced lines with three out of the four lines showing significant differences in the roots at week 5 (although week 4 also had the same trend in significance). Line KDb4-1

showed an increase in growth of roots whilst the KDb4-2 and KDb4-4 lines showed a decrease (Figure 3.15). This trend observed for the roots was also observed in the growth of the leaf tissue, although only KDb4-1 showed a significant difference. This variation in growth could be due to the location of the knock-down construct within the plant's genome and whether it has disrupted a gene associated with growth. The leaf and root growth was also visualised on MS media plated. Root length was measured and indicated that only the KDb4-1 line showed a significant difference having longer roots after 5 weeks of growth compared to the control (Figure 3.16). This same line had denser rosettes with an increased number of petioles, as seen in Figure 3.17, showing the various lines at age 2 and 5 weeks

The leaf area was measured for the two lines which were used for further studies. The 6 day single cotyledon and total leaf area was significantly higher in the pART control compared to both knock-down lines (Figure 3.18(A)), for single leaf KDb4-1 and KDb4-2, For total leaf area at 6 days KDb4-1 and KDb4-2 were both significantly lower compared to pART control. In addition, the silenced line KDb4-1 leaf area was smaller than the other silenced line, which is in agreement with the growth data (Figure 3.15). At day 15 there were a similar trend where the single leaf area for the pART control line was larger than both the silenced lines. However, for the total leaf area the KDb4-1 line was again higher due to more abundant leaves (Figure 3.18(B)). For the 5 week (35-36 days) the data collected included single leaf area, full rosette area, as well as all individual leaves averaged, and it was found that there was a significant decrease for KDb4-1 compared to pART control. Figure 3.18 (C) shows that as for the other plant ages, there was the same trend with individual leaf area being smaller for silenced line KDb4-1 but total area was slightly higher. This correlates with the weight data collected in Figure 3.12, which shows line KDb4-1 to have a higher weight, which is due to having more abundant smaller leaves. In summary, the leaf area of the pART control was significantly larger than the silenced lines; however, KDb4-1 line had a smaller leaf area but more abundant leaves.

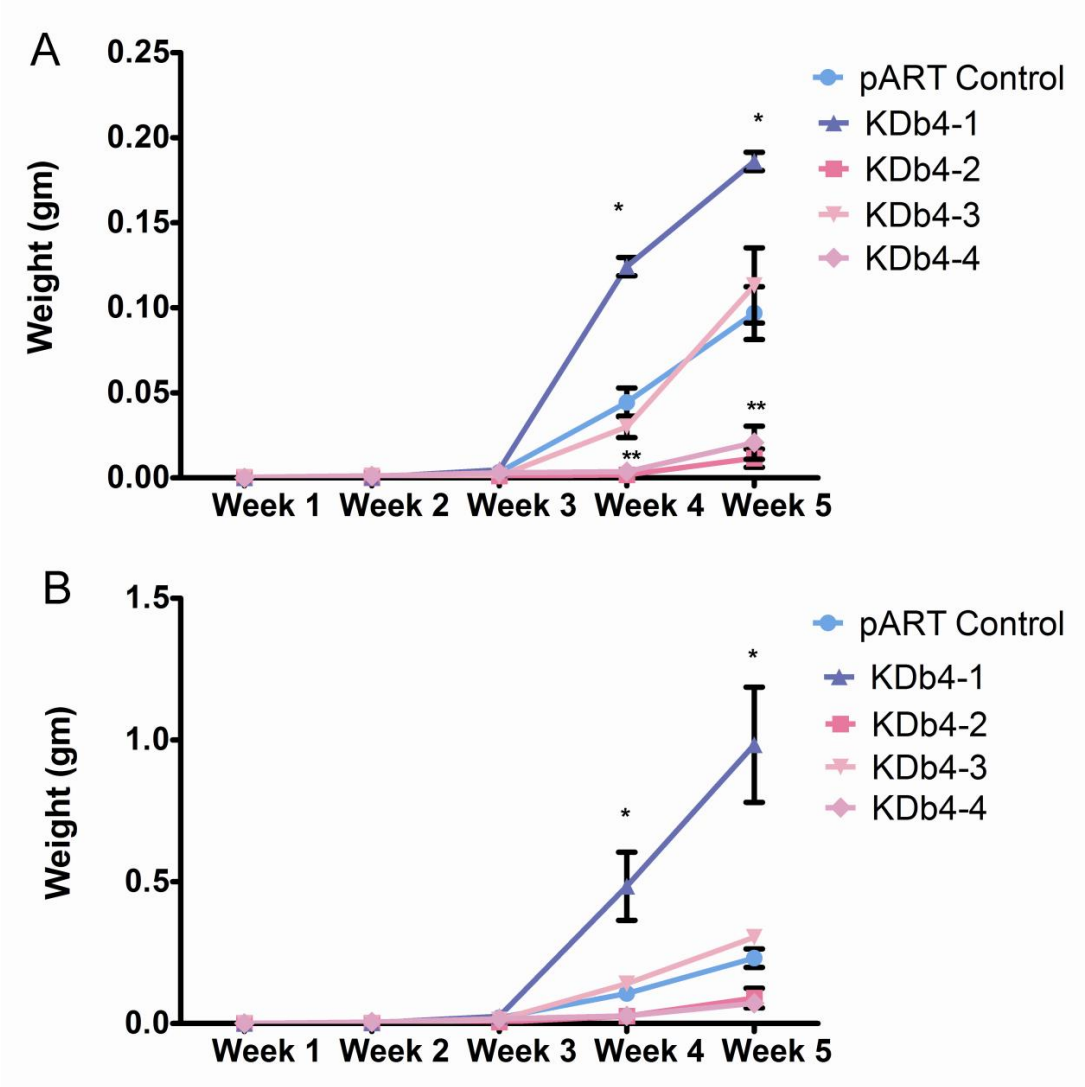

Figure 3.15 Growth rate for both roots and shoots of *ndb4* knock-down lines

Shoot and Roots were weighed weekley from *ndb4* knock-down lines and pART Control plants. The root (A) and shoot (B) measurements indicating variance between the knock-down lines and pART Control. Values are mean +/- SD for n=10 * indicates significant difference comparing *ndb4* knock-down lines to pART control. Roots, KDB4-1 (Mean diff= 0.08910, t= 11.02, P<0.001), KDB4-2 (Mean diff= -0.0853, t= 10.55, P<0.001), KDB4-4 (Mean diff= -0.07623, t= 9.429, P<0.001). Shoots, KDB4-1 (Mean diff= 0.7527, t= 10.96, P<0.001).

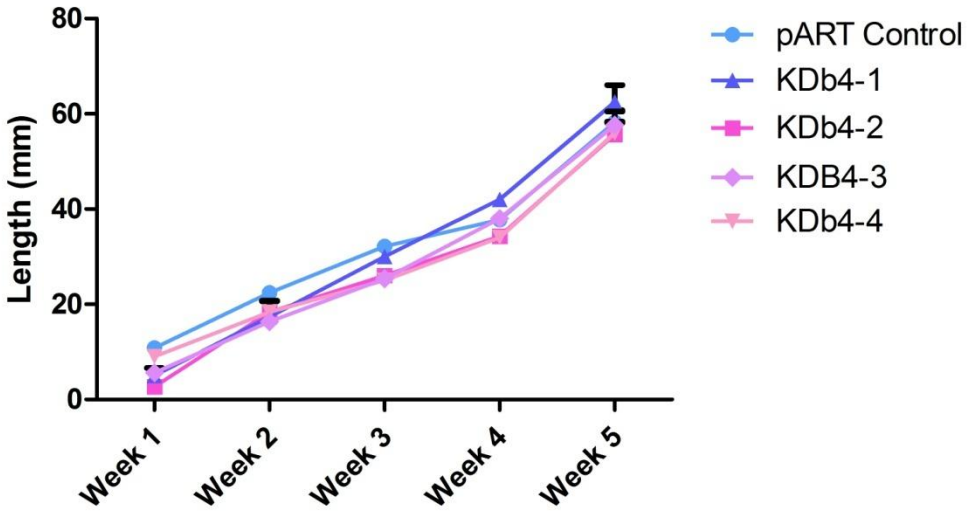

Figure 3.16 Root length measurements for *ndb4* knock-down lines

Root length was measured from plants growing on MS Media plate's weekley. Values are mean +/- SD for n=10. KDB4-1 (Mean diff= 4.267, t= 3.328, P<0.05).

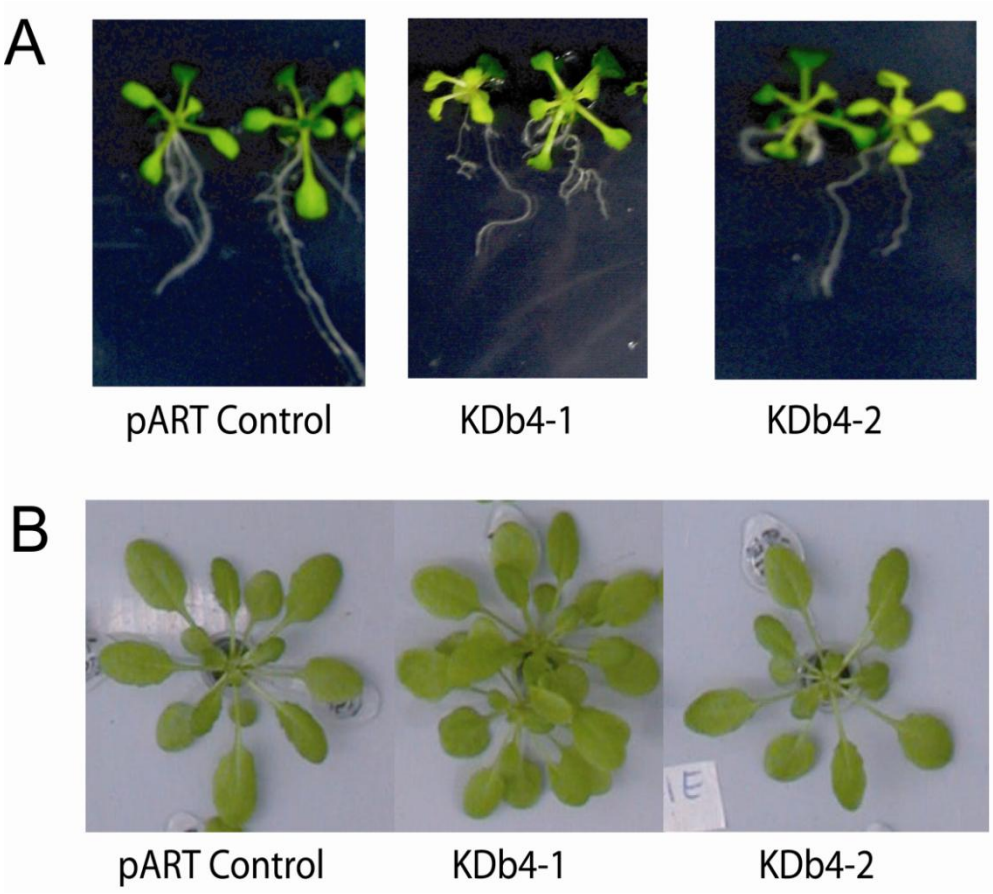

Figure 3.17 Visual observations of plants at 2 weeks and 5 weeks

Leaf development of *ndb4* mutants under unstressed conditions. pART empty vector control, and *ndb4* mutant plants were grown for a total of 5 weeks at 21 ^{o}C under ~120 µE (m^{-2} s^{-1}) of light with a 16/8 light/dark photoperiod. Photographs of rosettes were taken at the 5-6 rosette stage (14 days) and the 10-12 rosette stage (35 days after germination) and represent a minimum of *n*=3 biological replicates for each plant line. (A) 2 week growth on MS media plates and (B) 5 week growth in hydroponic set up.

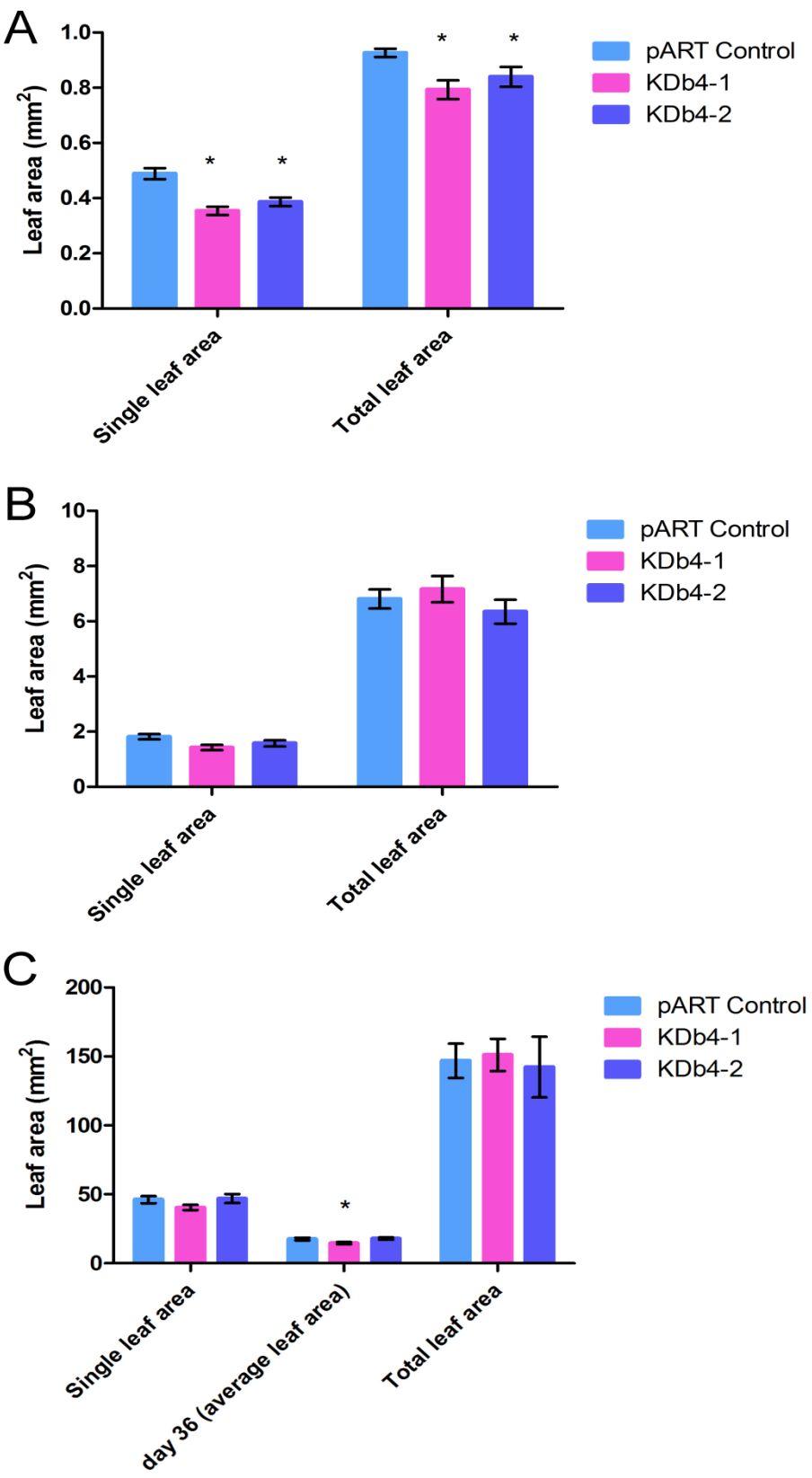
A
Leaf area (mm2)
1.0
0.8
0.6
0.4
0.2
0.0
*
*
*
Single leaf area
Total leaf area
pART Control
KDb4-1
KDb4-2
B
Leaf area (mm2)
10
8
6
4
2
0
Single leaf area
Total leaf area
pART Control
KDb4-1
KDb4-2
C
Leaf area (mm2)
200
150
100
50
0
*
Single leaf area
day 36 (average leaf area)
Total leaf area
pART Control
KDb4-1
KDb4-2

Figure 3.18 Leaf area analysis at 6 days, 15 days at 36 days

Average leaf area of *ndb4* mutants and appropriate controls at three stages of development: (A) 2-cotyledon stage (6 days), (B) 4-leaf stage (15 days), and (C) 10-12 rosette stage (35 days). Leaf area was calculated using Image J software. Error bars = ± SE of the mean (*n* = 20). Values are mean +/- SD for n=20 * indicates significant difference comparing *ndb4* knock-down lines to pART control. 6 day single leaf, KDb4-1 (Mean diff= -0.1353, t= 3.946, P<0.05), and KDb4-2 (Mean diff= -0.1021, t= 2.978, P<0.01). Total leaf area, KDb4-1 (Mean diff= -0.1328, t= 3.873, P<0.001), KDb4-2 (Mean diff= -0.08635, t= 2.518, P<0.05). Day 36, average leaf area, KDb4-1 (Mean diff= -2.963, t= 3.738, P<0.001).

3.5 Discussion

Post transcriptional suppression of targeted proteins can help to determine which specific putative gene encodes which protein. Until this study the NAD(P)H substrates specificities of the alternative dehydrogenases were not completely clear, despite experiments by (Geisler *et al.* 2007) examining preferred substrates of the *A. thaliana* alternative NAD(P)H DHs using fusion proteins in an *E. coli* host. There is still very limited knowledge known about the function of the alternative dehydrogenases compared to the alternative oxidase where a large amount of research has already been done (Clifton *et al.* 2006).

The pHANNIBAL vector was chosen as the knock-down vector as it has previously been demonstrated that it is effective at knock-down from only small bp regions about 100-200 bp in size (Wesley *et al.* 2003). As there is a high number of homologous DNA sequence regions within the alternative NAD(P)H dehydrogenase family we were limited in the choice of regions that were specific and unique to each gene family member. Therefore, from sequence alignments, it was only possible to select small regions of the sequence that had less chance of the other genes in the external dehydrogenase family being silenced. pHANNIBAL has been shown to have knock-down efficiency of up to 90%, although it has some experimental flaws which have been overcome by a new RNAi knock-down vector pHELLSGATE (Wesley *et al.* 2003; Wesley *et al.* 2004). The new knock-down vector eliminates the two rounds of directional cloning required by pHELLSGATE. For the preparation of any new knock-down vectors, it would be recommended to use the new pHELLSGATE knock-down vector and the gateway cloning system from Invitrogen. The pART vector was used for expression as it contains the Not I restriction site which allowed for ligation of the pHANNIBAl fragment containing the hairpin loop with knock-down regions. The pART vector also contains the NPT II gene which confers kanamycin resistance in plants. This allows for easy selection of plants that have taken the vector up, as those that haven’t will not be resistant to

kanamycin. Kanamycin resistance is an easy test to select for plants which are positive, as all plants can be placed on MS agar with the addition of kanamycin. Those plants that contain a cassette will be able to grow. This easy selection saves time as not every plant has to be tested at the molecular level which is time consuming. Only the plants which are resistant are tested to confirm the presence of the vector.

The knock-down efficiency of RNAi constructs can vary, although 300-500 bp are recommended. (Wesley *et al.* 2003) showed that smaller regions of sequence could be used including the 5'UTR which was found to be necessary for this homologous NDB gene family. Knock-down efficiency was determined by quantitative real time PCR which indicated varying knock-down of the mRNA for *ndb4* between the lines. The variation in knock-down is often observed due to the first step of RNAi knock-down known as the initiation step. This step which involves the cleavage of the triggering dsRNA into siRNAs of 21–26 nucleotides with 2-nucleotide overhangs, which correspond to both sense and antisense strands of a target gene (Kumar *et al.* 2003). As each vector will be targeted differently by this dicer complex the nucleotide blocks will be broken up differently and this will result in different knock-down patterns and hence efficiency (Helliwell *et al.* 2005). As the homology between the NDB gene family is quite high (Figure 3.1) there was a chance that some of the other dehydrogenases could be silenced as well. When looking at the 200 bp region used for knock-down *ndb4*, it can be seen that there is 56% identity with *ndb1* (Figure 3.1). This can explain why there was transcript knock-down of about 30% of *ndb1* for knock-down lines KDb4-1 and KDb4-2.

The most noticeable observation from QRT-PCR was the elevated transcript level of *ndb2* and *aox1a* when *ndb4* was silenced. This is not the first time *ndb2* and *aox1a* have been shown to exhibit co-expression. Both NDHs and AOX are encoded in two discrete gene subfamilies in higher plants. Members of the AOX1 subfamily, represented by AOX1a-d in *A. thaliana*, are induced by a range of stress stimuli and proposed to relate to a particular need under stress conditions (Clifton *et al.* 2005). It has been suggested that genes

displaying similar expression patterns may share regulatory pathways and have common binding sites for the relevant transcription factors (DeRisi *et al.* 1997; Spellman *et al.* 1998; Park *et al.* 2002). Clifton *et al.* (2005) observed the co-expression of AOX1a and NDB2 during many different stress conditions and suggest that the co-regulation is supported by the presence of common sequence elements with similar organisation within the sequence upstream of the coding region of both these genes. (Ho *et al.* 2008) also suggested a co-regulation of *ndb2* and *aox1a under addition of salicylic acid.* In this study, we observed that when *ndb4* was silenced, both *ndb2* and *aox1a* transcript levels increased, in agreement with these previous studies (Clifton *et al.* 2005; Ho *et al.* 2008) It was thought that the increase in *ndb2* initially could be due to the loss of *ndb4* and *ndb2* acting as a compensatory effect to take over the role from the loss of function caused by the *ndb4* gene. Elhafez *et al.* (2006) also suggested that *ndb2* and *aox1a* are primarily up regulated in response to a wide variety of treatments. AlthoughNDB4 has been hypothesized to function in plant growth and development based on its co-expression with the alternative oxidase AOX1c, there is also evidence in support of a similar role for NDB2. Although NDB2 is most well-recognized for its associated role with AOX1a in response to various stresses in the plant cell (Clifton et al., 2005; Elhafez et al., 2006; van Aken et al., 2009), *ndb2* transcript is evident at several time points throughout plant development and in several different plant tissues even without the addition of stress (Elhafez et al., 2006). Thus, it is likely that NDB2 serves additional roles in the plant other than merely as part of the stress response with AOX1a. Supporting this supposition, correlation of co-expression analysis and indicating a positive relationship with *ndb2*.

Thus, it seems likely that both NDB2 and NDB4 have similar non-stress related physiological roles in Arabidopsis and over-expression of either one may cause altered growth and development in the plant, specifically as observed in our study, by stimulating an increase in relative growth rate and subsequent increase in leaf area. This data was suggested from analysing genevestigator data (Genevestigator is a web-based application developed for biologists and medical researchers to rapidly find out in which tissues, at

which stages of development, and to what stimuli, drug treatments, diseases, or genetic modifications genes of given organisms are activated) where it was determined these genes respond to a large number of stresses (Elhafez *et al.* 2006). Hence it is possible that these two genes are responding together to co-ordinate an internal pathway within the ETC which directs excess NAD(P)H from the external dehydrogenases to AOX. It is possible that the lack of *ndb4* which may also have played a role in this stress response, results in higher *ndb2* in these plants to compensate for a lack of *ndb4*. The results of my work also support previous observations that these genes are co-regulated.

Analysis of the NAD(P)H oxidation activity of mitochondria isolated from the silenced plants from two different parental lines, showing different knock-down levels allowed the substrate specificity for both *ndb2* and *ndb4* to be suggested. From the perspective of enzyme function *in vivo*, substrate and affecter specificities must be placed in their metabolic context. External mitochondrial NAD(P)H dehydrogenases are directed toward the intermembrane space, which is metabolically and ionically connected to the cytosol via porin channels (Geisler *et al.* 2007). The pH of the plant cytosol is estimated to be 7.2–7.5 (Roberts *et al.* 1984; Felle 2001) but can decrease by 0.3–0.6 units upon light changes or hypoxia (Fox *et al.* 1995). The estimated concentration of free Ca^{2+} in the plant cytosol is below 1 uM (Moller 1997) but can increase dramatically in response to stress (Knight *et al.* 1996). The concentrations of free and total NADH in the plant cytosol are estimated to be around 0.5 and 55 µM, respectively (Heineke *et al.* 1991). NADPH concentrations are in both cases (free and total) are estimated to be around 150 µM (Igamberdiev *et al.* 2003). Line KDb4-1 with only limited *ndb4* knock-down and no observed *ndb2* transcript increase results in the decrease of both NADH and NADPH calcium independent activity. This data tells us that NDB4 uses both NADH and NADPH as a substrate but according to results it has a preference for NADH. This data correlates with what was observed in *E. coli* for the *A. thaliana* genes which indicated *ndb4* was a calcium independent NADH dehydrogenase (Geisler *et al.* 2007). For the silenced line KDb4-2, which had transcript increases for *ndb2*, there were

altered activities that suggested that *ndb2* was a calcium dependent NADH activity. Previously *ndb2* has been suggested to be a calcium dependent NADH dehydrogenase (Geisler *et al.* 2007). Geisler *et al.* 2007 also indicated that *ndb1* is a calcium dependent NADPH dehydrogenase. The slight increase that was observed for internal oxidation for knock-down line KDb4-2 correlates with QRT-PCR *nda1* increases seen. An increase in NDA1 along with ndb2 has been linked showing diurnal control (Elhafez *et al.* 2006). With *nda1*, *ndb2* and *aox1a* there is the potential to form a complete respiratory chain capable of oxidising internal and external NAD(P)H.

Immunoblots were done to confirm if protein levels corresponded to the transcript data. Previously, a 32 kDa protein that oxidised NADH was purified and localised to the outer surface of the IM or to the intermembrane space in maize mitochondria (Luethy *et al.* 1991b; Knudten *et al.* 1994). As well as this 32 kDa protein, a 43 kDa protein that had both NADH and NADPH dehydrogenase activity had been identified from red beet root (Luethy *et al.* 1991b; Menz *et al.* 1996b). This protein was localised to the inner surface of IM, hence this protein is an internal dehydrogenase. A 58 kDa protein with NADH dehydrogenase activity was also isolated from red beet root and maize. In maize this protein had both NADH and NADPH dehydrogenase activity and was isolated to the outer membrane (Menz *et al.* 1996a). The AtNDB proteins have predicted molecular masses of 63-65 kDa, including the putative presequence (Rasmusson *et al.* 2004). Results determined from immunoblots confirmed what was found in transcript data that *ndb4* expression was down in the KDb4-1 knock-down line and was also down in line KDb4-2 as well as NDB2 protein having higher abundance for KDb4-2. The AOX protein also had expected higher abundance. To confirm the 32 kDa band was an external NADPH dehydrogenase the band could be isolated and N-terminal sequencing done. It is possible this could be post-transcriptional modification occurring for one or more of the *ndb* genes.

This work has allowed us to generate a tool for looking at the biological implication for altered gene expression. By using a genetic, protein and physiology approach we were able to link a gene to function. Only one gene

could be matched to an activity, due to compensation from the other *ndb* genes. It has also helped to elucidate that these genes may play a more important role in the plants, hence why co-expression of these genes is seen. Although further work is needed to identify the remaining alternative dehydrogenases, this work has provided a method to be able to do this. In future it may be more beneficial to analyse over expressors to help determne substrate specificity due to the compensation between genes seen.

4 GENERATION OF A LETHAL PLANT FOR ALL OF THE EXTERNAL ALTERNATIVE NAD(P)H DEHYDROGENASES

4.1 Introduction

4.1.1. Knock-down of the *ndb* family

Previously a single external alternative dehydrogenase gene had been silenced using the RNAi knock-down vector pHANNIBAL (Chapter 3). Plants resulting from the knock-down of *ndb4* were able to grow at a similar rate although there were some significant physiological differences, such as significant changes in leaf area compared to Wt plants. It appeared from these experiments that when one gene was silenced another external ndb gene increased in transcript levels and appeared to a compensation for the loss of the silenced gene. This has been observed before when there was increased external NAD(P)H dehydrogenase activity in *nda1* mutation plants (Day *et al.* 1981; Moore *et al.* 2003). This compensatory effect, which may be due to gene redundancy in *A. thaliana*, interferes with the strategy of using gene knock-down to link gene to enzyme and examine the physiological impact of the absence or decrease in activity of one of the external NAD(P)H dehydrogenases. Thus, it was decided to explore a strategy where all four external dehydrogenase genes were silenced in the one plant it could be determined if these external dehydrogenase genes are required by the plant. Although external NAD(P)H oxidation has been known for a long time, its physiological importance is still not understood, even in red beet root which has been one of the most studies induction systems (Rasmusson *et al.* 2004). Although these genes have been identified in most species, they are not in every species. Although no physiological role has yet been completely identified, correlative evidence suggests that these enzymes play a role in the response of a plant under stress The alternative dehydrogenases give the plants the flexibility to fine tune the redox balance in the cytosol and mitochondrial matrix, which in turn acts to protect the plant (Finnegan *et al.*

2004). To determine if knock-down all four external dehydrogenases would generate viable plants a knock-down vector was created using a homologous region of sequence with high identity within the *ndb* gene family.

4.1.2. pHELLSGATE knock-down vector

Recently with the completion of the *A. thaliana* genome project; the advent of micro-array technology; and the ever increasing investigation into plant metabolic, perception and response pathways, a rapid, targeted way of silencingn genes would be of great interest (Arabidopsis Genome Initiative 2001). The RNAi silencing vector pHANNIBAL which had been used previously as the *ndb4* knock-down vector was successful at knock-down plants. The use of the knock-down vector pHANNIBAL is cumbersome in that it requires two rounds of directional cloning which can be timely, as well as a third round of cloning into an expression vector. To overcome the directional cloning issues of Phannibal, Helliwell *et al.* (2002) created a newer RNAi knock-down vector pHELLSGATE. This new knock-down vector takes advantage of Gateway technology which facilitates easy cloning of PCR fragments (Invitrogen, USA). With this technology, a PCR fragment is generated (bordered with recognition sites *att*B1 and *att*B2) which is directionally recombined in vitro into a plasmid containing *att*P1 and *att*P2 sites using the commercially available recombinase preparation (Invitrogen, USA). The system incorporates a negative selection marker (*ccd*B) that selects against E. Coli that do not have a suitable vector, resulting in a high frequency of recovery of recombined plasmids (Wesley *et al.* 2004). The pHELLSGATE vector was designed such that a single PCR product from primers with the appropriate *att*B1 and *att*B2 sites would be recombined into it simultaneously to form the two arms of the hairpin (Figure 4.1). The *ccd*B gene, which is lethal in standard *E. coli* strains such as DH5a was placed in the locations to be replaced by the arm sequences, ensuring that only recombinants containing both arms would be recovered.

Despite recent work on the external alternative NAD(P)H DH pathway there

is still limited knowledge known about their physiological function within the plant. Even though 7 putative *A. thaliana* alternative NAD(P)H dehydrogenase genes have been identified it has not been confirmed if all, some or any are essential in plant growth . The work in this chapter was done to help address this question with respect to the *ndb* gene family.

4.2 Aim

The overall aim of the following work was to generate *A. thaliana* knockdown plants for all of the external alternative dehydrogenase genes in the one plant with a homologous region. Then to determine if these plants were viable and knock-down was occurring. It was hoped to determine if the external alternative dehydrogenase enzymes are needed for viable plants, and if variation in knock-down occurred the substrate specificity could be confirmed for all genes.

4.3 Results

4.3.1. Identifying homologous region between all four external alternative dehydrogenases

Initially gene sequences for all seven putative alternative dehydrogenases were downloaded from MATDB from the MIPS website (Arabidopsis Genome Initiative 2000; Schoof *et al.* 2002). The seven genes were *ndb1* (AT4G28228), *ndb2* (AT4G05020), *ndb3* (AT4G21490), *ndb4* (AT2G20880), *nda1* (AT1G07180), *nda2* (At2G29990) and *ndc1* (At5G08740). Using the Angis Bioinformatics software alignments were done first between the four external encoding *ndb* genes, then with the three internal encoding *nda* and *ndc* genes. The ClustalW (accurate) algorithm (Thompson *et al.* 1994) was used to perform pairwise multiple DNA sequence alignments between the four external dehydrogenases, in the hope a homologous or identical region of the sequences could be found that was not high in identity to the internal dehydrogenases. Each pairwise multiple sequence alignment as well as

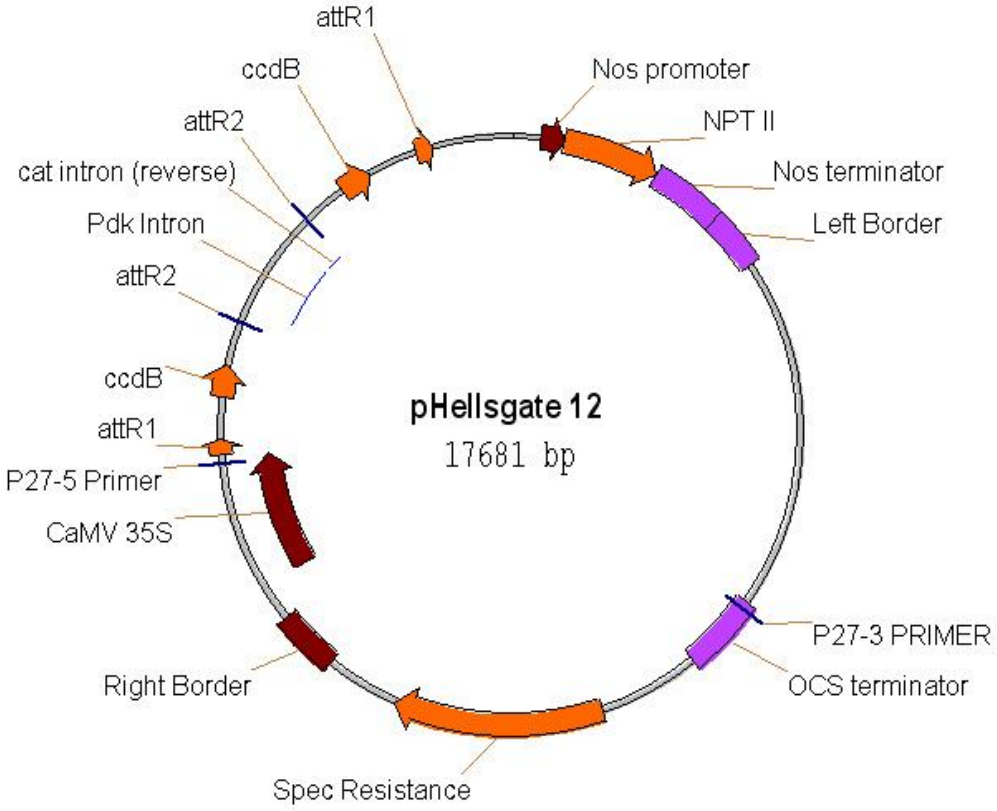

Figure 4.1 pHELLSGATE Vector map

The pHELLSGATE12 cloning map, where the two Intron loops are seen, as well as the *ccdB* lethal genes (Helliwell *et al.* 2002).

all four genes aligned together were viewed using the computer program GeneDoc. The four external genes were aligned separately, with the gene of origin being *ndb2*. A region was selected from multiple sequence alignments of all four genes as seen in Figure 4.2. The criteria that were set to optimise for selection of a sequence that would result in the most efficient knock-down were that the region needed to have the highest identity and a high number of blocks with 12 or more identical regions. This was found for all four of the external genes with this selected region of the *ndb2* sequence. Although the UTR does have success in silencing, when knock-down is required from a gene from a homologous gene family it is ideal to use the ORF as has been done for this knock-down vector, as the ORF will contain the moat similarity between gene family members. Although regions of between 300 and 1000 bp are ideal for knock-down (Wesley *et al.* 2004), in this case only a 173 bp region was selected as to avoid high identity with other related genes, such as the *Atnda* and *ndc* genes, and minimise preference for knock-down only 1 or 2 genes from the external *ndb* family. When a longer bp sequence was selected there was lower identity between the external dehydrogenase family, and higher identity with the internal genes. As seen in Figure 4.3(A-C) there was very little sequence identity with the remaining 3 alternative dehydrogenase genes, *nda1*, *nda2*, and *ndc1* and no regions with 12 or more blocks of identify. This should allow for a knock-down construct which will only silence the four external dehydrogenases and not the internal and *ndc1* genes. As seen in Table 4.1 the identity of this selected sequence between all four external dehydrogenases is quite high all above 76%. The identity between the selected sequence and the *nda*'s and *ndc1* is quite low and neither contains 12 blocks or more of identity.

4.3.2. Amplification of the homologous *ndb* knock-down region

4.3.2.1 Amplification of the *ndb2* gene

Although *ndb2* clones were available in the lab, they all had numerous errors. Hence it was decided to generate a new full length clone of *ndb2* from Wt plants. This gene was selected to be used for knock-down as it was the gene

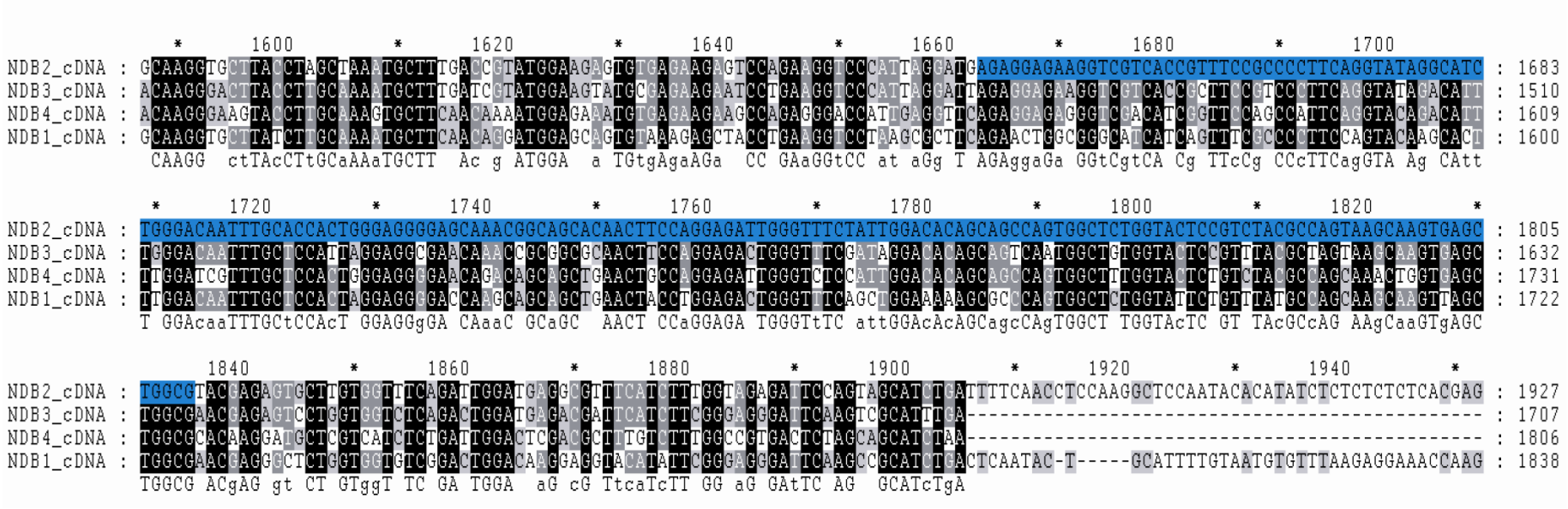

Figure 4.2 *ndb* family alignemnt with knock-down region from *nbd2* highlited in blue

Alignment of all four *Arabidopsis* external alternative NAD(P)H dehydrogenases with the 173 bp region used to generate the *ndb* RNAi lines highlighted in blue. Sequence with 100% identity is highlighted in black. A pair wise alignment was done. The region in blue highlights the region selected as *ndb* knock-down region. The areas of sequence homology are indicated by shading, the dashes (-) represent the gaps inserted to maximise the sequence alignments.

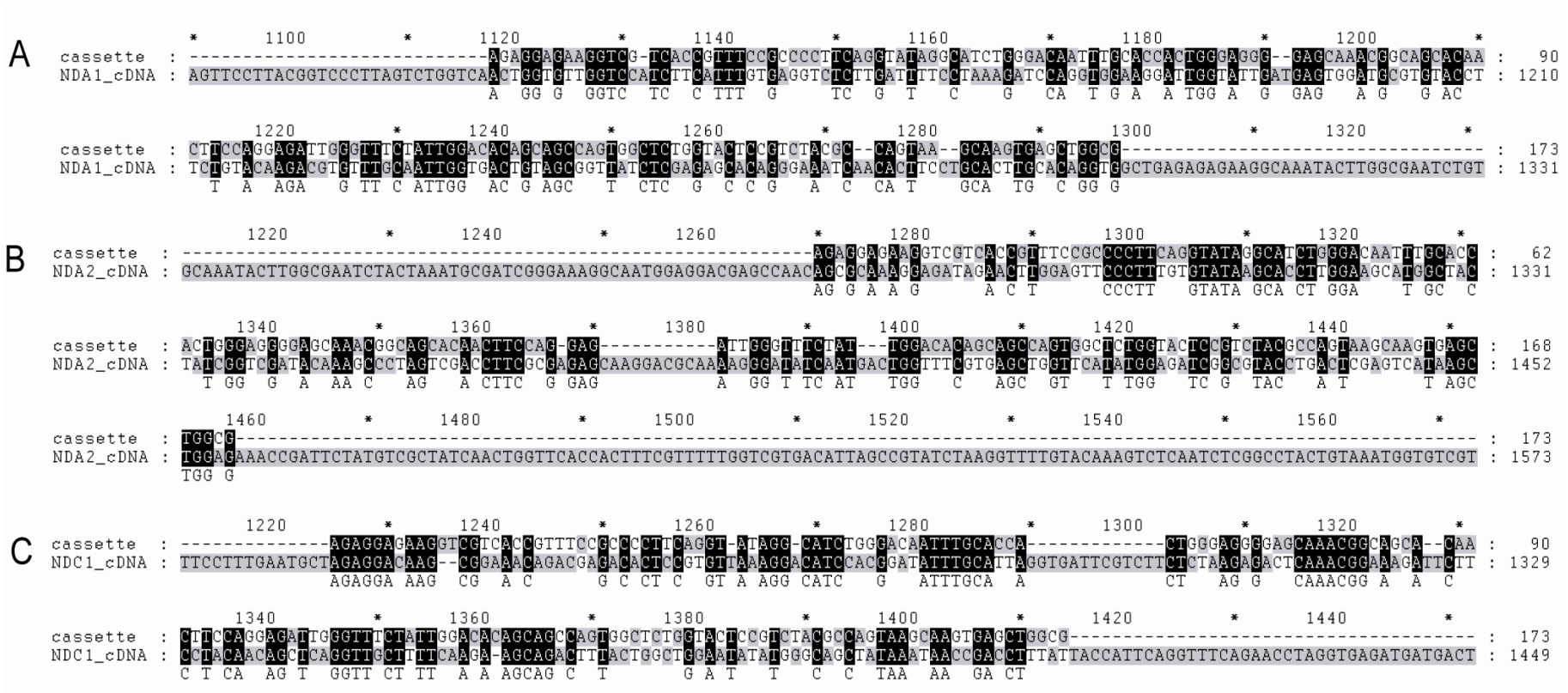

Figure 4.3 Individual alignments of *ndb* knock-down region with (A) *nda1*, (B) *nda2* and (C) *ndc1*

Alignment of the *ndb* knockdown region with (A) *nda1*, (B) *nda2* and (C) *ndc1* to determine the sequence similarity. A pair wise alignment was done with each pair.

of most interest to be silenced of the four, as it was also hoped to generate *ndb2* knock-down plants for future experiments to cross with the *ndb4* knock-down plants. Hence if this knock-down line only silences the gene it was selected against, it will be *ndb2*. RNA extractions were done using healthy 6 week old plant tissue (Figure 4.4).

4.3.3. Initial attempts to clone into pHANNIBAL knock-down vector

The first attempts to generate a knock-down vector for the homologous *ndb* gene region used pHANNIBAL vector. The primers were designed for PCR products to be amplified with primer pairs that allowed the same DNA sequence to be inserted into the vector in a sense and antisense direction. To amplify the antisense orientation product the forward primer required the *BamHI* recognition site and the reverse primer a *ClaI* recognition site (Table 2.1). For the sense orientation the forward primer required the *XhoI* site and the reverse primer the *KpnI* recognition site.

Once the PCR product to be used for cloning was amplified and sequenced successfully, digestion of both the pHANNIBAL vector and PCR product could occur. Initially the sense fragment was digestion both with *XhoI* and *KpnI* as well as single digests as a positive control to confirm digestion was occurring (Figure 4.5A). This sense fragment was successfully ligated into pHANNIBAL (Figure 4.5B). The next step was to ligate the antisence fragment into pHANNIBAL with the sense fragment. After several attempts and optimisation, a positive clone could not be generated. Hence it was decided to try the new gateway cloning method using pHELLSGATE.

4.3.4. Decision to move to pHELLSGATE knock-down vector

After initial trouble with pHANNIBAL and cloning it was decided to move to the newer knock-down vector pHELLSGATE and the gateway cloning system, to generate the knock-down vector rapidly.

Table 4.1 % identity with *ndb* knock-down region and remaining alternative DH genes

The sequence identity indicates which genes have a high identity with the homologous knockout region as determined from pairwise alignments (Section 2.3)

Gene	identity
NDA1	47%
NDA2	50%
NDB1	76%
NDB2	100%
NDB3	88%
NDB4	83%
NDC1	53%

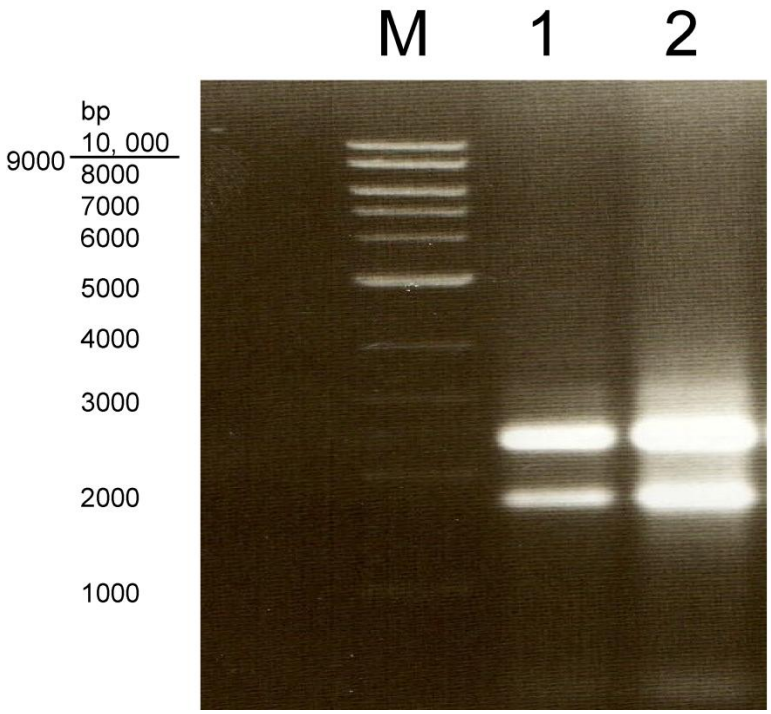

Figure 4.4 RNA of Wt Col plant tissue

RNA extractions were done on 100mg of *A. thaliana* leaf tissue to generate RNA for use to amplify *ndb2* gene.

M is 1Kb marker

Lane 1 Wt tissue #1

Lane 2 Wt tissue #2

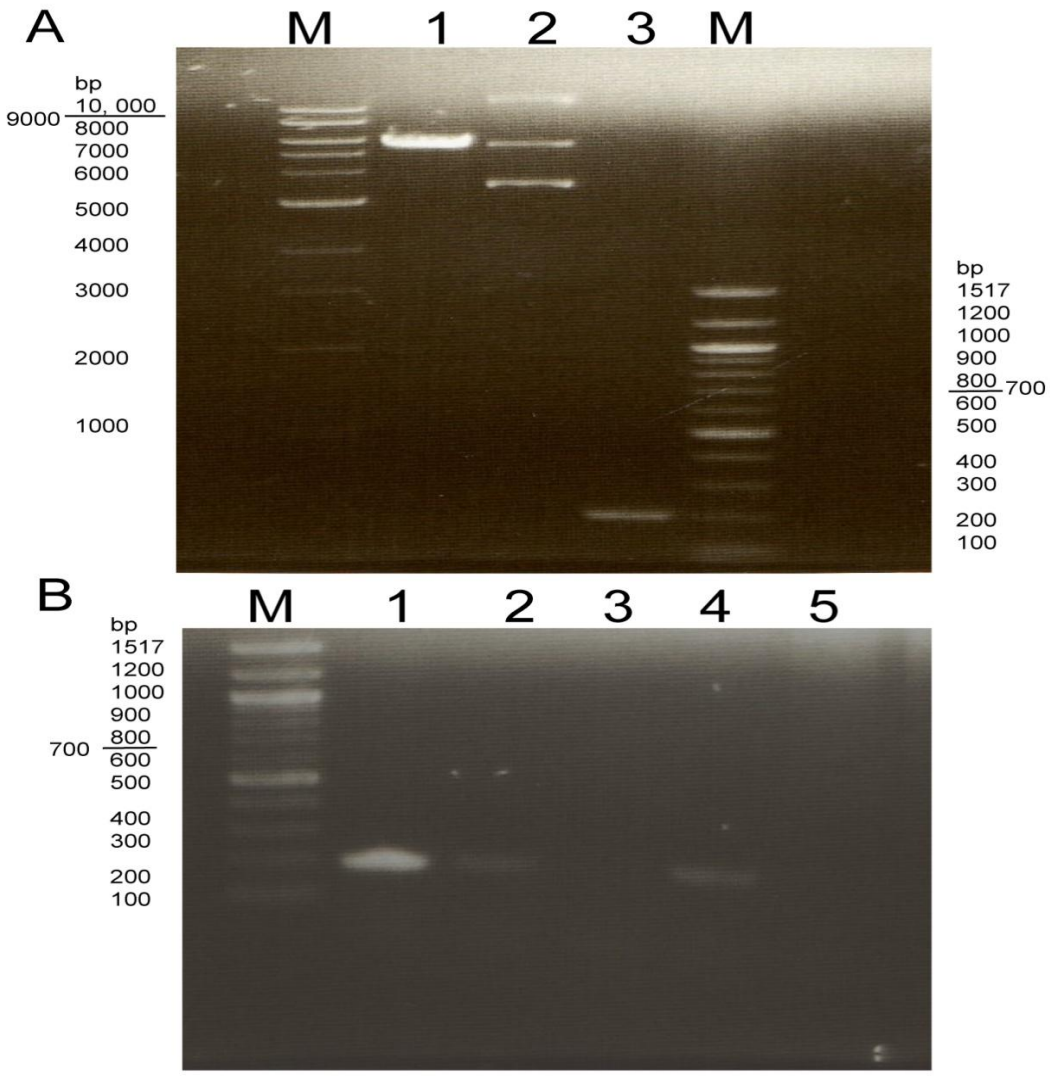

Figure 4.5 Visualisation of (A) PCR and pHANNIBAL vector digests and (B) PCR screen of sense fragment ligated into digested pHANNIBAL

Gel (A) shows sense PCR product and pHANNIBAL ready for ligation. PCR was conducted from A. thaliana cDNA. The pHANNIBAL vector was purified (B) After ligatiuon colonies were PCR Screened for the presence of a fragment containg the *ndb* knock-down region. Primers used were SenseCasF and SenseCasR (Table 2.1)

(A)

M 1Kb marker

Lane 1 Digested pHANNIBAL Vector

Lane 2 Undigested vector

Lane 3 Digested PCR product

M 100bp marker

(B)

M 100bp marker

Lane 1 Colony 1

Lane 2 Colony 2

Lane 3 Colony 3

Lane 4 Colony 4

Lane 5 - Control

For the gateway cloning system, PCR products generated must be bordered by *att*B recombination sites, this enables them to be recombine into an entry vector containing *att*P sites (pDONR^{TM}221). Primers were designed as specified by the Gateway cloning system (Invitrogen). The requirements for primers were:

Forward Primer: 5' GGGG- 25nt *att*B site – 18-25nt gene specific sequence

Reverse Primer: 5' GGGG- 25 *att*B2 site – 18-25nt gene specific sequence

PCR amplification with these new primers (Table 2.1) used the same conditions as had been previously used for the same gene specific sequence for the primers used for pHANNIBAL, hence no extra PCR optimisation was required. PCR product was produced for the *ndb* region (Figure 4.6).

4.3.5. Generating the pHELLSGATE 12 Vector

4.3.6. BP Recombination Reaction of Gateway Cloning – Creating an Entry Clone

The BP Recombination reaction of the Gateway Cloning System enabled the homologous *ndb* knock-down region PCR product to be recombined into a pDONR^{TM}221 (Invitrogen, USA) vector through an enzymatic reaction relying on *att* sites from the bacteriophage lambda contained on the PCR product and in the pDONR^{TM}221 vector (Figure 4.7). The recombined vector with PCR product were transformed into *E. coli* and then grown and selected on kanamycin selective LB plates. To confirm the presence of the *ndb* knock-down region fragment in the transformed colonies, a PCR screen of the colonies was conducted (Figure 4.8). Of the 8 colonies screened all were positive with a fragment of the expected size of 200 bp. These positive colonies would be used for the next recombination event into pHELLSGATE. The purified plasmids were sent for subsequent sequencing to confirm the correct *ndb* knock-down region was inserted into the pDONR^{TM}221 vector. Of the four colonies sequenced all contained the correct fragment with the correct sequence. Hence, any of these colonies could be use for the subsequent LR reaction.

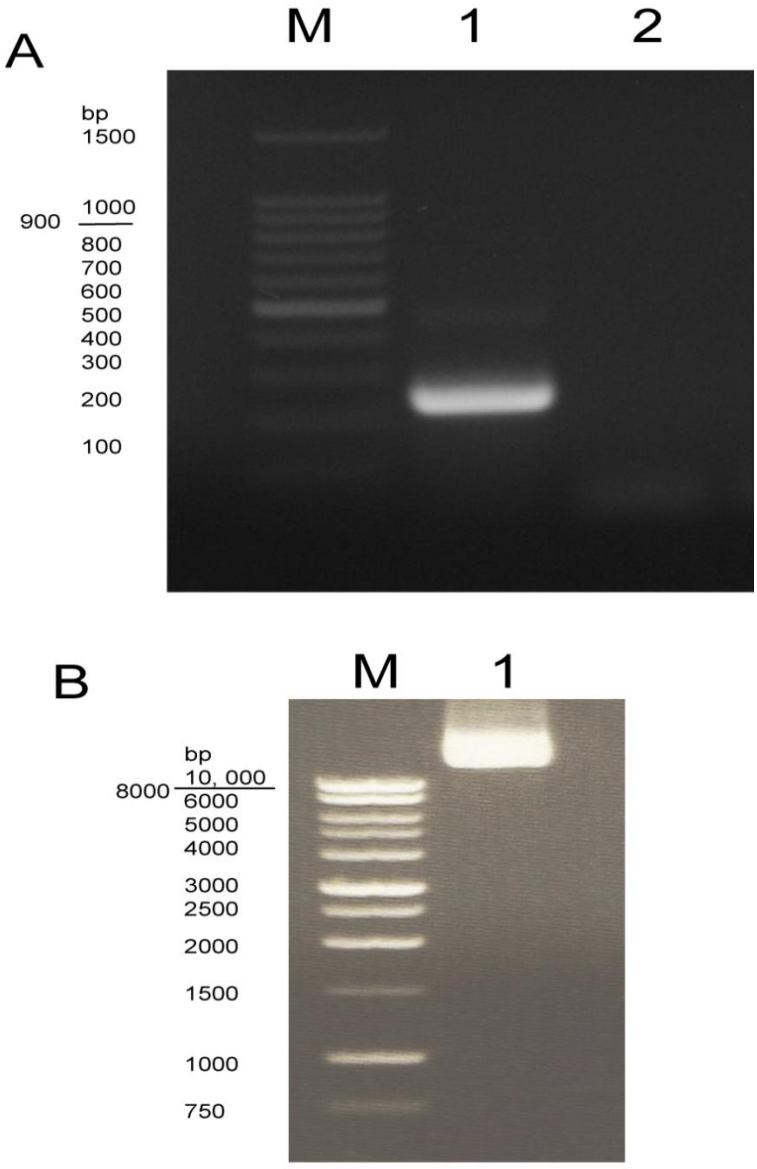

Figure 4.6 Visualisation of (A) PCR fragment ready for recombination into (B) pHELLSGATE vector

Gel (A) shows the PCR product conducted from A. thaliana cDNA of expected size of 200bp. (B) The pHANNIBAL vector was purified at the expected size of 17681bp. Primers used were pHellsB2F and pHellsB2R (Table 2.1)

(A)	(B)
M 100bp marker	M 1Kb marker
Lane 1 PCR product	Lane 1 pHELLSGATE vector

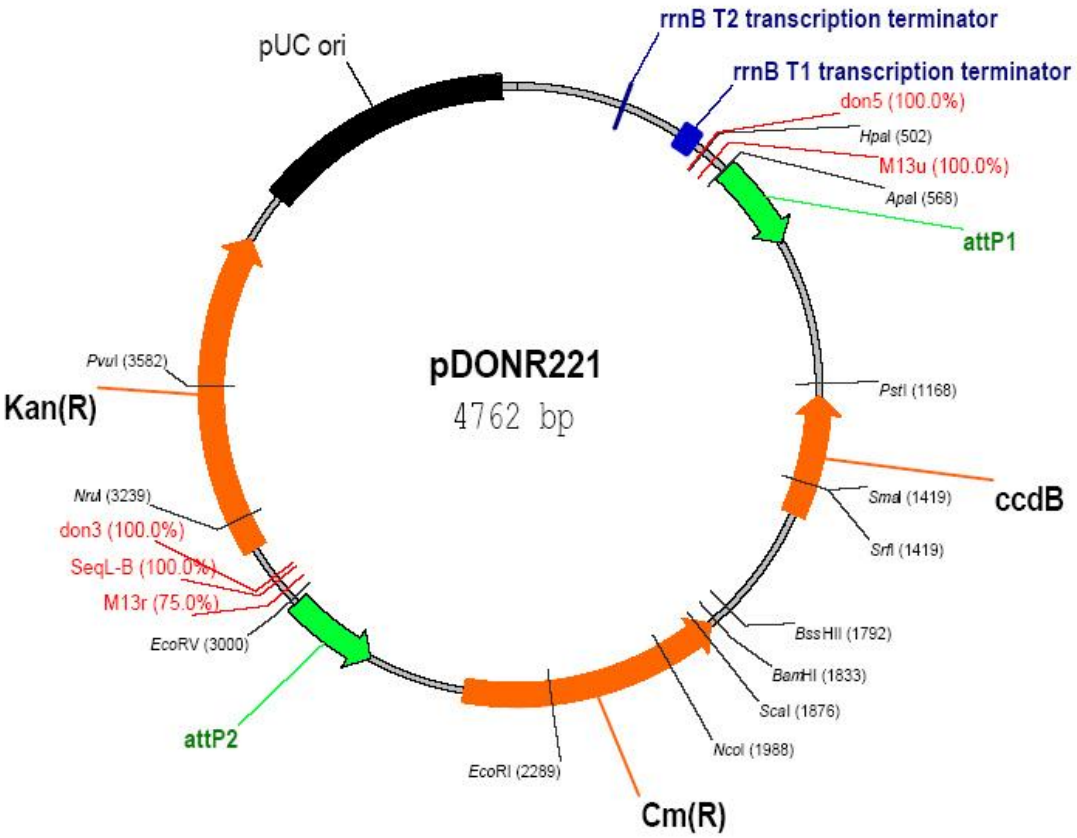

Figure 4.7 pDONR221 vector to be used as entry vector for recombination of the *ndb* knock-down fragment

The pDONR vector uses the attp1 and 2 sites seen in green for recombination (Invitrogen, USA).

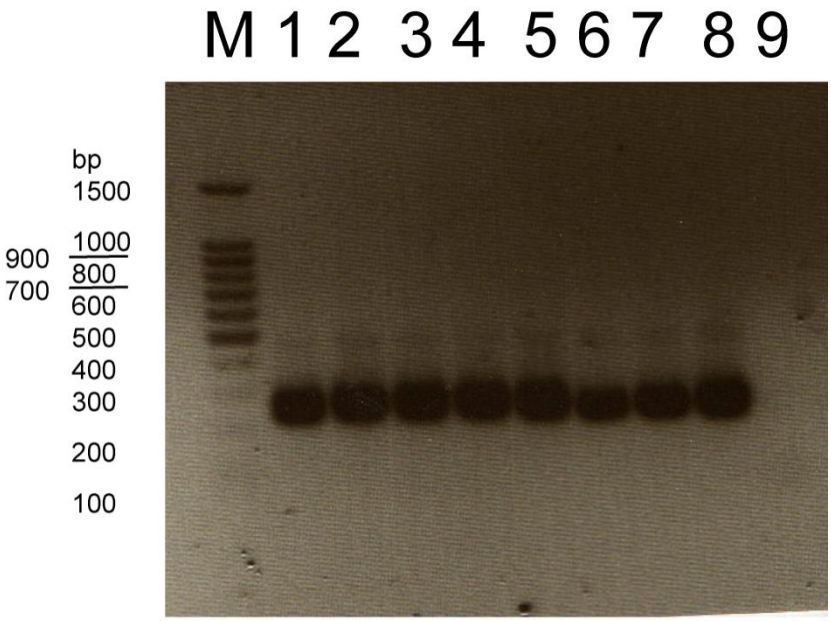

Figure 4.8 Confirmation of *ndb* knock-down region in pDONR vector
The gel shows the PCR screen of the PCR product in pDONR (Section 2.10.1). The PCR product was of expected size of 200 bp. PCR fragment corresponds to alignment in Figure 4.2. Primers used were pHellsB2F and pHellsB2R (Table 2.1).

M 100bp marker
Lane 1 Colony 1
Lane 2 Colony 2
Lane 3 Colony 3
Lane 4 Colony 4
Lane 5 Colony 5
Lane 6 Colony 6
Lane 7 Colony 7
Lane 8 Colony 8
Lane 9 – Control

4.3.7. LR Recombination of Gateway Cloning – Creating the hpRNA Construct

The *ndb* knock-down region fragment now present in the pDONR^{TM}221 vector, was transferred into the pHELLSGATE 12 (CSIRO) destination vector using the LR recombination reaction (Figure 4.9). As with the BP step a PCR screen was done on transformed colonies to confirm the presence of the *ndb* knock-down region. As seen in Figure 4.10 all four colonies screened were positive. The positive colonies were sent for sequencing of the RNAi ragment and all returned the correct sequence.

4.3.8. Transformation of *A. thaliana* by *A. tumefaciens*

pHELLSGATE was transformed into the GV3101 *A. tumefaciens* strain to facilitate delivery of the *ndb* knock-down region into wild type *A. thaliana.* Floral dipping was the method of choice for the generation of transgenic *A. thaliana* (Clough and Bent, 1998), as this has worked previously in the lab (Chapter 3). After 6 days, these plants were dipped again and placed in the glasshouse and allowed to set seed. This seed would be P1 seed, and was collected and stored in paper bags to dry.

4.3.9. Selection of T1 seed of pHELLSGATE containing *ndb* knock-down fragment

Both the empty pHELLSGATE 12 vector as a control and *ndb* silenced pHELLSGATE seeds were plated onto individual MS Media plates. Firstly seeds were plated in the 100's as to allow as many as possible to germinate and grow. All seeds that did germinate, progressed to a 2-leaf stage as a minimum, but only the seeds containing the vector with the kanamycin resistance gene would grow further. For both lines there were approximately 100 plants that were still green indicating the presence of the vector compared to bleached plants of which approximately 400 seeds for each line were originally plated. Obvious bleaching of chlorophyll from non-transformed

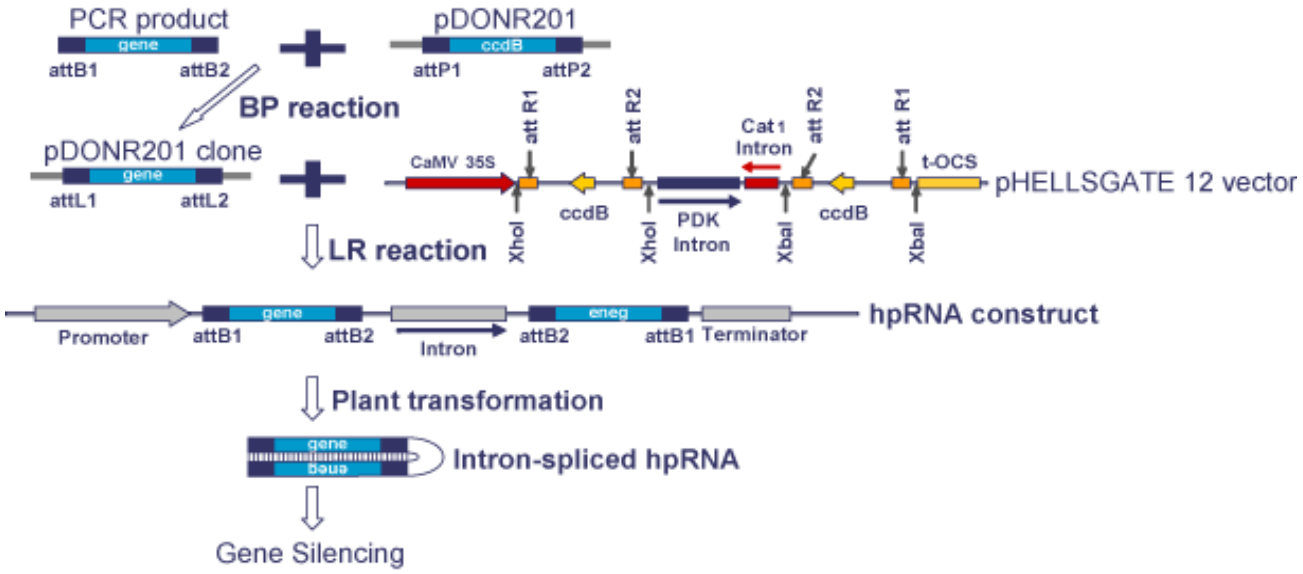

Figure 4.9 Recombination event between pDONR vector and pHELLSGATE vector (Wesley *et al.* 2003)

The figure explains the use of attP and attB sites which produces attL sites that can then recombine with attR sites in pHELLSGATE 12.

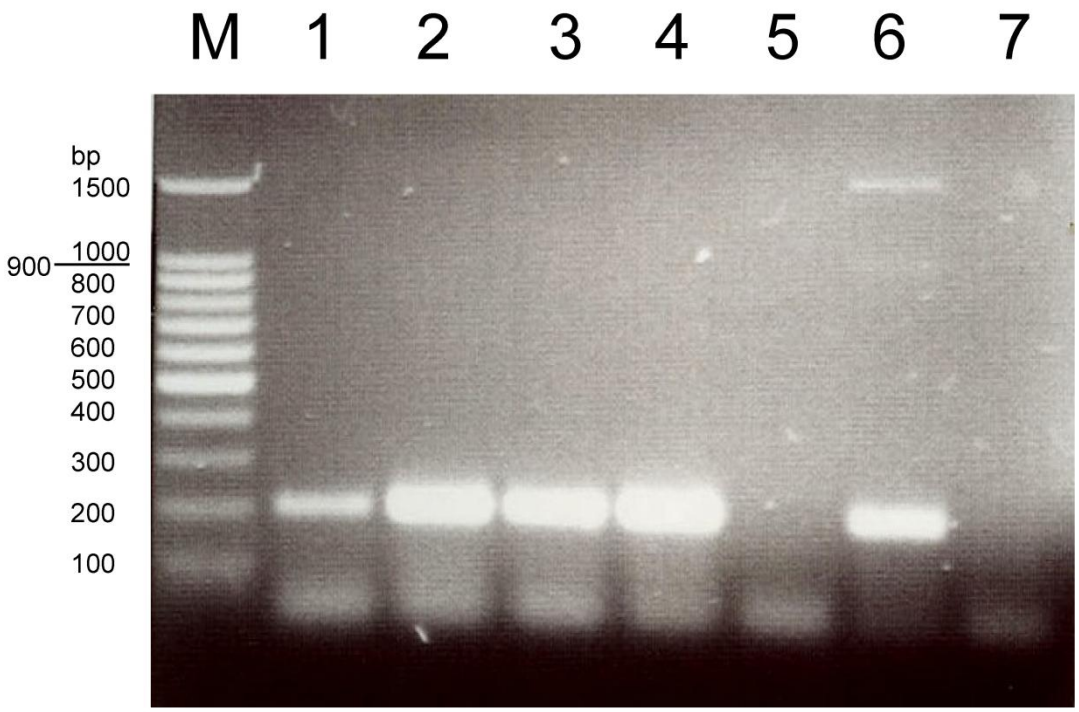

Figure 4.10 PCR Screen of pHELLSGATE with *ndb* knock-down region present

The gel shows the PCR screen, confirming the presence of PCR product in pHELLSGATE in *E. coli*. The PCR product was of expected size of 200bp. PCR fragment corresponds to alignment in Figure 4.2. Primers used were pHellsB2F and pHellsB2R (Table 2.1).

M 100bp marker

Lane 1 Colony 1

Lane 2 Colony 2

Lane 3 Colony 3

Lane 4 Colony 4

Lane 5 Empty pHELLSGATE

Lane 6 + Control (Plasmid)

Lane 7 - Control

A. thaliana plants was observed on the transformation plates, compared to those that were green and continued to grow, indicating the presence of either the empty vector or *ndb* silenced vector present in the genome (Figure 4.11).

The plants that had continued to grow were transferred to fresh MS media plates containing both kanamycin and cefotaxime, to allow the plants to continue to grow and further confirm these plants were kanamycin resistant. Empty pHELLSGATE vector, plants, continued to grow healthy at a rate comparable to Wt plants, also grown at the same time on non-selective plates. The plants containing the *ndb* silenced pHELLSGATE vector had reduced growth and after several weeks were still very small in size and most of the plants had no or severely stunted root growth. This can be observed in Figure 4.12 where it can be seen comparing empty vector control to the *ndb* knock-down pHELLSGATE vector there was a noticeable difference in growth. After several weeks and still no further growth the plants began to senesce and form clumps of tissue which appeared to be callus like with still none or very little root tissue compared to the control plants. These plants containing the ndb knck-down fragment vector never set seed, and hence were not viable and further generations could not be generated to carry out further experiments.

As there was still P1 seed remaining for both the empty vector control and the *ndb* knock-down vector the plating of the seed onto MS media containing kanamycin and cefotaxmine was repeated a total of three times and the same result was generated each time. This confirms that what was observed the first time was not due to experimental fault, and this was further supported as Wt and empty vector control plants could grown under the same conditions and treatments to the *ndb* knock-down plants.

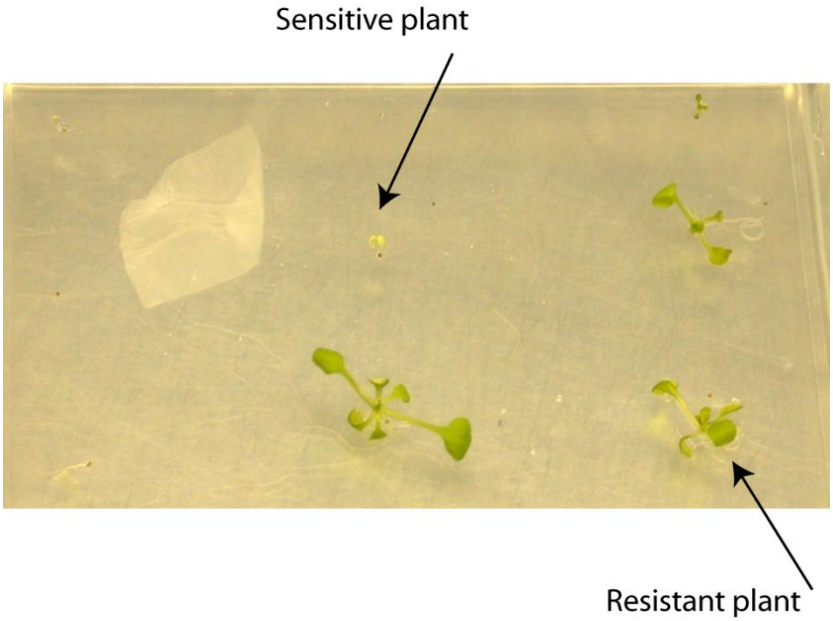

Figure 4.11 Comparison of Resistant to Sensitive plant for pHELLSGATE vector containing empty

Plants were germinated on MS Media with selection. The green resistant plant will contain the plasmid and hence kanamycin resistant gene NPT II. The bleached plants contain no vector and hence are not resistant.

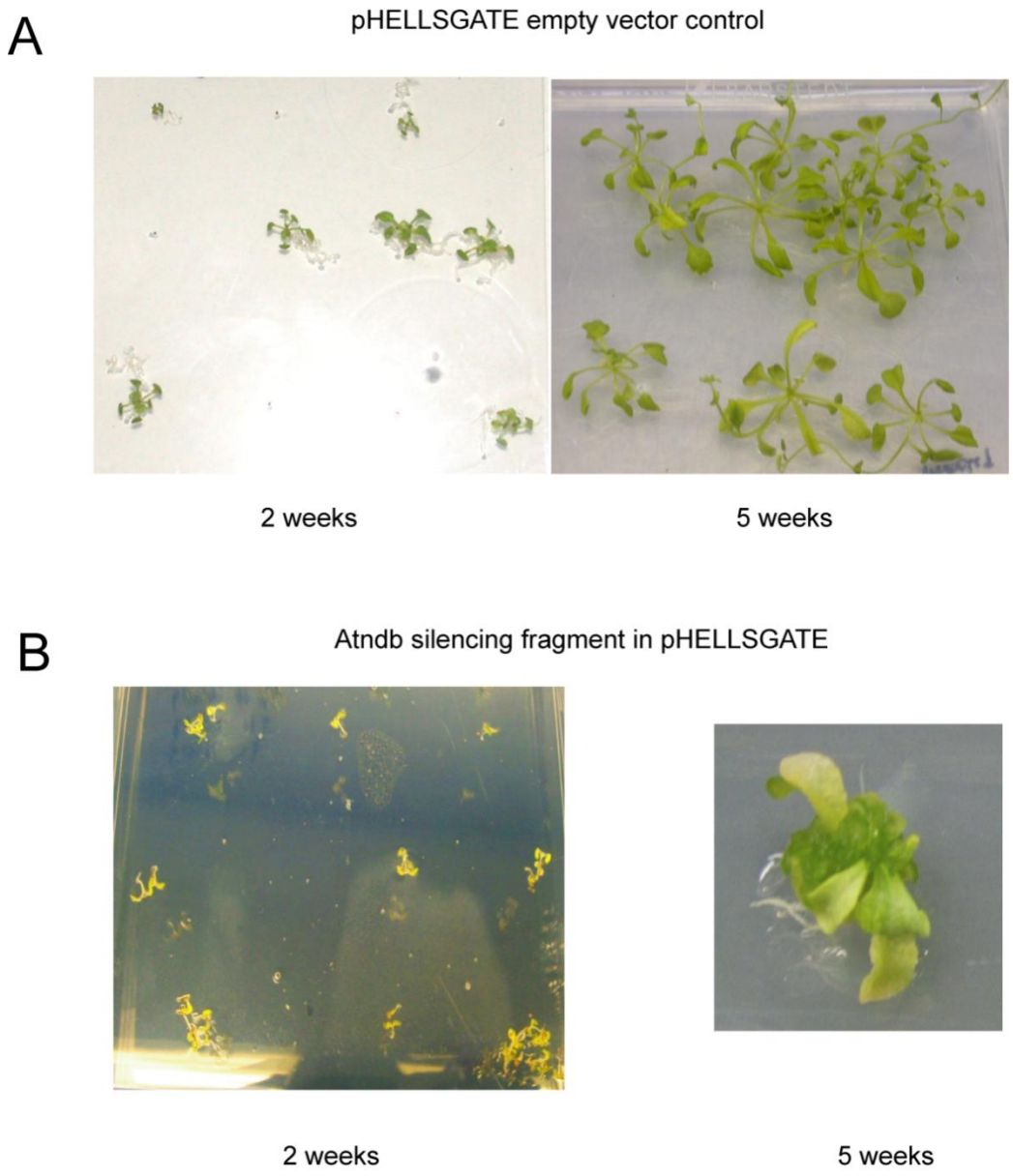

Figure 4.12 Comparison between (A) pHELLSGATE empty vector control at both 2 weeks and 5 weeks. (B) the *ndb* knock-down region in pHELLSGATE also at 2 weeks and at 5 weeks

pHELLSGATE empty vector control, and *ndb* knockdown line plants were grown for a total of 5 weeks at 21 ^{o}C under ~120 µE (m^{-2} s^{-1}) of light with a 16/8 light/dark photoperiod. Photographs of rosettes were taken at the 5-8 stage (14 days after germination) and 10-12 rosette stage (35 days after germination) and represent a minimum of *n*=3 biological replicates for each plant line.The empty vector control can be seen as healthy growing plants at both 2 and 5 weeks with normal growth. The knock-down line however has not grown in size and has unusual growth, with yellowing appearing in the leaves.

4.3.10. Conformation of pHELLSGATE vector in transformed plants

Extractions of genomic DNA were done on the small amount of leaf tissue that was generated for the *ndb* knock-down line as well as the empty vector control. The genomic DNA was then used as template for PCR. Primers used for screening were specifically designed for screening of pHELLSGATE 12 vector with the primers amplifying a 316 bp fragment. As seen in Figure 4.13A there was a fragment amplified at the expected size for both the empty vector control and the *ndb* knock-down vector at 316 bp. PCR was also done using the *ndb* knock-down region primers and there was a band at the expected size of 200 bp confirming that the *ndb* Knock-down vector did still contain the region and had been taken up into the plant (Figure 4.13B). Although no further experiments could be done we were able to confirm the presence of the control and knock-down vector in the respective plants.

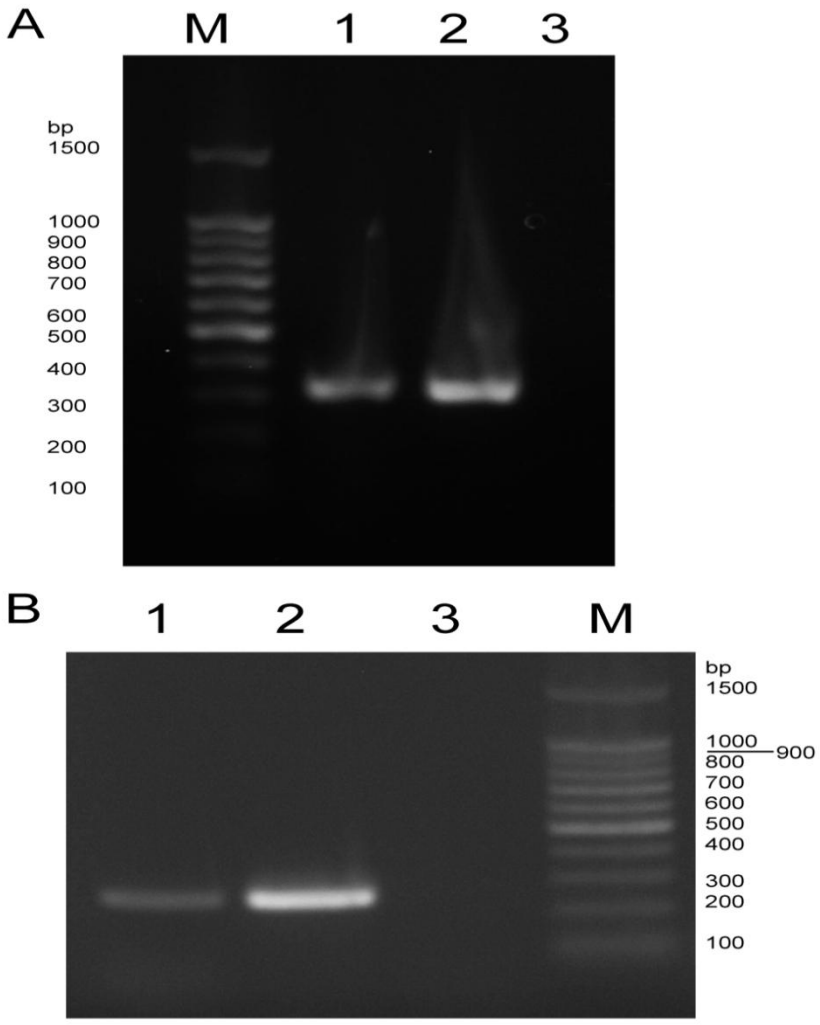

Figure 4.13 Confirmation of knock-down vector in plants from P1 seeds

Genomic DNA was used to screen plants from P1 seed of (A) pHELLSGATE empty vector and (B) *ndb* knock-down pHELLSAGTE plants. Gel (A) shows PCR screen of empty vector control. (B) shows the PCR screen of *ndb* knock-down plants. The PCR product was of expected size of 316 bp for empty vector, and (B) 200 bp for *ndb* knock-down region. PCR fragment corresponds to alignment in Figure 4.2. Primers used were (A) pHellsscreenF pHellsscreenR and (B) pHellsB2Fand pHellsB2R (Table 2.1).

(A)

M 100bp marker

Lane 1 Plant #1

Lane 2 Plant #2

Lane 4 - Control

(B)

Lane 1 Plant #1

Lane 2 Plant #2

Lane 3 - Control

M 100bp marker

4.4 Discussion

The pHANNIBAL vector originally used for knock-down has been used effectively and efficiently for a number of genes, but it is laborious when individually knock-down a large number of genes (Wesley *et al.* 2003). It takes a minimum of 2 weeks to clone a knock-down fragment using pHANNIBAL and into an expression vector such as pART, hence three full rounds of cloning are required, including sequencing. Hence if this is to be done for a large number of genes it would become quite time consuming. To overcome this time consuming cloning the pHELLSGATE vectors were designed. They use the commercially available Gateway cloning system (Invitrogen, USA). The Gateway Technology is a universal cloning method based on the site-specific

recombination properties of bacteriophage lambda (Landy 1989). It is a rapid and highly efficient was to move DNA sequences into multiple vector systems for functional analysis and protein expression (Hartley *et al.* 2000). There have been a series of HELLSGATE vectors become available, with each new vector providing improvements. The vector used for this work was pHELLSGATE 12, which was chosen due to more efficient knock-down, due to the use of the intermediate vector. Further, the two introns in opposite orientations mean that the final product of recombination will always produce a spliceable intron which has been shown to improve efficiency of knock-down (Wesley *et al.* 2004). Hence this pHELLSGATE 12 vector provided for efficient and effective knock-down for work with the *ndb* knock-down region for *A. thaliana*.

An important step for investigating the functions of the specific alternative NAD(P)H dehydrogenases is to generate gene-suppressed plant tools. This enables the specific effects of post transcriptional gene knock-down to be determined and can be attributed to the specific gene target. The components of the alterative oxidase have to date been well characterised and studied including knockout and over expressing plants, yet as to date

there is still little knowledge about the alternative NAD(P)H dehydrogenase proteins and their role in the plants (Rasmusson *et al.* 2004). They are found in all plant species to date and hence indicate a functioning role, yet their exact roles remain unclear (Elhafez *et al.* 2006). With the possible exception of red beetroots (Rayner *et al.* 1983), all plant mitochondria that have been investigated are able to oxidize external NADH and NADPH where tested (Moller *et al.* 1986; Moller 1997).

Previously gene knock-down has been done for *ndb4* (Chapter 3) which has helped to elucidate not only *ndb4* but also *ndb2* characteristics. Also work has been to attempt to silence done on *ndb1* which has suggested that it resulted in stunted growth and a possible role for *ndb1* during early growth development as these plant were also not able to grow to maturity (Cook 2007). This is the first time that all four external dehydrogenases have been attempted to be knocked out of the one plant together. There have been suggested roles for all of these external dehydrogenases as they display transcript increases under various stresses (Clifton *et al.* 2005), although it is mainly *ndb2* and *ndb4* that show the increases under stress, although often *ndb3* is too low in transcript to detect. *ndb1* has been suggested to be a housekeeping gene. As dual targeting of *ndb1* to the mitochondria and peroxisomes has just recently been shown, any *ndb1* functions may be combined activity from both the mitochondria as well as the peroxisomes (Carrie *et al.* 2008). However, there was no dual targeting detected for the remaining external dehydrogenases so any affect that would be seen by these genes is due purely to mitochondrial activity.

Previously it has been shown that the four external dehydrogenases have higher transcript levels in young roots (4-6 days) compared to older roots (Elhafez *et al.* 2006), indicating a possible link between these genes and growth, particularly root growth. It has also been reported that there are high levels of external dehydrogenase protein in young potato leaves (Svensson *et al.* 2001). This could explain the stunted or no root growth observed in the *ndb* silenced plants compared to the vector control and Wt plants. *ndb2* expression appears to be mainly isolated to the roots, as does *ndb3,*

although both are also found in the bud and flower. Whereas *ndb1* and *ndb4* appear to have expression found in not only roots, but also cotyledons and leaf tissue as well as the buds and flowers (Elhafez *et al.* 2006). This high expression of the external *ndb* genes early on in root growth could explain the lack of root growth observed in the *ndb* knock-down plants. Without these genes present which may play a role in the early stages of growth the roots were unable to grow normally and hence resulted in unhealthy plants with stunted growth. This has been one suggestion of why there are several homologs of these genes in *A. thaliana*, as they could represent isoforms expressed in a tissue-specific or developmental pattern (Rasmusson *et al.* 2004). This is further supported by data presented on the Genevestigator database (Zimmermann *et al.* 2004) which indicated that *ndb1* and *ndb2* have high expression early on during the plant growth, and then the two internal dehydrogenases have higher expression after initial plant growth occurs (Figure 4.14). Genevestigator data also indicates very high expression levels of *ndb2* in the roots compared to other alternative dehydrogenases. This data could suggest some role in the roots at an early age particularly for *ndb2*, and if silenced as assumed in these plants, without another external dehydrogenase to compensate for this loss the effect is detrimental to the plant. These results suggest that the role of this gene early on in plant growth is vital for normal functioning of the plant and suggesting that these enzymes are not wasteful, but play a key role in normal plant development as well as stress response.

This detrimental effect to the plant could also help to elucidate why these genes appear to be unregulated during stress. As seen from Figure 4.15, many of the uncoupling proteins, AOX's and alternative dehydrogenase genes are either up or down regulated during stress. It can be seen that the expression of *ndb2* and *nda2* are particularly coordinated. Interesting to note is that ndb1 transcripts appear not to respond to stress responses and hence, *ndb1* appears to act more like a housekeeping gene (Clifton *et al.* 2005; Elhafez *et al.* 2006).

Alternative respiration pathways are also associated with the synthesis of

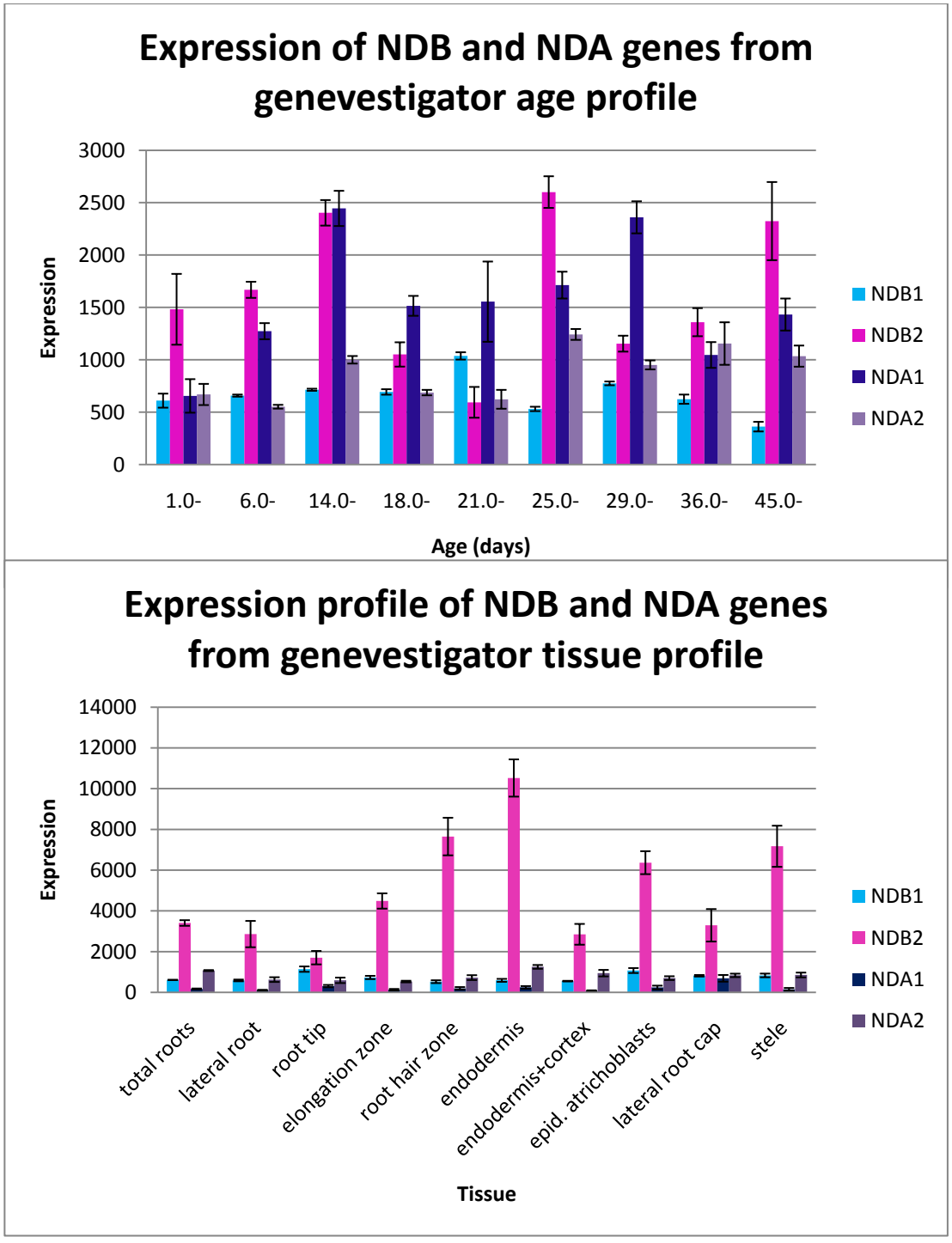

Figure 4.14 Genevestigator expression profiles for developmental stage and tissues profiles

The data presented (Zimmermann *et al.* 2004). The age profile shows all tissue available at that age. The tissue profile is done on mature plants.

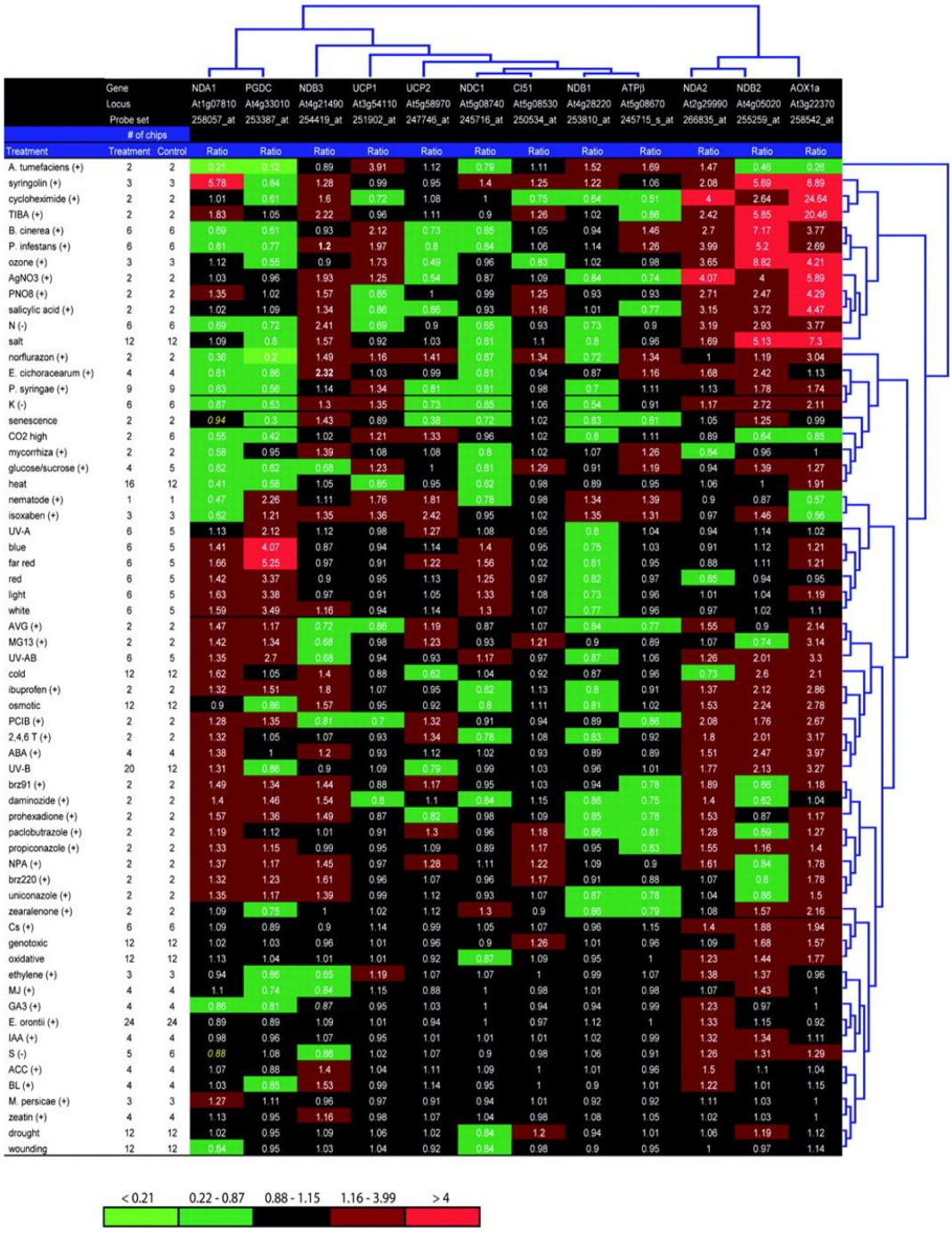

Figure 4.15 Stress induced expression of aox genes, Type II dehydrogenase genes and UCP genes from *A. thaliana*

The following is a summary of Genevestigator response viewer array data, showing the response of individual genes to a variety of stresses. Taken from *(Elhafez et al. 2006)*

various primary and secondary metabolites in the cell as they allow respiratory flux independent of the energy status of the cell. Thus the synthesis of these secondary metabolites could be absent or limited to minimal levels in these plants (Rakhmankulova *et al.* 2003). It has been suggested that the secondary metabolites of plants are involved in plant protection against biotic and abiotic stress factors, linking this function to external dehydrogenases (Matern 1991). In addition, the alternative oxidase is involved in the maintenance of high Krebs cycle functioning, and the intermediates produced in this cycle can be used for biomass synthesis (Palmer 1976). Hence there could be some link between stunted growth and the absence of these external dehydrogenases, due to limited synthesis of secondary metabolites, which result in loss of downstream signalling leading to healthy plants. The high level of adaptation that respiration expenses plants such as ruderal plants, may be related to uncoupling of respiration from energy mechanisms of the cyanide-resistant respiration and to an enhancement of the synthesis of secondary metabolites. In their turn, these mechanisms dramatically decrease the growth rate and prepare plants for transition to reproductive development (Rakhmankulova *et al.* 2003). This indicates a possible function of external dehydrogenases with secondary metabolites which controls growth, and without these metabolites there may not be control over growth, resulting in plants with stunted growth as observed.

It has been postulated that the external type II NADH dehydrogenases may be functionally redundant to the internal homologues (Rasmusson *et al.* 2008). In combination with export of reducing equivalents from the matrix via the malate/oxaloacetate shuttle for example, the external NADH dehydrogenases may oxidise reducing equivalents generated by Krebs cycle or glycine oxidation in the mitochondrial matrix. Consistently, external NADH oxidation has been shown to be up-regulated in mutants for internal NADH dehydrogenases (Sabar *et al.* 2000; Moore *et al.* 2003). There are reported cases where type II NADH dehydrogenases are able to substitute for complex I. Although it was not able to be tested due to non-viability of the plants, the lack of growth may signify that the internal and or complex 1 may

not be able to compensate for the loss of external dehydrogenase activity, and that these dehydrogenases may have a more important role in the plant than first though, especially involving root growth.

There has been recent research on complex 1 of the ETC, and in most cases the alternative dehydrogenases have been able to restore function, or replace the role of complex 1, indicating the external dehydrogenase have essential functions (Rasmusson *et al.* 2008). It has been reported that respiration can be restored in complex I-deficient mammalian cells by heterologous expression of the *S. cerevisiae* gene for the internal type II NADH dehydrogenase (Seo *et al.* 1998). Complex I-deficient *N. crassa* are fully viable but spore germination is delayed (Duarte *et al.* 2003). A mutant CMSII lacking complex I in *Nicotiana sylvestris* is a male sterility mutant and also results in a range of phenotypic differences compared to the wild type, including slower growth, increased levels of antioxidant systems, AOX capacity, and leaf amounts of NAD^+ and NADH, showing that the redox balance is substantially disturbed in this mutant (Noctor *et al.* 2004; Dutilleul *et al.* 2005; Vidal *et al.* 2007). These CMSII mutants have up regulation of both internal and external NADH oxidation, indicating both are able to bypass complex I (Sabar *et al.* 2000). This is further proof that the alternative dehydrogenases can fully compensate for complex I. Although since the type II NAD(P)H dehydrogenases do not contribute to the proton motive force, metabolite redox pair ratios will be partly released from coupling to the proton motive force. Consistently, there is strong evidence that the CMSII phenotype that is observed is caused not by the lack of complex I but by metabolite changes, including the high NADH concentrations in CMSII. So, the alternative NADH dehydrogenases may be redundant with complex I regarding NADH oxidation itself, but due to the lack of proton pumping by the type II enzymes, the molecules involved in the reaction will communicate differently with their metabolic context in the absence of complex I. Still, the observation that the complex I-deficient nuclear male sterility *N. sylvestris* mutant NMSI shows unchanged alternative NADH oxidation and displays a more severe phenotype than CMSII (Sabar *et al.* 2000) indicates that compensation of NADH oxidation in itself (without proton pumping) may have

beneficial effects on the growth and function of the mutant.

It has been proposed by Clifton *et al.* 2005 that AtAOX and ndb, a terminal oxidase and external NAD(P)H dehydrogenase, are capable of forming a simple but functional alternative respiratory chain allowing the oxidation of cytosolic NAD(P)H. The co-ordinated induction of these two activities enables formation of a distinct and self-contained biochemical pathway that may help maintain cellular redox balance of the cell. If this pathway is disrupted as may have been in these silenced *ndb* plants, it could be allowing the build up of ROS, which in turn is the reason the plants were senescing early, and not viable. These results are suggesting that these genes may play an important role in early development of the plant. Although single genes from the external *ndb* family have been silenced with success, as in Chapter 3 (Melino 2004; Cook 2007), these plants appeared to still be viable and healthy and most likely due to compensation between the external dehydrogenase family, but for these *ndb* knock-down plants, this was not possible and the role these dehydrogenases play could not be replaced, and hence resulted in nonviable plants.

Work in this chapter has been published in Smith, C.A., Melino, V.J., Sweetman, C., and Soole, K.L. (2009) Manipulation of alternative oxidase can influence salt tolerance in Arabidopsis thaliana. *Physiological Plantarum* **137**; 459-72

5 MANIPULATION OF ALTERNATIVE OXIDASE CAN INFLUENCE SALT TOLERANCE IN *ARABIDOPSIS THALIANA*

5.1 Introduction

5.1.1. Salinity Stress

Significant areas of cultivated land are affected by salinity in more than one hundred countries, although Australia has particularly high areas of land affected by salinity stress (Rengasamy 2006), hence soil salinity poses a serious threat to crop yield and future food production. Hence there is a need to find plants that will be able to sustain living in conditions with high salt. In Australia there is 2 million ha of land that has become saline since clearing began a century ago, and another 15 million ha are at risk of becoming saline in the next 50 years (Munns 2002). This amounts to a third of Australia's agricultural area. Irrigation systems are particularly prone to salinization, as irrigated land has at least twice the productivity of rain-fed land, it may produce one-third of the world's food. If plants are able to be developed that have higher salt tolerance then this will lead to higher yielding crops which will help to address important global issues.

When plants are under salt stress the build up of Na^+ becomes toxic. Na^+ will build up in the cytoplasm or the cell wall which will result in metabolic toxicity or osmotic imbalances. High salinity causes hyperosmotic stress and ion disequilibrium that produce secondary effects or pathologies (Hasegawa *et al.* 2000). When under salinity stress plants will either cope by avoiding the stress or by tolerating the salt stress. These tolerance mechanisms can be

categorised as those that function to minimise osmotic stress or ion equilibrium or alleviate the consequent secondary effects caused by these stresses (Yokoi *et al.* 2002).

5.1.2. Oxidative Stress

Oxidative stress is caused by an imbalance between the production of reactive oxygen and a biological system's ability to readily detoxify the reactive intermediates or easily repair the resulting damage (Moller 2001). This oxidative stress occurs as a result of many stresses, one of which is salinity stress. This is a result of salinity stress resulting in an osmotic in balance and hence damages the plant and as a result the biological system in this case the plant is unable to detoxify theses reactive oxygen species due to damage caused from osmotic imbalance. Oxidative stress is caused by this imbalance of reactive oxygen species (ROS) such as hydrogen peroxide (H_2O_2), superoxide (O_2-) and hydroxyle (OH) radicals. These ROS are very highly reactive and can alter normal cellular metabolism through oxidative damage to lipids, proteins and nucleic acids (Imlay 2003). This damage from ROS results in a decrease in enzyme activity, increase in membrane permeability and mutation in the DNA (Taylor *et al.* 2002). It has been estimated that approximately 1% of all oxygen consumed by plant tissue will result in the formation of ROS (Puntarulo *et al.* 1988).

5.1.3. AOX role in salinity stress

In plant cells, the major sites of ROS production are the chloroplast and mitochondria (Bartoli *et al.* 2004; Asada 2006). Whilst many of the ROS detoxification enzymes are located in these organelles and within the cytosol, plant mitochondria have an additional oxidase known as alternative oxidase (AOX), which has been proposed to play a role in ROS metabolism. Alternative oxidase branches from the electron transport chain accepting electrons from reduced ubiquinone and donating electrons directly to oxygen.

In this way, AOX can prevent over-reduction of the ubiquinone pool and minimise the potential of these electrons to form ROS by a non-enzymic reaction with oxygen (Moller 2001). Further, a link between AOX capacity and ROS formation for some abiotic stresses has been experimentally demonstrated, where altered AOX expression levels have impacted on the level of ROS formation during the stress. For example, in transgenic tobacco cell cultures with reduced expression of AOX using antisense expression, higher levels of ROS accumulated under increased phosphate stress than in wild-type cells (Yip *et al.* 2001). In *A. thaliana* lines over-expressing AOX, lower ROS levels were observed during chilling stress whereas lines with antisense suppressed AOX had higher ROS levels (Fiorani *et al.* 2005). More recently, *aox1a* mutants not expressing this gene, were shown to have high anthocyanin production, altered photosynthetic capacity increased superoxide levels and reduced root growth under combined moderate light and drought stress (Giraud *et al.* 2008). Altogether, these results lend support to the role of AOX in alleviating ROS formation, suggesting that AOX should also be considered as part of the plant oxidative stress response.

Stress conditions, such as low temperature (Vanlerberghe *et al.* 1992), drought and plant pathogen attack (Simons *et al.* 1999), appear to influence the Alternative Pathway activity, thus indicating that the Alternative Pathway may take part in stress response of plants (Day *et al.* 1995). For example, abundant evidence has been accumulated about the relationship between the Alternative Pathway and low temperature. However, knowledge about respiratory metabolism under saline stress conditions is not extensive. A large number of studies in a variety of species have indicated that AOX is induced at a gene, protein and activity level by a variety of treatments, generally labelled as stresses (Finnegan *et al.* 2004). From the current knowledge known about AOX in *A. thaliana*, Clifton *et al.* (2006) have summarized the signalling pathways that regulate the expression of the five AOX genes (Figure 5.1). The figure highlights that there are a number of organ, developmental, external and internal signals which act via a number of pathways to induce expression. The involvement of AOX in the response to salinity stress has been evident in early studies where an increase in the

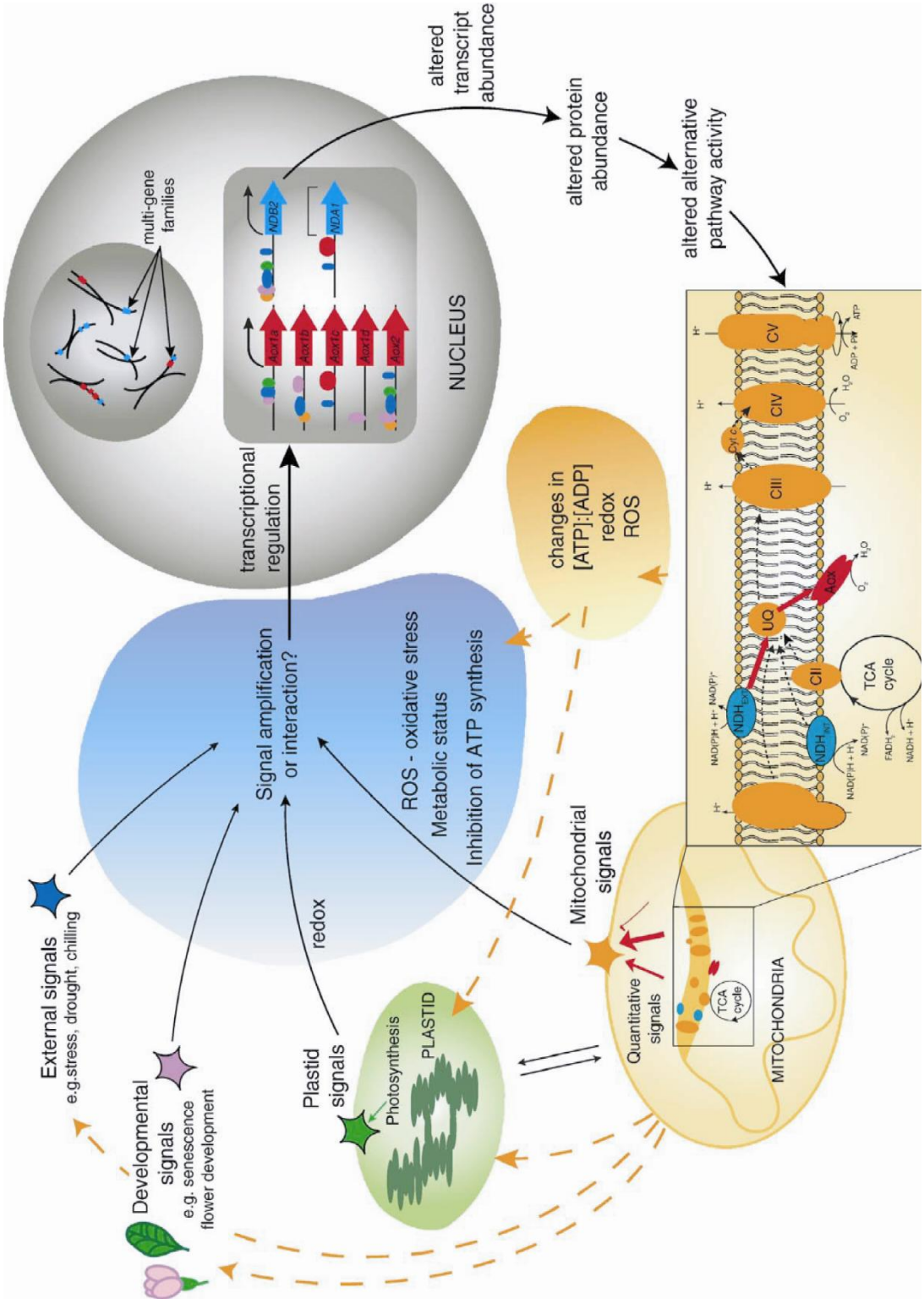

Figure 5.1 Overview of the signaling pathways that regulate expression of the five AOX genes in *A. thaliana*

The pathway highlights the signalling involved with activation of the AOX genes (Clifton *et al.* 2006).

AOX capacity was demonstrated in plants such as barley (Jolivet *et al.* 1990), soybean (Hilal *et al.* 1998) and more recently in carrot (Ferreira *et al.* 2008). However, the validity of certain assumptions used to determine AOX activities in the earlier studies have been called into question, such as the use of inhibitors to estimate AOX engagement rather than capacity (Millar *et al.* 1995). In addition, in microarray studies of salt-stressed *A. thaliana* plants it has been shown that one of the genes encoding AOX, *aox1a*, was expressed within three hours of NaCl exposure. Whether this is maintained or resulted in an increase in AOX capacity in the plant is not known. Interestingly, it is not known whether the other components of the alternative pathway of plant respiration, specifically the NAD(P)H dehydrogenases, respond to salt stress.

When plants are under salt stress the accumulation of Na^+ ions becomes toxic. Na^+ ions build up in the cytoplasm or the cell wall resulting in metabolic toxicity or osmotic imbalances. High salinity causes hyperosmotic stress and ion disequilibrium, both of which produce secondary effects or pathologies (Hasegawa *et al.* 2000). Salinity stress can also lead to a deficiency of K^+, which is an essential ion in the cell (Maathuis *et al.* 1999). Under salinity stress, plants will either cope by avoiding or tolerating the high salt environment. These tolerance mechanisms can be categorized as those that either function to minimize osmotic stress or ion equilibrium or to alleviate the secondary effects caused by these stresses (Munns *et al.* 2008).

A number of mechanisms exist by which some species of plants can minimise the damaging effects of salt stress, including detoxification mechanisms such as non-enzymic antioxidants and detoxifying enzymes which include superoxide dismutase (SOD), ascorbate peroxidise (APX), and glutathione reductase. The importance of the ROS protection pathway in salt stress and tolerance is evident from the observation that many of these enzymes increase with salt stress exposure of plants. For example, the *A. thaliana* pst1 mutant has high levels of SOD and APX when exposed to high levels of NaCl (Tsugane *et al.* 1999). Additionally forward and reverse genetic analyses have shown that alterations in the expression of these

enzymes can improve or diminish salt tolerance. The over-expression of glutathione-S-transferase and glutathione peroxidise in tobacco improved salt tolerance by reducing ROS-mediated cellular damage (Roxas *et al.* 1997; Roxas *et al.* 2000). More recently, an *A. thaliana* line with a null mutation in enh-1 was shown to be more sensitive to salt stress and accumulated higher levels of ROS compared to the wild type plant under salt stress. AtEnh-1 is thought to encode a rubredoxin-like protein which is involved in oxidative stress protection in microbes (Zhu *et al.* 2007).

5.1.4. Na^+ Transport

The main site of Na^+ toxicity for most plants is the leaf blade, where Na^+ accumulates after being deposited in the transpiration stream rather that in the roots (Munns 2002). As plants transpire 50 times more water that they retain in leaves, excluding Na^+ from the leaves is of most importance. The ability of plants to maintain an optimal K^+/Na^+ ratio in the cytosol is one of the key features of plant salinity tolerance (Munns *et al.* 2008). Plants try to maintain a normal ratio of Na^+/K^+ in the cells for healthy function. To do this there is thought to be several signalling pathways which may be involved when the plant is under salinity stress. The uptake of Na^+ into plant cells appears to occur at least partly through the transporter HKT1 (Laurie *et al.* 2002). In *A. thaliana*, Na^+ efflux is mediated by the plasma membrane Na^+/H^+ antiporter encoded by the SOS1 gene (Qiu *et al.* 2002) which drives Na^+ transport. As SOS1 facilitates Na^+ efflux into the root medium, it delays Na^+ accumulation in the cytoplasm. SOS1 appears also to control long-distance Na^+ transport between roots and leaves by mediating loading and unloading of Na^+ in the xylem and phloem (Zhu *et al.* 2007). Over expression of the SOS1 gene appears to confer increased salt tolerance, at least in part, in transgenic *A. thaliana* plants by these processes (Shi *et al.* 2003). It is thought that the AtHKT1 gene which acts to retrieve Na^+ from the xylem could be involved in signalling from salinity stress to help remove excess Na^+ from the leaves. It has been shown that when AtHKT1 is over expressed there is less Na+ accumulation in these lines, conferring salt tolerant plants

(Moller *et al.* 2007). These transport processes are reviewed by Munns and Tester (2008), and Tester and Davenport (2003). There is controversy regarding the mechanisms of Na^+ transport and flux into and out of the root xylem and to the shoot (Shi *et al.* 2003; Munns *et al.* 2008). It is clear that further work needs to be done on dissecting which flux is being effected in the AOX overexpressing lines, which may also assist in determining which transport system is being influenced by the altered cellular ROS levels.

5.1.5. Lines of *A. thaliana* overexpressing *aox1a*.

Previously a range of AOX mutants, both overexpressing and antisense lines were made (Umbach *et al.* 2005). Overexpression was confirmed at the protein level, where AOX expression was detected in a range of lines compared to Wt and pBI-Containing plants (vector control). In this study overexpressing lines XX1 and X6 and E9 were use. Line E9 is expressing a mutant form of AOX which is constitutively active. The E9 mutated form of *aox1a* lacks the regulatory cysteine residue that has been changed to glutamate. Thus, this form of AOX is not subject to inactivation by the formation of a disulfide bridge between the monomers and is highly active in the absence of keto-acids (Umbach *et al.* 2005). It was found that there was high expression of *aox1a* in both shoots and roots of plants from all of these lines, when stressed, and that only the monomeric form could be detected in E9 line.

Knowing that salinity has impacted on AOX in other species it was likely that the same response would be observed in *A. thaliana* plants, However, this need to be confirmed and if it was the case, then it may suggest that when AOX is over expressed in a plant, it may provide protection for the plant. It is thought that AOX with the alternative pathway acts to reduce ROS levels caused by stresses such as salinity, hence acting to protect the plant.

5.2 Aim

The overall aims of work in this chapter were to determine if AOX was up regulated under salt stress conditions in *A. thaliana* resulting in an increase AOX capacity and to determine if the other alternative dehydrogenases are co-regulated with AOX under salinity stress, which will link an increase in AOX with an increase in the alternative dehydrogenases. If AOX is up regulated, then the question is raised, would the overexpression of *aox1a* protect the plant against the deleterious effects of salinity stress.

5.3 Results

5.3.1. Alternative electron transport chain increases in response to salinity stress.

The use of shaking culture for biochemical analyses of *A. thaliana* seedlings has been previously reported (Moore *et al.* 2003). It is advantageous as it enables the rapid collection of sufficient amounts of material for organelle isolation and purification. It is also possible to separate tissues for smaller scale molecular biological analyses, when grown with care in the absence of fungicide.

Using the shaking culture system, seedlings were exposed to solution containing 100 mM NaCl. It has been shown that *A. thaliana* shows very low tolerance to salt and that at this concentration of NaCl can see a significant decrease in accumulation of dry matter compared to plants grown in the absence of salt (Munns *et al*. 2008). To confirm that the seedlings were under salinity stress, Na^+ and K^+ leaf and root content were measured. A significant increase in tissue level of Na^+, but not K^+ (Figure 5.2) was evident after only 24 hours of exposure in both shoots and roots. After 72 hours of exposure to salt, the Na^+ content continued to increase in leaves, being significantly different when compared to control plants but not in the roots, although the difference compared to the control was still significant.

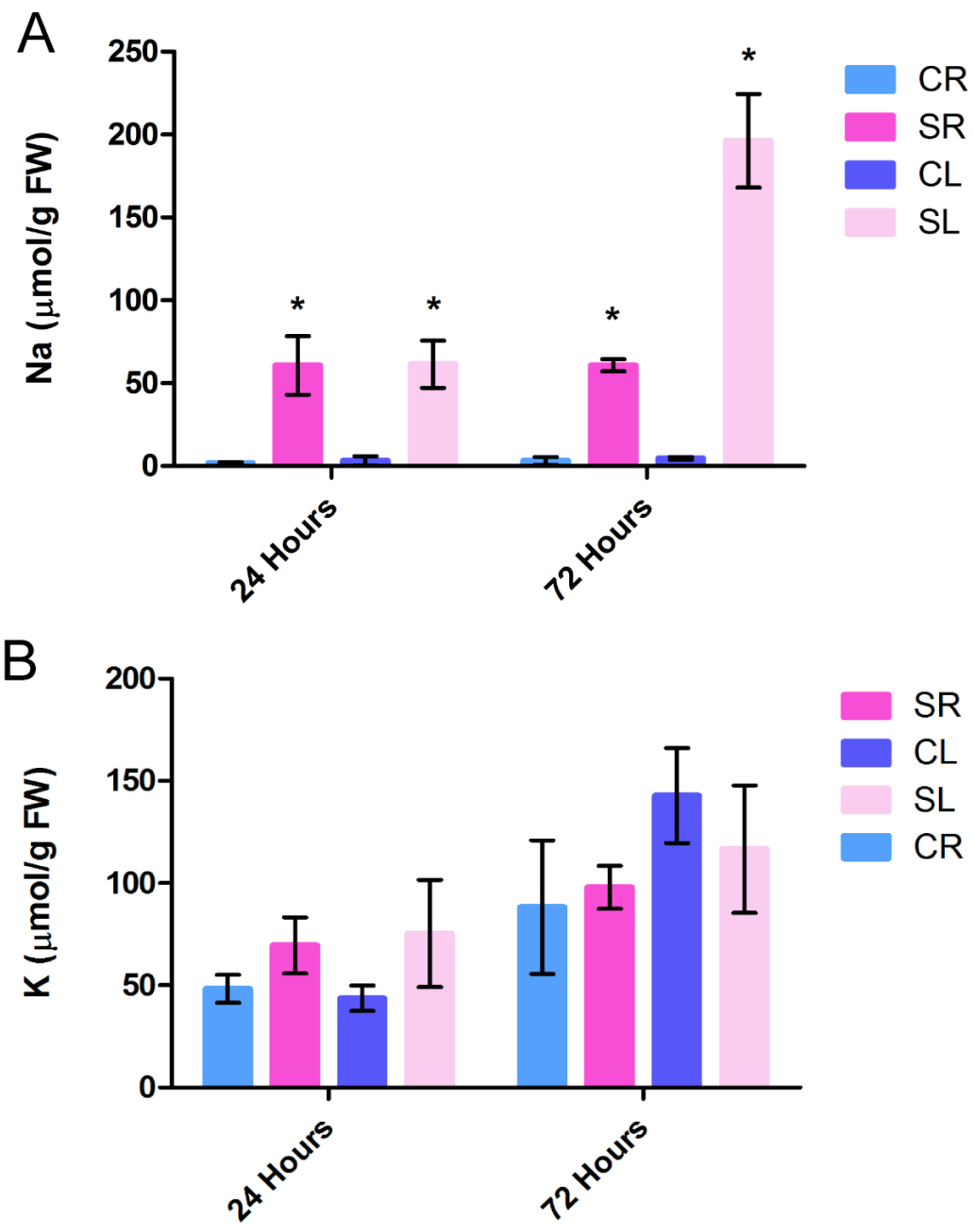

Figure 5.2: Na^+ and K^+ content in wild type *A. thaliana* tissue

Na^+ content (A) and K^+ content (B) were determined by flame photometry in root and leaf tissue of control (CR and CL) and salt-treated (SR and SL) plantlets growing in liquid culture. Tissue was harvested after 24 and 72 hours of exposure to 100 mM NaCl. The values are mean +/- SD for n=3. * are significantly different from the control treatment with P>0.05. At 24 Hours Na^+ Increase in shoots (Mean diff= 58.30, t= 5.523, P<0.001) and roots (Mean diff= 59.02, t= 5.591, P<0.001), at 72 Hour Na^+ increase in shoots (Mean diff= 191.5, t= 18.14, P<0.001) and roots (Mean diff= 57.63, t= 5.460, P<0.001)

Increased Na^+ content indicates that the seedlings were experiencing ion-specific toxicity and not only osmotic stress, which occurs within the early stages of salinity stress (Munns *et al.* 2008). The accumulation of Na^+ seen after 72 hours was due to the plant adjusting the osmotic stress, and a subsequent accumulation of Na^+ in the leaves (Munns *et al.* 2008). Initially at 24 hours K^+ increases in salinity stressed tissue as the K^+ is taken up by the cells, and after 72 hours the K^+ levels are relatively the same with no significant difference.

Mitochondria were isolated from the combined root and shoot tissue and showed an increase in AOX capacity after 24 hours of salt stress, which was maintained during the longer 72 hour stress (Table 5.1). After 72 hour of salinity stress, there was an increase in cytosolic NADH oxidation and a significant increase in cytosolic NADPH. There was no difference for the internal NAD(P)H oxidation. These results suggest that AOX together with an external alternative dehydrogenase respond together to the increased salinity stress. However, it is apparent that no internal dehydrogenase was responding. The external dehydrogenase and AOX are able to make their own pathway, which is most likely acting to reduce the quinol pool and help reduce ROS or allow metabolic flux for the synthesis of metabolites, such as osmoprotectants for example.

5.3.2. The response of the non-phosphorylating pathway to salt stress is regulated at the transcriptional level.

To confirm the activity increase seen for salinity stress in wild type tissue, the transcript response of the alternative pathway was determined. Previous microarray data have suggested that *aox1a* is one of the first genes to respond to salinity stress, (Kreps *et al.* 2002) suggesting that this increase in activity is regulated at the transcriptional level. Using QRT-PCR to determine relative transcript abundance, it was observed that there was an increase in transcript levels of the genes encoding these activities (Figure 5.3). After only six hours of salt stress there was a significant increase in *ndb2* in the roots,

Table 5.1. Salt treatment increases activity of the alternative oxidase and NAD(P)H dehydrogenase activities in *A thaliana* shaking cultures

Oxidation rates were determined using oxygen electrodes as described and are presented as nmol O_2.min.mg^{-1} protein. [a,b,c,d] indicate significant differences between mean values of the same annotation as determined by 2-way ANOVA (P>0.05). 72 Hours NADPH Oxidation (Mean diff= 62.00, t= 4.094, P<0.01).

	24 Hr		72 Hr	
	- NaCl	+ NaCl	- NaCl	+ NaCl
AOX capacity	0.0 ± 0.0[a]	13.2 ± 4.4[a]	8.2 ± 1.2[b]	36.4 ± 6.8[b]
Matrix NAD(P)H oxidation	20 ± 10	26 ± 10	13 ± 5	18 ± 6
Cytosolic NADH oxidation	81 ± 16	68 ± 14	64 ± 17	126 ± 25
Cytosolic NADPH oxidation	21 ± 6	17 ± 4[c]	25 ± 5[d]	48 ± 8[c,d]

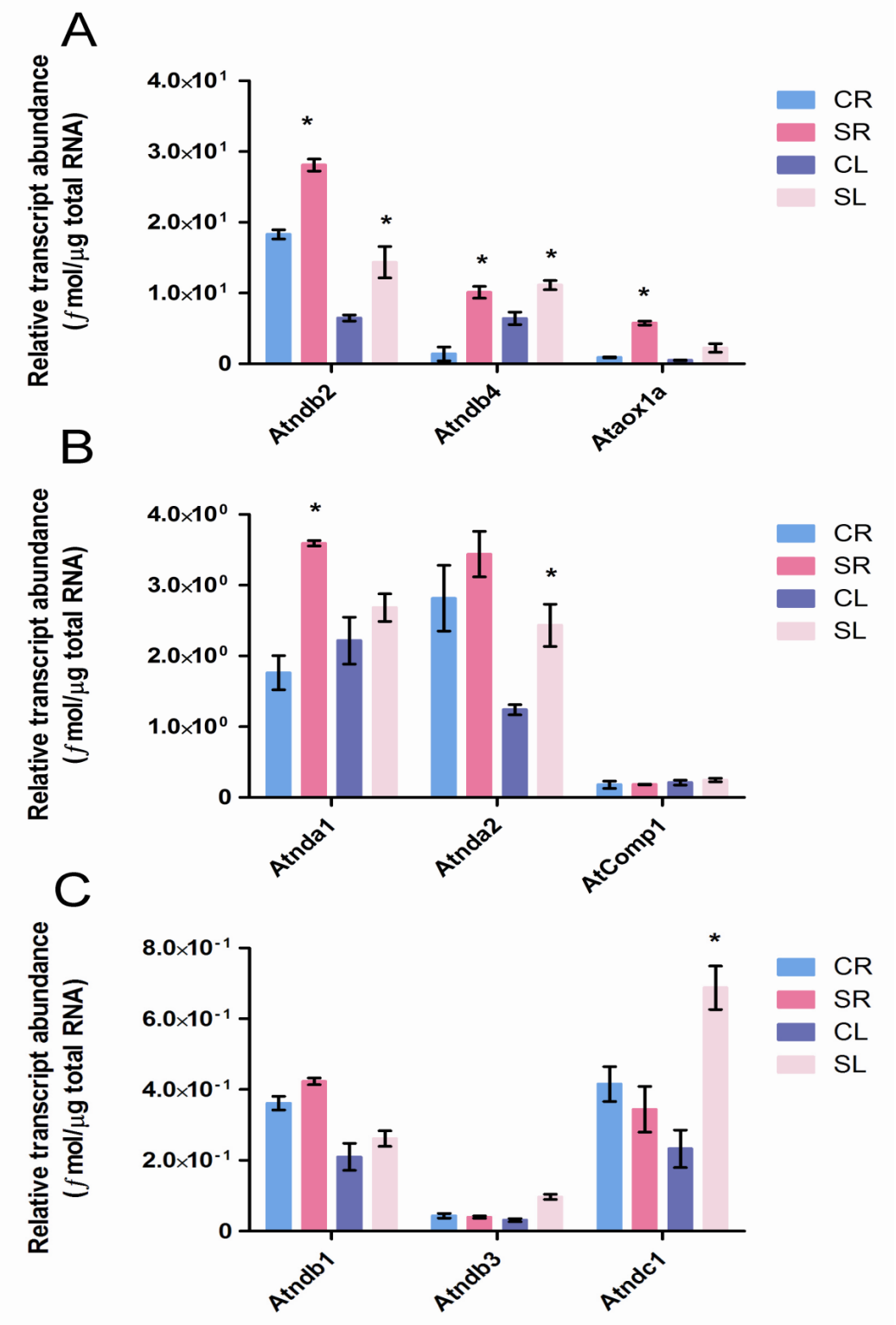
A
Relative transcript abundance
(fmol/μg total RNA)
4.0×10¹
3.0×10¹
2.0×10¹
1.0×10¹
0
Atndb2
Atndb4
Ataox1a
CR
SR
CL
SL
B
Relative transcript abundance
(fmol/μg total RNA)
4.0×10⁰
3.0×10⁰
2.0×10⁰
1.0×10⁰
0
Atnda1
Atnda2
AtComp1
CR
SR
CL
SL
C
Relative transcript abundance
(fmol/μg total RNA)
8.0×10⁻¹
6.0×10⁻¹
4.0×10⁻¹
2.0×10⁻¹
0
Atndb1
Atndb3
Atndc1
CR
SR
CL
SL

Figure 5.3 Regulation of the alternative pathway occurs at transcriptional level in roots and leaves for 6 hours salt stress

Relative transcript levels for genes encoding the non-phosphorylating pathway were determined by QRT-PCR. A, B and C are transcript levels after 6 hours of exposure of the plantlets to salt CR and CL refer to root and leave tissue grown in control liquid media, while SR and SL represents root and leaf tissue from plants in liquid culture with 100 mM NaCl. Atcomp1 is *A. thaliana* Complex 1. Values are mean +/- SD for n=3 with * being significant different from control tissue at P>0.05. 6 hours, *ndb2* roots (Mean diff= 9.800, t= 7.756, P<0.001), shoots (Mean diff= 7.870, t= 6.228, P<0.001). *ndb4* roots (Mean diff= 8.716, t= 6.898, P<0.001), shoots (Mean diff= 4.700, t= 3.720, P<0.01). aox1a roots (Mean diff= 4.872, t= 3.856, P<0.01). nda1 roots (Mean diff= 1.830, t= 5.670, P<0.001). Nda2 shoots (Mean diff= 1.193, t= 3.697, P<0.01). NDC1 shoots (Mean diff= 0.4550, t= 8.863, P<0.001).

and shoots, as well as *ndb4* for both roots and shoots. *aox1a* also had the same trend with a significant increase in just roots with salt stress. At 6 hours there was also a significant increase in *nda1* for roots. The shoots of both *nda2* and *ndc1* also had significant increases under salt stress.

Figure 5.4 shows the AOX protein level observed for extracted mitochondria at both 24 hours and 72 hours, which increased in conjunction with the 6hr and 72 hr transcript increase for *aox1a*. Hence the increase seen at the transcript level for *aox1a* was also observed at the protein level corresponding to the increase at 24 hours for protein. The increase in root *ndb4* transcript observed did not result in a significant increase in cytosolic NAD(P)H oxidation at 24 hours. It has been shown that *ndb4* and *ndb2* encode cytosolic NADPH and NAD(P)H oxidation activities respectively (Geisler *et al.* 2007). As both combined root and shoot mitochondria were used for biochemical activities, it is possible a dilution of the responses was observed at 24 hours of salt stress, due to the combined result of the shoot tissue masking the root response, as no increase in the *ndb4* transcript was observed in the shoots. The increase in NAD(P)H oxidation was not due to any increase in the phosphorylating pathway as there was no increase in complex I transcripts. While *nda1* transcript increased after 6 hours of salt stress in root tissue, the expression level was low with respect to that of *ndb2* and *ndb4* as seen in Figure 5.3. The same was seen for *ndc1* in salt stressed leaves. It is known that *nda1* encodes a matrix-facing NAD(P)H dehydrogenase (Elhafez *et al.* 2006), however there was no increase in matrix NAD(P)H oxidation was observed.

The longer term stress resulted in increased *ndb4* and *aox1a* transcripts in both root and shoot tissues at 72 hours (Figure 5.5). This was also seen at 24 hours. However, *ndb2* and *nda1* also slightly increased in the root in 72 hours of salt stress, which was not seen at 24 hours. Therefore, the prolonged salt stress for 72 hours has resulted in the maintenance of the increased *aox1a* and *ndb4* transcript levels. This also resulted in a high AOX capacity in the isolated mitochondria from the 72 salt stressed tissue, as well as a significant increase in cytosolic NADPH (and NADH) oxidation,

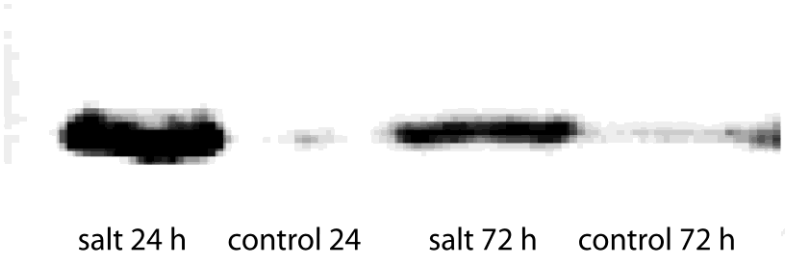

Figure 5.4 AOX protein levels increase during salt treatment

Protein abundance of AOX in Wt tissue subjected to 100mM of NaCl compared to control growth conditions from isolated Mitochondria. . Only the monomeric 34 kDa protein was detected under reduced conditions.

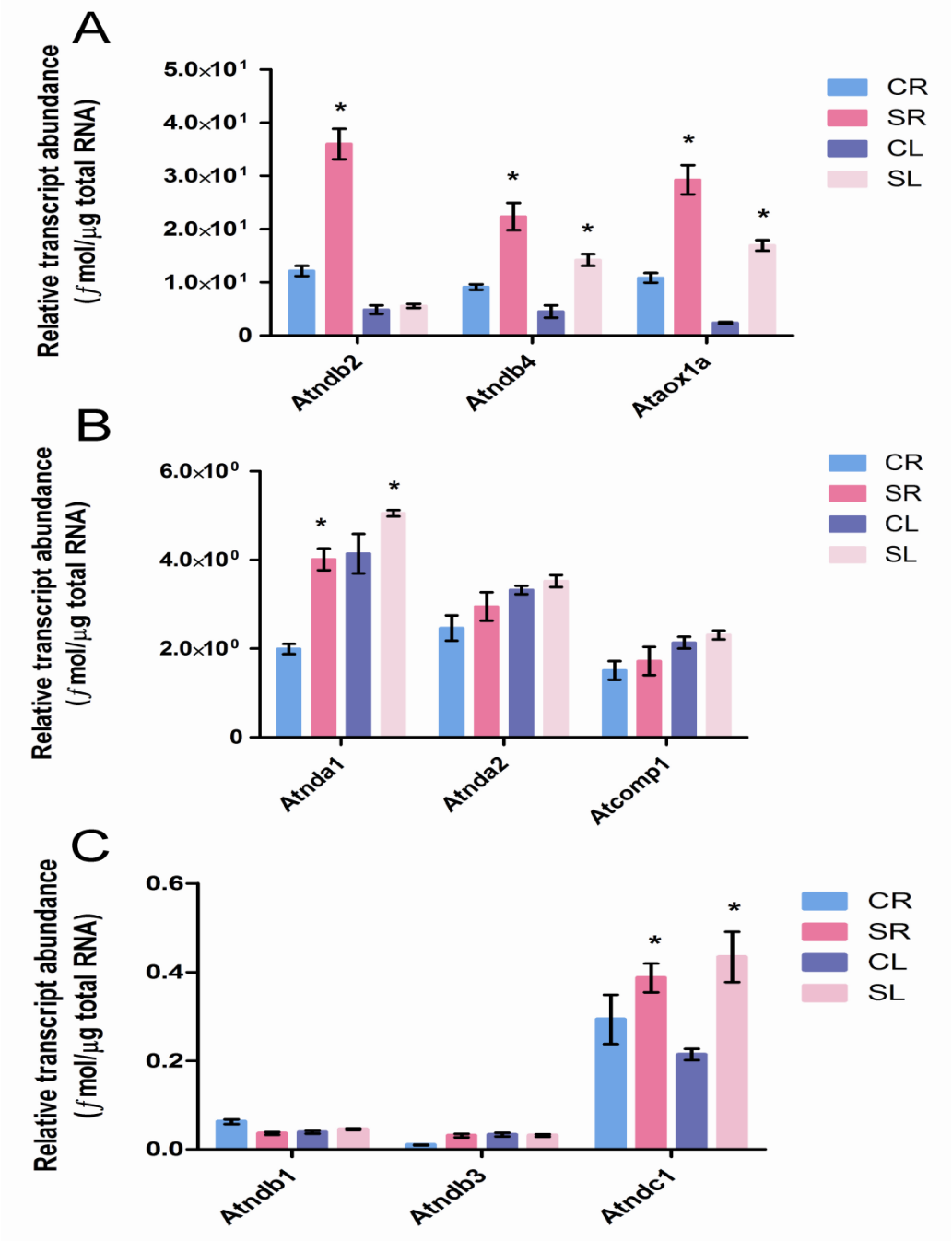

Figure 5.5 Regulation of the alternative pathway occurs at transcriptional level in roots and leaves for 72 hours salt stress

Relative transcript levels for genes encoding the non-phosphorylating pathway were determined by qRT-PCR. A, B and C are transcript levels after 72 hours of exposure of the plantlets to salt CR and CL refer to root and leave tissue grown in control liquid media, while SR and SL represents root and leaf tissue from plants in liquid culture with 100 mM NaCl. Values are mean +/- SD for n=3 with * being significant different from control tissue at P>0.05.

consistent with suggestions that *ndb4* and *ndb2* encode the cytosolic facing NAD(P)H dehydrogenases (Elhafez *et al.* 2006; Geisler *et al.* 2007). This increase in cytosolic NADPH activity was not seen at 24 hour salt stress. An analysis of publicly available microarray data from *A. thaliana* plants exposed to salt stress (100 mM) through the GENEVESTIGATOR database (Zimmermann *et al.* 2004), indicated that there increases in *ndb2*, *aox1a* and *nda1* upon salt stress. The microarray data were consistent with the QRT-PCR data in this study. Unfortunately there was no data for *ndb4* on this website.

Thus, it can be concluded that an alternative non-phosphorylating electron transport chain, composed of *ndb4*, *ndb2* and *aox1a* forms in root and shoot mitochondria during the initial response to salt stress and this non-phosphorylating ETC is maintained during prolonged salt stress.

5.3.3. Over-expression of AOX helps protect against oxidative stress induced by salt treatment.

Based on results presented from salinity stress response shown by wild type plants in this study and from previous work, where it has been observed that AOX increases under salinity stress, we now wanted to know what role AOX playing during salinity stress. Additionally, we wished to examine whether plants over-expressing AOX would show a level of resistance to the detrimental effects that this stress has on the plant. It has been shown that the cellular levels of ROS increase during salt stress (Hasegawa *et al.* 2000), and that in addition to the toxic effects of high levels of Na^+, the increase in ROS would further exacerbate damage to the cell and tissue. The role of AOX has been linked to lowering ROS production in the plant cell for many biological conditions, including stress (Moller 2001). Hence it is hypothesised that a role for AOX activity for salinity stress was to play a role in minimising the effect of oxidative stress. ROS levels were measured for hydroponically grown *A. thaliana* plants overexpressing AOX, and it is hypothesised that these plants would have lower ROS levels. The plant lines used in this study

were generated by Umbach *et al.* (2005), and were overexpressers of *aox1a* (lines X6 and XX-1) and a mutated form of *aox1a* (E9) as previously explained. pBI-Containing plants is the empty vector control used for these lines.

It was hypothesized that the *aox1a* transcript would be increased for these overexpressing mutants under normal conditions and this would be maintained under salinity conditions. Figure 5.6 shows that under controlled growth conditions, the X6, XX-1 and E9 lines showed higher levels of *aox1a* transcript than Wt plants, as expected. However, when exposed to salt stress, there was an additional increase in *aox1a* transcript, indicating that not only had the transcript been maintained, there was an additional increase in response to the salinity stress (Figure 5.6). These transcript increases under salinity stress were significant for XX1, X6, and for E9. The increased transcript levels under salinity conditions appeared to be the sum of the wild type response of the endogenous *aox1a* gene (Figure 5.3 and 5.5) plus the overexpression effect. Thus, the increased level of *aox1a* in the overexpressing lines was confirmed and their response to salt stress with an increase in *aox1a* expression was consistent with that observed for Wt tissue.

The oxidative stress effect of salt exposure was assessed using the Amplex Red assay. This assay is a direct quantitative measure of oxidative stress as it detects levels of H_2O_2 in tissue extracts. Knowing the *aox1a* transcript was further increased in salt stressed tissue it was expected that these plants would have reduced levels of ROS (H_2O_2) if AOX was playing a role of reducing ROS species as had been suggested. Salt stress caused a significant increase in H_2O_2 levels in the Wt and pBI-Containing plants lines for both roots and shoots (Figure 5.7). The 150 mM salinity stress imposed on these plants caused an increase in H_2O_2 levels, but as was hypothesized the increase was significantly lower when compared to pBI-Containing plants lines, for XX1 in roots, and shoots. These results suggest that when AOX activity is increased, it is able to reduce the highly reduced ubiquinone pool that was a result of exposure of the plants to salt. Hence, as hypothesized,

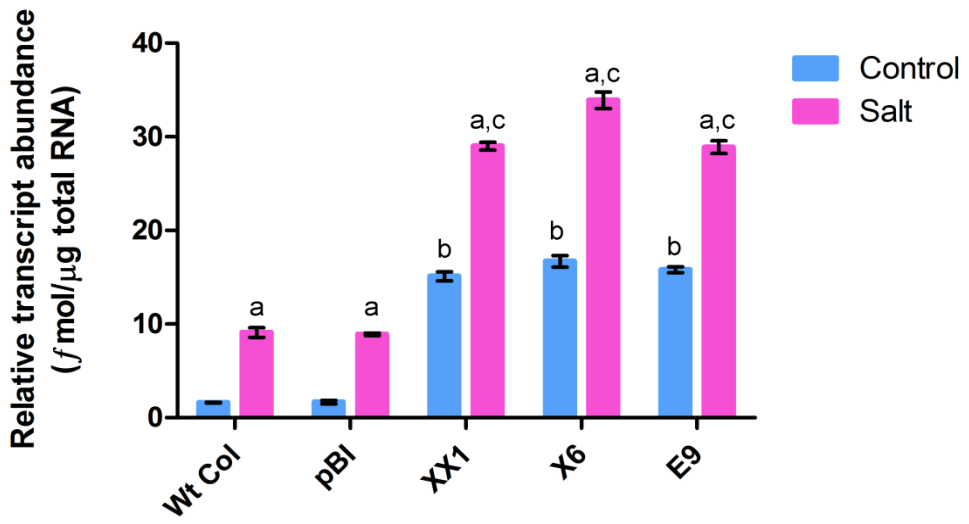

Figure 5.6 Transcript response of *aox1a* in AOX over-expression plant lines after salt stress

Transcript levels for *aox1a* were determined by qRT-PCR from leaves of plants grown hydroponically in the presence (salt) and absence (control) of 150 mM NaCl. Values represent means +/- SD for n=3, where [a] indicates significant difference when comparing control to salt treated plants. [b] and [c] indicate significant differences for Wt and pBI-Containing plants compared to AOX over expressing lines, where [b] is relevant for comparisons between control growth conditions and [c] is relevant for comparisons between salt growth conditions. XX1 (Mean diff= 19.90, t= 28.25, P<0.001), X6 (Mean diff= 24.80, t= 35.21, P<0.001), and E9 (Mean diff= 19.80, t= 28.11, P<0.001).

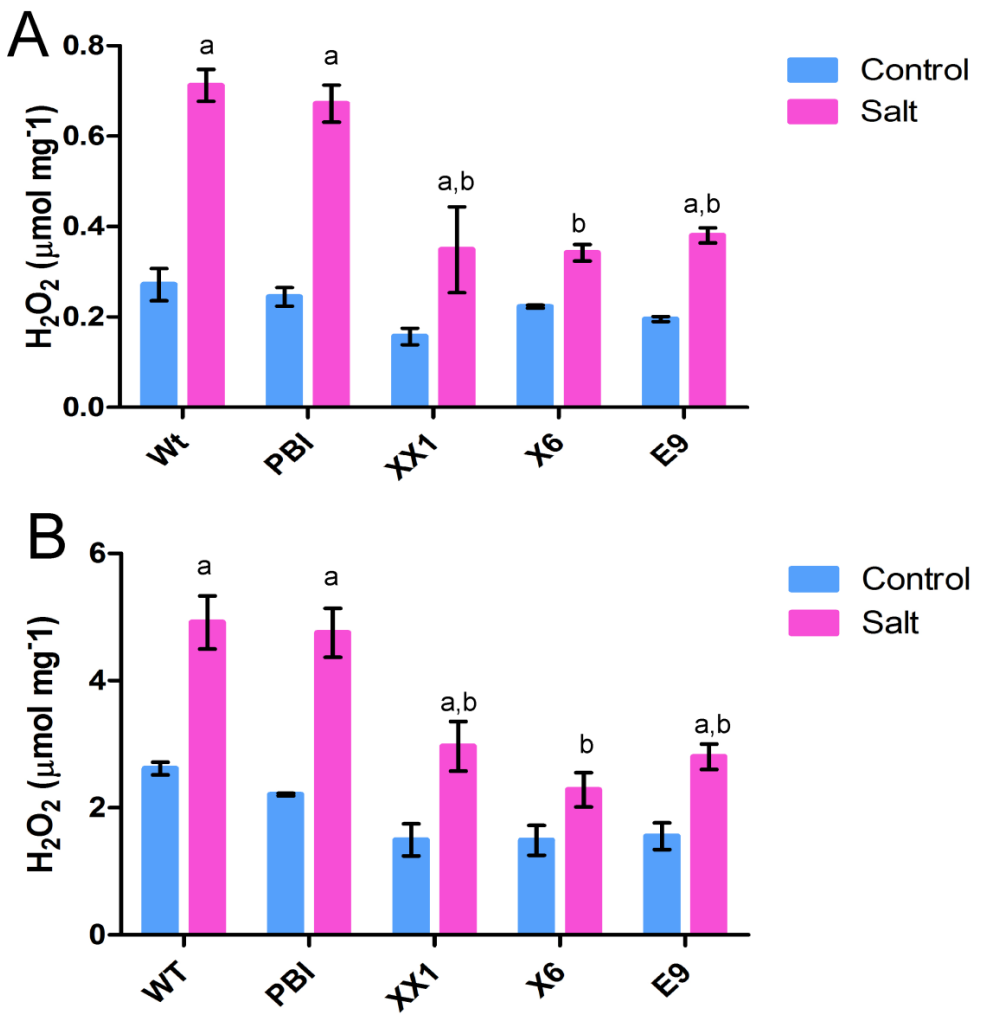

Figure 5.7 ROS levels in AOX overexpressers (A) roots and (B) shoots

ROS levels, specifically H_2O_2, were quantitatively determined using the Amplex Red assay in root (A) and leaf (B) tissue from plants grown in presence (salt) and absence (control) of 150mM NaCl in growth media for 10 days. Values are means +/- SD for n=3, where a indicates significant differences at P>0.05, when comparing control to salt treated plants and b for Wt and pBI-Containing plants compared to AOX over expressers under salt growth conditions. Wt, roots (Mean diff= .4277, t= 7.909, P<0.001), shoots (Mean diff= 2.545, t= 6.522, P<0.001). XX1 roots (Mean diff= -0.3233, t= 5.977, P<0.001) shoots (Mean diff= -1.949, t= 4.997, P<0.001).

with the increased AOX capacity, there was a minimisation of ROS formation which was protecting the plant against oxidative stress. The AOX overexpressing lines had a trend towards lower H_2O_2 levels under control conditions, although this was not significant at the P>0.05 level. This observation was consistent with a role of AOX in minimising ROS production also found by Umbach *et al.* (2005) when the cytochrome pathway was compromised.

5.3.4. Overexpression of *aox1a* improved the growth rate during salt stress.

Na^+ tolerance can be defined by the ability of a plant to grow in a solution or soil containing NaCl (Munns *et al.* 2008). The salinity tolerance of AOX overexpressing plants was assessed by measuring the impact on relative growth rate (RGR) over 10 days of salt exposure. It was hypothesized that if plants overexpressing AOX were more tolerant of NaCl due to the ability to reduce ROS species they would have a higher relative growth rate than the control. In the Wt and pBI-Containing plants plants, there was a significant decrease in RGR for both root and shoot tissue as shown in Figure 5.8 for Wt and pBI-Containing plants. This was as expected as *A. thaliana* plants have been reported to be quite sensitive to salinity stress (Munns *et al.* 2008), although when AOX was present they appear to have an increased tolerance. Under salinity conditions, there were significantly increased growth rates for the AOX overexpressers such as XX1 in roots, and shoots. Under controlled treatment conditions the AOX overexpressers had lower RGR compared to Wt and pBI-Containing plants. The XX-1 line showed a marginal, but significant reduction in root and shoot RGR. While the X6 line showed the same trend as XX-1 line for RGR, it was only significant for the shoot tissue, and the RGR of the E9 line was not significantly different from either the Wt or pBI-Containing plants lines. More dramatic though, was the significantly higher root and shoot RGR displayed by all AOX overexpresser lines after salt stress. The overexpresser lines showed an increase of 60% root and 40% shoot RGR compared to the Wt and pBI-Containing plants

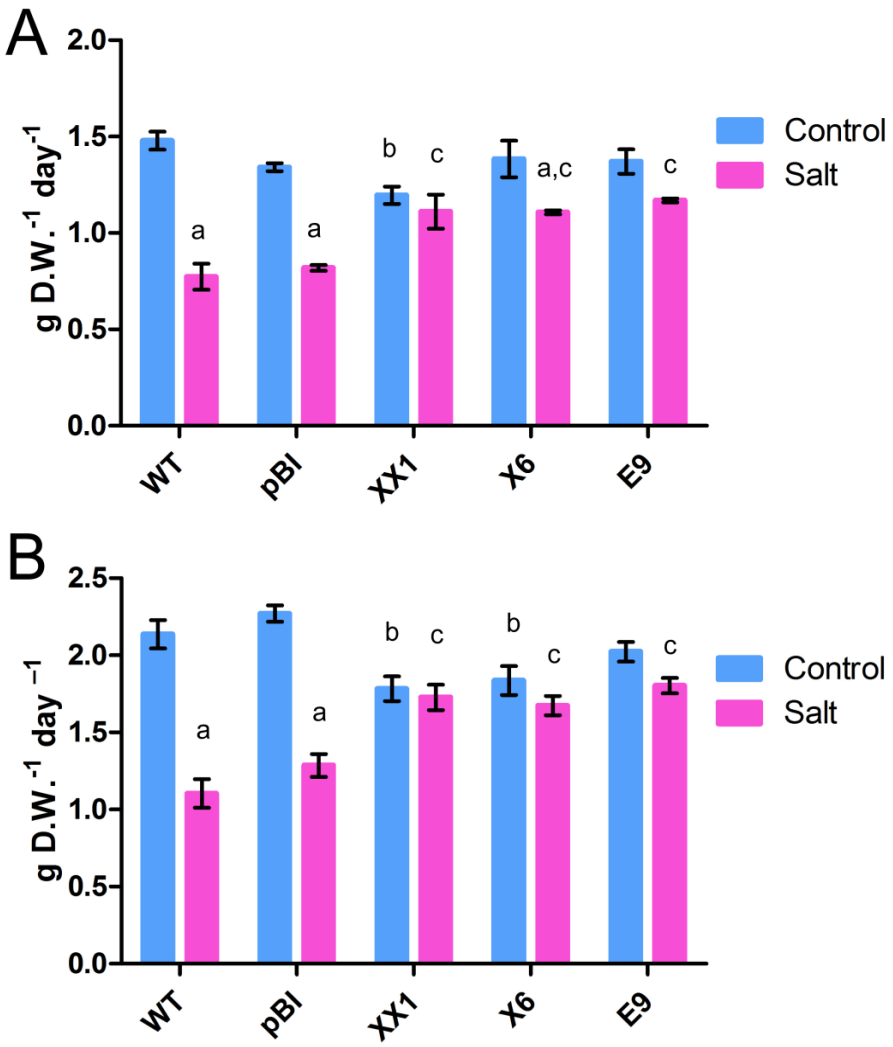

Figure 5.8 Over-expression of AOX results in higher growth rates during salt stress

The RGR was determined for roots (A) and leaves (B) of plants grown hydroponically in the presence (salt) and absence (control) of 150 mM NaCl for 10 days. Values are means +/- SD for n=3, where [a] indicates significant difference, P>0.05 when comparing control to salt treated plants, [b] and [c] indicate significant difference for Wt and pBI-Containing plants compared to AOX overexpresser lines under (b) control condition and (c) salt conditions. Wt, roots (Mean diff= 1.193, t= 3.697, P<0.01), shoots (Mean diff= 1.193, t= 3.697, P<0.01). XX1, roots (Mean diff= 0.3370, t= 4.325, P<0.001), shoots (Mean diff= 0.6235, t= 5.819, P<0.001). XX1, root (Mean diff= -0.2838, t= 3.641, P<0.01), shoot (Mean diff= -0.3527, t= 3.292, P<0.01). X6, shoot (Mean diff= -0.2992, t= 2.792, P<0.05).

plants during salinity stress (Figure 5.8).The different response between Wt and overexpressing lines was visually evident after 10 days (Figure 5.9).

5.3.5. Overexpression of *aox1a* altered the Na^+ and K^+ balance, reducing Na^+ shoot content.

Salinity tolerance can also be defined as the ability of a plant to reduce Na^+ shoot content (Maathuis *et al.* 1999; Munns *et al.* 2008). Therefore the Na^+ and K^+ content of the AOX overexpressers and control plants were determined. Figure 5.10 and 5.11 showed that salt stress increased the content of Na^+ and lowered the K^+ content in both roots and shoots of Wt and pBI-Containing plants plants, in agreement with the shaking culture experiments (Figure 5.2). The AOX overexpresser lines had lower shoot Na^+ levels and higher shoot K^+ content. However, it was found that there was higher root Na^+ content and no difference in K^+ content, indicating these plant lines retained a higher root Na^+ content and lower Na^+ shoot content (Figure 5.10). The Na^+/K^+ ratio reflected the differences as seen in Figure 5.10 and 11. Where for the roots there was no difference or a slightly higher ratio for XX1 which was significant at a higher P level. There was a significant lower ratio for the shoots for all three lines; XX1, X6, and E9. Interestingly, even under normal growth conditions, the AOX overexpresser lines had a significantly higher K^+ level in the shoots, and a trend towards a higher K^+ content in the roots.

Thus, these AOX overexpresser lines demonstrated an altered ionic balance for Na^+ and K^+ that resulted in lower shoot Na^+ content with retention in the root, indicative of increased salinity tolerance and suggesting a change in long distance transport of Na^+ in these plants.

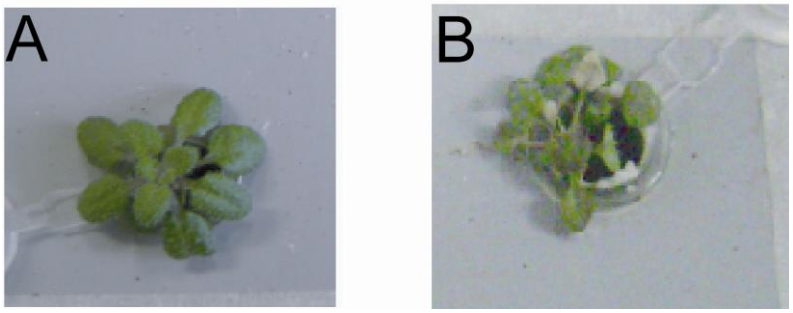

Figure 5.9 Visualization of plants growing under salt stress conditions
Photographs of a XX-1 plant (C) grown in 100mM NaCl for 10 days compared to a pBI-Containing plants control plant (D) under the same salt conditions, indicate the AOX overexpresser lines showed increased growth.

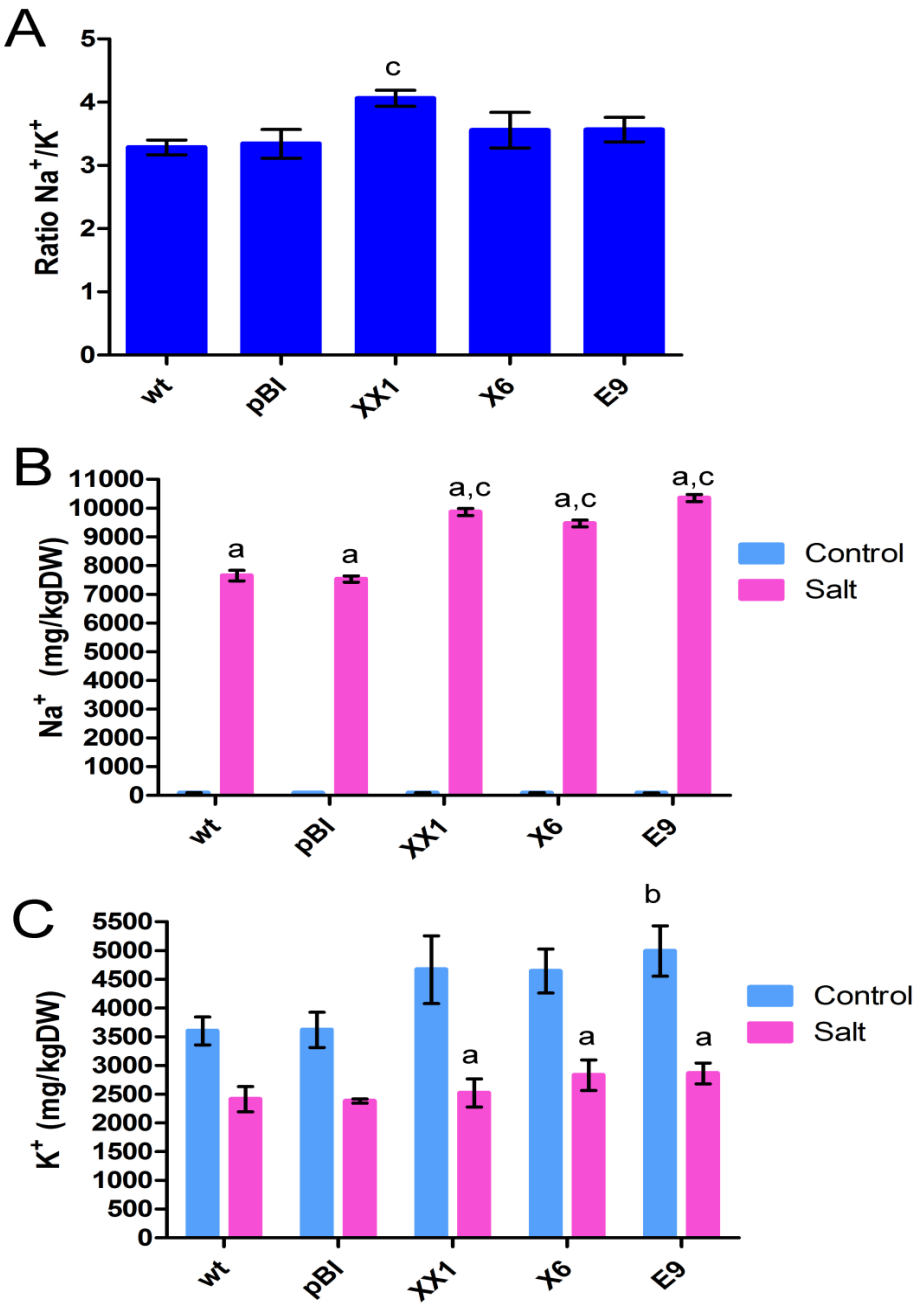

Figure 5.10 Overexpression of *aox1a* affects the root Na^+ and K^+ content
The ratio of Na^+/K^+ for the root (A) tissue after growth in 150 mM NaCl for 10 days. The Na^+ content of the root (B) and K^+ content of the root (C) were determined y ICPOES analysis. Values are the mean +/-SD for n=3 where, [a] indicates significant difference when comparing control to salt treated, [b] and [c] indicate significant difference for Wt and pBI-Containing plants compared to AOX- over expressing lines under (b) control condition and (c) salt conditions. Ratio Na^+/K^+ XX1 (Mean diff= -0.7203, t= 4.434, P<0.05).

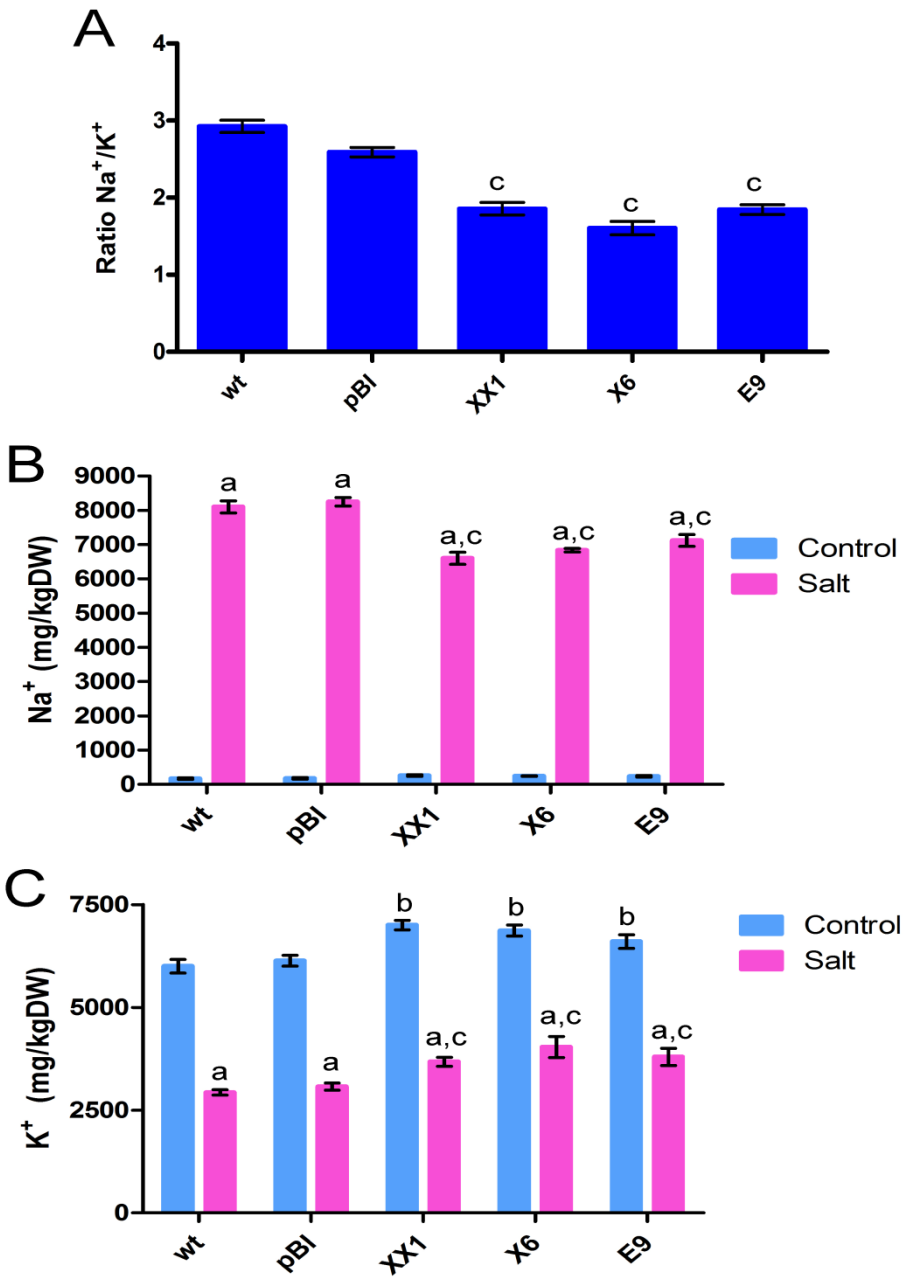

Figure 5.11 Overexpression of *aox1a* affects the shoot Na^+ and K^+ content

The ratio of Na^+/K^+ for the shoot (A) tissue after growth in 150 mM NaCl for 10 days. The Na^+ content of the shoot (B) and K^+ content of the shoot (C) were determined y ICPOES analysis. Values are the mean +/- SD for n=3 where, ^{a} indicates significant difference when comparing control to salt treated, ^{b} and ^{c} indicate significant difference for Wt and pBI-Containing plants compared to AOX- over expressing lines under (b) control condition and (c) salt conditions. Ratio Na^+/K^+ XX1 (Mean diff= 0.7347, t= 6.899, P<0.001), X6 (Mean diff= 0.9855, t= 9.255, P<0.001), and E9 (Mean diff= 0.7456, t= 7.002, P<0.001).

5.4 Discussion

If AOX is up regulated, then the question we have tried to answer is, would the overexpression of *aox1a* in *A thaliana* protect the plant against the deleterious effects of salinity stress. Although there have been recent studies of AOX under salinity stress for various species. An earlier microarray study has also observed that aox1a increased after only 3 hr after exposure to salt stress (Kreps et al. 2002). From the work presented in this study, I have shown that AOX transcript, activity and protein all increase in response to salinity stress. Also the alternative NAD(P)H dehydrogenases responded to salinity stress which has led to the proposal that a reduced non-phosphorylating electron transport chain composed of cytosolic NAD(P)H dehydrogenases (*ndb2, ndb4*) and alternative oxidase (*aox1a*) forms in response to salinity stress.

Although there has been varying functions suggested for AOX, there has been less proposed as functions for the alternative dehydrogenases, although one of these is the link to metabolic flexibility in a plant. It has been suggested that AOX may enable the release of respiration from adenylate control, thus allowing the continued production of biosynthetic precursors and/or flux through primary metabolism. It may also be the non-phosphorylating pathway which allows this to occur and hence facilitate protection during the early stages of salinity stress, which is why plants with AOX overexpressed were better protected. However, there is much more evidence for the role of AOX in the minimisation of ROS levels in plants cells (Moller 2001) The increase in AOX has been linked to the ability to keep the UQ pool in a more oxidised state and minimise the harmful formation of ROS species by stopping these high energy electrons in the reduced ubiquinone interacting with molecular oxygen (Amirsadeghi *et al.* 2006).

The response of a plant to salinity stress resulted in a reduction in growth and can be due to two different effects that are, an osmotic effect of the salt in the solution bathing the plant and the toxic effect of the salt within the plant

(Munns *et al.* 2008). These occur in two phases, a rapid response to the increase in external osmotic pressure, which has an immediate impact on growth and a slower response due to the accumulation of Na^+ in the leaves or other tissues, which results in a longer term growth response. Data presented here indicated an immediate response with AOX and an NAD(P)H dehydrogenase, which was supported in microarray studies (Kreps *et al.* 2002; Zimmermann *et al.* 2004), this increase is maintained, suggesting a role for this pathway in both the short and long term responses to salt stress.

Salinity stress is well documented to result in the accumulation of ROS (Gomez *et al*. 1999; Borsani *et al*. 2001), and it has been suggested that AOX to plays a role in minimising ROS and hence in minimising this harmful effect of salinity stress. This data has linked higher expression of AOX resulting in decreased ROS and a tolerance to salinity stress. The plants overexpressing the *aox1a* gene showed lower H_2O_2 (ROS) levels during salt stress for both root and shoot tissues. This observation agreed with previous data on the same AOX overexpressing lines, where there were lower levels of ROS generation when the cytochrome pathway was inhibited by KCN treatment and during cold stress (Fiorani *et al.* 2005; Umbach *et al.* 2005). The decrease of ROS for *A. thaliana* overexpressing AOX lines was linked to an increase in AOX capacity as well. Although suspension cell cultures of tobacco overexpressing AOX have shown a difference in the expression of other oxidative stress enzymes such as, Mn-supoxide dismutase, peroxidoredoxins, glutathione reductase and ascorbate peroxidise (Maxwell *et al.* 1999), these AOX overexpressing lines did not, as determined by (Umbach *et al.* 2005). Hence, in this plant under these conditions it appeared that AOX alone can protect the plant from oxidative damage, in this case caused from salinity stress.

For the AOX overexpressers grown under control/optimal conditions, it was found that there was no difference in root RGR and approximately 20% reduction in shoot RGR. This decrease in shoot RGR may reflect the hypothesised inefficiency that would be expected in plants where respiratory electron flow occurs through a greater proportion of a non-ATP producing

pathway. Although under salinity stress conditions, the AOX overexpressers had higher RGR compared to Wt, this may have been due primarily to their lower Na^+ levels in shoots. Growing or surviving in a saline soil imposes some costs to the plant; the cost of excluding salt, of intracellular compartmentation, and of excreting it through salt glands (Yeo 1983). High salinity is a stress condition that affects plant growth and crop production (Xiong *et al.* 2002), as the plants ability to take up water is reduced due to the osmotic balance and hence causes decreased growth rate and a long cascade of metabolic changes (Munns 2002). Hence the improved RGR of these AOX overexpressers is an indication of tolerance and the ability of these plants to adapt to saline conditions. Suggesting the overexpression of AOX improves the RGR of both shoots and roots of salt stressed plants due the minimisation of ROS species, and hence ROS related damage to the *A. thaliana* plants.

As well as lowered ROS levels and improved growth, the AOX overexpressing lines showed a novel response of altered ionic homeostasis (lower leaf Na^+ levels, and higher root Na^+ levels) compared to Wt plants. The improved salinity tolerance is suggested to be a result of Na^+ being exported out of the leaves or stopping the flow up the leaves, as it is a build up of Na^+ in the leaf tissue which results in Na^+ toxicity. The net delivery of Na^+ to the xylem has four distinct components; influx into the cells in the outer part of the root; efflux back out from these cells to the soil or bathing media; efflux from the cells in the inner root cells into the xylem and influx back into these cells from the xylem before transpiration delivers the Na^+ to the shoot (Munns *et al.* 2008). Hence the lower leaf Na^+ content observed maybe a consequence of potential changes in any of these fluxes, including a higher efflux of Na^+ from xylem into inner root cells (or xylem, retrieval) or higher efflux out of outer root cells into soil/media.

Salt exclusion functions to reduce the rate at which salt accumulates in transpiring organs. There are several mechanisms by which salt is excluded from leaves such as selectivity of uptake by root cells. It is still unclear which cell types control the selectivity of ions from the soil solution. There is

evidence for a preferential loading of K^+ rather than Na^+ by the stelar cells that is under genetic control (Gorham *et al.* 1990). Or the exclusion could be due to the removal of salt from the xylem in the upper part of the roots, the stem, petiole or leaf sheaths (Munns 2002). In many species, Na^+ is retained in the upper part of the root system and in the lower part of the shoot, indicating an exchange of K^+ for Na^+ by the cells lining the transpiration stream. There was evidence of exclusion from the leaves on AOX overexpressers compared to the Wt plants which indicates tolerance. This may be due to ROS signalling and the activation of Na^+ and K^+ transporters which aid in exclusion.

The major transport systems involved in these processes include; SOS-1, a Na-H antiporter at the cell:soil interface and the cell:xylem interface, and; HKT-1, a high-affinity K^+ transporter which also mediates Na^+ transport (Davenport *et al.* 2007; Munns *et al.* 2008). It is known SOS-1 participates in the retrieval of Na from the xylem, as overexpression of SOS-1 produced plants with increased salt tolerance.

The link between ROS and long distance Na^+ transport and the effect of overexpression of AOX is unknown. It appears, from the data that increased AOX results in lower ROS levels, which then results lower shoot Na^+ levels. The mechanisms by AOX overexpression and salt stress-induced ROS, regulate ion transport is unclear. It is known ROS induces K^+ efflux from *A. thaliana* roots (Cuin *et al.* 2007). The level of root cytoplasmic K^+ has been shown to influence Na^+ shoot levels and hence Na^+ tolerance (Maathuis *et al.* 1999), However, Zhu *et al.* (2007), suggest that ROS may interfere with the selectivity of the transporter proteins or disturb the cytoplasmic pH, and hence this altered pH may lead to a disruption of transporter proteins. Hence the ability of the plant to retain cytoplasmic K^+ has been linked to salinity tolerance not only in *A. thaliana*, but other plants, including wheat (Cuin *et al.* 2008). It is interesting to note that under controlled growth conditions, the AOX overexpressers had higher K^+ levels in leaf than in the leaves of Wt lines. The lower ROS effect may also influence cytoplasmic K^+ levels by this mechanism under these conditions, thus giving the AOX overexpressing

plants a significant advantage before the Na^+ stress is applied. Thus, it appears that more work with the AOX overexpressing lines is needed, to determine the mechanism by which lower ROS levels are mediated by the alteration in long distance Na^+ transport. However, recently it has been shown that ROS levels increase the stability of SOS-1 mRNA levels (Chung *et al.* 2008). If this is so, then lower ROS levels in the AOX overexpressing lines would result in a decrease the amount of SOS-1 transporter. If this transporter is involved in Na^+ influx into the xylem, as suggested (Shi *et al.* 1999) then a lower level of this protein would result in lower net influx of Na^+ into the xylem. However, as mentioned previously, the involvement of this transporter in xylem Na^+ loading is controversial (Munns *et al.* 2008) and the effect of ROS on HKT1, the other Na^+ transport system, needs clarification. One mechanism through which ROS may influence Na^+ tissue levels is through the effect of ROS on K^+ transport. It has been shown that ROS inhibit K^+ channels in guard cells of *Vicia faba* (Kohler *et al.* 2003). Further, ROS induces K^+ efflux from *A. thaliana* roots (Cuin *et al.* 2007). The level of root cytoplasmic K^+ has been shown to influence Na+ shoot levels and hence Na+ tolerance (Maathuis *et al.* 1999), thus the ability of the plant to retain cytoplasmic K^+ has been linked to salinity tolerance not only in *A. thaliana*, but other plants, including wheat (Cuin *et al.* 2008). The lower ROS effect thus, may also influence cytoplasmic K^+ levels by this mechanism under these conditions, thus giving the overexpressing plants a significant advantage before the Na^+ stress is applied.

Although the AOX overexpressing lines displayed a slightly lower growth rate, it maybe that plant varieties with higher active AOX levels have a significant adaptive advantage over varieties with lower AOX activity. This observation with salt stress supports the hypothesis that AOX can play a critical role in cell reprogramming under stress whether this is by a temporary increase in AOX activity in response to the stress, or by an adaptive advantage in plant lines/genotypes that have naturally higher AOX activity. As an increase in the alternative dehydrogenases occurred under salinity stress, it would be interesting to observe if further tolerance is achieved by plant with already increased AOX and alternative NAD(P)H dehydrogenases.

Although AOX and alternative NAD(P)H dehydrogenases increase under salinity stress, it has been suggested that an already increased transcript of AOX appears to help with re-programming of cells to induce salt tolerance. Hence would a plant with already increased AOX and an alternative NAD(P)H dehydrogenase provide further tolerance due to cell reprogramming? This is a question that is explored in the next chapter.

6 UP REGULATION OF THE ALTERNATIVE PATHWAY CAN PROTECT AGAINST SALT TOLERANCE IN *ARABIDOPSIS THALIANA*

6.1 Introduction

6.1.1. Conferring salt tolerance on plants with modified alternative pathways

As discussed in the previous chapter, stress growth conditions can influence expression of the alternative pathway, suggesting that the alternative pathway may be involved in the stress response of plants. There have been many previous reports that suggest that AOX protects the plant under salinity stress, (Section 5.1.3) and results from this study suggests that this occurs by reducing or avoiding the build up of ROS (Section 5.3.3). Previous experiments with both wild type *A. thaliana* and AOX overexpressers indicate that AOX was up-regulated at the transcriptional level resulting in an increase in protein abundance and AOX capacity. This up-regulation of AOX did result in reduced ROS in these lines and lead to a salt tolerant line with improved RGR and altered Na^+/K^+ ratio due to the plant avoiding Na^+ build up.

The results from these AOX overexpresser lines suggested that when AOX was already up-regulated prior to the addition of salt, the plant was in a pre-prepared state for the stress and hence could adapt more quickly to the salinity stress applied. In Wt plants, it has been shown, in this study, that when AOX was up-regulated, so were members of the alternative dehydrogenases mainly *ndb2* an *ndb4* and *nda1*. Hence it was hypothesized that if an external and internal alternative dehydrogenase were up-regulated as well as AOX prior to stress, then an *A. thaliana* plant line with increased constitutive expression of these genes would be better equipped to cope with the stress.

6.1.2. Alternative pathway over expressing lines

Previously in chapter three *A. thaliana* plants over expressing certain family members of the alternative pathway were characterised. In this chapter, these lines were exposed to salinity stress to determine if the plants are better equipped to cope with this stress, due to the up regulation of the alternative respiratory pathway prior to stress. Four lines were used for analysing the stress as all had varying levels of expression of different members of the alternative pathway genes. Line KDb4-1 was used as *Aox1a* was up-regulated 2-fold but there was only slight up regulation of *nda1*. KDb4-2 had the highest level of knock-down of *ndb4* and up regulation of *Aox1a* as well as *ndb2*. KDb4-4 showed a similar expression pattern to KDb4-2, as did KDb4-3 but with not as efficient knock-down of *ndb4* (Chapter 3).

As it is thought that by having members of the electron transport chain up-regulated may assist the plant prior to stress exposure, it was thought that a microarray analysis may assist in determining any other genes which may be activated or down regulated as a result of the altered expression of the alternative dehydrogenases in these plant lines. Microarray has already been used previously to examine the stress response of plants when lacking *Aox1a* (Giraud *et al.* 2008). It was found that the absence of AOX1a leads to changes in the transcriptome in *A. thaliana* even under normal conditions. They concluded that changes in the transcript level of genes involved in ROS defence, signalling and proteins located on the mitochondria indicated that signalling for gene expression was altered.

The microarray work in this chapter was analysed with the help of Dr Michelle Barthet from School of Biological Sciences, University of Sydney.

6.2 Aim

Thus the major aim of this chapter was to analyze the transcriptome changes of *A. thaliana* lines with altered pathways in the alternative electron transport chain. It is hypothesized that there will be changes in the metabolism and stress pathways with possible changes relating to the production of ROS and signaling. It is thought these changes in plants overexpressing alternative pathway genes could result in the plants being adapted to environmental stresses. It is hypothesized that the gene expression profile reflects a pre-adaption to stress and hence these plants are more prepared to cope with stresses. Hence suggesting when salinity stress was applied to these plants they will cope better that Wt plant and show better tolerance. As salinity stress involves an alteration in the ionic balance in the plant (Munns and Tester, 2008), it was thought there could be changes in metal ions within the leaf and root tissue of these plants, thus a more detailed ionic profile was performed on the transgenic stressed and unstressed plants.

6.3 Results

6.3.1. An altered transcriptome is apparent from the knockdown of *ndb4*.

Microarray analyses were performed on mRNA extracted from plants grown in hydroponics as described in section 2.2. An analysis of the array from the pART control and KDb4-1 lines showed significant differences between the transcriptome. Using a false discovery rate (FDR) correction factor of Q = 0.1 and a fold change of >3, 252 transcripts were altered for p all, and 145 when p is <0.5 (Table 6.1), Indicating there was a wide spread rearrangement of the KDb4-1 transcriptome. These large differences are supported by PCA (Figure 6.1). Based on principal component 1 (PC1), there is a large difference between pART control and the knock-down line KDb4-1.

Microarray data suggests changes in the area of development, abiotic, and

Table 6.1 Changes in Transcriptome abundance between pART control and KDb4-1

Changes in transcriptome abundance between pART control and KDb4-1, where FC (All) refers to the number of genes called present in the array.

	p All	p<0.5
FC all	14622	3538
FC 1.5	3539	2129
FC > 3.0	252	145

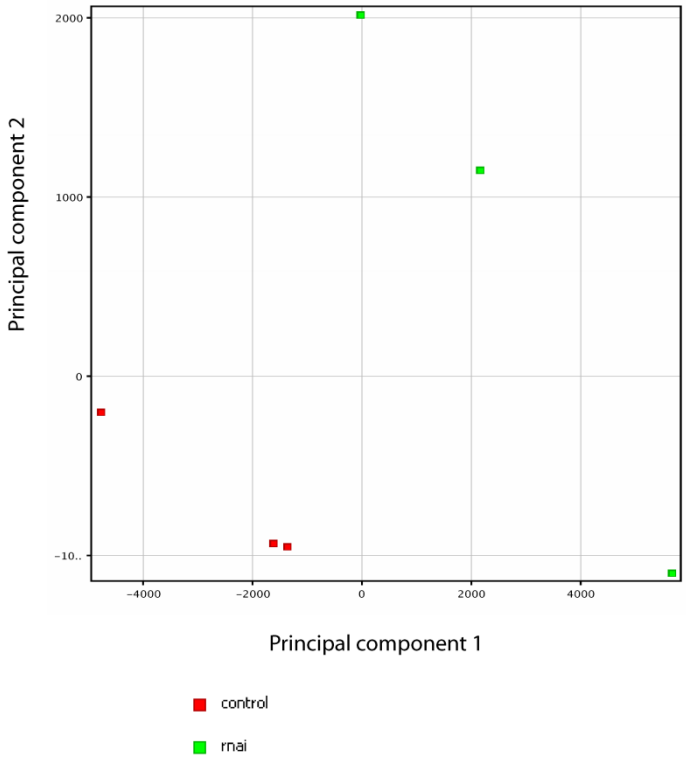

Figure 6.1 PCA to determine differences between pART control and KDb4-1

A PCA of the above changes to obtain an overall view of the differences between the control and knock-down line.

redox pathways (Figure 6.2). There were a large number of developmental genes up-regulated. The number of genes that have been shown to be altered in the KDb4-1 line, and the variety of groupings they represent, stresses that it is not just the mitochondria that has been affected by that there is a global effect due to the change in *ndb4* expression (Figure 6.2 and Figure 6.3). This change in gene expression thus impacts on other pathways in the plant. It was evident from microarray data that altered *ndb4* expression significantly impacted several anti-oxidant pathways, both in and outside the mitochondria (Figure 6.2, Table 6.2). In the mitochondria, transcript levels of genes from each enzyme family of the alternative respiratory pathway were significantly altered. Notably, transcript abundance of the internal alternative dehydrogenase *nda1* increased almost 3-fold in KDb4-1. Thetranscription of alternative oxidase was also affected; *Aox1a* transcript abundance increased 1.7 fold in KDb4-1. Overall, transcripts for 28 genes involved redox regulation and metabolic transport in the mitochondria were up-regulated in the RNAi KDb4-1 mutant (Table 6.2). The large number of changes seen for stress genes may be a result of the plant having AOX up-regulated. Due to the altered the *ndb4* expression there has been a decrease in NAD(P)H oxidation, hence the cell has responded by altering its gene expression profile, which includes *Aox1a* as well as these stress responsive genes. All these changes are indicative of an altered equilibrium of signalling relating particularly to stress in KDb4-1 plants. This confirms that a knockdown of *ndb4* has a significant effect outside the mitochondria. These results suggest that an altered electron transport chain is resulting in changes which link with an altered ROS signalling pathway. A number of heat-responsive genes were up-regulated in these lines as well (Figure 6.2), further confirmation that the plant has altered signalling pathways.

To gain an overview of these changes in the KDb4-1 line compared to the pART control, the significant changes with a fold change of ±1.5 or more were displayed using MapMan software (Thimm *et al.* 2004). It was hypothesized that there would be changes in the phosphorylating electron transport chain as seen observed by QRT-PCR and mitochondrial activities (Figure 3.9-11).The development-related phenotype observed in the *ndb4*

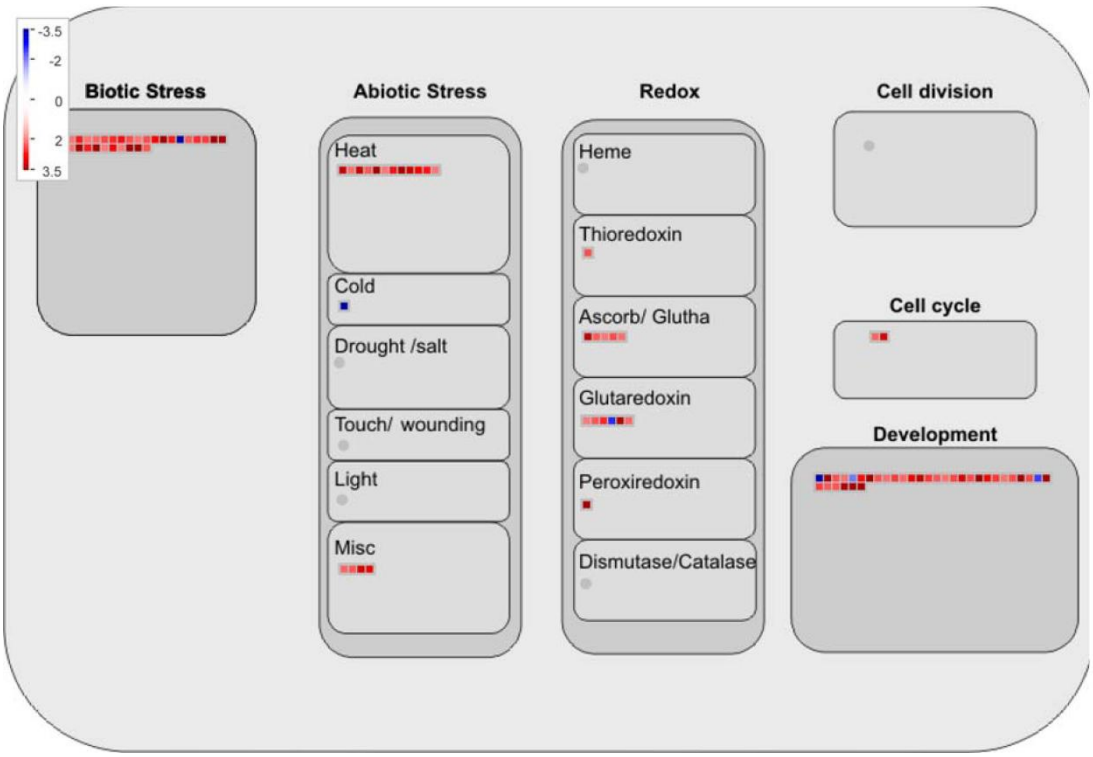

Figure 6.2 Cellular response overview of the transcriptome changes for KDb4-1 compared to pART control

Overview of the changes in transcript abundance associated with cellular response, changes after FDR correction. Changes are displayed using MapMan software (Thimm *et al.* 2004). Increases in transcript are shown in red, and decreases are shown in blue.

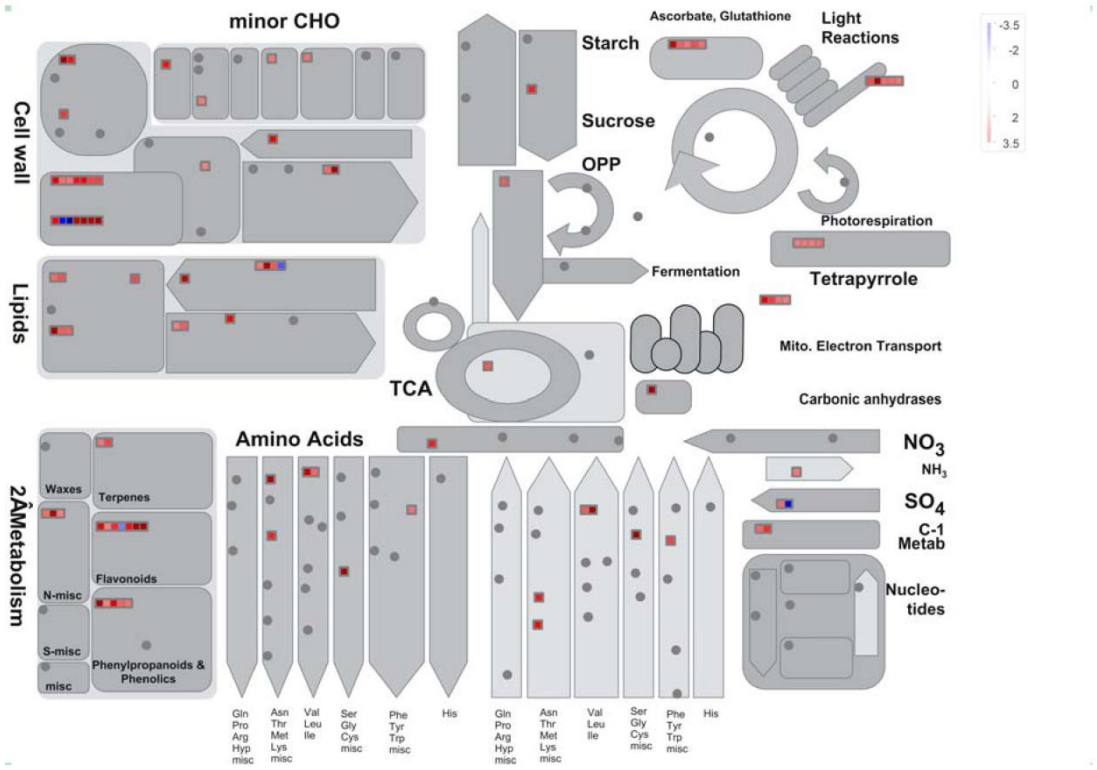

Figure 6.3 Metabolism overview of the transcriptome changes for KDb4-1 compared to pART control

Overview of the changes in transcript abundance associated with primary metabolism, changes after FDR correction. Changes are displayed using MapMan software (Thimm *et al.* 2004). Increases in transcript are shown in red, and decreases are shown in blue.

Table 6.2 Microarray fold change of ±1.5 difference for genes of KDb4-1 compared to pART control

Table is separated into types of genes. Transcript fold change compaing pART control to KDb4-1 is given, The id is determined from Microarray elements.

id	Type of Gene	Description	Fold Change
245928_s_at	Development storage proteins	VSP2 (VEGETATIVE STORAGE PROTEIN 2); acid phosphatase Has acid phosphatase activity dependent on the presence of divalent cations (Mg2+, Co2+, Zn2+, Mn2+) and anti-insect activity. Insects fed with the protein show a retarded development. Induced in response to abscisic acid, jasmonic acid, salt, water deficiency and wounding	-5.215
245038_at	Development storage proteins	PLP2 (PHOSPHOLIPASE A 2A); nutrient reservoir encodes a lipid acyl hydrolase with wide substrate specificity that accumulates upon infection by fungal and bacterial pathogens. Protein is localized in the cytoplasm in healthy leaves, and in membranes in infected cells.	4.224
249923_at	Development storage proteins	pepsin	2.327
250877_at	Development storage proteins	SDP1 (SUGAR-DEPENDENT1); triacylglycerol lipase Encodes a triacylglycerol lipase that is involved in storage lipid breakdown during seed germination. The mutant plant exhibits a much slower rate of postgerminative growth than the wild type.	1.529
256534_at	Development storage proteins	patatin-related	1.542
250648_at	Development late embryogenesis abundant	late embryogenesis abundant group 1 domain-containing protein / LEA group 1 domain-containing	2.103
259426_at	Development late embryogenesis abundant	LEA14 (LATE EMBRYOGENESIS ABUNDANT 14) Encodes late-embryogenesis abundant protein whose mRNA levels are induced in response to wounding and light stress. Might be involved in protection against dessication.	1.631
248524_s_at	Development unspecified	squamosa promoter-binding protein, putative	1.972
267460_at	Development unspecified	SPL3 (SQUAMOSA PROMOTER BINDING PROTEIN-LIKE 3); transcription factor Encodes a member of the SPL (squamosa-promoter binding protein-like) gene family, a novel gene family encoding DNA binding proteins and putative transcription factors. Contains the SBP-box, which encodes the SBP-domain, required and sufficient for interaction with DNA. It binds DNA, may directly regulate AP1, and is involved in regulation of flowering and vegetative phase change. Its temporal expression is regulated by the microRNA miR156. The target site for	1.529

		the microRNA is in the	
267482_s_at	Development unspecified	COP1-interacting protein	1.67
245247_at	Development unspecified	SCL13 (SCARECROW-LIKE 13); transcription factor Encodes a scarecrow-like protein (SCL13). Member of GRAS gene family	1.93
245934_at	Development unspecified	ANAC082 (Arabidopsis NAC domain containing protein 82); transcription	1.663
245982_at	Development unspecified	nodulin MtN3 family protein	1.849
245987_at	Development unspecified	ANAC083 (Arabidopsis NAC domain containing protein 83); transcription factor	1.751
246335_at	Development unspecified	ACD1 (ACCELERATED CELL DEATH 1, PHEOPHORBIDE A OXYGENASE) Encodes a pheide a oxygenase (PAO). Accelerated cell death (acd1) mutants show rapid, spreading necrotic responses to both virulent and avirulent Pseudomonas syringae pv. maculicola or pv. tomato pathogens and to ethylene.	1.788
246515_at	Development unspecified	F-box family	1.53
246525_at	Development unspecified	CO (CONSTANS); transcription factor/ zinc ion binding Encodes a protein showing similarities to zinc finger transcription factors, involved in regulation of flowering under long days. Acts upstream of FT and SOC1	-2.051
246600_at	Development unspecified	SAG101 (SENESCENCE-ASSOCIATED GENE 101); triacylglycerol lipase encodes an acyl hydrolase involved in senescence.	1.764
247707_at	Development unspecified	scarecrow-like transcription factor 11 (SCL11)	1.798
248198_at	Development unspecified	WD-40 repeat family protein	1.633
248347_at	Development unspecified	transducin family protein / WD-40 repeat family protein Encodes a transducin protein whose gene expression is induced by UV-B. This induction is reduced in hy5 mutant and may be a target of HY5 during UV-B response.	1.673
248467_at	Development unspecified	nodulin MtN3 family protein	-1.772
248496_at	Development unspecified	nodulin MtN3 family	2.74
248642_at	Development unspecified	senescence-associated protein-related	1.872
249467_at	Development unspecified	ANAC092/ATNAC2/ATNAC6 (Arabidopsis NAC domain containing protein 92); protein heterodimerization/ protein homodimerization/ transcription factor Encodes a transcription factor. This gene is up-regulated in response to salt stress in wildtype as well as NTHK1 transgenic lines although in the latter case the induction was drastically reduced. It was also up-regulated by ABA, ACC and NAA treatment, although in the latter two cases, the induction occurred relatively late when compared with NaCl or ABA treatments.	3.635

249595_at	Development unspecified	seven in absentia (SINA) family	1.691
249944_at	Development unspecified	ANAC089 (Arabidopsis NAC domain containing protein 89); transcription factor	1.617
250024_at	Development unspecified	ANAC087; transcription factor	2.331
250372_at	Development unspecified	senescence-associated protein-related	2.136
251283_at	Development unspecified	seven in absentia (SINA) family protein	1.666
251360_at	Development unspecified	embryo-abundant protein	1.55
251686_at	Development unspecified	AtATG18d (Arabidopsis thaliana homolog of yeast autophagy 18 (ATG18) d	1.997
251884_at	Development unspecified	embryo-abundant protein-related	2.464
251892_at	Development unspecified	WRI1 (WRINKLED 1); DNA binding / transcription factor WRINKLED1 encodes transcription factor of the AP2/ERWEBP class. Protein has two plant-specific (AP2/EREB) DNA-binding domains and is involved in the control of storage compound biosynthesis in Arabidopsis. Mutants have wrinkled seed phenotype, due to a defect in the incorporation of sucrose and glucose into triacylglycerols. Transgenic sGsL plants (21-day-old) grown on 6% sucrose for 24 hours had 2-fold increase in levels of expressions (sGsL line carries a single copy of T-DNA containing the Spomin::GUS-Spomin::LUC dual reporter genes in the upper arm of chromosome 5 of ecotype Col-0. The sporamin .minimal. promoter directs sugar-inducible expression of the LUC and GUS reporters in leaves).	1.615
252234_at	Development unspecified	ATPSK4 (PHYTOSULFOKINE 4 PRECURSOR); growth factor Phytosulfokine 3 precursor, coding for a unique plant peptide growth factor. Plants overexpressing this gene (under a 35S promoter), develop normal cotyledons and hypocotyls but their growth, in particular that of their roots, was faster than that of wildtype.	1.668
252591_at	Development unspecified	TET3 (TETRASPANIN3) Member of TETRASPANIN family	1.679
253056_at	Development unspecified	SHR (SHORT ROOT); transcription factor Involved in radial organization of the root and shoot axial organs. Essential for normal shoot gravitropism. The protein moves in a highly specific manner from the cells of the stele in which it is synthesized outward	1.662
253113_at	Development unspecified	senescence/dehydration-associated protein	2.176
253161_at	Development unspecified	SEN1 (DARK INDUCIBLE 1) Senescence-associated gene that is strongly induced by phosphate starvation. Transcripts are differentially regulated at the level of mRNA stability at different times of day. mRNAs are targets of the mRNA degradation pathway mediated by the downstream (DST) instability	2.923

		determinant.	
253829_at	Development unspecified	nodulin MtN21 family	3.255
253872_at	Development unspecified	RD26 (RESPONSIVE TO DESSICATION 26); transcription factor Encodes a NAC transcription factor induced in response to dessication. It is localized to the nucleus and acts as a transcriptional activator in ABA-mediated dehydration response.	1.65
254318_at	Development unspecified	embryo-abundant protein-related	2.503
255129_at	Development unspecified	nodulin MtN21 family protein	2.274
255575_at	Development unspecified	nodulin MtN21 family	2.068
255585_at	Development unspecified	ANAC069 (Arabidopsis NAC domain containing protein 69); transcription factor	1.613
255641_at	Development unspecified	similar to PREDICTED:	2.391
255799_at	Development unspecified	DET1 (DE-ETIOLATED 1) Encodes a nuclear-localized protein that acts as a repressor of photomorphogenesis and may be involved in chromatin remodeling.	1.517
255957_at	Development unspecified	senescence-associated protein-related	-1.672
256225_at	Development unspecified	dormancy/auxin associated family protein	1.551
256273_at	Development unspecified	TET6 (TETRASPANIN6) Member of TETRASPANIN family	1.616
256300_at	Development unspecified	NAP (NAC-LIKE, ACTIVATED BY AP3/PI); transcription factor Encodes a member of the NAC transcription factor gene family. It is expressed in floral primordia and up-regulated by AP3 and PI. Its expression is associated with leaf senescence	3.056
256967_at	Development unspecified	transducin family protein / WD-40 repeat family protein similar to transducin family protein / WD-40 repeat family protein [Arabidopsis thaliana] (TAIR:AT2G43770.1)	1.789
257271_at	Development unspecified	nodulin MtN3 family	-1.972
257661_at	Development unspecified	WD-40 repeat family protein	1.535
257823_at	Development unspecified	nodulin, putative	1.71
258146_at	Development unspecified	transducin family protein / WD-40 repeat family protein	1.754
258170_at	Development unspecified	senescence/dehydration-associated protein-related	1.711
258497_at	Development unspecified	COL2 (CONSTANS-LIKE 2); transcription factor/ zinc ion binding homologous to the flowering-time gene CONSTANS (CO) encoding zinc-finger proteins	2.364
258809_at	Development unspecified	ANAC047 (Arabidopsis NAC domain containing protein 47); transcription factor	5.375
258813_at	Development unspecified	ANAC046 (Arabidopsis NAC domain containing protein 46); transcription factor	2.781
259705_at	Development unspecified	ANAC032 (Arabidopsis NAC domain containing protein 32); transcription factor	-1.559

259792_at	Development unspecified	CAD1 (CONSTITUTIVELY ACTIVATED CELL DEATH 1); oxidoreductase Encodes a protein containing a domain with significant homology to the MACPF (membrane attack complex and perforin) domain of complements and perforin proteins that are involved in innate immunity in animals. Transgenic cad1-1 mutant plants show lesions seen in the hypersensitive response, as well as a spontaneous activation of expression of pathogenesis-related genes and leading to a 32-fold increase in salicylic acid (SA). CAD1 is postulated to act as a negative regulator controlling SA-mediated pathway of programmed cell death in plant immunity.	2.495
259871_at	Development unspecified	nodulin, putative	1.61
260137_at	Development unspecified	senescence-associated family protein	2.098
260156_at	Development unspecified	NAM (Arabidopsis NAC domain containing protein 18); transcription factor Transcription factor with a NAC domain. Homologous to the petunia gene NAM which is required for the development of the shoot. Expressed in the embryo.	2.365
260203_at	Development unspecified	ANAC019 (Arabidopsis NAC domain containing protein 19); transcription factor encodes a NAC transcription factor whose expression is induced by drought, high salt, and abscisic acid. This gene binds to ERD1 promoter in vitro	5.992
260447_at	Development unspecified	COP1-interacting protein-related	-1.536
260526_at	Development unspecified	nucleotide binding	1.74
260878_at	Development unspecified	SCL1 (SCARECROW-LIKE 1); transcription factor Encodes a scarecrow-like protein (SCL1). Member of GRAS gene family.	1.682
261177_at	Development unspecified	male sterility MS5 family protein	2.36
261335_at	Development unspecified	nodulin MtN21 family protein	1.551
261576_at	Development unspecified	nodulin MtN21 family protein	1.606
261860_at	Development unspecified	SCL5; transcription factor Encodes a scarecrow-like protein (SCL5). Member of GRAS gene family.	1.572
262162_at	Development unspecified	senescence-associated protein-related (InterPro:IPR007650)	-2.45
262170_at	Development unspecified	senescence-associated protein-related	1.516
262216_at	Development unspecified	nodulin family protein	1.593
262261_at	Development unspecified	CLE17 (CLAVATA3/ESR-RELATED 17); receptor binding Member of a large family of putative ligands homologous to the Clavata3 gene. Consists of a single exon.	1.565
262561_at	Development	esterase/lipase/thioesterase family protein	1.524

	unspecified		
263584_at	Development unspecified	ANAC036 (Arabidopsis NAC domain containing protein 36); transcription factor	1.926
263633_at	Development unspecified	SCL21 (SCARECROW-LIKE 21); transcription factor Encodes a scarecrow-like protein (SCL21). Member of GRAS gene family.	1.584
264211_at	Development unspecified	GI (GIGANTEA) Together with CONSTANTS (CO) and FLOWERING LOCUS T (FT), GIGANTEA promotes flowering under long days in a circadian clock-controlled flowering pathway. GI acts earlier than CO and FT in the pathway by increasing CO and FT mRNA abundance. Located in the nucleus. Regulates several developmental processes, including photoperiod-mediated flowering, phytochrome B signaling, circadian clock, carbohydrate metabolism, and cold stress response. The gene's transcription is controlled by the circadian clock and it is post-transcriptionally regulated by light and dark.	3.749
264261_at	Development unspecified	nicotianamine synthase, putative	3.749
264489_at	Development unspecified	squamosa promoter-binding protein-like 10 (SPL10	2.454
264261_at	Development unspecified	nicotianamine synthase, putative	3.749
264758_at	Development unspecified	F-box family protein	1.573
264787_at	Development unspecified	ERD7 (EARLY-RESPONSIVE TO DEHYDRATION 7)	1.996
265075_at	Development unspecified	embryo-abundant protein-related	2.271
265260_at	Development unspecified	ANAC042 (Arabidopsis NAC domain containing protein 42); transcription factor Identical to Putative NAC domain-containing protein 42 (ANAC042) [Arabidopsis Thaliana] (GB:Q9SK55)	2.3
266368_at	Development unspecified	embryo-abundant protein-related	1.857
266728_at	Development unspecified	CAAX amino terminal protease family protein	1.741
266775_at	Development unspecified	scarecrow transcription factor family protein	1.97
266799_at	Development unspecified	ATPSK2 (PHYTOSULFOKINE 2 PRECURSOR); growth factor Phytosulfokine 2 precursor, coding for a unique plant peptide growth factor	3.411
266965_at	Development unspecified	nodulin MtN21 family protein	11.646
266993_at	Development unspecified	nodulin family protein	5.25
267293_at	Development unspecified	TET8 (TETRASPANIN8) Member of TETRASPANIN family	1.743
263345_s_at	PS lightreaction photosystem II LHC-II	LHCB2.2 (Photosystem II light harvesting complex gene 2.2); chlorophyll binding Encodes Lhcb2.2. Belongs to the Lhc super-gene family encodes the light-harvesting	2.376

		chlorophyll a/b-binding (LHC) proteins that constitute the antenna system of the photosynthetic apparatus.	
248151_at	PS lightreaction photosystem II LHC-II	LHCB3 (LIGHT-HARVESTING CHLOROPHYLL BINDING PROTEIN 3) Lhcb3 protein is a component of the main light harvesting chlorophyll a/b-protein complex of Photosystem II (LHC II).	1.57
258239_at	PS lightreaction photosystem II LHC-II	LHCB2:4 (Photosystem II light harvesting complex gene 2.3); chlorophyll binding Encodes Lhcb2.4. Belongs to the Lhc super-gene family encodes the light-harvesting chlorophyll a/b-binding (LHC) proteins that constitute the antenna system of the photosynthetic apparatus.	4.009
258993_at	PS lightreaction photosystem II LHC-II	LHCB4.2 (LIGHT HARVESTING COMPLEX PSII); chlorophyll binding Lhcb4.2 protein (Lhcb4.2, protein involved in the light harvesting complex of phototystem II	2.156
259491_at	PS lightreaction photosystem II LHC-II	LHCB6 (LIGHT HARVESTING COMPLEX PSII); chlorophyll binding Lhcb6 protein (Lhcb6), light harvesting complex of photosystem II.	1.514
265722_at	PS lightreaction photosystem II LHC-II	LHCB4.3 (LIGHT HARVESTING COMPLEX PSII); chlorophyll binding Lhcb4:3 protein (Lhcb4.3, light harvesting complex of photosystem II	1.892
244963_at	PS lightreaction photosystem II PSII polypeptide subunits	PSII cytochrome b559	1.926
244964_at	PS lightreaction photosystem II PSII polypeptide subunits	PSII cytochrome b559. There have been many speculations about the function of Cyt b559, but the most favored at present is that it plays a protective role by acting as an electron acceptor or electron donor under conditions when electron flow through PSII is not optimized.	2.139
244972_at	PS lightreaction photosystem II PSII polypeptide subunits	encodes for CP47, subunit of the photosystem II reaction center	1.514
244973_at	PS lightreaction photosystem II PSII polypeptide subunits	Encodes photosystem II 5 kD protein subunit PSII-T. This is a plastid-encoded gene (PsbTc) which also has a nuclear-encoded paralog (PsbTn).	1.744
245001_at	PS lightreaction photosystem II PSII polypeptide subunits	PSII low MW protein	1.819
245021_at	PS lightreaction photosystem II PSII polypeptide subunits	PSII component	1.603
265149_at	PS lightreaction photosystem II PSII polypeptide subunits	photosystem II 5 kD protein	1.586
259840_at	PS.lightreaction. photosystem	photosystem I reaction center subunit VI, chloroplast, putative / PSI-H, putative	1.506

	I.PSI polypeptide subunits	(PSAH2)	
263114_at	PS.lightreaction photosystem I PSI polypeptide subunits	PSAD-2 (photosystem I subunit D-2) Encodes a protein predicted by sequence similarity with spinach PsaD to be photosystem I reaction center subunit II (PsaD2)	2.067
244934_at	PS.lightreaction NADH DH	NADH dehydrogenase ND6	1.625
255488_at	PS lightreaction state transition	protein kinase family protein	-1.781
265998_at	PS calvin cyle GAP	ALDH11A3 (Aldehyde dehydrogenase 11A3); 3-chloroallyl aldehyde dehydrogenase/ glyceraldehyde-3-phosphate dehydrogenase (NADP+) Encodes a protein with non-phosphorylating NADP-dependent glyceraldehyde-3-phosphate dehydrogenase activity. The activity of the enzyme was determined from leaf extracts; the enzyme has not been purified to confirm activity. InterPro domain NAD-dependent aldehyde dehydrogenase; (InterPro:IPR012303); contains InterPro domain Aldehyde dehydrogenase; (InterPro:IPR002086)	1.63
256020_at	Tetrapyrrole synthesis glu-tRNA reductase	HEMA1; glutamyl-tRNA reductase Encodes a protein with glutamyl-tRNA reductase (GluTR) activity, catalyzing the NADPH-dependent reduction of Glu-tRNA(Glu) to glutamate 1-semialdehyde (GSA) with the release of free tRNA(Glu). It is involved in the early steps of chlorophyll biosynthesis.	2.024
251664_at	Tetrapyrrole synthesis magnesium-protoporphyrin IX monomethyl ester (oxidative) cyclase	AT103 (DICARBOXYLATE DIIRON 1) Encodes a putative ZIP protein with varying mRNA accumulation in leaves, stems and roots. Has a consensus carboxylate-bridged di-iron binding site.	1.801
248197_at	Tetrapyrrole synthesis protochlorophyllide reductase	PORA (Protochlorophyllide reductase A); oxidoreductase/ protochlorophyllide reductase light-dependent NADPH:protochlorophyllide oxidoreductase A Identical to Protochlorophyllide reductase A, chloroplast precursor (EC 1.3.1.33) (PCR A) (NADPH-protochlorophyllide oxidoreductase A) (POR A) (PORA) [Arabidopsis Thaliana] (GB:Q42536;GB:Q9FK22)	1.531
253871_at	Tetrapyrrole synthesis protochlorophyllide reductase	PORB (PROTOCHLOROPHYLLIDE OXIDOREDUCTASE B); oxidoreductase/ protochlorophyllide reductase light-dependent NADPH:protochlorophyllide oxidoreductase B	1.733
245242_at	Tetrapyrrole synthesis chlorophyll b synthase	CH1 (CHLORINA 1); chlorophyll a oxygenase Encodes chlorophyllide a oxygenase which converts chlorophyllide a to chlorophyllide b by catalyzing two successive hydroxylations at the 7-methyl group of chlorophyllide a . Mutants are deficient in pigments that associate with thylakoid membrane proteins, lacking chlorophyll b and light-harvesting	2.061

		proteins of photosystem II. The protein was shown through cross-linking experiments to interact with Toc75, Toc34, Tic40, Tic20 and Tic22.	
246870_at	Tetrapyrrole synthesis ferrochelatase	ferrochelatase I	1.798
251519_at	Tetrapyrrole synthesis regulation	GUN4 (Genomes uncoupled 4) GUN, genomes uncoupled, is necessary for coupling the expression of some nuclear genes to the functional state of the chloroplast. Binds to the magnesium chelatase complex and promotes formation of the substrate,a tetrapyrrole signaling molecule. Porphyrin-binding protein that enhances the activity of Mg-chelatase. Although required for chlorophyll accumulation under normal growth conditions, GUN4 is not essential for chlorophyll synthesis.	2.055
249091_at	Tetrapyrrole synthesis unspecified	ATCLH2 (Chlorophyll-chlorophyllido hydrolase 2) Encodes a chlorophyllase, the first enzyme in chlorophyll degradation. It catalyzes the hydrolysis of the ester bond to chlorophyllide and phytol. AtCLH2 has a typical signal sequence for the chloroplast. Gene expression does not respond to methyljasmonate, a known promoter of senescence and chlorophyll degradation.	2.136
248659_at	Cell cycle	cyclin family protein	2.183
254526_at	Cell cycle	cyclin family protein	1.517
257619_at	Cell cycle	ICK3 (kip-related protein 5); cyclin-dependent protein kinase inhibitor Kip-related protein (KRP) gene, encodes CDK (cyclin-dependent kinase) inhibitor (CKI), negative regulator of cell division. A member of seven KRP genes found in Arabidopsis thaliana. Differential expression patterns for distinct KRPs were revealed by in situ hybridization.	1.64
260307_at	Cell cycle	cyclin-related	1.63
261780_at	Cell cycle	CYCB2;4 (CYCLIN B2;4); cyclin-dependent protein kinase regulator core cell cycle genes	1.641
264697_at	Cell cycle	CYCD1;1 (CYCLIN D1;1); cyclin-dependent protein kinase regulator Encodes a D-type cyclin that physically interacts with CDC2A. Its expression is up-regulated early during germination.	1.678
246644_at	Cell cycle peptidylprolyl isomerase	peptidyl-prolyl cis-trans isomerase	1.541
248657_at	Cell cycle peptidylprolyl isomerase	peptidyl-prolyl cis-trans isomerase, putative / FK506-binding protein, putative	3.124
251932_at	Cell cycle peptidylprolyl isomerase	PAS1 (PASTICCINO 1); FK506 binding / peptidyl-prolyl cis-trans isomerase Immunophilin-like protein	1.581
245210_at	Cell division	Ran GTPase binding / chromatin binding / zinc ion binding (InterPro:IPR000408); contains InterPro domain Regulator of chromosome condensation/beta-lactamase-	1.551

		inhibitor protein II; (InterPro:IPR009091); contains InterPro domain Disease resistance/zinc finger/chromosome condensation-like region; (InterPro:IPR013591); contains InterPro domain Pleckstrin homology-type; (InterPro:IPR011993); contains InterPro domain Zinc finger, FYVE-type; (InterPro:IPR000306)	
246536_at	Cell division	structural maintenance of chromosomes (SMC) family protein (MSS2)	1.766
248693_at	Cell division	regulator of chromosome condensation (RCC1) family protein	1.741
250382_at	Cell division	UVB-resistance protein-related / regulator of chromosome condensation (RCC1) family protein	1.655
250617_at	Cell division	(ARABIDOPSIS MEI2-LIKE); RNA binding AML4 A member of mei2-like gene family, predominantly plant-based family of genes encoding RNA binding proteins with characteristic presence of a highly conserved RNA binding motif first described in the mei2 gene of the fission yeast S. pombe. In silico analyses reveal nine mei2 -like genes in *A. thaliana*. They were grouped into four distinct clades, based on overall sequence similarity and subfamily-specific sequence elements. AML4 is a member of two sister clades of mei2-like gene family, AML1 through AML5, and belongs to the clade named ALM14. AML4 is expressed during embryo development (heart and torpedo stage) and in vegetative and floral apices.	1.61
251975_at	Cell division	cell division cycle protein 48, putative / CDC48, putative	1.913
253148_at	Cell division	CYCB2;2 (CYCLIN B2;2); cyclin-dependent protein kinase regulator	1.599
254679_at	Cell division	AML3 (ARABIDOPSIS MEI2-LIKE); RNA binding A member of mei2-like gene family, predominantly plant-based family of genes encoding RNA binding proteins with characteristic presence of a highly conserved RNA binding motif first described in the mei2 gene of the fission yeast S. pombe. In silico analyses reveal nine mei2 -like genes in *A. thaliana*. They were grouped into four distinct clades, based on overall sequence similarity and subfamily-specific sequence elements. AML3 is a member of two sister clades of mei2-like gene family, AML1 through AML5, and belongs to the clade named ALM235. Among mei2-like genes, AML3 is the transcript with highest frequency of alternative splicing. Expression was detected during early embryo development (heart and torpedo stage); no accumulation was detected in vegetative and floral apices, as revealed by in situ hybridization.	1.518
258085_at	Cell division	regulator of chromosome condensation (RCC1) family protein	1.725

259125_at	Cell division	regulator of chromosome condensation (RCC1) family protein	1.731
259334_at	Cell division	ankyrin repeat family protein / regulator of chromosome condensation (RCC1) family protein	1.81
261917_at	Cell division	regulator of chromosome condensation (RCC1) family protein / zinc finger protein-related	1.537
263534_at	Redox ascorbate and glutathione	ATMAPR2 (ARABIDOPSIS THALIANA MEMBRANE-ASSOCIATED PROGESTERONE BINDING PROTEIN 2); heme binding / transition metal ion binding	1.534
256892_at	Redox ascorbate and glutathione	oxidoreductase, 2OG-Fe(II) oxygenase family protein	1.582
256922_at	Redox ascorbate and glutathione	oxidoreductase, 2OG-Fe(II) oxygenase family protein	3.274
260545_at	Redox ascorbate and glutathione	ATGPX3 (GLUTATHIONE PEROXIDASE 3); glutathione peroxidase Glutathione peroxidase. Functions as both a redox transducer and a scavenger in abscisic acid and drought stress responses. Interacts with ABI2 and ABI1.	1.7
262638_at	Redox ascorbate and glutathione	2-oxoglutarate-dependent dioxygenase, putative encodes a protein whose sequence is similar to 2-oxoglutarate-dependent dioxygenase	2.239
262831_at	Redox ascorbate and glutathione	similar to ACYB-2 (Arabidopsis cytochrome b561 -2), carbon-monoxide oxygenase [Arabidopsis thaliana] (TAIR:AT4G25570.1)	2.066
264383_at	Redox ascorbate and glutathione	ATGPX1 (GLUTATHIONE PEROXIDASE 1); glutathione peroxidase Encodes glutathione peroxidase.	1.517
246021_at	Redox ascorbate and glutathione ascorbate	L-ascorbate oxidase, putative	1.577
250916_at	Redox ascorbate and glutathione ascorbate	monodehydroascorbate reductase, putative	1.871
252862_at	Redox ascorbate and glutathione ascorbate	L-ascorbate oxidase, putative	2.366
257227_at	Redox ascorbate and glutathione ascorbate	ATMDAR4 (MONODEHYDROASCORBATE REDUCTASE 4); monodehydroascorbate reductase (NADH) Encodes a peroxisome membrane-bound monodehydroascorbate reductase, involved in the ascorbate-glutathione cycle which removes toxic H2O2	2.12
253307_at	Redox ascorbate and glutathione ascorbate L-galactose dehydrogenase	L-galactose dehydrogenase (L-GalDH) Encodes a L-galactose dehydrogenase, involved in ascorbate biosynthesis	1.509
254890_at	Redox	ATGPX6 (GLUTATHIONE PEROXIDASE 6);	1.811

	ascorbate and glutathione glutathione	glutathione peroxidase Encodes glutathione peroxidase.	
263426_at	Redox ascorbate and glutathione glutathione	ATGPX2 (GLUTATHIONE PEROXIDASE 2); glutathione peroxidase glutathione peroxidase GPx	1.619
245392_at	Redox glutaredoxins	glutaredoxin family protein Identical to Monothiol glutaredoxin-S4 (AtGrxS4)	2.019
245504_at	Redox glutaredoxins	glutaredoxin family protein Identical to Monothiol glutaredoxin-S8 (AtGrxS8)	1.8
245505_at	Redox glutaredoxins	glutaredoxin family protein Identical to Monothiol glutaredoxin-S5 (AtGrxS5)	2.295
245506_at	Redox glutaredoxins	glutaredoxin family protein Identical to Monothiol glutaredoxin-S3 (AtGrxS3)	1.806
247418_at	Redox glutaredoxins	glutaredoxin, putative Identical to Glutaredoxin-C1 (AtGrxC1)	1.539
249996_at	Redox glutaredoxins	glutaredoxin family protein Identical to Monothiol glutaredoxin-S2 (AtGrxS2	1.861
253382_at	Redox glutaredoxins	glutaredoxin family protein Identical to Glutaredoxin-C6 (AtGrxC6)	-1.532
256583_at	Redox glutaredoxins	glutaredoxin family protein	2.594
260831_at	Redox glutaredoxins	glutaredoxin family protein Identical to Monothiol glutaredoxin-S11 (AtGrxS11)	-2.591
263168_at	Redox glutaredoxins	glutaredoxin family protein Identical to Putative monothiol glutaredoxin-S1 (AtGrxS1)	3.41
265067_at	Redox glutaredoxins	glutaredoxin family protein Identical to Monothiol glutaredoxin-S13 (AtGrxS13)	2.169
264923_s_at	Redox peroxiredoxin	TPX2 (THIOREDOXIN-DEPENDENT PEROXIDASE 2); antioxidant thioredoxin-dependent peroxidase 2	9.808
257338_s_at	Mitochondrial electron transport / ATP synthesis NADH-DH localisation not clear	Mitochondrial NADH dehydrogenase subunit 5. The gene is trans-spliced from three different pre-cursors, NAD5a, NAD5b and NAD5c.	1.68
260767_s_at	Mitochondrial electron transport / ATP synthesis NADH-DH localisation not clear	NADH-ubiquinone oxidoreductase-related	1.522
252091_at	Mitochondrial electron transport / ATP synthesis NADH-DH localisation not clear	zinc finger (DHHC type) family protein	1.59
256057_at	Mitochondrial electron transport / ATP synthesis NADH-DH type II internal matrix	NDA1 (ALTERNATIVE NAD(P)H DEHYDROGENASE 1); NADH dehydrogenase Internal NAD(P)H dehydrogenase in mitochondria. The predicted protein sequence has high homology with other designated NAD(P)H	2.938

		DHs from microorganisms; the capacity for matrix NAD(P)H oxidation via the rotenone-insensitive pathway is significantly reduced in the Atndi1 mutant plant line; the in vitro translation product of AtNDI1 is imported into isolated mitochondria and located on the inside of the inner membrane.	
256209_at	Mitochondrial electron transport / ATP synthesis electron transfer flavoprotein	ETFALPHA (ELECTRON TRANSFER FLAVOPROTEIN ALPHA); FAD binding / electron carrier Encodes the electron transfer flavoprotein ETF alpha, a putative subunit of the mitochondrial electron transfer flavoprotein complex (ETF beta is At5g43430.1) in Arabidopsis. Mutations of the ETF beta gene results in accelerated senescence and early death compared to wild-type during extended darkness.	1.554
260536_at	Mitochondrial electron transport / ATP synthesis electron transfer flavoprotein	ETFQO (ELECTRON-TRANSFER FLAVOPROTEIN:UBIQUINONE OXIDOREDUCTASE); catalytic/ electron acceptor Encodes a unique electron-transfer flavoprotein:ubiquinone oxidoreductase that is localized to the mitochondrion. Mutants are more sensitive to sugar starvation when plants are kept in the dark for long periods.	1.775
258452_at	Mitochondrial electron transport / ATP synthesis alternative oxidase	AOX1A (alternative oxidase 1A); alternative oxidase Encodes an isoform of alternative oxidase that is expressed in rosettes, flowers, and root. The alternative oxidase of plant mitochondria transfers electrons from the ubiquinone pool to oxygen without energy conservations. It is regulated through transcriptional control and by pyruvate. Plays a role in shoot acclimation to low temperature. Also is capable of ameliorating reactive oxygen species production when the cytochrome pathway is inhibited.	1.695
246944_at	Mitochondrial electron transport / ATP synthesis cytochrome c reductase	ubiquinol-cytochrome C reductase complex 14 kDa protein, putative	2.482
263509_s_at	Mitochondrial electron transport / ATP synthesis cytochrome c oxidase	Encodes cytochrome c oxidase subunit 3.	1.516
246404_at	Mitochondrial electron transport / ATP synthesis cytochrome c oxidase	membrane bound O-acyl transferase (MBOAT) family protein	1.686
253072_at	Mitochondrial electron transport / ATP synthesis cytochrome c	cytochrome c oxidase-related	1.502

	oxidase		
257333_at	Mitochondrial electron transport / ATP synthesis cytochrome c oxidase	cytochrome c oxidase subunit 1	2.095
259446_at	Mitochondrial electron transport / ATP synthesis cytochrome c oxidase	cytochrome c oxidase assembly protein CtaG / Cox11 family	1.614
259594_at	Mitochondrial electron transport / ATP synthesis cytochrome c oxidase	similar to Os03g0850600	1.565
254120_at	Mitochondrial electron transport / ATP synthesis uncoupling protein	mitochondrial substrate carrier family protein	1.736
265228_s_at	Mitochondrial electron transport / ATP synthesis F1-ATPase	ATPase subunit 1	1.554
266012_s_at	Mitochondrial electron transport / ATP synthesis F1-ATPase	ATPase subunit 6	1.898
244901_at	mitochondrial electron transport / ATP synthesis F1-ATPase	encodes a plant b subunit of mitochondrial ATP synthase based on structural similarity and the presence in the F(0) complex.	2.021
250863_at	Mitochondrial electron transport / ATP synthesis F1-ATPase	F1F0-ATPase inhibitor protein, putative	1.593
256184_at	Mitochondrial electron transport / ATP synthesis F1-ATPase	ATP synthase epsilon chain, mitochondrial	1.543
264038_at	Mitochondrial electron transport / ATP synthesis unspecified	coenzyme Q biosynthesis Coq4 family protein / ubiquinone biosynthesis Coq4 family protein Ubiquinone biosynthesis protein COQ4 homolog	1.766
249372_at	OPP oxidative PP G6PD	G6PD6 (GLUCOSE-6-PHOSPHATE DEHYDROGENASE 6); glucose-6-phosphate 1-dehydrogenase Encodes a cytosolic glucose-6-phosphate dehydrogenase that is insensitive to reduction by DTT and whose	1.544

		mRNA is expressed ubiquitously.	
264513_at	OPP oxidative PP G6PD	G6PD4 (GLUCOSE-6-PHOSPHATE DEHYDROGENASE 4); glucose-6-phosphate 1-dehydrogenase Encodes a protein similar to glucose-6-phosphate dehydrogenase but, based on amino acid differences in the active site and lack of activity, does not encode a functional G6PDH. The amino acid sequence for the consensus sequence of the G6PDH active site (DHYLGKE) differs in three places in this protein. gc exon splice site at 20574 is based on protein alignment, and is not confirmed experimentally.	1.675
259748_at	OPP oxidative PP 6-phosphogluconate dehydrogenase	6-phosphogluconate dehydrogenase NAD-binding domain-containing protein	1.771
263986_at	Gluconeogenese/ glyoxylate cycle citrate synthase	CSY3 (CITRATE SYNTHASE 3); citrate (SI)-synthase Encodes a peroxisomal citrate synthase that is expressed throughout seedling and shoot development.	1.726
245528_at	Gluconeogenese/ glyoxylate cycle pyruvate dikinase	PPDK (PYRUVATE ORTHOPHOSPHATE DIKINASE); kinase/ pyruvate, phosphate dikinase The product of this long transcript was shown to be targeted to the chloroplast, whereas the shorter transcript (no targeting sequence) accumulates in the cytosol. They were also found in slightly different tissues.	1.803
261355_at	TCA / org Transformation other organic acid transformations malic	ATNADP-ME4 (NADP-MALIC ENZYME 4); malate dehydrogenase (oxaloacetate-decarboxylating) (NADP+)/ malic enzyme/ oxidoreductase, acting on NADH or NADPH, NAD or NADP as acceptor The malic enzyme (EC 1.1.1.40) encoded by AtNADP-ME4 is localized to chloroplasts. The gene is expressed throughout the whole plant and during embryogenesis and germination. A possible involvement in the fatty acid biosynthesis has been proposed.	1.544
246396_at	TCA / org Transformation carbonic anhydrases	carbonic anhydrase family protein / carbonate dehydratase family protein	1.515
252011_at	TCA / org transformation carbonic anhydrases	carbonic anhydrase family protein	1.782
265170_at	TCA / org transformation carbonic anhydrases	carbonic anhydrase, putative / carbonate dehydratase, putative	4.701

mutants was further investigated using microarray to assess global changes in the transcriptome as a result of altered *ndb4* expression. Transcript abundance for genes involved in cell division/ differentiation, and plant development were significantly increased in the KDb4-1 compared to controls at day 6 (cotyledon stage) of development (Figure 6.2). Of specific importance, transcript abundance of the phytosulfokine 3 precursor ATPSK2, the expression of which has been directly related to plant growth rate (Yang *et al.* 2001) was significantly increased (fold change of 3.411) in the KDb4-1 RNAi line compared to empty vector control (Table 6.2). There were increases in transcript abundance for genes encoding proteins involved in cell wall modification and lipid synthesis, there were also genes up-regulated in antioxidant defence (Figure 6.3). There were also a noticeable number of genes associated with secondary metabolism that were up-regulated. It has already been suggested in Chapter 4, that the secondary metabolites of plants are involved in plant protection against biotic and abiotic stress factors. Many of these genes may be up-regulated as the plant is in a stressed state due to the perturbation of expression of the external dehydrogenases and hence altering the NADH:NAD^+ ratio in the cell.

Microarray was also used to analyse the members of the electron transport chain. The results indicate that *Aox1a* was up-regulated as observed in QRT-PCR, as well as *nda1* (Table 6.3). Unfortunately *ndb4* is not available on the microarray chip, so could not confirm the knock-down observed using qRT-PCR (Chapter 3). Another gene family which was up-regulated encode malate transporters. The two genes SLAH2 and SLAH3 had fold change increases of 2.7 and 2.1 respectively. The increase in malate transporter expression could be a result of the knock-down of *ndb4* and the limited external NAD(P)H oxidation capacity. If this gene expression has change altered the flux of malate transport, it is possible that this flux would be limiting in the cell thus, metabolite shuttles would be required to transport reducing equivalents into the matrix for oxidation. In this case, it would be malate shuttling NADH into the mitochondrial matrix, the malate/OAA or malate/aspartate shuttle. Hence microarray analysis has shown that there were global changes in gene expression and that other

Table 6.3 Electron transport gene changes from Microarray

The fold change for genes from the ETC, showing the change observed, highlighted in red is the increase fold changed that is also seen in QRT-PCR

Fold Change	Probe ID	Gene
1.1353675	245716_at	ndc1
-1.050818	247746_at	ucp2
1.2899561	249343_at	Complex II
-1.0175669	251902_at	ucp1
1.1695048	253810_at	ndb1
1.2582437	255259_at	ndb2
2.9377708	256057_at	nda1
1.6949816	258452_at	aox1a
-1.0564849	262593_at	Complex III
-1.1866189	266835_at	nda2

pathways were affected from the knockdown of *ndb4*.

6.3.2. Response of *ndb4* knockdown lines to salt stress

It was hypothesized that as the *Aox1a* transcript was up-regulated in *ndb4* knockdown lines they are mimicking the AOX overexpressing lines used in Chapter 5. Further, in some of these lines, *ndb2* was also up-regulated under normal growth conditions. It has been shown that both these genes increase in expression in response to salinity stress in Wt tissue along with *nda1*, hence the effect of salt stress was analysed in these plants. Figure 6.4 shows that when exposed to 150mM salt stress for 10 days, there was an additional increase in *Aox1a* transcript as observed for the AOX overexpresser lines, indicating that not only had the over-expression of the transcript been maintained, expression of the endogenous gene was still responding to the stress signals, and had increased. Further this was a significant increase for both root, and shoot. This increased transcript under salinity conditions appears to be the sum of the background response observed in wild type tissue (Figure 6.4). As also expected the transcript for *ndb2* and *nda1* was further increased under salinity conditions. For *ndb2* there were significant changes under salinity stress i.e. for root, and shoot, as well as for *nda1* for root, and shoot. Thus, the increased level of *Aox1a*, *ndb2* and *nda1* transcripts in the over-expressing lines was confirmed and their response to salt stress with an increase in expression was as expected from the Wt response (Chapter 5).

6.3.3. Increased *ndb2* and *Aox1a* results in decreased ROS accumulation

The oxidative stress effect of salt exposure was assessed using the Amplex Red assay as before (Chapter 5). Knowing that the *Aox1a* over expressers had reduced ROS (H_2O_2) under salinity stress compared to the pBI-Containing plants, it was hypothesized that these plants with increases in alternative dehydrogenases and AOX would also confer less ROS

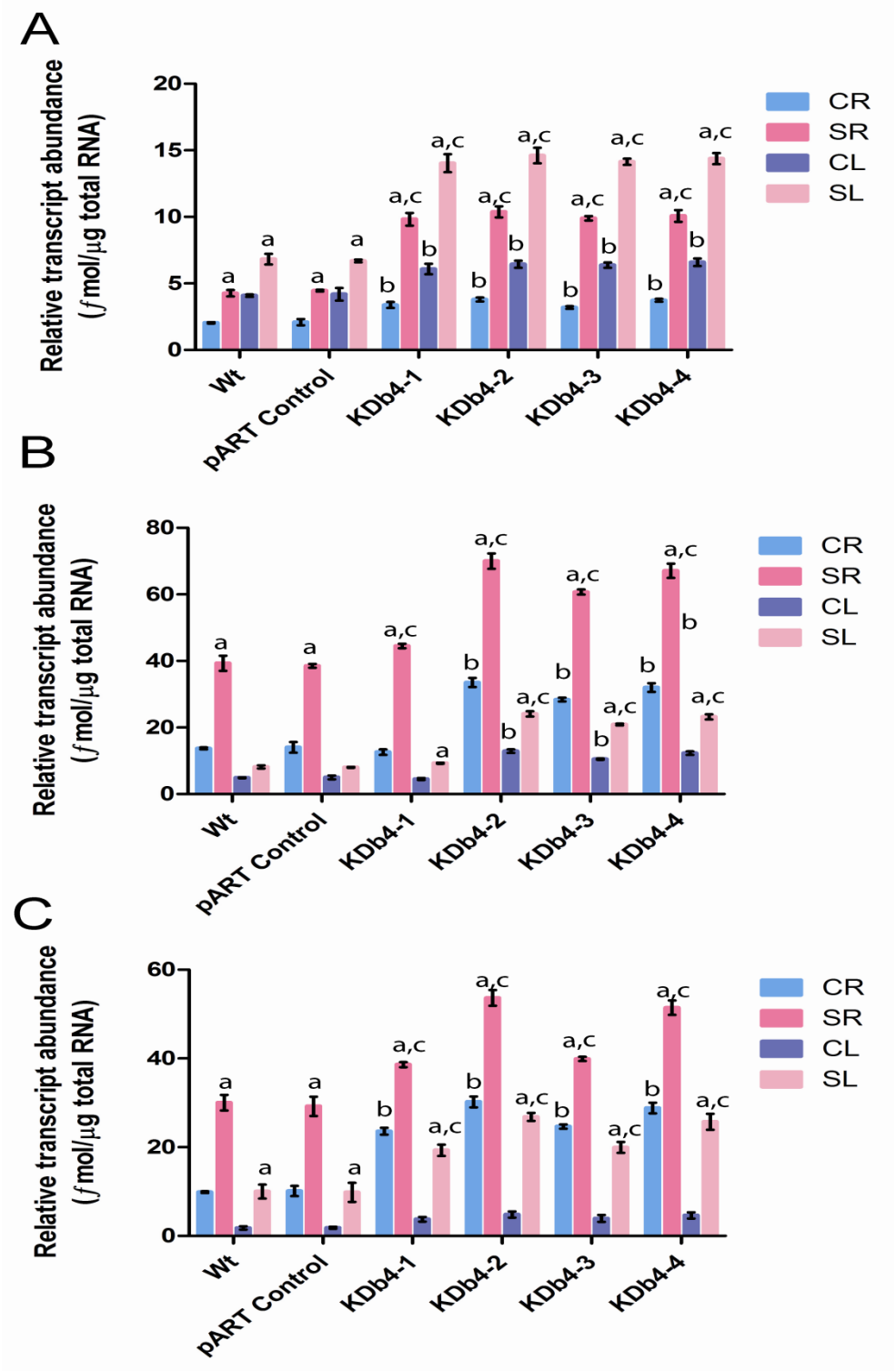
A
Relative transcript abundance
(fmol/µg total RNA)
20
15
10
5
0
CR
SR
CL
SL
Wt
pART Control
KDb4-1
KDb4-2
KDb4-3
KDb4-4
B
Relative transcript abundance
(fmol/µg total RNA)
80
60
40
20
0
CR
SR
CL
SL
Wt
pART Control
KDb4-1
KDb4-2
KDb4-3
KDb4-4
C
Relative transcript abundance
(fmol/µg total RNA)
60
40
20
0
CR
SR
CL
SL
Wt
pART Control
KDb4-1
KDb4-2
KDb4-3
KDb4-4

Figure 6.4 Transcript responses of *Aox1a*, *ndb2* and *nda1* in *ndb4* knock-down lines after salt stress

Transcript levels for and (A) *nda1*, (B) *ndb2*, and (C) *Aox1a* were determined by qRT-PCR from leaves of plants grown hydroponically in the presence (salt) and absence (control) of 150 mM NaCl. Values represent means +/- SD for n=3, where [a] indicates significant difference when comparing control to salt treated plants. [b] and [c] indicate significant differences for Control compared to *ndb4* knock-down lines, where [b] is relevant for comparisons between control growth conditions and [c] is relevant for comparisons between salt growth conditions. *Aox1a*, KDb4-2 root (Mean diff= 23.63, t= 13.68, P >0.001), shoot, (Mean diff= 16.82, t= 9.738, P >0.001). *ndb2*, KDb4-2 root (Mean diff= 30.71, t= 15.96, P >0.001), shoot (Mean diff= 15.91, t= 8.270, P >0.001). *nda1*, KDb4-2 root, (Mean diff= 6.107, t= 13.06, P >0.001), shoot (Mean diff= 7.785, t= 16.64, P >0.001).

accumulation in these tissues. Figure 6.5 shows that for the root tissue there was reduced ROS in the *ndb4* knock-down lines compared to pART control. This was significantly lower for KDb4-2 line for both normal growth conditions, and under salinity stress of 150mM for 10 days. Interestingly, the levels were not any lower than what was observed for the *Aox1a* over expressers (Figure 5.7) However in the leaf tissue there was also significantly less ROS for the *ndb4* knock-down lines, especially KDb4-2 which was significantly lower under both normal and salinity conditions. This low level of H_2O_2 was expected and even lower levels of ROS were generated than seen in the *Aox1a* alone over expressers, suggesting that these plants may show even better tolerance. These results suggest that when *ndb2*, *nda1* and *Aox1a* expression and activity is increased, it is able to keep ubiquinone pool and the cell, in a less reduced state minimising the potential production of ROS during the stress. Hence as was hypothesized with increased alternative pathway enzymes activity there was a minimisation of ROS formation, protecting the plant against oxidative stress.

6.3.4. Over-expression of AOX improved the growth rate during salt stress

It was hypothesized that if these plants over expressing alternative pathways genes were more tolerant of salinity stress compared to both control plants and the AOX over expressers alone based on ROS species formation, then they would have a higher relative growth rate. This was evident under normal growth conditions where there was no significant decrease in the RGR for both shoot and root data when comparing the pART control to the *ndb4* knock-down lines. For shoot growth rates, the *ndb4* knock-down plants had a significant increase in RGR when comparing to the pART control under salinity conditions, as seen for KDb4-2 (Figure 6.6). It appears these plants have more protection under normal growth conditions as a higher RGR was observed for these plants with altered alternative pathways compared to an up-regulation of *Aox1a* alone. Results for the root tissue line showed the same trend as shoot data, with no significant decrease in growth rate under

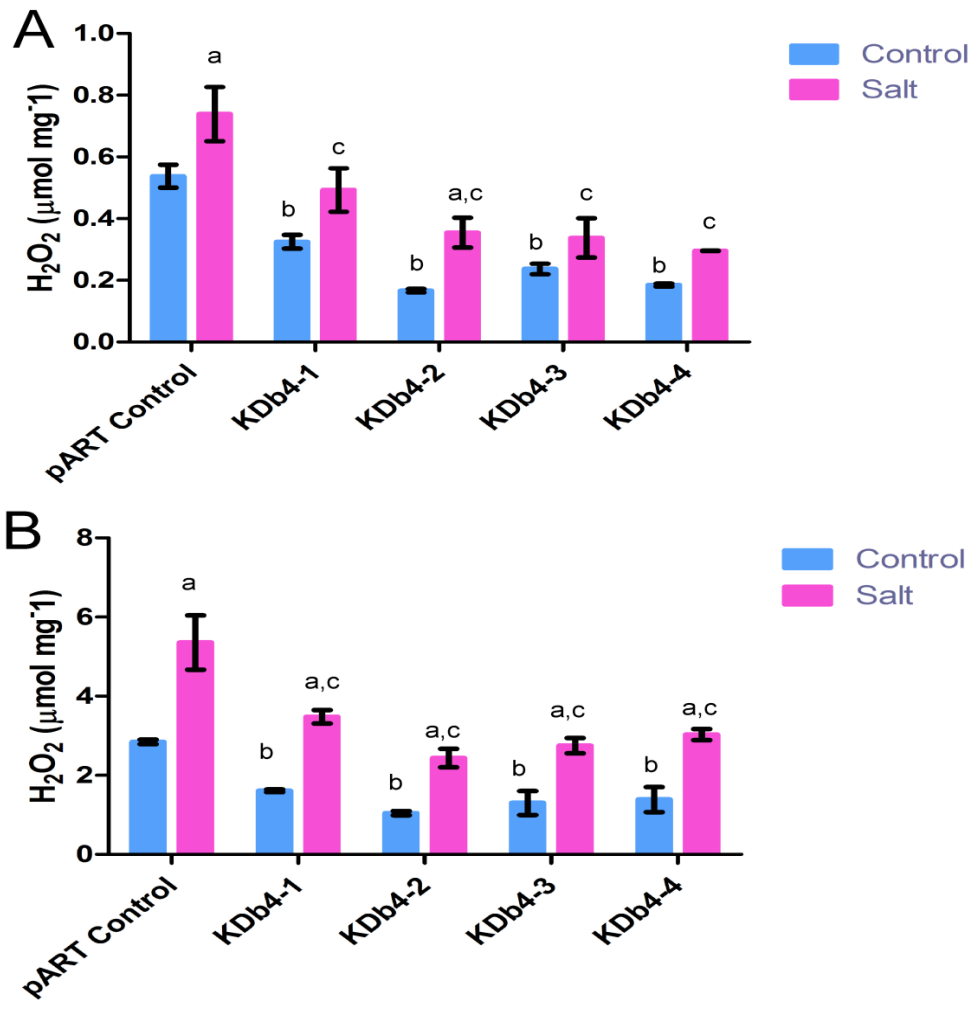

Figure 6.5 ROS levels in *ndb4* knock-down lines (A) roots and (B) shoots

ROS levels, specifically H_2O_2, were quantitatively determined by Amplex Red Assay in root (A) and leaf (B) tissue from plants grown in presence (salt) and absence (control) of 150 mM NaCl in growth media for 10 days. Values are means +/- SD for n=3, where [a] indicates significant difference when comparing control to salt treated plants. [b] and [c] indicate significant differences for pART compared to *ndb4* knock-down lines, where [b] is relevant for comparisons between control growth conditions and [c] is relevant for comparisons between salt growth conditions. Root, KDb4-2, normal growth conditions (Mean diff= -0.3709, t= 5.685, P >0.001), salinity stress (Mean diff= -0.3838, t= 5.883, P >0.001). Leaf KDb4-2, normal growth conditions (Mean diff= -1.802, t= 4.477, P >0.001), salinity stress (Mean diff= -2.925, t= 7.266, P>0.001).

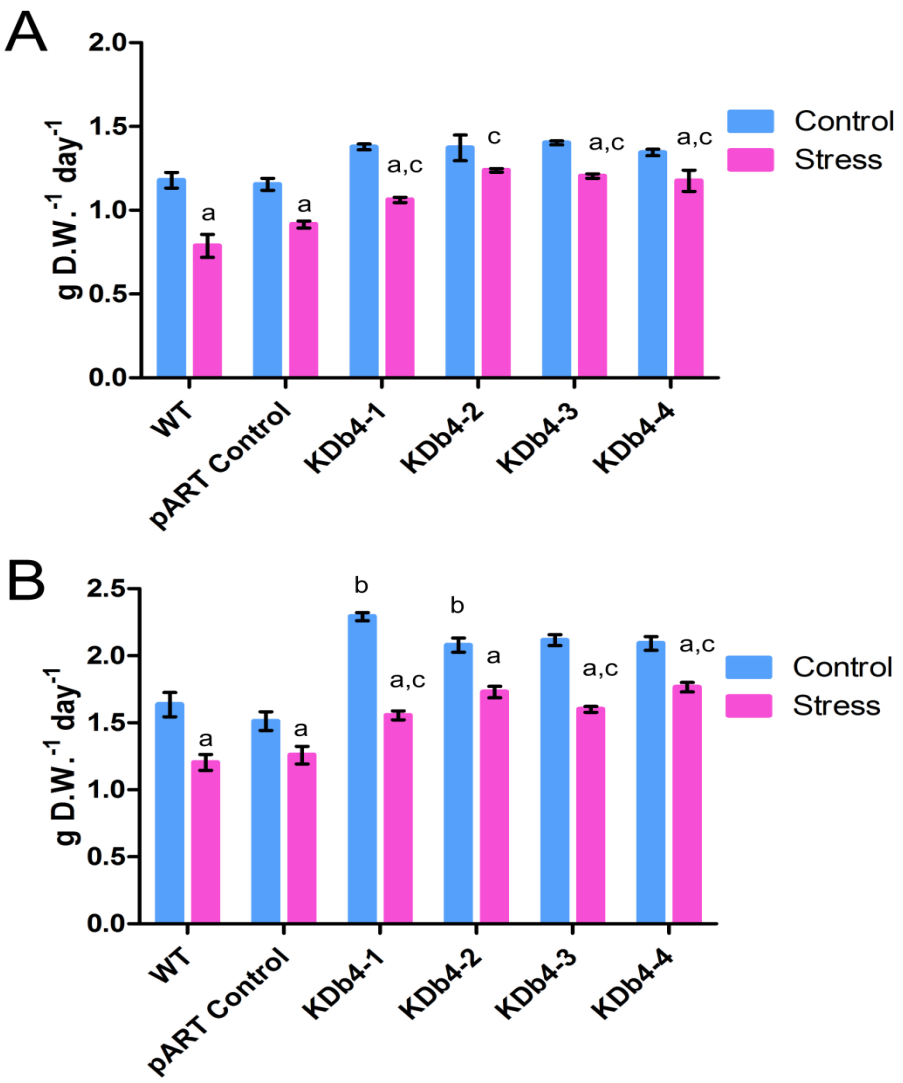

Figure 6.6 An increase in the alternative pathway results in higher growth rates during salt stress

Relative growth rate of *ndb4* mutant and control plants. Relative growth rate (RGR) was calculated by change in fresh weight of either rosette leaves or roots, from week 4 to week 5 of plant development using the equation (LN(mean fresh weight 5 weeks) – LN(mean fresh weight 4 weeks)/ time, where time = 1 week. (A) Roots and (B) leaves of plants grown hydroponically in the presence (salt) and absence (control) of 150 mM NaCl for 10 days. Values are means +/- SD for n=3, where [a] indicates significant difference, P>0.05 when comparing control to salt treated plants, [b] and [c] indicate significant difference for Wt and pART control compared to *ndb4* knock-down lines under (b) control condition and (c) salt conditions. Root, KDb4-2, salinity stress (Mean diff= 0.4230, t= 7.362, P >0.001). Leaf, KDb4-2, salinity stress (Mean diff= 0.5708, t= 12.22, P >0.001).

normal growth conditions. There was a significant increase in RGR when comparing pART to KDb4-2 under salinity conditions. This was expected, but it was noticed that for the *ndb4* knock-down lines there was no significant difference between RGR for KDb4-2 compared to normal and salt conditions. This is indicative of a plant that is well adapted to cope with stress before the stress is applied. The three knock-down lines with *ndb2*, *nda1* and *Aox1a* up-regulated showed tolerance to salt which was hypothesised to be linked to a minimisation of ROS species, hence allowing for an improved RGR.

6.3.5. Over-expression of AOX altered the Na^+ and K^+ balance, reducing Na^+ shoot content

An analysis of the ion balance with the AOX over expressers had shown a change in Na^+/K^+ ratio's, thus it was expected that an altered ratio would also be seen with these lines. It was hypothesized that tolerance of salt by the *ndb4* silencers would follow the same trend as AOX over expressers with a lower level of build up of Na^+ in the shoots.

Figure 6.7 and 6.8 shows the plants displayed an altered ion balance when subjected to the salt treatment (Figure 5.10 and 5.11). In the *ndb4* knock-down lines, although the root tissue behaved with the same trend, the shoot tissue however showed a significant decrease in the K^+ concentration under normal conditions i.e. for KDb4-2 and under salt stress conditions. These lines appear to have decreased K^+ levels and this occurs even more so under salt stress. Indicating K^+ level was not high in the *ndb4* knock-down lines compared to Wt.

As a more significant change was seen for the increase in Na^+ in the roots of the *ndb4* knock-down lines a higher Na^+/K^+ ratio was seen which was significant i.e. KDb4-2. The ratio for the leaf tissue also showed a more dramatic change with a significant decrease i.e. for KDb4-2, due to the lower Na^+ taken up by the leaf tissue in these lines. This result indicates the plants

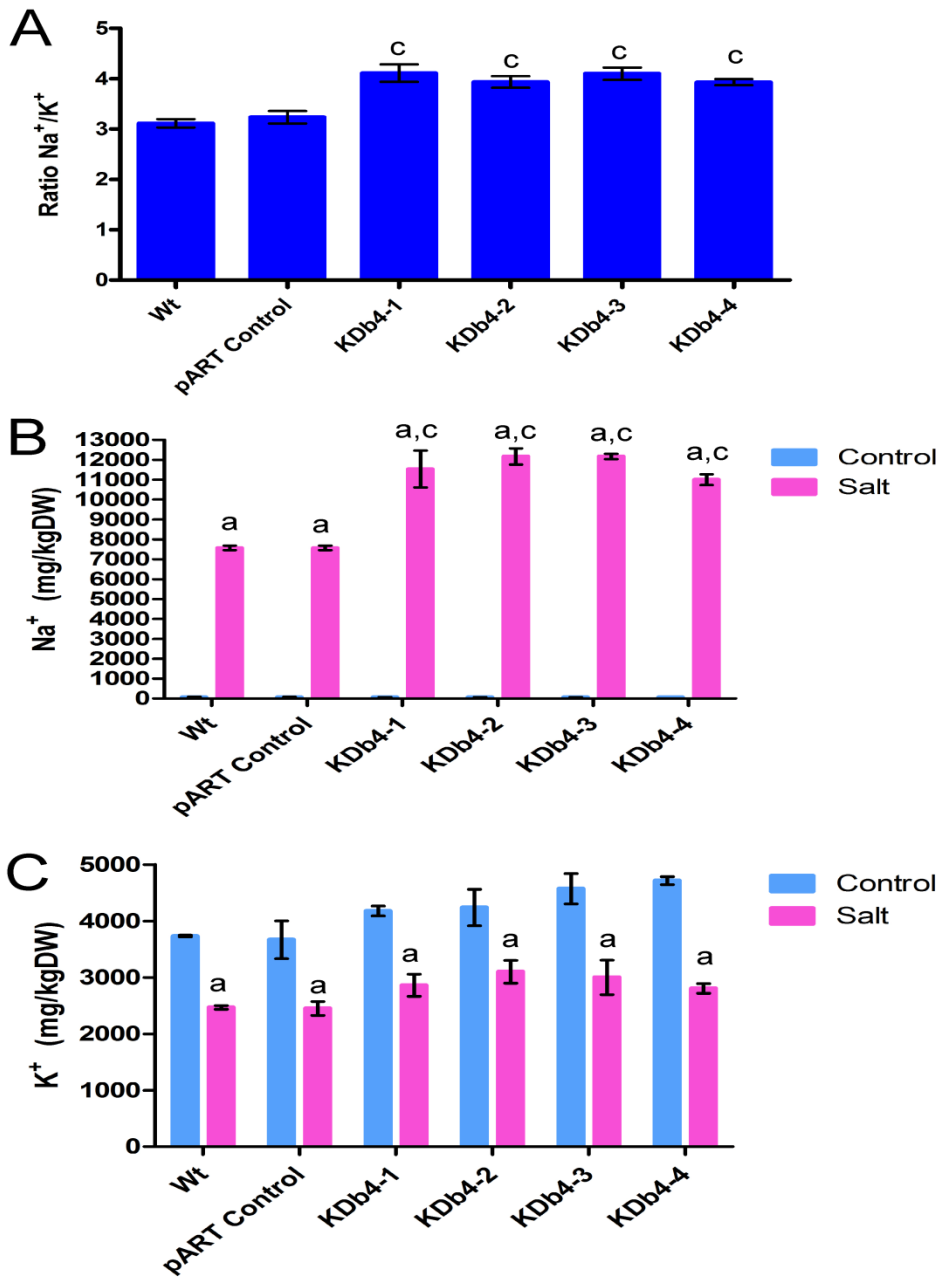

Figure 6.7 Alteration of the alternative pathway affects the root Na^+ and K^+ content

The ratio of Na^+/K^+ for the (A) root tissue after growth in 150 mM NaCl for 10 days. The Na^+ content of the (B) root and K^+ content of the (C) root were determined by ICPOES analysis. Values are the mean +/- SD for n=3 where, [a] indicates significant difference when comparing control to salt treated, [b] and [c] indicate significant difference for Wt and pART control compared to *ndb4* knock-down lines under (b) control condition and (c) salt conditions. Na^+/K^+, KDb4-2 (Mean diff= -0.8219, t= 4.881, P >0.01).

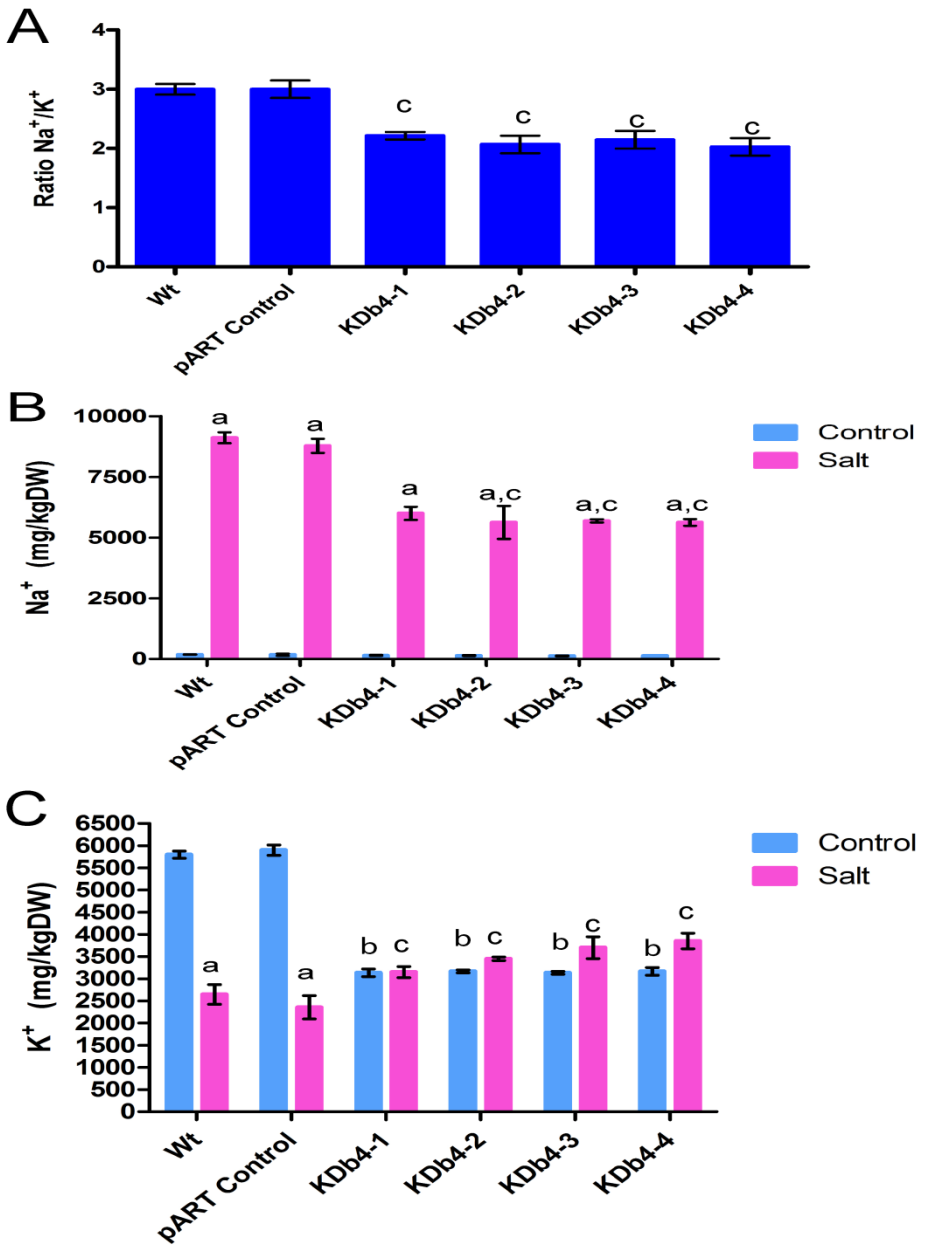

Figure 6.8 Alteration of the alternative pathway affects the leaf Na^+ and K^+ content

The ratio of Na^+/K^+ for the (A) leaf tissue after growth in 150 mM NaCl for 10 days. The Na^+ content of the leaf (B) and K^+ content of the (C) leaf were determined by ICPOES analysis. Values are the mean +/- SD for n=3 where, [a] indicates significant difference when comparing control to salt treated, [b] and [c] indicate significant difference for Wt and pART control compared to *ndb4* knock-down lines under (b) control condition and (c) salt conditions. Na^+/K^+ , KDb4-2 (Mean diff= 0.9306, t= 5.090, P >0.01) K^+ KDb4-2, Control conditions, (Mean diff= -2633, t= 12.56, P >0.001) salt conditions (Mean diff= 805.6, t= 3.842, P >0.01).

have more chance of survival as they appear to either take up less Na^+ to the leaf tissue of retain less. This is important as it is the build up of Na^+ in leaf tissue which becomes toxic to the plant, and hence this results in tolerance (Munns *et al.* 2008).

Thus, these *ndb4* silenced lines that over express the alternative pathway, demonstrated an altered ionic balance for Na^+ and K^+ that results in a lowered shoot Na^+ content with retention in the root, indicative of increase salinity tolerance and suggesting a change in long distance transport of Na^+ in these plants.

6.3.6. Disruption of the metal ion balance in plants as a result of salinity stress

Knowing that Na^+ an K^+ concentrations had changed as a result of salinity stress it was thought that other metal ions, particularly Ca^{2+} could be changing during salinity stress as a result of the change in ion balances to allow the plant to tolerate salt stress. As Zinc and Boron had both previously been suggested to have a change in metal ions under salinity stress (Tinker *et al.* 1984; Alpaslan *et al.* 2001), the level of these ions were also investigated. It was hypothesized that there would be a change in the balance of metal ions under salinity stress. For calcium there were no significant changes observed for the root tissue, although there was a trend towards higher calcium in the salt stressed tissue. However, no significant difference was seen between the pART control and *ndb4* knock-down lines (Figure 6.9). However for the leaf tissue there was significantly higher calcium content in two of the knock-down lines under salinity stress compared to normal growth conditions, KDb4-2, and KDb4-4. Additional calcium is added to solution with NaCl, as Na^+ can affect theactivity of calcium making it less available via a competition effect. Hence the extra calcium is added so the effects are not due to a calcium deficiency, but Na^+ toxicity. So in the *ndb4* knock-down lines the increase in calcium may be due to the lower levels of Na^+ that these plants have allowing more ability to

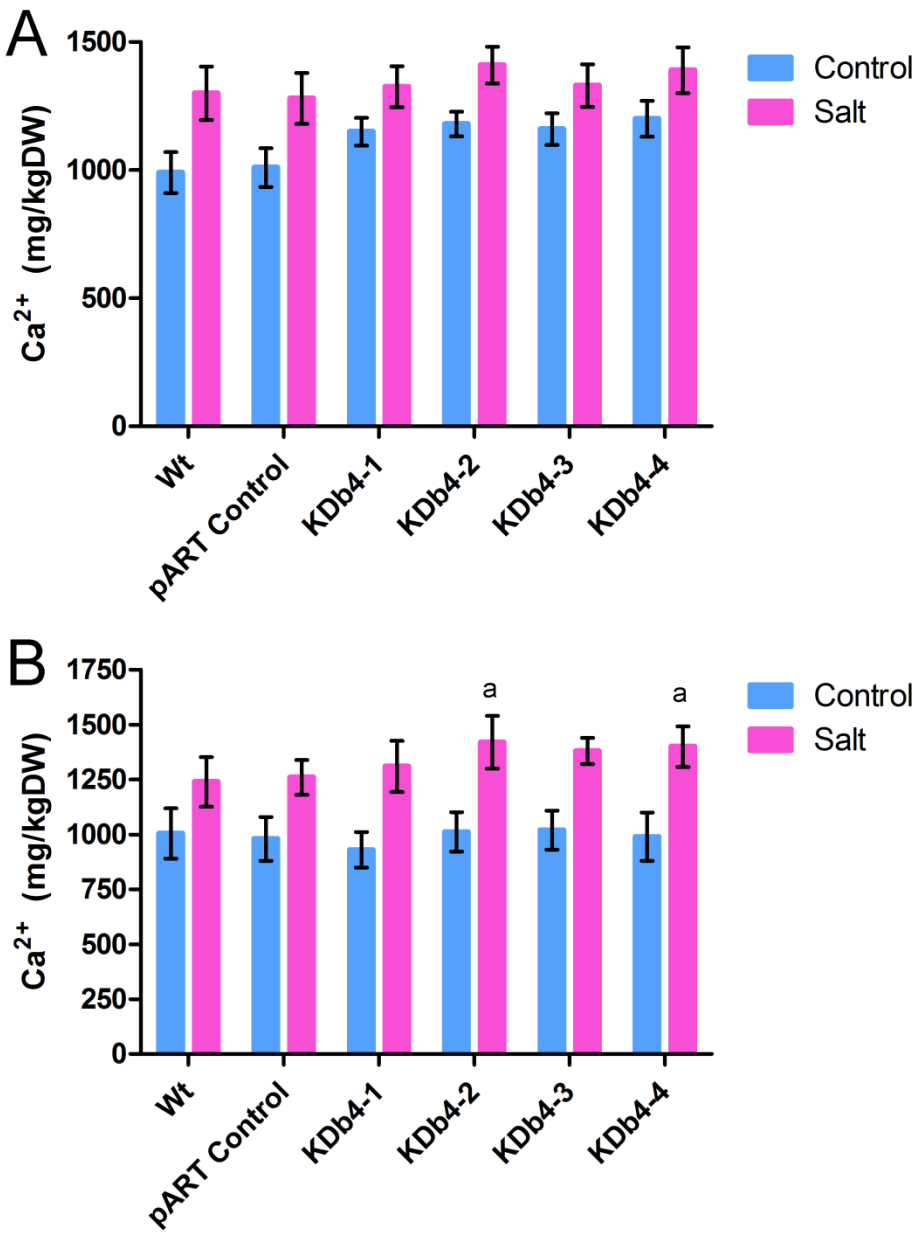

Figure 6.9 Alteration of the alternative pathway affects the leaf Ca^{2+} content

The Ca^{2+} content of the (A) root tissue after growth in 150 mM NaCl for 10 day and the Ca^{2+} content of the (B) leaf were determined by ICPOES analysis. Values are the mean +/- SD for n=3 where, [a] indicates significant difference when comparing control to salt treated, [b] and [c] indicate significant difference for Wt and pART control compared to *ndb4* knock-down lines under (b) control condition and (c) salt conditions. Leaf tissue salt stress KDb4-2, (Mean diff= 408.0, t= 2.922, P >0.05). KDb4-4, (Mean diff= 410.0, t= 2.936, P >0.05).

move calcium up to the leaves as its not being competed out.

For boron, a significant increase was seen for all lines under salinity stress, although, the increase was significantly less for *ndb4* knock-down lines in both roots (e.g. KDb4-2) and shoots (Figure 6.10). The increase in boron under salinity conditions was thought to be due to the passive movement due to membrane damage as a result of salinity increase (Alpaslan *et al.* 2001). This suggests that these lines may be maintaining better membrane integrity.

Zinc showed a different pattern to the other two ions as there was a decrease during salinity stress, and a trend towards an increase in the *ndb4* knock-down lines, compared to control for both roots and shoots (Figure 6.11). This decrease in zinc is suggested to be due to a stronger competition by salt cations at the root surface (Tinker *et al.* 1984). There was significantly more zinc in control growth conditions for shoots for the knock-down lines, i.e. KDb4-2, compared to control, although this was significantly reduced under salinity stress. The increase of Zinc in the knock-down lines indicates there was less competition in these lines for Zinc uptake compared to the control lines, a suggestion that this may be due to the change of ion balance in these lines. It is known that Nicotianamine synthase (AtNAS) is involved in transporting micronutrient metal ions in plants (Klatte *et al.* 2009), we also see this gene up-regulated 3.749 fold in KDB4-1 (Table 6.2), providing a possible link between the ion balance change seen in the *ndb4* knock-down lines.

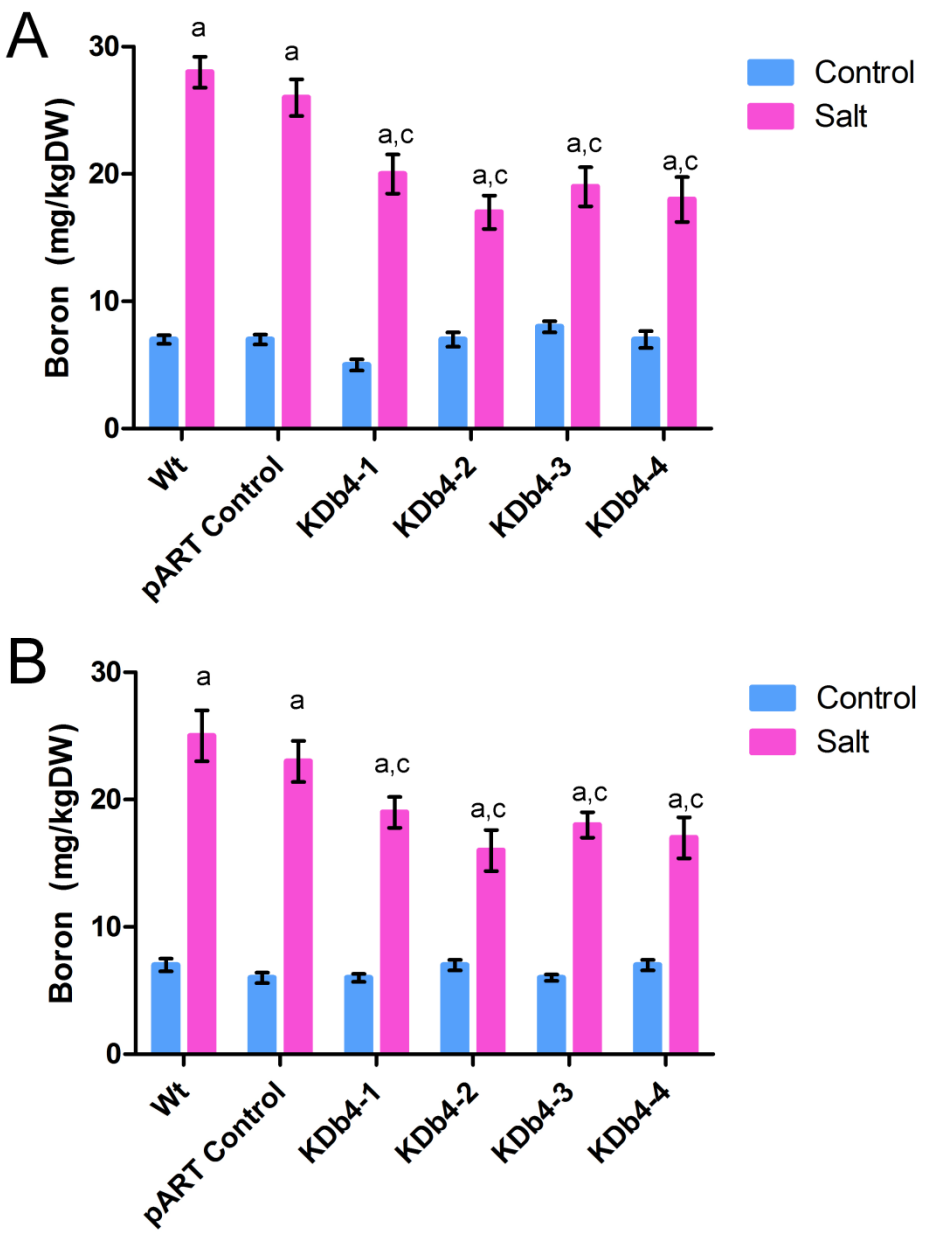

Figure 6.10 Alteration of the alternative pathway affects the leaf boron content

The B^{3+} content of the (A) root tissue after growth in 150 mM NaCl for 10 day and the B^{3+} content of the (B) leaf were determined by ICPOES analysis. Values are the mean +/- SD for n=3 where, [a] indicates significant difference when comparing control to salt treated, [b] and [c] indicate significant difference for Wt and pART control compared to *ndb4* knock-down lines under (b) control condition and (c) salt conditions. Salinity stress KDb4-2, roots (Mean diff= -11.00, t= 7.082, P >0.001), shoots (Mean diff= -9.000, t= 5.692, P >0.001).

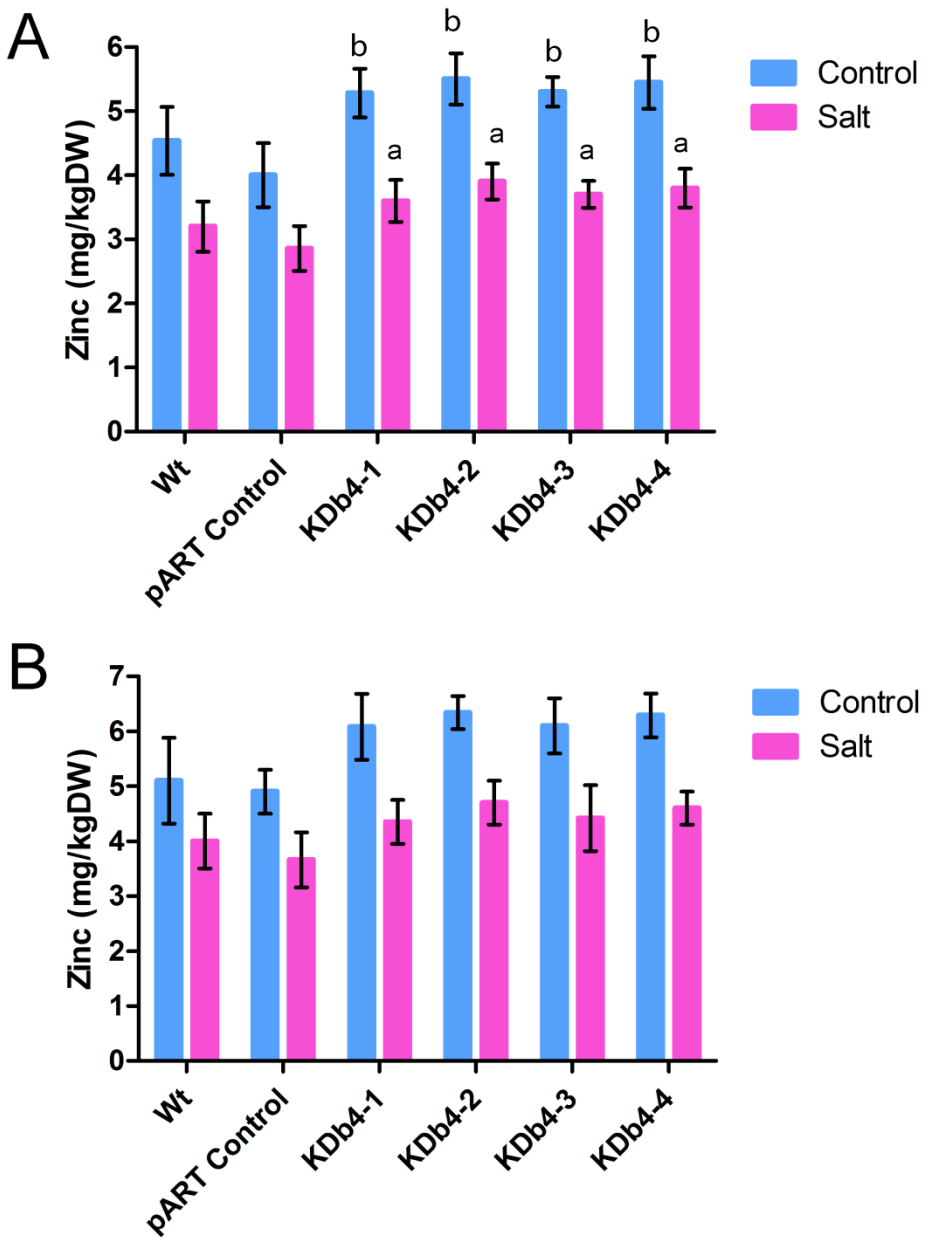

Figure 6.11 Alteration of the alternative pathway affects the leaf zinc content

The zinc content of the (A) root tissue after growth in 150 mM NaCl for 10 day and the zinc content of the (B) leaf were determined by ICPOES analysis. Values are the mean +/- SD for n=3 where, [a] indicates significant difference when comparing control to salt treated, [b] and [c] indicate significant difference for Wt and pART control compared to *ndb4* knock-down lines under (b) control condition and (c) salt conditions. Control KDb4-2, shoots, (Mean diff= 1.504, t= 2.868, P >0.05), salinity stress (Mean diff= -1.604, t= 3.058, P >0.05).

6.4 Discussion

Based on results generated for the AOX over expressers under salinity conditions (Chapter 5) and confirming that AOX did provide tolerance to salt stress by decreasing ROS it would be interesting to observe what would result if other members of the alternative respiratory pathway were also up-regulated. The *ndb4* knock-down lines had *ndb2* and *nda1* as well as *Aox1a* up-regulated, thus it was possible to test this hypothesis using the *ndb4* silenced lines. Additionally, it was hoped that the data would help to understand any benefit of the alternative dehydrogenases under salt stress, as very little has been done to look at the regulation of these genes and the role that play during salt stress. It is known that the NAD(P)H dehydrogenases alleviate excess NAD(P)H when concentrations are increased, suggesting that complex I activity is inadequate under these conditions. Hence the external dehydrogenases may help to minimize ROS using this NAD(P)H oxidation overflow (Moller 2001).

The microarray data suggested that a number of pathways are already turned on in these *ndb4* knock-down lines, even prior to stress, hence these plants may already be experiencing a state of stress. Previous microarray data on AOX mutants indicated changes in oxidative stress genes as was observed for these *ndb4* knock-down lines. It was found that several of these genes responded with an increase in transcript while others had a down regulation of transcript. This suggests that there is an altered equilibrium of signaling in those *Aox1a* T-DNA plants (Giraud *et al.* 2008). This data further confirmed that AOX activity is linked to oxidative stress which is the pattern seen in this work. A disruption in the mitochondrial electron transport chain can lead to alterations in ROS in various other organelles due to the complexity and interactions of the ROS signaling and defense networks. The data presented here confirms that changes in the genes of the ETC has a greater effect outside the mitochondrion in terms of altering metabolism, and the antioxidant defense compared with within the mitochondrion.

There were also several antioxidant genes which had changed transcripts in the KDb4-1 line, as well as numerous oxidoreductase genes (Table 6.2). These results suggest that an altered electron transport chain is resulting in changes which link with an altered ROS signalling pathway, due to the changes seen for abiotic, biotic, redox antioxidant pathways in the microarray data. These pathways have altered transcripts due to the knock-down of *ndb4* which appears to result in altered ROS signalling pathway. This suggests that when members of the alternative pathway are already being expressed, the plant is in an altered state to cope with environmental stress. The functional analysis of heat-responsive gene expression suggests that the plant transcriptome is rapidly adjusted, most likely due to a changed signalling pathway caused by the alteration of alternative pathway genes (Kant *et al.* 2008).

The increase seen for the expression of malate transporters could be due to the lack of NAD(P)H oxidising power on the outer surface of the mitochondrial membrane, which leads to up-regulation of substrate shuttles, such as the malate-oxaloacetate exchange, to take reductant into the mitochondrial matrix as malate. At higher malate concentrations the rotenone-insensitive NADH dehydrogenase is increasingly important and has increased electron transport capacity (Walker *et al.* 1983). With higher malate concentrations an increasing portion of electrons from malate reduce O_2 through the alternative oxidase (Walker *et al.* 1983). An increase in intramitochondrial NAD(P)H levels could lead to a need for increased internal type II NDAs. The transcript increases observed for *nda1* fit with this model.

Like the results seen for AOX over expressers, these plants also resulted in decreased ROS levels and a tolerance to salinity stress for the *ndb4* knock-down plants with higher expression of the alternative pathway genes. In normal plant tissue, ROS such as H_2O_2 will provide a mechanism to amplify the intensity of some signals by crossing over of signalling that lead to an induction of AOX (Vanlerberghe *et al.* 1996), and it would seem the alternative NAD(P)H dehydrogenases. Although it is becoming apparent that AOX has a bigger role than just alleviating ROS. There has been four

suggested pathways that lead to the induction of specific AOX genes and possibly the alternative dehydrogenases genes could also be responding to similar pathways; a ROS dependent pathway, a redox pathway linked to plastid dysfunction, a pathway triggered by ATP depletion and a pathway triggered by ATP depletion, as well as a pathway triggered by altered metabolic conditions (Clifton *et al.* 2005; Zarkovic *et al.* 2005; Clifton *et al.* 2006). Having confirmed that AOX can prevent ROS formation, it may be dependent on how much excess alternative pathway capacity is present before the imposition of the stress, which we have indicated is the case based on results which indicate AOX can be up-regulated under stress and protect the plant. However if these genes are already turned on as was the case for the *ndb4* knock-down lines the plant will already be signalling pathways relating to stress such as ROS and in turn before the plant is stressed it is already in a changed state to cope with the stress.

The improved growth rate seen for the *ndb4* knock-down line under salt is an indication that the alteration of this pathway could provide improved crops for farmers whose land has high salt content. The improved growth rate is an indication that theses lines are able to maintain intracellular water potential, below the water potential in growth medium to enable the cells to take up water required for growth (Moller *et al.* 2007). The changes in plant growth under salinity conditions are a result of osmotic effect, and similar to that seen from drought responses (Munns *et al.* 2008). It has been found that when Ca^{2+} was added to a saline media solution there was improved leaf elongation (Cramer 1992), hence why Ca^{2+} was added to our solution, and an indication of why an increase in calcium is seen in the salt stressed plant. High salinity results in increased cytosolic Ca^{2+} that is transported from the apoplast and intracellular compartments, with the resultant transient Ca^{2+} increase potentiates stress signal transduction and leads to salt adaptation (Knight *et al.* 1997). Ca^{2+} signalling in salinity stress has been previously researched and shown to be important in the activation of the SOS (Salt-Overly-Sensitive) signalling pathway which acts to regulate Na^{+} and K^{+} homeostasis. Munns and Tester (2008) argue that thermodynamically, SOS-1 cannot participate in xylem retrieval, but rather in efflux into the xylem, and

that it is more likely that over expression of SOS-1 increases the efflux of Na^+ from the outer root cells into the soil. Although there has been no research into a link between AOX and SOS-1 as yet, results suggest similar pathways of response and leads to possible further research into salt tolerant plants. The first step would be to look at transcript of SOS-1 in the *ndb4* knock-down lines to determine if there is a link.

Like the AOX over expressers, the *ndb4* knock-down lines also showed a novel response of altered ionic homeostasis (lower leaf Na^+ levels, and higher root Na^+ levels) compared to Wt plants. The *ndb4* knock-down lines showed even further improved salinity tolerance as a result of even more Na^+ being exported out of the leaves or the stop of the flow up into the leaves. Although the difference seen with the *ndb4* knock-down lines was a decreased K^+ content in the leaf tissue of the knock-down lines, there was increased K^+ in the roots. K^+ is an essential ion to plants; the K^+ of roots was increased, and is likely involved in signalling and in transporters to move Na^+ out of the leaf tissue to aid in salt tolerance.

The increase in boron is likely to be a passive movement, and is likely to be increased under salinity conditions due to a damaged membrane. Boron in high concentrations is toxic to the plant as is can limit plant growth and often high Boron is found in saline soils and saline well water (Dhankhar *et al.* 1980). As the *ndb4 knock-down* lines had less Boron it is an indication there was less membrane damage in these plants and hence less Boron was able to be taken up. Conformation of this is that previously salt excluder plants are more resistant to boron toxicity since their salt exclusion mechanism control the excessive uptake of Boron as we observed (Alpaslan *et al.* 2001). An opposite result was seen for zinc where a decrease under salinity conditions occurred, which was previously also suggested by Tinker *et al* (1984). Zinc is out competed by other ions such as cadmium, and hence Cadmium is taken up by the plants in preference to zinc (Khoshgoftar *et al.* 2004). The increase in zinc in the *ndb4* knock-down lines further supports salinity tolerance as reduced zinc can often lead to increased plasma membrane permeability of root cells, where these lines had more zinc and hence further supports the

decrease seen for boron which is also a result of damaged membrane. Nicotianamine is mobile in the plant and has been detected in root and leaf cells as well as in phloem sap. It can bind metal ions like Fe, Zn, copper, and nickel (Scholz *et al.* 1992; Schmiedeberg *et al.* 2003). The *ndb4* knock-down plants have an increase in Nicotianamine Synthase which is the enzyme responsible for producing Nicotianamine (Klatte *et al.* 2009). Suggesting these plants may be using Nicotianamine to help move metal ions around the plant and uptake from the soil, hence why higher levels of zinc are found in the *Atnb4* knock-down lines compared to control.

All the results presented support and conclude that the *Atnbd4* knock-down lines with increased transcript of *ndb2*, *Aox1a* and *nda1* in 3 of the lines had improved salt tolerance and hence have shown that by increasing the transcript of these genes we have been able to have reduced ROS as a result of a suggested changed signalling withing these plants which in turn increases growth rate and is able to remove Na^+ from leaf tissue of plants which would normally result in toxicity to the plants.

7 GENERAL DISCUSSION/CONCLUSION

There were three main aims in this study. Firstly, an aim was to generate a transgenic *A. thaliana* line with complete suppression of the *ndb4* gene to confirm that it encodes an external NAD(P)H dehydrogenase and its calcium dependence. Secondly, it was also hoped that it would be possible to elucidate the role of the external facing alternative NAD(P)H dehydrogenases by reducing or eliminating expression of all the four external dehydrogenases in one plant line. The third aim was to look at the response of the alternative pathway including alternative oxidase (AOX) to stress growth conditions, specifically salinity stress. These aims were achieved with using RNAi technology to generate transgenic plants with silenced expression of the *ndb4* gene and these plants were characterised under normal growth condition and their response to salinity stress was determined.

Until now the substrate specificity of alternative NAD(P)H dehydrogenases had not been confirmed in *A. thaliana*. To date, some of the *A. thaliana* genes had been cloned into *E. coli* and their substrate specificity analysed, this had yet to be confirmed *in planta* (Geisler *et al.* 2007). The substrate specificity for *ndb4* and *ndb2* was confirmed *in planta* during this project. Indicating the specificity observed for *ndb1* by Geisler *et al.* (2007) is likely to also be correct. Figure 7.1 summarises what we now know about the substrate specificity of the external alternative NAD(P)H dehydrogenases and whether they are stimulated by calcium or not as determined from this study and Geisler *et al.* (2007). It was determined from this study that *ndb2* is an NAD(P)H dehydrogenase which is calcium dependent, with a preference for NADH, and that *ndb4* is an NAD(P)H dehydrogenase calcium independent dehydrogenase also with a preference for NADH. Previous work (not confirmed in *A. thaliana*) suggests that *ndb1* is calcium independent NADPH (Geisler *et al.* 2007). As *ndb2* and *ndb4* both use NADH as a substrate, it explains why there was an increase in NADH oxidation capacity when *ndb4* was silenced as there also was an increase

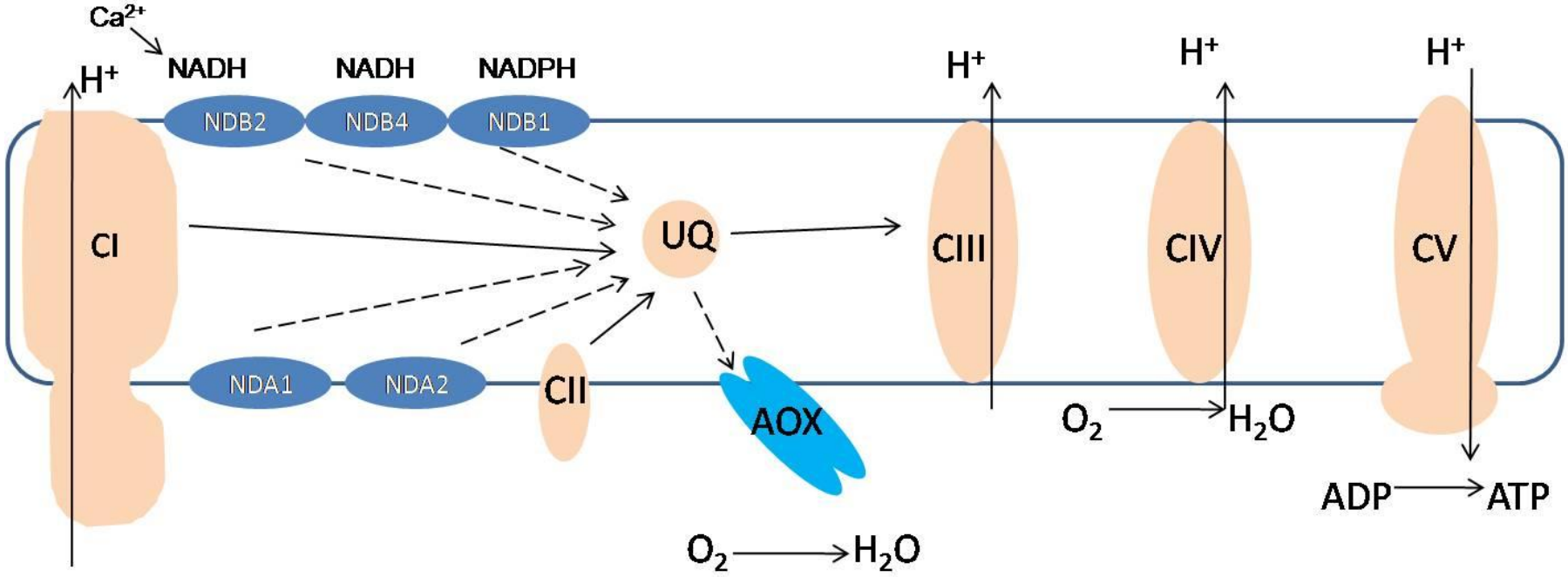

Figure 7.1 The electron chain showing the elucidated substrates for external dehydrogenases

It was concluded that NDB1 is a calcium independent NADPH (Gielsler *et al* 2007). NDB2 is a calcium dependent NADH and NDB4 is a calcium independent NADH.

in *ndb2* expression, thus compensating for the loss of *ndb4* as the products of both genes can use the same substrate.

Evidence that the external dehydrogenases are required for normal cell function in plants hasn't been extensively investigated. Research into the non-phosphorylating pathway of plant respiration has focussed on AOX showing it to be present across a wide range of species and that it is found in most kingdoms, even the animal kingdom (McDonald *et al.* 2004; McDonald 2008). It is likely that the alternative NAD(P)H dehydrogenases may also be wide spread and due to their widespread presence suggests that they may play an essential biological function. A phylogenetic analysis of bacterial, plant, fungal, and protist NAD(P)H dehydrogenase-like protein sequences (Michalecka *et al.* 2003) shows the wide-spread presence of these genes/proteins (Figure 7.2). There are three distinct subgroups separated on sequence features, suggesting that there are three families (nda, ndb, and ndc) of type II NAD(P)H dehydrogenase genes present in plants. The NDA and NDB sequences of plants appear closely related to the fungal and protest sequences, while At-NDC1 and the rice NDC homolog cluster with cyanobacterial proteins (Michalecka *et al.* 2003). In this study, I have shown that when a plant with a RNAi knock-down vector containing a knock-down region for all four external alternative NAD(P)H dehydrogenases were grown, it resulted in plants that were not viable and had stunted growth. This indicates that at least one if not all of these dehydrogenases may be essential for plant development. It has been shown in this study that both AOX and the alternative dehydrogenases play a role in the reduction of ROS, as the *ndb4* knock-down lines with both *Aox1a* and *ndb2* up regulated showed lower levels of H_2O_2 when compared to lines over expressing Ataox1a alone. Thus, without these dehydrogenases and an increased level of ROS can accumulate as the alternative electron chain will not function optimally without an external dehydrogenase. This is summarised in Figure 7.3 where without the functioning alternative dehydrogenases ROS accumulates at Complex I.

Clifton *et al.* (2005) proposed the co-expression of AOX and NDH that are

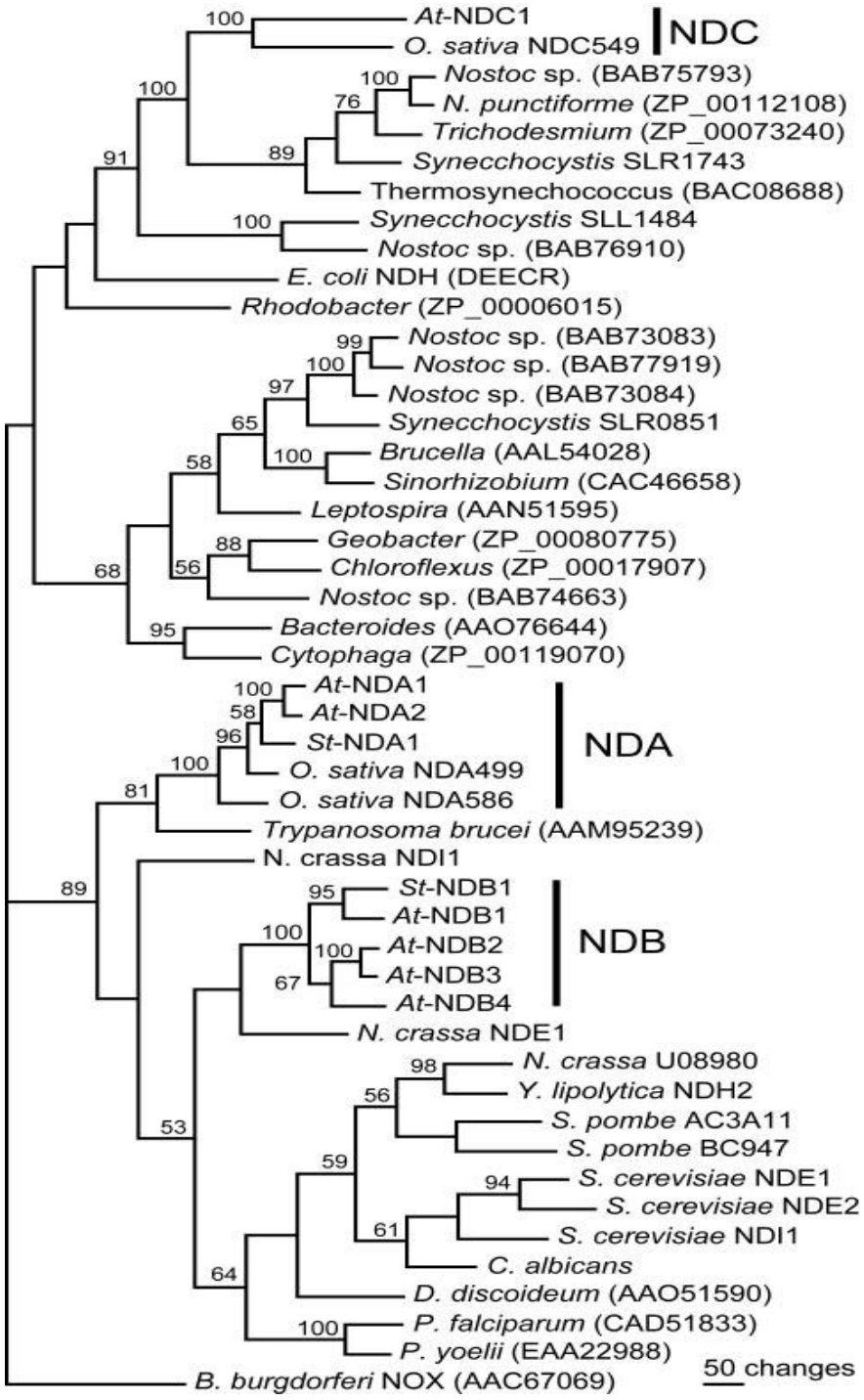

Figure 7.2 Phylogenetic analysis of bacterial, plant, fungal, and protest NAD(P)H dehydrogenase-like protein sequences

Sequences were aligned using ClustalW in MacVector 7.1 software (Accelrys Inc., San Diego). Alignments were manually inspected and edited, assuring correct matches of conserved regions (Michalecka *et al.* 2003).

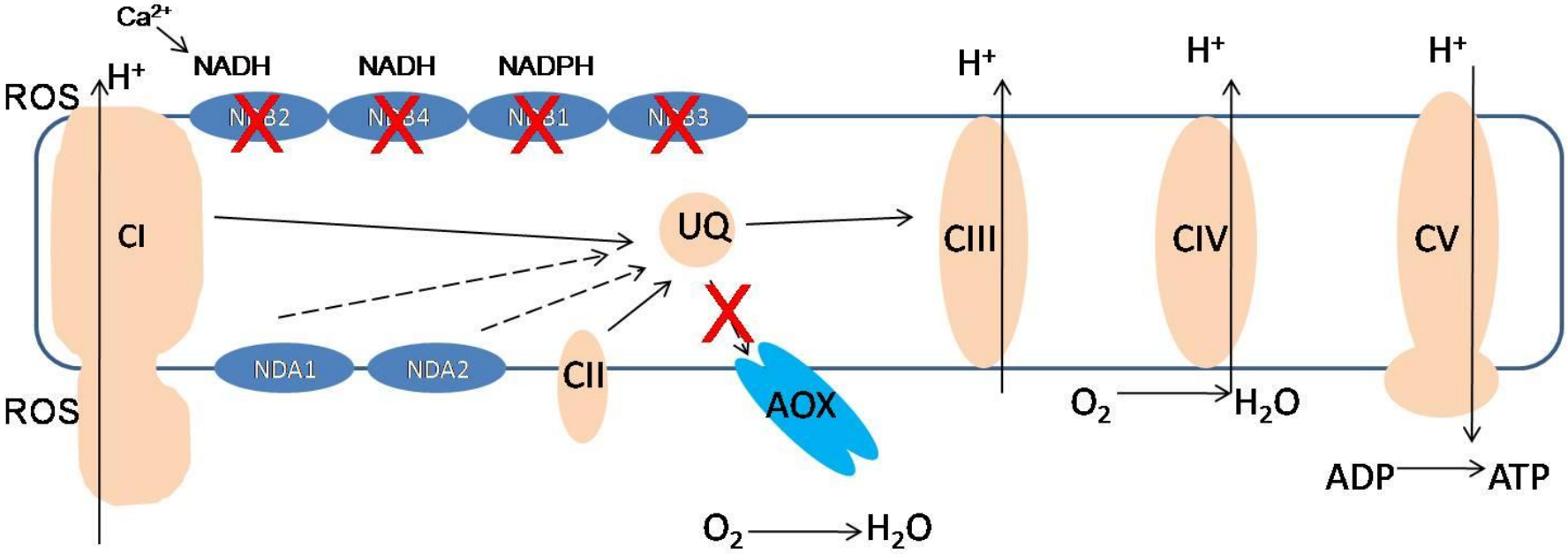

Figure 7.3 The electron chain showing the four external dehydrogenases silenced

An RNAi construct designed to recognize all four genes led to a seedling-lethal phenotype.

capable of forming a simple but functional alternative respiratory chain, allowing oxidation of cytosolic NAD(P)H in a manner which is uncoupled from oxidative phosphorylation. This was shown for AOX1a and NDB2 in this study during salt stress and in transgenic lines disturbed in *ndb4* expression. This co-regulation may be due to the presence of common sequence elements in the promoter regions of these genes, such as CAREs for AOX1a and NDB2 (Ho *et al.* 2008). Due to this co-expression it has been suggested by Clifton *et al.* (2005) that the products of *Aox1a* and *ndb2* genes are capable of forming a simple but functional alternative respiratory chain (Figure 7.1). This alternative respiratory pathway allows oxidation of cytosolic NAD(P)H from oxidative phosphorylation, and may be useful in helping maintain redox balance of the cell, and turnover of carbon pathways.

Results presented confirmed that a 'self contained' alternative electron transport chain is up-regulated under saline conditions in Wild type plants, (Figure 7.4). The up-regulation of the alternative pathway under stress is a result of trying to lower the ROS levels, this work supports previous work for citrus cell cultures which showed improved protection from salt stress with an increase in AOX (Ferreira *et al.* 2008). An *A. thaliana* mutant *enh1-1* that enhances the salt sensitivity of a *sos3-1* and also caused increased salt sensitivity by itself. This *A. thaliana enh-1* mutant showed greater sensitivity to salt stress as it had higher ROS levels and higher seedling Na^+ content than the Wt (Zhu *et al.* 2007). Although it was observed that when AOX was up-regulated prior to stress, an improved response to salinity stress was observed, and showed an indication of tolerance, due to the improved RGR and lower shoot Na^+ levels. Clifton *et al.* (2006) proposed the possibly that when there is altered AOX expression, it can induce a stress response, act as a modulator of existing programs, and an initiate novel expression programs. AOX may be more than just a terminal oxidase but also be an initiator of cellular reprogramming which acts to trigger novel expression. The results presented in this work follow this proposition indicating that when AOX was up-regulated there was a change in the reprogramming which allowed for the plant to become tolerant by activating certain pathways for

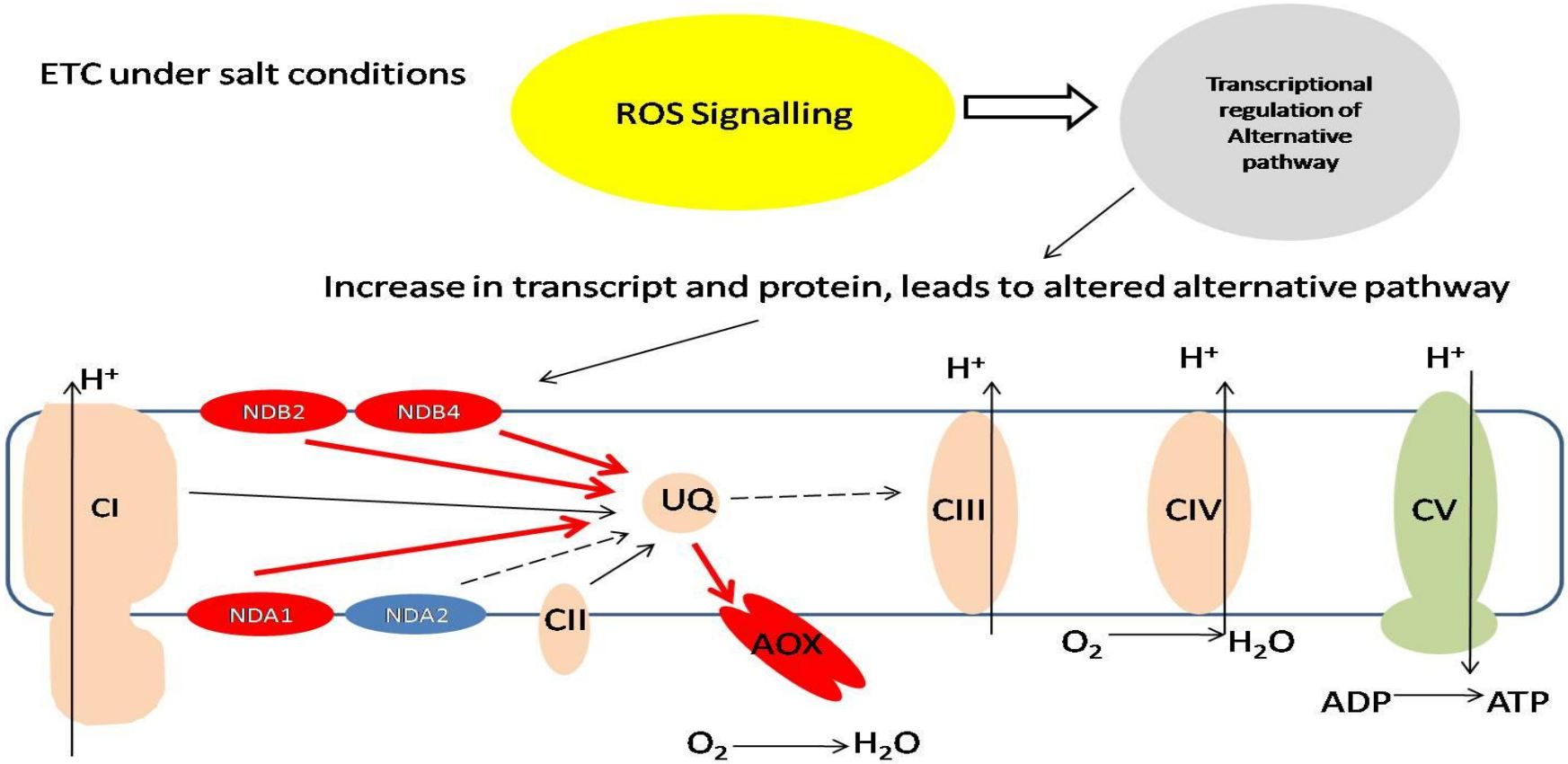

Figure 7.4 The electron chain under salt stress conditions

Under salt stress conditions the alternative pathway is up regulated which aids in protection

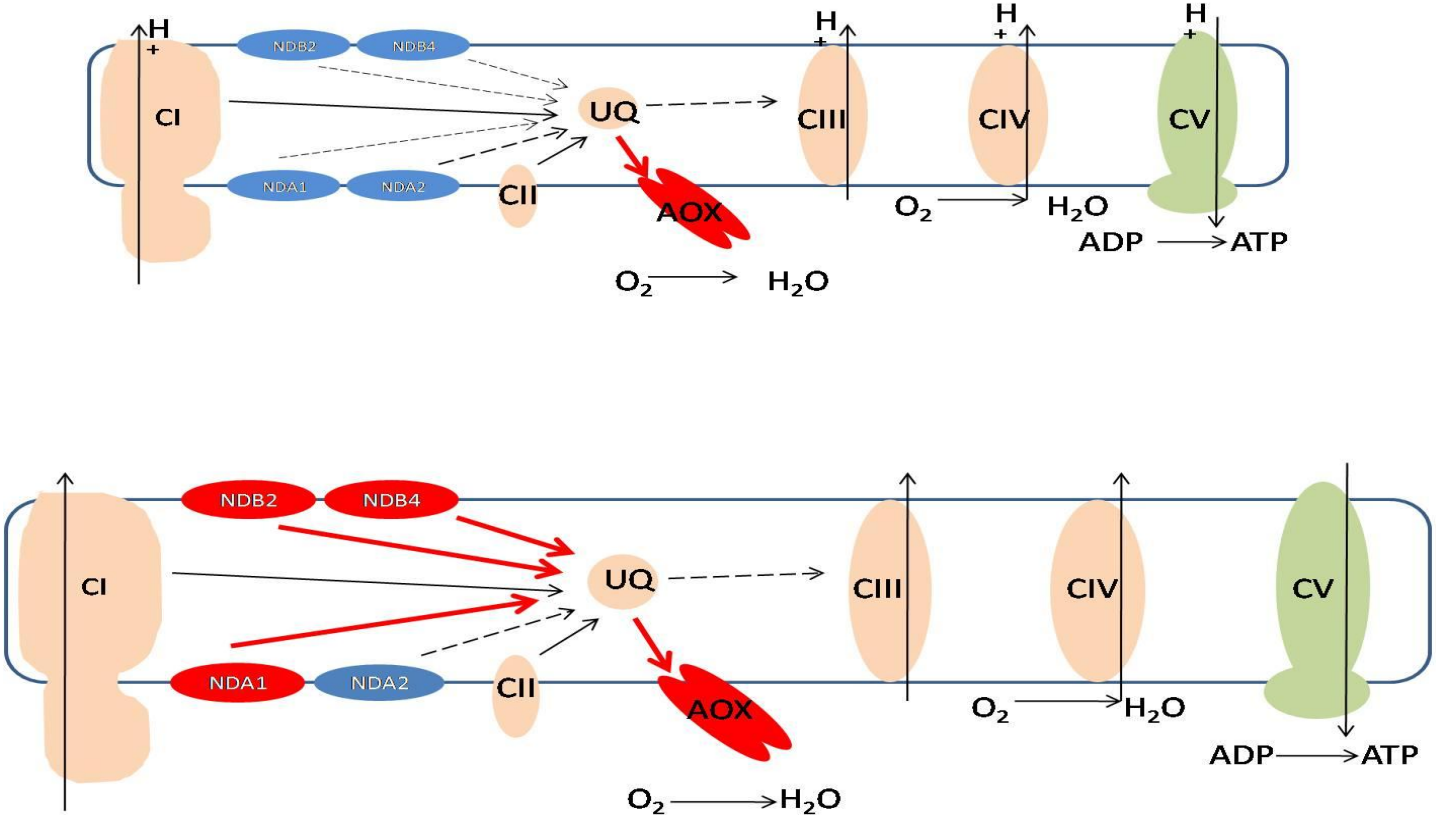

Figure 7.5 The electron chain showing AOX up regulated prior to stress and after stress

(A) AOX is already turned on, so when stress is applied, the plants are better equipped to lower ROS levels quickly due to AOX up regulation and hence generate tolerant plants. (B) Tolerance is further improved when both AOX and the non-phosphorylating pathway is already turned on in plants.

signalling, such as the changes in Na^+ and K^+ transport. The results presented in this work support a dual role for AOX and the alternative dehydrogenases in that together they act both as an alternative electron chain with an external, internal dehydrogenases and AOX able to make their own pathway, as well as a mediator of a cellular response to changing conditions. The summary of this can be seen in Figure 7.5. This is supported by Clifton *et al.* (2006) who also suggest a dual role for AOX. This is not without precedent as it has been documented that cytochrome c also plays a dual role, again both in electron transport and signalling of programme cell death (Balk *et al.* 1999). If a plant can be in a position to be ready to adapt to a stress response before a stress is applied it may be a valuable tool for the agricultural market.

High salinity is a stress condition that affects plant growth and crop production (Xiong *et al.* 2002), as the plant's ability to take up water is reduced due to the osmotic balance and hence causes decreased growth rate and a long cascade of metabolic changes (Munns 2002). Once salinity stress is induced there are various biochemical and physiological responses that occur to help the plant survive (Seki *et al.* 2003). Some of the responses of the plant are a buildup of ROS, which cause oxidative damage to different cellular components. If plants were able to alleviate this oxidative damage caused from ROS, then the plant may have enhanced resistance to salt stress (Apse *et al.* 2002), and in an ever changing global climate, if a plant is able to cope to stresses such as salinity, it may assist in improving crop yield.

When not only AOX was up-regulated prior to salinity stress but also an internal and external dehydrogenases were up-regulated, an increased tolerance, as determined by the lower shoot Na^+ content and improved RGR, was achieved (Figure 7.6). The biological outcome of ROS signalling is intrinsically related to the nature of the ROS signal and is dose dependent. Low doses of O_2 and H_2O_2 have been shown to induce protective mechanisms and acclimation responses against oxidative and abiotic stress, while high doses trigger cell death (Gechev *et al.* 2006). Hence with the ETC

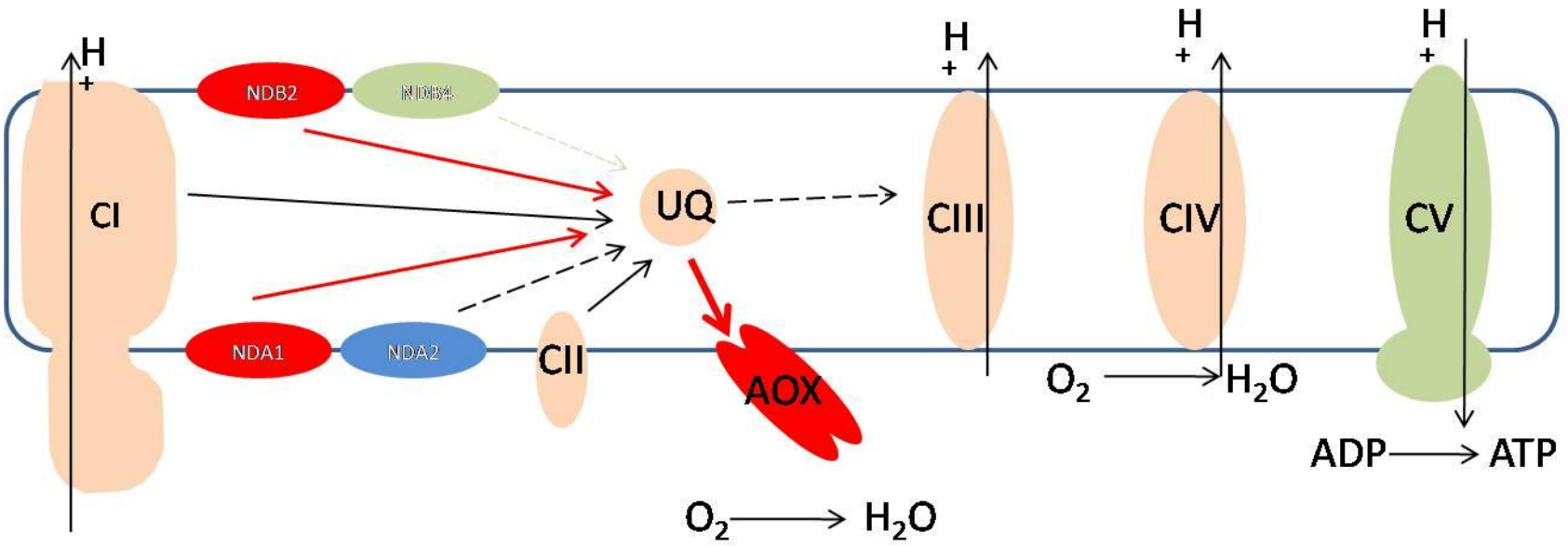

Figure 7.6 The electron chain showing AOX, NDA1 and NDB2 up regulated prior to stress

The alternative pathway is already turned on, so when stress is applied the plants are better equipped to lower ROS levels quickly due to alternative pathway up regulation and hence generate tolerant plants.

prior to stress, only low levels of ROS can be eliminated, as the alternative pathway is up regulated and it reduces ROS levels. Hence in these over-expressing plants, unlike the Wt plants, a high dose of H_2O_2 cannot accumulate, protecting these plants from death. These redox changes are sensed by the plant cell as a 'warning' message and, depending on the situation, genetic programs leading to stress acclimation or programmed cell death are switched on (Gechev *et al.* 2006). The small transient increases in H_2O_2 serve as signals triggering stress acclimation against subsequent more severe abiotic or oxidative stress. Protective roles for H_2O_2 have already been demonstrated against chilling, salt, high light and heat, and oxidative stress (Karpinski *et al.* 1999), confirming the protection we saw due to a signalled stress response. However, there is still controversy over how Na^+ tolerance is achieved. It is suggested that Na^+ retrieval from the xylem is the primary controller of lower shoot Na^+ in *A. thaliana* and the primary determinant of this is HKT1 (Munns *et al.* 2008). However, other authors suggest that SOS-1 participates in the retrieval of Na^+ from the xylem, as over expression of SOS-1 produced plants with increased salt tolerance (Shi *et al.* 2003). The mechanisms of how Na^+ transport is affected still needs further research. Hence future work with both the AOX overexpressing lines and the *ndb4* knock-down lines needs to determine if there is a link between ROS, AOX and the HKT-1 or SOS-1 gene in these lines. This would help to further understand the role ROS is having on Na^+ transport and subsequent salinity tolerance.

In conclusion this work has helped to elucidate the substrate specificities of several external NAD(P)H dehydrogenases, as well as indicating that the external dehydrogenases may be essential in the plant. From the data presented it can be concluded that the alternative pathway with the involvement of not just AOX but also alternative NAD(P)H dehydrogenases result in protecting the plant by signalling stress responses in the plant, specifically salinity stress. This aids the plant under such a stress by providing protection not just by reducing ROS but also signalling which results in the removal of toxic Na. Hence these dehydrogenases appear to play a dual and critical important role in the plant.

Future work leading on from this project will involve looking into the HKT1 and SOS1 genes and trying to understand the role these genes have on salinity stress and if there is a link with the *Aox1a* and *Atndb* genes. Another direction for these genes is to look at other stresses such as heat, high light and drought and a combination of these stresses which are conditions that could be found naturally in arid environments. Future work with the alternative pathway will also involve the further characterization of the remaining alternative dehydrogenase and AOX genes. The tools for identifying and characterizing these genes have been established with QRT-PCR assays and available antibodies for protein analysis. As part of the characterisation of all the alternative dehydrogenase genes and AOX genes multiple knockdown/out plants could be created for combinations such as *ndb2*, *ndb4* and *Aox1a*, as well as many other combinations. With work already completed and expected future work the results should elucidate substrate specificity for all genes and establish physiological significance within the plant.

APPENDIX

APPENDIX A - BUFFERS / REAGENTS / SOLUTIONS / MEDIA

All reagents listed below were of molecular grade and supplied by Sigma-Aldrich® (Australia) unless otherwise specified. Solutions requiring sterilisation were autoclaved on a fluid cycle at 121°C for 15 minutes, unless otherwise specified.

A.1 SDS-PAGE Gel Electrophoresis

Resolving Gel - 10%

375mM Tris-HCl (Progen, Australia) *pH 8.8*, 0.1% (w/v) SDS (ICN Biomedical, Ohio), 10% (w/v) Acrylamide, 0.27% (w/v) Bis, 0.4% (v/v) TEMED, 0.05% (w/v) Ammonium persulphate (Bio-Rad, CA) – *Add Last*

Stacking Gel – 4%

125mM Tris-HCl (Progen, Australia) *pH 6.8*, 0.1% (w/v) SDS (ICN Biomedical, Ohio), 4% (w/v) Acrylamide, 0.1% (w/v) Bis, 0.2% (v/v) TEMED, 0.05% (w/v) Ammonium persulphate (Bio-Rad, CA) – *Add Last*

Running Buffer

190mM Glycine, 24mM Tris-Base, 3.4mM SDS (ICN Biomedical, Ohio)

4x Denaturing Loading Buffer

250mM Tris *pH 6.8*, 8% (w/v) SDS (ICN Biomedical, Ohio), 40% (w/v) Glycerol, 0.01% (w/v) Bromophenol Blue

Add 400mM DTT to a small aliquot prior to use

A.2 Western Blots

Transfer Buffer

199mM Glycine, 48.05mM Trizma-base, 3.46mM SDS (ICN Biomedical, Ohio), 20% (v/v) Methanol (Chem-Supply, SA)

10x TBS Buffer

100 mM Tris-HCl, *pH to 7.6,* 1.5M NaCl (Chem-Supply, SA)

1x TBST Buffer

10% (v/v) 10x TBS Buffer, 1% (v/v) Polyoxyethylene Sorbitan Monolaurate (Tween-20)

Coomassie Brilliant Blue R250 Stain

0.25% (w/v) Coomassie Brilliant Blue R250, 45% (v/v) Methanol (Chem-Supply, SA), 10% (v/v) Glacial Acetic Acid (Chem-Supply, SA)

Coomassie Blue Destain

45% (v/v) Methanol (Chem-Supply, SA), 10% (v/v) Glacial Acetic Acid (Chem-Supply, SA)

Blocking Buffer

5% (w/v) Diploma Skim Milk Powder in 1x TBST Buffer

Centrifuge at 3500g for 15 min in Jouan CR312 Centrifuge to settle insoluble powder, use supernatant only.

Stripping Buffer

2% SDS, 100 uM B-ME, 50 mM Tris pH 6.8, to final volume of 50mL for each membrane, and heated to 50ºC prior to use.

A.3 Media Broth/Plates

LB Broth

0.1% (w/v) Tryptone (Oxoid, England), 0.5% (w/v) Yeast Extract (Oxoid, England), 0.5% (w/v) NaCl (Chem-Supply, SA) *pH to 7 and Autoclaved*

Selective LB Broth

Allow autoclaved LB Broth to cool, 0.1% (v/v) Glucose ((BDH) AnalR, Victoria),

Antibiotics as required:

Streptomycin 50µg/ml

Ampicillin 100µg/ml

Spectinomycin

Gentamycin

Rifampicin

LB Plates

0.1% (w/v) Tryptone (Oxoid, England), 0.5% (w/v) Yeast Extract (Oxoid, England), 0.5% (w/v) NaCl (Chem-Supply, SA), 1.5% (w/v) Agar (MoBio, CA), *pH to 7 and Autoclaved and allow to cool*

Selective LB Plates

0.1% (w/v) Tryptone (Oxoid, England), 0.5% (w/v) Yeast Extract (Oxoid, England), 0.5% (w/v) NaCl (Chem-Supply, SA), 1.5% Agar (MoBio, CA), *pH to 7 and Autoclaved and allow to cool*

Antibiotics as required:

Ampicillin 100µg/ml

Streptomycin 50µg/ml

Spectinomycin

Gentamycin

Rifampicin

MS Plates

1% (w/v) Sucrose, ½ Murasige and Skoog salts (2.15g/L), pH 5.6-5.8 0.7% (w/v) Agar (MoBio, CA), *Autoclave and allow to cool*, 1% (v/v) Gamborgs

Vitamins Solution 1000x

Selective MS Plates

1% (w/v) Sucrose, ½ Murasige and Skoog salts (2.15g/L), pH 5.6-5.8 0.7% (w/v) Agar (MoBio, CA), *Autoclave and allow to cool*, 1% (v/v) Gamborgs Vitamins Solution 1000x*. Antibiotics as required:* Kanamycin 250µg/ml

A.4 Antibiotics (Stock Solutions)

All stock solutions suspended in distilled water, filter sterilised and stored at -20ºC unless otherwise stated.

Streptomycin (50mg/ml), Ampicillin (100mg/ml), Spectinomycin (50mg/ml), Kanamycin (30mg/ml), Rifampicin (25mg/ml in 99.8% Molecular grade methanol), Cefotaxime/Claforan (50mg/ml) (austratec, Australia)

A.5 Seed and Plant Culture

Coco Mix 3 Soil

540L Coco Peat, 180L Waikerie Sand, *Mix and Steam 1 hour*, 540g Dolimite Lime, 1.8kg Ag Lime, 720g Hydrated Lime, 540g Gypsum, 540g Superphosphate, 1.35kg Iron Sulphate, 90g Iron Chelate, 540g Micromax, 1.35kg $^{Ca2+}$ Nitrate, *Allow to cool*, 1.8kg Osmocote Mini, *pH 6-6.5*

Micronutrient Stock Solution for Hoagland's

46.2mM H_3BO_3, ((BDH) AnalR, Victoria), 9.14mM $MnCl_2.4H_2O$, 0.765mM $ZnSO_4.7H_2O$ (Univar, Victoria), 0.32mM $CuSO_4.5H_2O$ ((BDH) AnalR, Victoria), 1.03mM $Na_2MoO_4.2H_2O$ ((BDH) AnalR, Victoria),

½ Strength Complete Hoagland's Media

2.5mM KNO_3, 2.5mM $Ca(NO_3)_2$, 1mM $MgSO_4$ ((BDH) AnalR, Victoria), 0.5mM KH_2PO_4 (Chem-Supply, SA), 0.05% (v/v) Micronutrient Stock Solution

0.447mM $FeCl_3.6H_2O$ (Chem-Supply, SA), 1.02mM Na EDTA (Univar, Victoria),
Add together and mix before adding to final solution

pH 5.8 with KOH/HCl

Agar Bullets

0.7% (w/v) Agar (MoBio, CA) in ½ strength complete Hoagland's Media and pour into Eppendorf tubes, *cut the end off the tube before using*

Salt Treated ½ Strength Complete Hoagland's Media

To ½ strength Hoagland's add NaCl (Chem-Supply, SA) and $CaCl_2$ (Chem-Supply, SA) to desired concentration

Seed Sterilisation Buffer

15ml 12.5% Bleach (ACE Chemicals, SA), 30ml milliQ water, 4 drops Triton X-114

A.6 Gel Electrophoresis

Ethidium Bromide

10mg into 1ml Distilled water

50x TAE Buffer

1.98M Tris Base, 50mM EDTA *pH 8*, 22.8% (v/v) Glacial Acetic Acid (Chem-Supply, SA)

DEPC treat for RNA

A.7 DNA/RNA/Protein Extraction

GTC Buffer

4M Guanidinium Isothiocyanate, 25mM Sodium Citrate *pH 7.0,* 0.5% (w/v) SDS (ICN Biomedical, Ohio), 100mM β-mercaptoethanol

DNA Extraction Buffer

100mM Tris *pH 8,* 50mM EDTA *pH 8,* 500mM NaCl, 10mM B-mercaptoethanol

A.8 Mitochondrial isolation and assays

Isolation Media

0.3M Sucrose (Merck), 10mM KH_2PO_4, 10mM MOPS, 2mM EDTA (AJAX Chemicals), 1%(W/V) PVP-40, pH 7.5. On the day of use 20mM IsoAscorbic Acid, 4mM L-cysteine, Bring pH down to 7.5 again, 1% (W/V) BSA.

Percoll Gradients

If making 4 gradients

	High	Low
Percoll	19.6ml	19.6ml
PVP-40(20%)	15.4ml	
H20		15.4ml
2 x wash	35ml	35ml
BSA	70mg	70mg

2 X Wash Media

0.6 M Sucrose, 20mM TES, pH 7.2

Standard Reaction Media

0.3 M Sucrose, 10mM TES, 10mM KH_2PO_4, 2mM $MgCl_2$, pH 7.2

APPENDIX B – QUANTITATIVE REAL TIME PCR

B.1 Example of curves generated from QRT-PCR

The following is an example of the amplification generated for QRT-PCR and standard curve generated

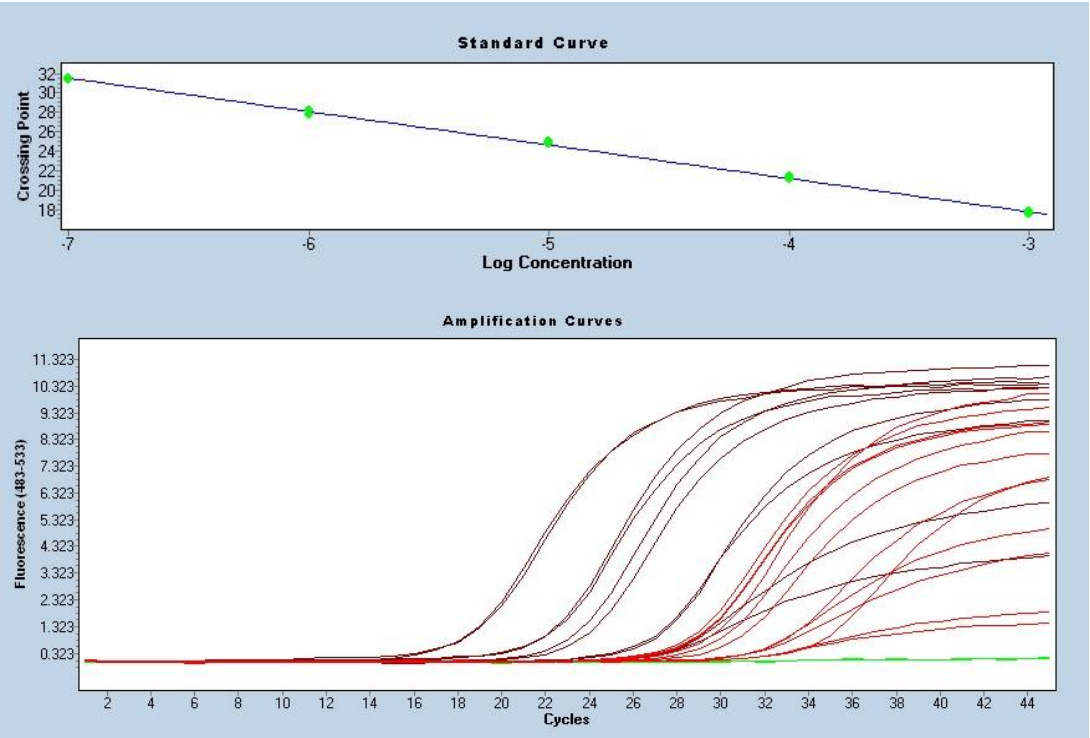

B.2 *ndb4* absolute values

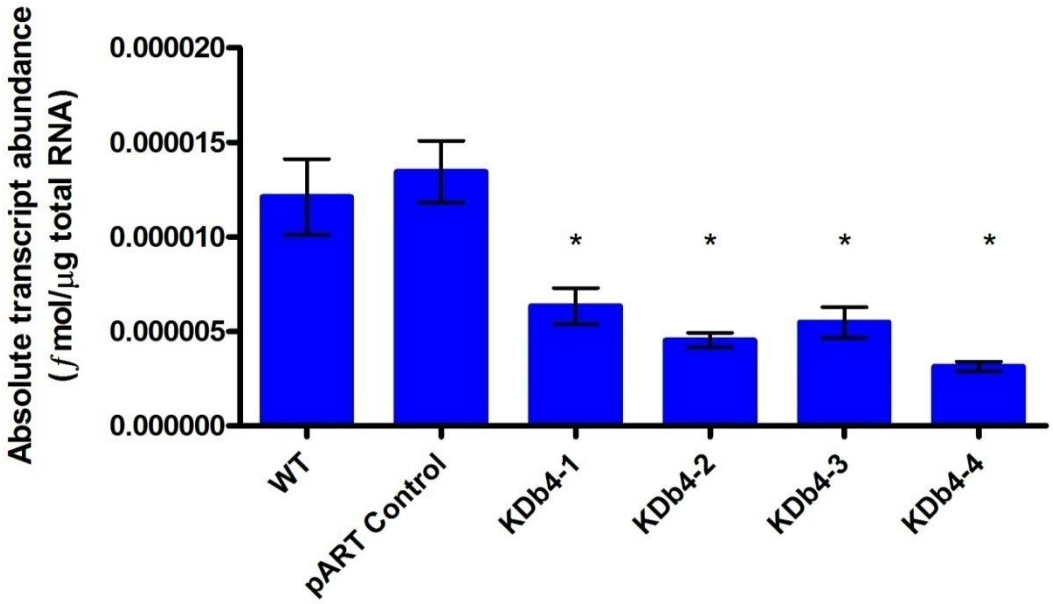

Transcript levels for absolute *ndb4* determined by qRT-PCR, as described in section 2.32. Values are mean +/- SD for n=6 with * being significantly different from the control at P>0.05.

APPENDIX C – CHI SQUARE RESULTS

The data collected from the transgenic lines grown on MS agar and MS agar supplemented with Kanamycin were used to calculate segregation ratios. The ratios were calculated using the Web Chi Square Calculator (Ball et al., 1996).

Mutant Plant Strain: **42A 31**

	Germinated	**Growth**	**Total**
MS Agar	2	37	39
MS + K Agar	6	22	38
Total	8	59	67

Degrees of freedom: 1
Chi-square = 4.119
p is less than or equal to 0.0424.
The distribution is significant.

Mutant Plant Strain: **25 B 23**

	Germinated	**Growth**	**Total**
MS Agar	1	29	30
MS + K Agar	8	22	30
Total	9	51	60

Degrees of freedom: 1
Chi-square = 6.405
p is less than or equal to 0.011
The distribution is significant

Mutant Plant Strain:**4 A 31**

	Germinated	**Growth**	**Total**
MS Agar	1	26	27
MS + K Agar	8	25	33
Total	9	51	66

Degrees of freedom: 1
Chi-square = 4.913
p is less than or equal to 0.027
The distribution is significant

Mutant Plant Strain: **3 B 22**

	Germinated	**Growth**	**Total**
MS Agar	18	3	21
MS + K Agar	21	0	21
Total	39	3	42

Degrees of freedom: 1
Chi-square = 3.231
For significance at the .05 level, chi-square should be greater than or equal to 3.84.
The distribution is not significant.
p is greater than or equal to 0.072

Mutant Plant Strain: **3 A 31**

	Germinated	**Growth**	**Total**
MS Agar	9	23	32
MS + K Agar	2	24	26
Total	11	47	58

Degrees of freedom: 1
Chi-square = 3.897
p is less than or equal to 0.048
The distribution is significant.

Mutant Plant Strain: **26 B 32**

Degrees of freedom: 1
Chi-square = 2.222

	Germinated	Growth	Total
MS Agar	5	39	22
MS + K Agar	5	14	44
Total	12	54	66

For significance at the .05 level, chi-square should be greater than or equal to 3.84.
The distribution is not significant.
p is greater than or equal to 0.136.

Mutant Plant Strain: **41 A 31**

	Germinated	Growth	Total
MS Agar	15	3	18
MS + K Agar	19	0	19
Total	34	3	37

Degrees of freedom: 1
Chi-square = 3.446
For significance at the .05 level, chi-square should be greater than or equal to 3.84.
The distribution is not significant.
p is greater than or equal to 0.063.

Mutant Plant Strain: **26 B 22**

	Germinated	Growth	Total
MS Agar	16	2	18
MS + K Agar	23	0	23
Total	39	2	31

Degrees of freedom: 1
Chi-square = 2.687
For significance at the .05 level, chi-square should be greater than or equal to 3.84.
The distribution is not significant.
p is greater than or equal to 0.101

Mutant Plant Strain: **5 A 32**

	Germinated	Growth	Total
MS Agar	8	32	40
MS + K Agar	13	21	34
Total	21	53	74

Degrees of freedom: 1
Chi-square = 3.007
For significance at the .05 level, chi-square should be greater than or equal to 3.84.
The distribution is not significant.
p is greater than or equal to 0.083

Mutant Plant Strain: **1 B 21**

	Germinated	Growth	Total
MS Agar	2	32	34
MS + K Agar	1	26	37
Total	3	68	71

Degrees of freedom: 1
Chi-square = 0.443
For significance at the .05 level, chi-square should be greater than or equal to 3.84.
The distribution is not significant.
p is greater than or equal to 0.506

Mutant Plant Strain: **2 A 32**

	Germinated	Growth	Total
MS Agar	2	33	35
MS + K Agar	7	21	28
Total	9	54	63

Degrees of freedom: 1
Chi-square = 4.725
p is less than or equal to 0.030
The distribution is significant.

Mutant Plant Strain: **3 A 24**

	Germinated	Growth	Total
MS Agar	1	31	32
MS + K Agar	8	23	31
Total	9	54	63

Degrees of freedom: 1
Chi-square = 6.615
p is less than or equal to 0.010
The distribution is significant.

Mutant Plant Strain: **1 B 15**

	Germinated	Growth	Total
MS Agar	1	29	30
MS + K Agar	2	22	24
Total	3	51	54

Degrees of freedom: 1
Chi-square = 0.635
For significance at the .05 level, chi-square should be greater than or equal to 3.84.
The distribution is not significant.
p is greater than or equal to 0.426

Mutant Plant Strain: **4 A 22**

	Germinated	Growth	Total
MS Agar	3	33	36
MS + K Agar	9	24	33
Total	12	57	60

Degrees of freedom: 1
Chi-square = 4.299
p is less than or equal to 0.038
The distribution is significant.

Mutant Plant Strain: **6 A 25**

	Germinated	Growth	Total
MS Agar	18	3	21
MS + K Agar	24	0	24
Total	42	3	45

Degrees of freedom: 1
Chi-square = 3.673
For significance at the .05 level, chi-square should be greater than or equal to 3.84.
The distribution is not significant.
p is greater than or equal to 0.055

REFERENCES

Agius, S. C., A. G. rasmusson and I. M. Moller (2001). NAD(P) turnover in plant mitochondira. *Aust. J. Plant Physio.* **28**: 461-470.

Alpaslan, M. and A. Gunes (2001). Interactive effects of boron and salinity stress on the growth, membrane permeability and mineral composition of tomato and cucumber plants. *Plant and Soil* **236**(1): 123-128.

Amirsadeghi, S., C. A. Robson, A. E. McDonald and G. C. Vanlerberghe (2006). Changes in plant mitochondrial electron transport alter cellular levels of reactive oxygen species and susceptibility to cell death signaling molecules. *Plant and Cell Physiology* **47**(11): 1509-1519.

Andersson, M. E. and P. Nordlund (1999). A revised model of the active site of alternative oxidase. *FEBS Lett* **448**: 17-22.

Apel, K. and H. Hirt (2004). Reactive oxygen species: metabolism, oxidative stress, and signal transduction. *Annu Rev Plant Biol* **55**: 373-99.

Apse, M. P. and E. Blumwald (2002). Engineering salt tolerance in plants. *Curr Opin Biotechnol* **13**(2): 146-50.

Arron, G. P. and G. E. Edwards (1979). Oxidation of reduced nicotinamide adenine dinucleotide phosphate by plant mitochondria. *Can J Biochem* **57**(12): 1392-9.

Arron, G. P. and G. E. Edwards (1980). Oxidation of Reduced Nicotinamide Adenine Dinucleotide Phosphate by Potato Mitochondria: INHIBITION BY SULFHYDRYL REAGENTS. *Plant Physiol* **65**(4): 591-594.

Asada, K. (2006). Production and scavenging of reactive oxygen species in chloroplasts and their functions. *Plant Physiol* **141**(2): 391-6.

Balk, J., C. J. Leaver and P. F. McCabe (1999). Translocation of cytochrome c from the mitochondria to the cytosol occurs during heat-induced programmed cell death in cucumber plants. *FEBS Lett* **463**(1-2): 151-4.

Bartoli, C. G., F. Gomez, D. E. Martinez and J. J. Guiamet (2004). Mitochondria are the main target for oxidative damage in leaves of wheat (Triticum aestivum L.). *J Exp Bot* **55**(403): 1663-9.

Benjamini, Y. and Y. Hochberg (1995). Controlling the false discovery rate: a practical and powerful approach to multiple testing. *J Roy Statist Soc Ser B* **57**: 289-300.

Berthold, D. A., N. Voevodskaya, P. Stenmark, A. Graslund and P. Nordlund (2002). EPR studies of the mitochondrial alternative oxidase. Evidence for a diiron carboxylate center. *J Biol Chem* **277**(46): 43608-14.

Borsani, O., V. Valpuesta and M. A. Botella (2001). Evidence for a role of

salicylic acid in the oxidative damage generated by NaCl and osmotic stress in Arabidopsis seedlings. *Plant Physiol* **126**(3): 1024-30.

Carneiro, P., M. Duarte and A. Videira (2004). The main external alternative NAD(P)H dehydrogenase of Neurospora crassa mitochondria. *Biochim Biophys Acta* **1608**(1): 45-52.

Carneiro, P., M. Duarte and A. Videira (2007). The external alternative NAD(P)H dehydrogenase NDE3 is localized both in the mitochondria and in the cytoplasm of Neurospora crassa. *J Mol Biol* **368**(4): 1114-21.

Carrie, C., M. W. Murcha, K. Kuehn, O. Duncan, M. Barthet, P. M. Smith, H. Eubel, E. Meyer, D. A. Day, A. H. Millar and J. Whelan (2008). Type II NAD(P)H dehydrogenases are targeted to mitochondria and chloroplasts or peroxisomes in Arabidopsis thaliana. *FEBS Lett* **582**(20): 3073-9.

Chaudhuri, M., W. Ajayi and G. C. Hill (1998). Biochemical and molecular properties of the Trypanosoma brucei alternative oxidase. *Molec Biochem Parasitol* **95**: 53-68.

Chomczynski, P. and N. Sacchi (1987). Single-step method of RNA isolation by acid guanidinium thiocyanate-phenol-chloroform extraction. *Anal Biochem* **162**(1): 156-9.

Chomczynski, P. and N. Sacchi (2006). The single-step method of RNA isolation by acid guanidinium thiocyanate-phenol-chloroform extraction: twenty-something years on. *Nat Protoc* **1**(2): 581-5.

Chuang, C. F. and E. M. Meyerowitz (2000). Specific and heritable genetic interference by double-stranded RNA in Arabidopsis thaliana. *Proc Natl Acad Sci U S A* **97**(9): 4985-90.

Chung, J. S., J. K. Zhu, R. A. Bressan, P. M. Hasegawa and H. Shi (2008). Reactive oxygen species mediate Na+-induced SOS1 mRNA stability in Arabidopsis. *Plant J* **53**(3): 554-65.

Clifton, R., R. Lister, K. L. Parker, P. G. Sappl, D. Elhafez, A. H. Millar, D. A. Day and J. Whelan (2005). Stress-induced co-expression of alternative respiratory chain components in Arabidopsis thaliana. *Plant Mol Biol* **58**(2): 193-212.

Clifton, R., A. H. Millar and J. Whelan (2006). Alternative oxidases in Arabidopsis: A comparative analysis of differential expression in the gene family provides new insights into function of non-phosphorylating bypasses. *Biochimica Et Biophysica Acta-Bioenergetics* **1757**(7): 730-741.

Clough, S. J. and A. F. Bent (1998). Floral dip: a simplified method for Agrobacterium-mediated transformation of Arabidopsis thaliana. *Plant J* **16**(6): 735-43.

Coleman, J. O. and J. M. Palmer (1971). Role of Ca(2+) in the oxidation of exogenous NADH by plant mitochondria. *FEBS Lett* **17**(2): 203-208.

Considine, M. J., D. O. Daley and J. Whelan (2001). The expression of alternative oxidase and uncoupling protein during fruit ripening in mango. *Plant Physiol* **126**(4): 1619-29.

Considine, M. J., R. C. Holtzapffel, D. A. Day, J. Whelan and A. H. Millar (2002). Molecular distinction between alternative oxidase from monocots and dicots. *Plant Physiol* **129**(3): 949-53.

Cook , P. A. (2007). Post-Transcriptional Gene Silencing of an Alternative NAD(P)H Dehydrogenase in *Arabidopsis thaliana* and the response of the Alternative Oxidase to Salinity Stress in Barley. School of Biological Sciences, Flinders University. **Bachelor of Biotechnology**.

Cramer, G. R. (1992). Kinetics of Maize Leaf Elongation : III. Silver Thiosulfate Increases the Yield Threshold of Salt-Stressed Plants, but Ethylene Is Not Involved. *Plant Physiol* **100**(2): 1044-1047.

Cuin, T. A., S. A. Betts, R. Chalmandrier and S. Shabala (2008). A root's ability to retain K+ correlates with salt tolerance in wheat. *J Exp Bot* **59**(10): 2697-706.

Cuin, T. A. and S. Shabala (2007). Compatible solutes reduce ROS-induced potassium efflux in Arabidopsis roots. *Plant Cell Environ* **30**(7): 875-85.

Davenport, R. J., A. Munoz-Mayor, D. Jha, P. A. Essah, A. Rus and M. Tester (2007). The Na+ transporter AtHKT1;1 controls retrieval of Na+ from the xylem in Arabidopsis. *Plant Cell Environ* **30**(4): 497-507.

Day, D. A., J. Whelan, A. H. Millar, J. N. Siedow and J. T. Wiskich (1995). Regulation of Alternative Oxidase in Plants and Fungi. *Aust J Plant Physiol* **22**: 497-509.

Day, D. A. and J. T. Wiskich (1981). Glycine Metabolism and Oxalacetate Transport by Pea Leaf Mitochondria. *Plant Physiol* **68**(2): 425-429.

DeRisi, J. L., V. R. Iyer and P. O. Brown (1997). Exploring the metabolic and genetic control of gene expression on a genomic scale. *Science* **278**(5338): 680-6.

Dhankhar, D. P. and S. S. Dahiya (1980). The effect of different levels of boron and soil salinity on the yield of dry matter and its mineral composition in Ber (Zizyphus rotundifola). Int Symp. Salt Affected Soils. Carnal, India**:** 396-403.

Dizengremel, P. (1983). Effect of Triton X-100 on the cyanide-resistant pathway in plant mitochondria. *Physiol. Veg* **21**: 743-752.

Dry, I. B. and J. T. Wiskich (1987). 2-Oxoglutarate dehydrogenase and pyruvate dehydrogenase activities in plant mitochondria: interaction via a common coenzyme a pool. *Arch Biochem Biophys* **257**(1): 92-9.

Duarte, M., M. Peters, U. Schulte and A. Videira (2003). The internal

alternative NADH dehydrogenase of Neurospora crassa mitochondria. *Biochem J* **371**(Pt 3): 1005-11.

Dutilleul, C., C. Lelarge, J. L. Prioul, R. De Paepe, C. H. Foyer and G. Noctor (2005). Mitochondria-driven changes in leaf NAD status exert a crucial influence on the control of nitrate assimilation and the integration of carbon and nitrogen metabolism. *Plant Physiol* **139**(1): 64-78.

Elhafez, D., M. W. Murcha, R. Clifton, K. L. Soole, D. A. Day and J. Whelan (2005). Characterisation of Mitochondrial Alternative NAD(P)H Dehydrogenases in Arabidopsis: Intraorganelle Location and Expression. *Plant Cell Physiol*.

Elhafez, D., M. W. Murcha, R. Clifton, K. L. Soole, D. A. Day and J. Whelan (2006). Characterization of mitochondrial alternative NAD(P)H dehydrogenases in Arabidopsis: intraorganelle location and expression. *Plant Cell Physiol* **47**(1): 43-54.

Elthon, T. E., R. L. Nickels and L. McIntosh (1989). Mitochondrial events during development of thermogenesis in Sauromatum guttatum (Schott). *Planta* **180**(82-89).

Escobar, M. A., K. A. Franklin, A. S. Svensson, M. G. Salter, G. C. Whitelam and A. G. Rasmusson (2004). Light regulation of the Arabidopsis respiratory chain. Multiple discrete photoreceptor responses contribute to induction of type II NAD(P)H dehydrogenase genes. *Plant Physiol* **136**(1): 2710-21.

Escobar, M. A., D. A. Geisler and A. G. Rasmusson (2006a). Reorganization of the alternative pathways of the Arabidopsis respiratory chain by nitrogen supply: opposing effects of ammonium and nitrate. *Plant J* **45**(5): 775-88.

Escobar, M. A., D. A. Geisler and A. G. Rasmusson (2006b). Reorganization of the alternative pathways of the Arabidopsis respiratory chain by nitrogen supply: opposing effects of ammonium and nitrate. *Plant Journal* **45**(5): 775-788.

Felle, H. (2001). pH: Signal and Messenger in Plant Cells. *Plant Biology* **3**: 577-591.

Ferreira, A. L., J. D. Arrabaca, V. Vaz-Pinto and M. E. Lima-Costa (2008). Induction of alternative oxidase chain under salt stress conditions. *Biologica Plantarum* **52**: 66-71.

Finnegan, P. M., K. L. Soole and A. L. Umbach (2004). 'Alternative Mitochondrial Electron Transport Proteins in Higher Plants'. *Plant Mitochondria, From Genome to Function*. H. A. M. D.Day, J. Whelan. **17**.

Finnegan, P. M., J. Whelan, A. H. Millar, Q. Zhang, M. K. Smith, J. T. Wiskich and D. A. Day (1997). Differential expression of the multigene family encoding the soybean mitochondrial alternative oxidase. *Plant Physiol* **114**(2): 455-66.

Fiorani, F., A. L. Umbach and J. N. Siedow (2005). The alternative oxidase of plant mitochondria is involved in the acclimation of shoot growth at low temperature. A study of Arabidopsis AOX1a transgenic plants. *Plant Physiology* **139**(4): 1795-1805.

Fox, G. G., N. R. Mccallan and R. G. Ratcliffe (1995). Manipulating Cytoplasmic Ph under Anoxia - a Critical Test of the Role of Ph in the Switch from Aerobic to Anaerobic Metabolism. *Planta* **195**(3): 324-330.

Fredlund, K. M., A. G. Rasmusson and I. M. Moller (1991a). Oxidation of external NAD(P)H by purified mitochondria from fresh and aged beetroot (*Beta vulgaris* L.). *Plant Physiol* **97**: 99-103.

Fredlund, K. M., A. G. Rasmusson and I. M. Moller (1991b). Oxidation of External NAD(P)H by Purified Mitochondria from Fresh and Aged Red Beetroots (Beta vulgaris L.). *Plant Physiol* **97**(1): 99-103.

Fridovich, I. (1978). The biology of oxygen radicals. *Science* **201**(4359): 875-80.

Gechev, T. S., F. Van Breusegem, J. M. Stone, I. Denev and C. Laloi (2006). Reactive oxygen species as signals that modulate plant stress responses and programmed cell death. *Bioessays* **28**(11): 1091-1101.

Geisler, D. A., C. Broselid, L. Hederstedt and A. G. Rasmusson (2007). Ca2+-binding and Ca2+-independent respiratory NADH and NADPH dehydrogenases of Arabidopsis thaliana. *Journal of Biological Chemistry* **282**(39): 28455-28464.

Giraud, E., L. H. Ho, R. Clifton, A. Carroll, G. Estavillo, Y. F. Tan, K. A. Howell, A. Ivanova, B. J. Pogson, A. H. Millar and J. Whelan (2008). The absence of ALTERNATIVE OXIDASE1a in Arabidopsis results in acute sensitivity to combined light and drought stress. *Plant Physiol* **147**(2): 595-610.

Gomez, J. M., J. A. Hernandez, A. Jimenez, L. A. del Rio and F. Sevilla (1999). Differential response of antioxidative enzymes of chloroplast and mitochondria to long term NaCl stress of pea plants. *Free Radic. Res.* **31**: s11-s118.

Gorham, J., R. G. Wyn Jones and A. Bristol (1990). Partial characterization of the trait for enhanced K+-Na+ discrimination in the D genome of wheat. *Planta* **180**: 590-597.

Gutierres, S., M. Sabar, C. Lelandais, P. Chetrit, P. Diolez, H. Degand, M. Boutry, F. Vedel, Y. de Kouchkovsky and R. De Paepe (1997). Lack of mitochondrial and nuclear-encoded subunits of complex I and alteration of the respiratory chain in Nicotiana sylvestris mitochondrial deletion mutants. *Proc Natl Acad Sci U S A* **94**(7): 3436-41.

Hartley, J. L., G. F. Temple and M. A. Brasch (2000). DNA cloning using in vitro site-specific recombination. *Genome Res* **10**(11): 1788-95.

Hasegawa, P. M., R. A. Bressan, J. K. Zhu and H. J. Bohnert (2000). Plant cellular and molecular responses to high salinity. *Annual Review of Plant Physiology and Plant Molecular Biology* **51**: 463-499.

Heineke, D., B. Riens, H. Grosse, P. Hoferichter, U. Peter, U. I. Flugge and H. W. Heldt (1991). Redox Transfer across the Inner Chloroplast Envelope Membrane. *Plant Physiol* **95**(4): 1131-1137.

Helliwell, C. A. and P. M. Waterhouse (2005). Constructs and methods for hairpin RNA-mediated gene silencing in plants. *Methods Enzymol* **392**: 24-35.

Helliwell, C. A., S. V. Wesley, A. J. Wielopolska and P. M. Waterhouse (2002). High-throughput vectors for efficient gene silencing in plants. *Functional Plant Biology* **29**: 1217-1225.

Hilal, M., A. M. Zenoff, G. Ponessa, H. Moreno and E. M. Massa (1998). Saline stress alters the temporal patterns of xylem differentiation and alternative oxidase expression in developing soybean roots. *Plant Physiol* **117**(2): 695-701.

Ho, L. H., E. Giraud, R. Lister, D. Thirkettle-Watts, J. Low, R. Clifton, K. A. Howell, C. Carrie, T. Donald and J. Whelan (2007). Characterization of the regulatory and expression context of an alternative oxidase gene provides insights into cyanide-insensitive respiration during growth and development. *Plant Physiol* **143**(4): 1519-33.

Ho, L. H., E. Giraud, V. Uggalla, R. Lister, R. Clifton, A. Glen, D. Thirkettle-Watts, O. Van Aken and J. Whelan (2008). Identification of regulatory pathways controlling gene expression of stress-responsive mitochondrial proteins in Arabidopsis. *Plant Physiol* **147**(4): 1858-73.

Holtzapffel, R. C., J. Castelli, P. M. Finnegan, A. H. Millar, J. Whelan and D. A. Day (2003). A tomato alternative oxidase protein with altered regulatory properties. *Biochim Biophys Acta* **1606**(1-3): 153-62.

Humphreys, T. E. and E. E. Conn (1956). The oxidation of reduced diphosphopyridine nucleotide by lupine mitochondria. *Arch Biochem Biophys* **60**(1): 226-43.

Igamberdiev, A. U. and P. Gardestrom (2003). Regulation of NAD- and NADP-dependent isocitrate dehydrogenases by reduction levels of pyridine nucleotides in mitochondria and cytosol of pea leaves. *Biochim Biophys Acta* **1606**(1-3): 117-25.

Imlay, J. A. (2003). Pathways of oxidative damage. *Annu Rev Microbiol* **57**: 395-418.

Initiative, A. G. (2000). Analysis of the genome sequence of the flowering plant Arabidopsis thaliana. *Nature* **408**(6814): 796-815.

Ito, Y., D. Saisho, M. Nakazono, N. Tsutsumi and A. Hirai (1997). Transcript

levels of tandem-arranged alternative oxidase genes in rice are increased by low temperature. *Gene* **203**(2): 121-9.

Jarmuszkiewicz, W., M. Behrendt, R. Navet and F. E. Sluse (2002). Uncoupling protein and alternative oxidase of Dictyostelium discoideum: occurrence, properties and protein expression during vegetative life and starvation-induced early development. *FEBS Lett* **532**(3): 459-64.

Jolivet, Y., J. C. Pireaux and P. Dizengremel (1990). Changes in Properties of Barley Leaf Mitochondria Isolated from NaCl-Treated Plants. *Plant Physiol* **94**(2): 641-646.

Joseph-Horne, T., J. Babij, P. M. Wood, D. Hollomon and R. B. Sessions (2000). New sequence data enable modelling of the fungal alternative oxidase and explain an absence of regulation by pyruvate. *FEBS Lett* **481**(2): 141-6.

Kant, P., M. Gordon, S. Kant, G. Zolla, O. Davydov, Y. M. Heimer, V. Chalifa-Caspi, R. Shaked and S. Barak (2008). Functional-genomics-based identification of genes that regulate Arabidopsis responses to multiple abiotic stresses. *Plant Cell Environ* **31**(6): 697-714.

Karpinski, S., H. Reynolds, B. Karpinska, G. Wingsle, G. Creissen and P. Mullineaux (1999). Systemic signaling and acclimation in response to excess excitation energy in Arabidopsis. *Science* **284**(5414): 654-7.

Karpova, O. V., E. V. Kuzmin, T. E. Elthon and K. J. NeWton (2002). Differential expression of alternative oxidase genes in maize mitochondrial mutants. *Plant Cell* **14**(12): 3271-84.

Khoshgoftar, A. H., H. Shariatmadari, N. Karimian, M. Kalbasi, S. E. A. T. M. van der Zee and D. R. Parker (2004). Salinity and Zinc Application Effects on Phytoavailability of Cadmium and Zinc. *Soil Sci. Soc. Sm J* **68**: 1885-1889.

Klatte, M., Schuler, M., Wirtz, M., Fink-Straube, C., Hell, R., and P. Bauer (2009). The Analysis of Arabidopsis Nicotianamine Synthase Mutans Reveals Functions for Nicotianamine in Seed Iron Liading and Iron Deficiency Responses. *Plant Physiol* **150**: 257-271

Knight, H., A. J. Trewavas and M. R. Knight (1997). $^{Ca2+}$ signalling in Arabidopsis thaliana responding to drought and salinity. *Plant J* **12**(5): 1067-78.

Knight, H., A. J. Trewavas and M. R. Knight (1996). Cold calcium signaling in Arabidopsis involves two cellular pools and a change in calcium signature after acclimation. *Plant Cell* **8**(3): 489-503.

Knudten, A. F., J. J. Thelen, M. H. Luethy and T. E. Elthon (1994). Purification, Characterization, and Submitochondrial Localization of the 32-Kilodalton NADH Dehydrogenase from Maize. *Plant Physiol* **106**(3): 1115-1122.

Kohler, B., A. Hills and M. R. Blatt (2003). Control of guard cell ion channels by hydrogen peroxide and abscisic acid indicates their action through alternate signaling pathways. *Plant Physiol* **131**(2): 385-8.

Kosugi, S. and Y. Ohashi (2002). DNA binding and dimerization specificity and potential targets for the TCP protein family. *Plant J* **30**(3): 337-48.

Kosugi, S., I. Suzuka, Y. Ohashi, T. Murakami and Y. Arai (1991). Upstream sequences of rice proliferating cell nuclear antigen (PCNA) gene mediate expression of PCNA-GUS chimeric gene in meristems of transgenic tobacco plants. *Nucleic Acids Res* **19**(7): 1571-6.

Kreps, J. A., Y. Wu, H. S. Chang, T. Zhu, X. Wang and J. F. Harper (2002). Transcriptome changes for Arabidopsis in response to salt, osmotic, and cold stress. *Plant Physiol* **130**(4): 2129-41.

Kumar, R., D. S. Conklin and V. Mittal (2003). High-throughput selection of effective RNAi probes for gene silencing. *Genome Res* **13**(10): 2333-40.

Lam, E., N. Kato and M. LaWton (2001). Programmed cell death, mitochondria and the plant hypersensitive response. *Nature* **411**(6839): 848-53.

Landy, A. (1989). Dynamic, structural, and regulatory aspects of lambda site-specific recombination. *Annu Rev Biochem* **58**: 913-49.

Laurie, S., K. A. Feeney, F. J. Maathuis, P. J. Heard, S. J. Brown and R. A. Leigh (2002). A role for HKT1 in sodium uptake by wheat roots. *Plant J* **32**(2): 139-49.

Leach, G. R., K. Krab, D. G. Whitehouse and A. L. Moore (1996). Kinetic analysis of the mitochondrial quinol-oxidizing enzymes during development of thermogenesis in Arum maculatum L. *Biochem J* **317 (Pt 1)**: 313-9.

Levin, J. Z., A. J. de Framond, A. Tuttle, M. W. Bauer and P. B. Heifetz (2000). Methods of double-stranded RNA-mediated gene inactivation in Arabidopsis and their use to define an essential gene in methionine biosynthesis. *Plant Mol Biol* **44**(6): 759-75.

Luethy, M. H., M. K. Hayes and T. E. Elthon (1991a). Partial Purification and Characterisation of three NAD(P)H dehydrogenases from *Beta vulgaris* mitochondria. *Plant Physiol* **97**: 1317-1322.

Luethy, M. H., M. K. Hayes and T. E. Elthon (1991b). Partial Purification and Characterization of Three NAD(P)H Dehydrogenases from Beta vulgaris Mitochondria. *Plant Physiol* **97**(4): 1317-1322.

Luethy, M. H., J. J. Thelen, A. F. Knudten and T. E. Elthon (1995). Purification, Characterization, and Submitochondrial Localization of a 58-Kilodalton NAD(P)H Dehydrogenase. *Plant Physiol* **107**(2): 443-450.

Maathuis, F. J. M. and A. Amtmann (1999). K+ nutrition and Na+ toxicity: The

basis of cellular K+/Na+ ratios. *Annals of Botany* **84**(2): 123-133.

Mackenzie, S. and L. McIntosh (1999). Higher plant mitochondria. *Plant Cell* **11**(4): 571-86.

Matern, U. (1991). Coumarins and other phenylpropanoid compounds in the defense response of plant cells. *Planta Med* **57**(7 Suppl): S15-20.

Maxwell, D. P., Y. Wang and L. McIntosh (1999). The alternative oxidase lowers mitochondrial reactive oxygen production in plant cells. *Proc Natl Acad Sci U S A* **96**(14): 8271-6.

McCabe, T. C., P. M. Finnegan, A. Harvey Millar, D. A. Day and J. Whelan (1998). Differential expression of alternative oxidase genes in soybean cotyledons during postgerminative development. *Plant Physiol* **118**(2): 675-82.

McDonald, A. (2009). Alternative oxidase: what information can protein sequence comparisons give us? *Physiologia Plantarum* **137**: 328-341.

McDonald, A. E. (2008). Alternative oxidase: an inter-kingdom perspective on the function and regulation of this broadly distributed 'cyanide-resistant' terminal oxidase. *Functional Plant Biology* **35**(7): 535-552.

McDonald, A. and G. Vanlerberghe (2004). Branched mitochondrial electron transport in the Animalia: presence of alternative oxidase in several animal phyla. *IUBMB Life* **56**(6): 333-41.

McNulty, A. K. and W. R. Cummins (1987). The relationship between respiration and temperature in leaves of the arctic plant Saxifraga cernua. *Plant Cell Environ* **10**(319–325).

Meeuse, B. J. D. (1975). Thermogenic respiration in Aroids. *Annu Rev Plant Biol* **26**: 117–126.

Meeuse, B. J. D. and R. G. Buggelin (1969). Time, space, light and darkness in the metabolic flare-up of the Sauromatum appen-dix. *Acta Bot Neerl* **18**: 159-172.

Melino, V. J. (2004). Gene silencing of an alternative NAD(P)H dehydrogn\enase via post-transcriptonal suppression in *Arabidopsis thaliana*. School of Biological Sciences, Flinders University. **Bachelor of Biotechnology**.

Melo, A. M., M. Duarte, I. M. Moller, H. Prokisch, P. L. Dolan, L. Pinto, M. A. Nelson and A. Videira (2001). The external calcium-dependent NADPH dehydrogenase from Neurospora crassa mitochondria. *J Biol Chem* **276**(6): 3947-51.

Melo, A. M. P., T. H. Roberts and I. M. Moller (1996). Evidence for the presence of two rotenone-insensitive NAD(P)H dehydrogenases on the inner surface of the inner membrane of potato tuber mitochondria. *Biochem*

Biophys Acta **1276**: 133-139.

Menz, R. I. and D. A. Day (1996a). Identification and Characterization of an Inducible NAD(P)H Dehydrogenase from Red Beetroot Mitochondria. *Plant Physiol* **112**(2): 607-613.

Menz, R. I. and D. A. Day (1996b). Purification and characterization of a 43-kDa rotenone-insensitive NADH dehydrogenase from plant mitochondria. *J Biol Chem* **271**(38): 23117-20.

Michalecka, A. M., S. C. Agius, I. M. Moller and A. G. Rasmusson (2004). Identification of a mitochondrial external NADPH dehydrogenase by overexpression in transgenic Nicotiana sylvestris. *Plant J* **37**(3): 415-25.

Michalecka, A. M., A. S. Svensson, F. I. Johansson, S. C. Agius, U. Johanson, A. Brennicke, S. Binder and A. G. Rasmusson (2003). Arabidopsis genes encoding mitochondrial type II NAD(P)H dehydrogenases have different evolutionary origin and show distinct responses to light. *Plant Physiol* **133**(2): 642-52.

Millar, A. H., O. K. Atkin, H. Lambers, J. T. Wiskich and D. A. Day (1995). A critique of the use of inhibitors to estimate partitioning of electrons between mitochondrial respiratory pathways in plants. *Physiol Plant* **95**: 523-532.

Millar, A. H., J. Whelan and I. Small (2006). Recent surprises in protein targeting to mitochondria and plastids. *Curr Opin Plant Biol* **9**(6): 610-5.

Minagawa, N., S. Sakajo, T. Komiyama and A. Yoshimoto (1990). Essential role of ferrous iron in cyanide-resistant respiration in Hansenula anomala. *FEBS Lett* **267**(1): 114-6.

Moller, I. M. (1997). The oxidation of cytosolic NAD(P)H by external NAD(P)H dehydrogenases in the respiratory chain of plant mitocondria. *Physiologia Plantarum* **100**: 85-90.

Moller, I. M. (2001). PLANT MITOCHONDRIA AND OXIDATIVE STRESS: Electron Transport, NADPH Turnover, and Metabolism of Reactive Oxygen Species. *Annu Rev Plant Physiol Plant Mol Biol* **52**: 561-591.

Moller, I. M. and W. Lin (1986). Membrane-Bound NAD(P)H Dehydrogenases in Higher Plant Cells. *Annual Review of Plant Physiology* **37**(309-334).

Moller, I. M. and J. M. Palmer (1981). The inhibition of exogenous NAD(P)H oxidation in plant mitochondria by chelators and mersalyl as a function of pH. *Physiol. Plant* **53**: 413-420.

Moller, I. M. and A. G. Rasmusson (1998). The role of NADP in the mitochondrial matrix. *Trends Plant Sci* **3**: 21-27.

Moller, I. M., A. G. Rasmusson and K. M. Fredlund (1993). NAD(P)H-ubiquinone oxidoreductases in plant mitochondria. *J Bioenerg Biomembr*

25(4): 377-84.

Moller, I. M., T. H. Roberts and A. G. Rasmusson (1996). Ubiquinone-1 Induces External Deamino-NADH Oxidation in Potato Tuber Mitochondria. *Plant Physiol* **112**(1): 75-78.

Moller, I. S. and M. Tester (2007). Salinity tolerance of Arabidopsis: a good model for cereals? *Trends in Plant Science* **12**(12): 534-540.

Moore, A. L. and J. N. Siedow (1991). The regulation and nature of the cyanide-resistant alternative oxidase of plant mitochondria. *Biochim Biophys Acta* **1059**(2): 121-40.

Moore, C. S., R. J. Cook-Johnson, C. Rudhe, J. Whelan, D. A. Day, J. T. Wiskich and K. L. Soole (2003). Identification of AtNDI1, an internal non-phosphorylating NAD(P)H dehydrogenase in Arabidopsis mitochondria. *Plant Physiol* **133**(4): 1968-78.

Munns, R. (2002). Comparative physiology of salt and water stress. *Plant Cell and Environment* **25**(2): 239-250.

Munns, R. and M. Tester (2008). Mechanisms of salinity tolerance. *Annu Rev Plant Biol* **59**: 651-81.

Murashige, T. and F. Skoog (1962). A revised medium for rapid growth and bioassays with tobacco tissue cultures. *Plant Physiol* **15**: 473-497.

Nash, D. and J. T. Wiskich (1983a). Properties of substantially chlorophyll-free pea leaf mitochondria prepared by sucrose density gradient centrifugation. *Plant Physiol* **71**(627-634).

Nash, D. and J. T. Wiskich (1983b). Properties of Substantially Chlorophyll-Free Pea Leaf Mitochondria Prepared by Sucrose Density Gradient Separation. *Plant Physiol* **71**(3): 627-634.

Nelson, D. L. and M. M. Cox (2000). *Lehninger Principles of Biochemistry (3rd Ed)*, Freeman, New York.

Noctor, G., C. Dutilleul, R. De Paepe and C. H. Foyer (2004). Use of mitochondrial electron transport mutants to evaluate the effects of redox state on photosynthesis, stress tolerance and the integration of carbon/nitrogen metabolism. *J Exp Bot* **55**(394): 49-57.

Ordentlich, A., R. A. Linzer and I. Raskin (1991). Alternative respiration and heat evolution in plants. *Plant Physiol* **97**(1545–1550).

Palmer, J. M. (1976). The Organization and Regulation of Electron Transport in Plant Mitochondria. *Annual Review of Plant Physiology* **27**(1): 133-157.

Park, P. J., A. J. Butte and I. S. Kohane (2002). Comparing expression profiles of genes with similar promoter regions. *Bioinformatics* **18**(12): 1576-84.

Picault, N., M. Hodges, L. Palmieri and F. Palmieri (2004). The growing family of mitochondrial carriers in Arabidopsis. *Trends Plant Sci* **9**(3): 138-46.

Puntarulo, S., R. A. Sanchez and A. Boveris (1988). Hydrogen Peroxide Metabolism in Soybean Embryonic Axes at the Onset of Germination. *Plant Physiol* **86**(2): 626-630.

Qiu, Q. S., Y. Guo, M. A. Dietrich, K. S. Schumaker and J. K. Zhu (2002). Regulation of SOS1, a plasma membrane Na^+/H^+ exchanger in *Arabidopsis thaliana*, by SOS2 and SOS3. *Proc Nat Acad Sci USA* **99**: 843-8441.

Rakhmankulova, Z. F., V. V. Fedyaev, O. A. Podashevka and I. Y. Usmanov (2003). Alternative Respiration Pathways and Secondary Metabolism in Plants with Different Adaptive Strategies under Mineral Deficiency. *Russian Journal of Plant Physiology* **50**: 206-212.

Rasmusson, A. G., D. A. Geisler and I. M. Møller (2008). The multiplicity of dehydrogenases in the electron transport chain of plant mitochondria. *Mitochondrion* **8**(1): 47-60.

Rasmusson, A. G., V. V. Heiser, E. Zabaleta, A. Brennicke and L. Grohmann (1998). Physiological, biochemical and molecular aspects of mitochondrial complex I in plants. *Biochim Biophys Acta* **1364**(2): 101-11.

Rasmusson, A. G. and I. M. Moller (1991). Effect of calcium ions and inhibitors on internal NAD(P)H dehydrogenases in plant mitochondria. *Eur J Biochem* **202**(2): 617-23.

Rasmusson, A. G., K. L. Soole and T. E. Elthon (2004). Alternative NAD(P)H dehydrogenases of plant mitochondria. *Annu Rev Plant Biol* **55**: 23-39.

Rayner, J. R. and J. T. Wiskich (1983). Development of NADH oxidation by Red Beet Mitochondira and Aging of the Tissues. *Aust. J. Plant Physio.* **10**: 55-63.

Rengasamy, P. (2006). World salinization with emphasis on Australia. *J Exp Bot* **57**(5): 1017-23.

Rhoads, D. M. and L. McIntosh (1991). Isolation and characterization of a cDNA clone encoding an alternative oxidase protein of Sauromatum guttatum (Schott). *Proc Natl Acad Sci U S A* **88**(6): 2122-6.

Rinalducci, S., L. Murgiano and L. Zolla (2008). Redox proteomics: basic principles and future perspectives for the detection of protein oxidation in plants. *J Exp Bot* **59**(14): 3781-801.

Roberts, J. K., J. Callis, D. Wemmer, V. Walbot and O. Jardetzky (1984). Mechanisms of cytoplasmic pH regulation in hypoxic maize root tips and its role in survival under hypoxia. *Proc Natl Acad Sci U S A* **81**(11): 3379-83.

Roberts, T. H., K. M. Fredlund and I. M. Moller (1995). Direct evidence for the presence of two external NAD(P)H dehydrogenases coupled to the electron

transport chain in plant mitochondria. *FEBS Lett* **373**(3): 307-9.

Roxas, V. P., S. A. Lodhi, D. K. Garrett, J. R. Mahan and R. D. Allen (2000). Stress tolerance in transgenic tobacco seedlings that overexpress glutathione S-transferase/glutathione peroxidase. *Plant Cell Physiol* **41**(11): 1229-34.

Roxas, V. P., R. K. Smith, Jr., E. R. Allen and R. D. Allen (1997). Overexpression of glutathione S-transferase/glutathione peroxidase enhances the growth of transgenic tobacco seedlings during stress. *Nat Biotechnol* **15**(10): 988-91.

Sabar, M., R. De Paepe and Y. de Kouchkovsky (2000). Complex I impairment, respiratory compensations, and photosynthetic decrease in nuclear and mitochondrial male sterile mutants of Nicotiana sylvestris. *Plant Physiol* **124**(3): 1239-50.

Saisho, D., E. Nambara, S. Naito, N. Tsutsumi, A. Hirai and M. Nakazono (1997). Characterization of the gene family for alternative oxidase from Arabidopsis thaliana. *Plant Mol Biol* **35**(5): 585-96.

Sambrook, J., D. W. Russell and Cold Spring Harbor Laboratory. (2001). *Molecular cloning : a laboratory manual*. Cold Spring Harbor, N.Y., Cold Spring Harbor Laboratory.

Schmiedeberg, L., Kruger, C., Stephan, U. W., Baumlein, H. and R, Hell (2003) Synthesis and proof-of-function of a [^{14}C]-labelled form of the plant iron chelator nicotianamine using recombinant nicotianamine synthase from barley. *Physiol Plant* **118**: 430-438

Scholz, G., Becker, R., Pich, A., and U. W. Stephan (1992) Nicotianamine: a common constituent of strategy-I and strategy-II of iron acquisition by plants. A review. J Plant Nutr **15**: 1647-1665

Schoof, H., P. Zaccaria, H. Gundlach, K. Lemcke, S. Rudd, G. Kolesov, R. Arnold, H. W. Mewes and K. F. Mayer (2002). MIPS Arabidopsis thaliana Database (MAtDB): an integrated biological knowledge resource based on the first complete plant genome. *Nucleic Acids Res* **30**(1): 91-3.

Seki, M., A. Kamei, K. Yamaguchi-Shinozaki and K. Shinozaki (2003). Molecular responses to drought, salinity and frost: common and different paths for plant protection. *Current Opinion in Biotechnology* **14**(2): 194-199.

Seo, B. B., T. Kitajima-Ihara, E. K. Chan, I. E. Scheffler, A. Matsuno-Yagi and T. Yagi (1998). Molecular remedy of complex I defects: rotenone-insensitive internal NADH-quinone oxidoreductase of Saccharomyces cerevisiae mitochondria restores the NADH oxidase activity of complex I-deficient mammalian cells. *Proc Natl Acad Sci U S A* **95**(16): 9167-71.

Shi, H., B. H. Lee, S. J. Wu and J. K. Zhu (2003). Overexpression of a plasma membrane Na+/H+ antiporter gene improves salt tolerance in Arabidopsis thaliana. *Nat Biotechnol* **21**(1): 81-5.

Shin, R., R. H. Berg and D. P. Schachtman (2005). Reactive oxygen species and root hairs in Arabidopsis root response to nitrogen, phosphorus and potassium deficiency. *Plant Cell Physiol* **46**(8): 1350-7.

Siedow, J. N. and A. L. Umbach (1995). Plant Mitochondrial Electron Transfer and Molecular Biology. *The Plant Cell* **7**: 821-831.

Siedow, J. N., J. Whelan, A. Kearns, J. T. \Wiskich and D. A. Day (1992). Topology of the alternative oxidase in soybean mitochondria. *Molecular, Biochemical and Physiological Aspects of Plant Respiration*. H. Lambers and L. H. W. van der Plas, Academic Publishing, The Hague**:** 19-27.

Simons, B. H., F. F. Millenaar, L. Mulder, L. C. Van Loon and H. Lambers (1999). Enhanced expression and activation of the alternative oxidase during infection of Arabidopsis with Pseudomonas syringae pv tomato. *Plant Physiol* **120**(2): 529-38.

Sluse, F. E. and W. Jarmuszkiewicz (2002). Uncoupling proteins outside the animal and plant kingdoms: functional and evolutionary aspects. *FEBS Lett* **510**(3): 117-20.

Smith, N. A., S. P. Singh, M. B. Wang, P. A. Stoutjesdijk, A. G. Green and P. M. Waterhouse (2000). Total silencing by intron-spliced hairpin RNAs. *Nature* **407**(6802): 319-20.

Smith, T. A. (1985). Polyamines. *Annual Review of Plant Physiology* **36**(1): 117-143.

Soole, K. L., I. B. Dry and J. T. Wiskich (1990). Oxidation of NADH by plany mitochondria; kinetics and effects of calcium ions. *Physiol. Plant* **80**: 75-82.

Spellman, P. T., G. Sherlock, M. Q. Zhang, V. R. Iyer, K. Anders, M. B. Eisen, P. O. Brown, D. Botstein and B. Futcher (1998). Comprehensive identification of cell cycle-regulated genes of the yeast Saccharomyces cerevisiae by microarray hybridization. *Mol Biol Cell* **9**(12): 3273-97.

Svensson, A. S., F. I. Johansson, I. M. Moller and A. G. Rasmusson (2002). Cold stress decreases the capacity for respiratory NADH oxidation in potato leaves. *FEBS Lett* **517**(1-3): 79-82.

Svensson, A. S. and A. G. Rasmusson (2001). Light-dependent gene expression for proteins in the respiratory chain of potato leaves. *Plant J* **28**(1): 73-82.

Sweetlove, L. J., A. Lytovchenko, M. Morgan, A. Nunes-Nesi, N. L. Taylor, C. J. Baxter, I. Eickmeier and A. R. Fernie (2006). Mitochondrial uncoupling protein is required for efficient photosynthesis. *Proc Natl Acad Sci U S A* **103**(51): 19587-92.

Taiz, L. and E. Zeiger (2002). *Plant Physiology (3rd Ed)*.

Taylor, N. L., D. A. Day and A. H. Millar (2002). Environmental stress causes

oxidative damage to plant mitochondria leading to inhibition of glycine decarboxylase. *J Biol Chem* **277**(45): 42663-8.

Thimm, O., O. Blasing, Y. Gibon, A. Nagel, S. Meyer, P. Kruger, J. Selbig, L. A. Muller, S. Y. Rhee and M. Stitt (2004). MAPMAN: a user-driven tool to display genomics data sets onto diagrams of metabolic pathways and other biological processes. *Plant J* **37**(6): 914-39.

Thirkettle-Watts, D., T. C. McCabe, R. Clifton, C. Moore, P. M. Finnegan, D. A. Day and J. Whelan (2003). Analysis of the alternative oxidase promoters from soybean. *Plant Physiol* **133**(3): 1158-69.

Thompson, J. D., D. G. Higgins and T. J. Gibson (1994a). CLUSTAL W: improving the sensitivity of progressive multiple sequence alignment through sequence weighting, position-specific gap penalties and weight matrix choice. *Nucleic Acids Res* **22**(22): 4673-80.

Thompson, J. D., D. G. Higgins and T. J. Gibson (1994b). CLUSTAL W: Improving The Sensitivity Of Progressive Multiple Sequence Alignment Through Sequence Weighting, Position-Specific Gap Penalties And Weight Matrix Choice. *Nucleic Acids Research* **22**(22): 4673-4680.

Tinker, P. B. and A. Lauchli (1984). *Advances in plant nutrition*. San Deego, CA, Academic Publishers.

Tsugane, K., K. Kobayashi, Y. Niwa, Y. Ohba, K. Wada and H. Kobayashi (1999). A recessive Arabidopsis mutant that grows photoautotrophically under salt stress shows enhanced active oxygen detoxification. *Plant Cell* **11**(7): 1195-206.

Umbach, A. L., F. Fiorani and J. N. Siedow (2005). Characterization of transformed Arabidopsis with altered alternative oxidase levels and analysis of effects on reactive oxygen species in tissue. *Plant Physiology* **139**(4): 1806-1820.

Vanlerberghe, G. C. and L. McIntosh (1992). Lower Growth Temperature Increases Alternative Pathway Capacity and Alternative Oxidase Protein in Tobacco. *Plant Physiol* **100**(1): 115-119.

Vanlerberghe, G. C. and L. McLntosh (1996). Signals Regulating the Expression of the Nuclear Gene Encoding Alternative Oxidase of Plant Mitochondria. *Plant Physiol* **111**(2): 589-595.

Vanlerberghe, G. C., C. A. Robson and J. Y. Yip (2002). Induction of mitochondrial alternative oxidase in response to a cell signal pathway down-regulating the cytochrome pathway prevents programmed cell death. *Plant Physiol* **129**(4): 1829-42.

Venus, J. C. and D. R. Causton (1979). Plant Growth Analysis: The Use of the Richards Function as an Alternative to Polynomial Exponentials. *Ann Bot* **43**(5): 623-632.

Vercesi, A. E., I. S. Martins, M. A. P. Silva, H. M. F. Leite, I. M. Cuccovia and H. Chalmovich (1995). PUMPing Plants. *Nature* **375**: 24.

Vidal, G., M. Ribas-Carbo, M. Garmier, G. Dubertret, A. G. Rasmusson, C. Mathieu, C. H. Foyer and R. De Paepe (2007). Lack of respiratory chain complex I impairs alternative oxidase engagement and modulates redox signaling during elicitor-induced cell death in tobacco. *Plant Cell* **19**(2): 640-55.

Walker, G. H. and D. J. Oliver (1983). Changes in the electron transport chain of pea leaf mitochondria metabolizing malate. *Arch Biochem Biophys* **225**(2): 847-53.

Waterhouse, P. M., M. W. Graham and M. B. Wang (1998). Virus resistance and gene silencing in plants can be induced by simultaneous expression of sense and antisense RNA. *Proc Natl Acad Sci U S A* **95**(23): 13959-64.

Waterhouse, P. M., M. B. Wang and T. Lough (2001). Gene silencing as an adaptive defence against viruses. *Nature* **411**(6839): 834-42.

Wesley, S. V., C. Helliwell, M. B. Wang and P. Waterhouse (2004). Posttranscriptional gene silencing in plants. *Methods Mol Biol* **265**: 117-29.

Wesley, S. V., C. A. Helliwell, N. A. Smith, M. B. Wang, D. T. Rouse, Q. Liu, P. S. Gooding, S. P. Singh, D. Abbott, P. A. Stoutjesdijk, S. P. Robinson, A. P. Gleave, A. G. Green and P. M. Waterhouse (2001). Construct design for efficient, effective and high-throughput gene silencing in plants. *Plant J* **27**(6): 581-90.

Wesley, S. V., Q. Liu, A. Wielopolska, G. Ellacott, N. Smith, S. Singh and C. Helliwell (2003). Custom knock-outs with hairpin RNA-mediated gene silencing. *Methods Mol Biol* **236**: 273-86.

Whelan, J., A. H. Millar and D. A. Day (1996). The alternative oxidase is encoded in a multigene family in soybean. *Planta* **198**(2): 197-201.

Wilson, R. H. and B. N. Smith (1971). Uncoupling of Sauromatum spadix mitochondria as a mechanism of thermogenesis. *Z Pflanzenphysiol* **65**: 124-129.

Xiong, L., K. S. Schumaker and J. K. Zhu (2002). Cell signaling during cold, drought, and salt stress. *Plant Cell* **14 Suppl**: S165-83.

Yagi, T. (1991). Bacterial NADH-quinone oxidoreductases. *J Bioenerg Biomembr* **23**(2): 211-25.

Yang, H., Matsubayashi, Y., Nakamura, K. and Y. Sakagami (2001). Diversity of Arabidopsis gene encoding precursors for phytosulfokine, a peptide growth factor. *Plant Physiol* **127**: 842-851.

Yeo, A. R. (1983). Salinity resistance: Physiologies and prices. *Physiologia Plantarum* **58**: 214-222.

Yip, J. Y. and G. C. Vanlerberghe (2001). Mitochondrial alternative oxidase acts to dampen the generation of active oxygen species during a period of rapid respiration induced to support a high rate of nutrient uptake. *Physiol Plant* **112**(3): 327-333.

Yokoi, S., F. J. Quintero, B. Cubero, M. T. Ruiz, R. A. Bressan, P. M. Hasegawa and J. M. Pardo (2002). Differential expression and function of Arabidopsis thaliana NHX Na+/H+ antiporters in the salt stress response. *Plant J* **30**(5): 529-39.

Zarkovic, J., S. L. Anderson and D. M. Rhoads (2005). A reporter gene system used to study developmental expression of alternative oxidase and isolate mitochondrial retrograde regulation mutants in Arabidopsis. *Plant Mol Biol* **57**(6): 871-88.

Zhang, Q., L. Mischis and J. T. Wiskich (1996). Respiratory responses of pea and wheat seedlings to chloramphenicol treatment. *Aust. J. Plant Physio.* **23**: 583-592.

Zhu, J., X. Fu, Y. D. Koo, J. K. Zhu, F. E. Jenney, Jr., M. W. Adams, Y. Zhu, H. Shi, D. J. Yun, P. M. Hasegawa and R. A. Bressan (2007). An enhancer mutant of Arabidopsis salt overly sensitive 3 mediates both ion homeostasis and the oxidative stress response. *Mol Cell Biol* **27**(14): 5214-24.

Zimmermann, P., M. Hirsch-Hoffmann, L. Hennig and W. Gruissem (2004). GENEVESTIGATOR. Arabidopsis microarray database and analysis toolbox. *Plant Physiol* **136**(1): 2621-32.

Zottini, M., G. Mandolino and D. Zannoni (1993). Oxidation of External NAD(P)H by Mitochondria from Taproots and Tissue Cultures of Sugar Beet (Beta vulgaris). *Plant Physiol* **102**(2): 579-585.